

**DEVELOPMENT AND CHARACTERIZATION OF RAFFIA PALM FIBER
REINFORCED POLYMER MATRIX COMPOSITES**

A Thesis Submitted to the College of
Graduate and Postdoctoral Studies
In Partial Fulfillment of the Requirements
For the Degree of Master of Science
In the Department of Mechanical Engineering
University of Saskatchewan
Saskatoon

By

Opeoluwa Elijah Fadele

PERMISSION TO USE

In presenting this thesis in partial fulfillment of the requirements for a Postgraduate degree from the University of Saskatchewan, I agree that the Libraries of this University may make it freely available for inspection. I further agree that permission for copying of this thesis in any manner, in whole or in part, for scholarly purposes may be granted by Prof. Ikechukwuka Oguocha and Prof. Akindele Odeshi, the professors who supervised my thesis work or in their absence, by the Head of the Department or the Dean of the College in which my thesis work was done. It is understood that any copying or publication or use of this thesis or parts thereof for financial gain shall not be allowed without my written permission. It is also understood that due recognition shall be given to me and to the University of Saskatchewan in any scholarly use which may be made of any material in my thesis.

Requests for permission to copy or to make other uses of materials in this thesis in whole or part should be addressed to:

Head of the Department of Mechanical Engineering
57 Campus Drive
University of Saskatchewan
Saskatoon, Saskatchewan S7N 5A9
Canada

OR

Dean
College of Graduate and Postdoctoral Studies
University of Saskatchewan
116 Thorvaldson Building, 110 Science Place
Saskatoon, Saskatchewan S7N 5C9
Canada

ABSTRACT

Due to high energy consumption and environmental pollution generated in the processing and use of synthetic fibers, the need for replacement of these fibers with natural fibers in composites manufacture has increased. The advantages of natural fibers over synthetic fibers include low cost, biodegradability and non-toxicity. In this study, as received raffia palm fibers (RPF) and those whose surface were chemically modified using 10 wt.% NaOH for 5 h at 60°C and 0.6 M H₂SO₄ for 2 h at 100°C were compression molded to produce HDPE matrix composites containing 5, 10, 20, and 30 wt.% of RPFs. Morphological, thermal, tensile, physical and structural properties of the fibers before and after treatment were investigated using scanning electron microscopy (SEM), differential scanning calorimetry (DSC), InstronTM machine and Fourier transform infrared spectroscopy (FTIRS). The effects of chemical treatments of the fiber and varying fiber loadings on the mechanical, physical and thermal properties of RPFs reinforced HDPE composites were investigated. Mechanical and thermal properties of the composites were investigated using InstronTM machine and the differential scanning calorimetry (DSC), respectively. The effect of chemical modification on water uptake of the composites was also studied.

Surface chemical treatment of the RPFs by soaking in 10 wt.% NaOH for 5 h at 60°C or 0.6 M H₂SO₄ for 2 h at 100°C resulted in 22% increase in the cellulose content of the fiber. SEM results showed that the RPF comprises of several elemental fibers, which are tightly packed together with each having its lumen at the center. FTIR spectroscopy results indicated reduction and disappearance of some non-cellulosic components in the treated RPFs. Although, there was an increase in the degradation temperature of the treated fibers, tensile strength and water absorption capacity of the treated fibers reduced in comparison to non-treated fibers. The use of RPFs (surface treated or not) in reinforcing HDPE led to increase in tensile modulus, flexural strength, flexural modulus and crystallization temperature of the composite when compared to unreinforced HDPE. The rate of water absorption for composites containing treated fibers is lower than that for composites containing untreated fiber. The tensile strength, impact strength and melting temperature of HDPE decreased with addition of either untreated or treated RPFs. Results also showed that increasing fiber content decreased the tensile strength, flexural strength, impact energy and the melting temperature of the composites. However, increase in tensile modulus, flexural

modulus, water absorption and crystallization temperature of the composites was observed as the fiber content was increased.

ACKNOWLEDGEMENTS

I would like to express my sincere gratitude to my supervisors, Prof. Ikechukwuka Oguocha and Prof. Akindele Odeshi for the opportunity to carry out my M.Sc. study under their guidance. The kindness, time, professional and scientific contributions to the success of my study are deeply appreciated. The contributions of Prof. Duncan Cree and Prof. Tabil Lope, my advisory committee members are greatly appreciated. I thank Dr. Majid Soleimani for his time, advice, insightful and valuable comments which have remarkably contributed to the success of this study.

My appreciations also go to Mr. Rob Peace and Dr. Chithra Karunakaran for their time, advice and patience in training me on most of the equipment used during my MSc. program. The extensive technical support received from Mr. Nan Fang Zhao, Dr. Melanie Fauchoux, Prof. Lee Wilson and Abdalla Karoyo in carrying out many of my experiments is also acknowledged. My appreciation also goes to Fraser Waldie my contact at Nova Chemicals Corporation who ensure I got the right HDPE polymer for my research. I am grateful.

I would like to sincerely appreciate the efforts of my parents, Pastor and Pastor (Mrs.) Fadele for their support, prayers, words of encouragement; they gave to me both morally and financially. I pray that the Almighty God will give them life and strength to eat the good fruit of their labour. To my uncle (Pastor James Fadel) who took it upon himself to see me succeed in my academic pursuit, daddy I am eternally grateful.

To my friends Emmanuel Awoyele, Ahmed Tiamiyu, and Jimmy Fung, your contribution and moral supports towards the completion of this thesis cannot be quantified. Thank you. Lastly, I am very grateful to everybody who has been a source of help, inspiration and guide, and my second family (Jesus House Family), I am grateful to have met you. God, bless you all.

DEDICATION

I DEDICATE MY THESIS FIRST TO THE SOURCE OF ALL LIFE AND MY KING
(JESUS), TO MY PARENTS, AND MY UNCLE, YOU MEAN SO MUCH MORE TO ME.

TABLE OF CONTENTS

PERMISSION TO USE	i
ABSTRACT	ii
ACKNOWLEDGEMENTS	iv
DEDICATION	v
TABLE OF CONTENTS	vi
LIST OF TABLES	xi
LIST OF FIGURES	xiii
LIST OF ABBREVIATIONS AND SYMBOLS	xviii
CHAPTER 1: INTRODUCTION	1
1.1 Overview	1
1.2 Objectives	3
1.3 Thesis organization	3
CHAPTER 2: LITERATURE REVIEW	4
2.1 Composites Materials	4
2.2 Classification of Composite Materials Based on the Matrix	4
2.2.1 Metal Matrix Composites	5
2.2.2 Ceramics Matrix Composites	5
2.2.3 Polymer Matrix Composites	6
2.3 Type of Reinforcements for Composite Materials	6
2.3.1 Particles	6
2.3.2 Whiskers	7
2.3.3 Fibers	7
2.3.3.1 Synthetic Fibers	7
2.3.3.2 Natural Fibers	7
2.4 Chemical Composition of Natural Fibers	8
2.5 Characterization of Natural Fibers	10

2.5.1	Moisture Adsorption	11
2.5.2	Water Absorption	12
2.5.3	Thermal Conductivity	12
2.5.4	Thermal Analysis of Natural Fibers	12
2.5.5	FTIR and Raman Spectroscopy	13
2.6	Chemical Treatment of Natural Fibers	13
2.6.1	Sodium Hydroxide (NaOH) Treatment	14
2.6.2	Sulphuric Acid (H ₂ SO ₄) Treatment	15
2.6.3	Silane Treatment	15
2.7	Processing Techniques for Natural Fiber Reinforced Composites	16
2.7.1	Extrusion Molding and Extrusion Compounding	16
2.7.2	Compression Molding	18
2.7.3	Injection Molding	18
2.8	Characterization of Natural Fibers Reinforced Polymer Matrix Composites	19
2.8.1	Water Absorption	19
2.8.2	Thermal Properties	20
2.8.3	Mechanical Properties	21
2.9	Application of Natural Fiber Reinforced Polymer Matrix Composites	22
2.10	Summary	22
CHAPTER 3:	MATERIALS AND EXPERIMENTAL METHODS	24
3.1	Materials	24
3.2	Characterization of Raffia Palm Fibers (RPF)	25
3.2.1	Length Measurement	25
3.2.2	Density Measurement	25
3.2.3	Determination of Chemical Composition of RPFs	27
3.2.4	Sample Preparation for Microscopy	28
3.2.5	Mid Infrared Spectromicroscopy (Mid – IRS)	28
3.2.6	Tensile Test	30
3.2.7	Statistical Analysis	30
3.2.8	Moisture Adsorption of RPFs	31

3.2.9	Water Absorption of RPFs	32
3.2.10	X-ray Diffraction (XRD)	32
3.2.11	Chemical Treatments of RPFs	33
3.2.12	Colour Measurement	34
3.2.13	Differential Scanning Calorimetry (DSC)	35
3.2.14	FTIR and Raman Spectroscopy	36
3.3	Manufacture of RPF Reinforced High Density Polyethylene Composites	37
3.3.1	Extrusion Machine and Process of Mixture	38
3.3.2	Compression Molding Equipment and Process	40
3.4	Characterization of RPF Reinforced HDPE Composites	42
3.4.1	Density Measurement	42
3.4.2	Tensile Test of Composites	43
3.4.3	Flexural Test of Composites	45
3.4.4	Charpy Impact Test of Composites	46
3.4.5	Water Absorption	48
3.4.6	Thermal Analysis	48
3.4.7	Microscopic Investigations of Composites	49
CHAPTER 4:	RESULTS AND DISCUSSION	50
4.1	Characterization of Raffia Palm Fiber (RPF)	50
4.1.1	Chemical Composition of RPF	50
4.1.2	Microstructure of RPF	53
4.1.3	Moisture Adsorption and Water Absorption	57
4.1.4	Mechanical Properties	60
4.1.5	Statistical Analysis	64
4.1.6	Colour Measurements of RPFs	66
4.1.7	Synchrotron Based Fourier Transform Infrared Spectromicroscopy	67
4.1.8	FT-Infrared and Raman Spectroscopy	71
4.1.9	X-ray Diffraction	74
4.1.10	DSC Measurements	75
4.2	Characterization of RPF Reinforced Polymer Composite	79

4.2.1	The Effect of Fiber Addition on the Density of High Density Polyethylene	80
4.2.2	Tensile Properties Raffia Palm Fiber Reinforced HDPE	83
4.2.3	Fractography of Failed Tensile Specimens	85
4.2.4	The Effect of Fiber Reinforcement on the Flexural Properties of HDPE	87
4.2.5	The Effect of Fiber Addition on the Energy Absorbed of HDPE	89
4.2.6	SEM Analysis of Fractured Charpy Impact Samples	91
4.2.7	The Effect of Fiber Addition on Thermo-Physical Properties of HDPE	92
4.2.8	The Influence of Fiber Addition on the Water Absorption Capacity of HDPE	96
4.3	Summary	99
CHAPTER 5:	CONCLUSIONS AND RECOMMENDATIONS	101
5.1	Conclusions	101
5.2	Recommendations for Future Work	102
REFERENCES	103
APPENDICES	119
APPENDIX A	120
	Ankom Fiber ADF, NDF and ADL Methods	
APPENDIX B	131
	Statistical Analysis of Variation of RPF Colour with Fiber Treatment	
APPENDIX C	134
	Result and Statistical Analysis of the Effect of Fiber Content and Fiber Treatment on the Density of RPF reinforced HDPE	
APPENDIX D	139
	Result and Statistical Analysis of the Effect of Fiber Content and Fiber Treatment on the Tensile Properties of RPF reinforced HDPE	
APPENDIX E	148
	Result and Statistical Analysis of the Effect of Fiber Content and Fiber Treatment on the Flexural Properties of RPF reinforced HDPE	

APPENDIX F 157
Result and Statistical Analysis of the Effect of Fiber Content and Fiber Treatment on the Impact Strength of RPF reinforced HDPE

APPENDIX G 166
Result of the Effect of Fiber Content and Fiber Treatment on the Density of RPF reinforced HDPE

APPENDIX H 167
Result and Statistical Analysis of the Effect of Fiber Content and Fiber Treatment on the Water Absorption Behaviour of RPF reinforced HDPE

LIST OF TABLES

Table 2.1	Chemical composition of some natural fibers.	10
Table 2.2	Mechanical properties of some natural and synthetic fibers.	11
Table 3.1	Humidity generator setup parameters.	31
Table 4.1	Chemical composition (as received basis) of raffia palm fibers.	51
Table 4.2	Chemical composition (dry matter basis) of raffia palm fibers.	52
Table 4.3	Mechanical properties of chemically treated raffia palm fibers.	64
Table 4.4	ANOVA test results for tensile strength of raffia palm fibers with varying fiber lengths of 45, 70, 95, 120 and 145 mm.	64
Table 4.5	ANOVA test results for %elongation for 25 mm gauge length of raffia palm fibers with varying fiber lengths of 45, 50, 55, 60, 65, 70 and 75 mm.	65
Table 4.6	ANOVA test results for tensile strength for 50 mm gauge length of raffia palm fibers with varying crosshead speed of 0.5, 1, 1.5 and 2 mm/min.	65
Table 4.7	ANOVA test results of fiber treatments on the tensile strength at 45 mm fiber length of raffia palm fibers.	66
Table 4.8	ANOVA test results of fiber treatments on % elongation at 25 mm gauge length of raffia palm fibers.	66
Table 4.9	Variation of raffia palm fiber colour with NaOH and H ₂ SO ₄ treatment.	66
Table 4.10	Thermal properties of untreated and treated raffia palm fibers obtained from differential scanning calorimetry analysis.	79
Table B.1	ANOVA results for colour variations of raffia palm fibers with fiber treatment.	131
Table C.1	Effect of raffia palm fiber addition on the density of high density polyethylene composites.	134
Table C.2	SigmaPlot two-way analysis of variance of the effect of fiber content and fiber treatment on the density of raffia palm fiber reinforced high density polyethylene.	134
Table D.1	Effect of raffia palm fiber addition on the tensile properties of high density polyethylene composites.	139
Table D.2	SigmaPlot two-way analysis of variance of the effect of fiber content and fiber treatment on the tensile strength of raffia palm fiber reinforced high density polyethylene.	139

Table D.3	SigmaPlot two-way analysis of variance of the effect of fiber content and fiber treatment on the Young's modulus of raffia palm fiber reinforced high density polyethylene.	143
Table E.1	Effect of raffia palm fiber content on the flexural properties of high density polyethylene composites.	148
Table E.2	SigmaPlot two-way analysis of variance of the effect of fiber content and fiber treatment on the flexural strength of raffia palm fiber reinforced high density polyethylene.	148
Table E.3	SigmaPlot two-way analysis of variance of the effect of fiber content and fiber treatment on the flexural modulus of raffia palm fiber reinforced high density polyethylene.	152
Table F.1	Impact properties of unreinforced and raffia palm fiber reinforced high density polyethylene at different temperatures.	157
Table F.2	SigmaPlot three-way analysis of variance of the effect fiber content, fiber treatment and temperature on the impact strength of raffia palm fiber reinforced high density polyethylene.	158
Table G.1	Effect of untreated and treated raffia palm fibers on thermo-physical properties of high density polyethylene composites.	166
Table H.1	Effect of untreated and treated raffia palm fibers on water absorption behaviour of high density polyethylene composites.	167
Table H.2	SigmaPlot two-way analysis of variance of the effect fiber content and fiber treatment on the water absorption behaviour of raffia palm fiber reinforced high density polyethylene.	167

LIST OF FIGURES

Figure 1.1	Photo showing (a) the location of raffia palm tree and (b) raffia palm tree.	2
Figure 2.1	Classification of natural fibers according to origin.	8
Figure 2.2	Applications of natural fiber reinforced polymer matrix composites.	23
Figure 3.1	Photographs of raffia palm fiber (a) before cleaning and (b) after washing and drying.	24
Figure 3.2	Flowchart for raffia palm fiber processing, treatment and characterization.	25
Figure 3.3	Images of (a) weighing instrument for ground raffia palm fibers and (b) gas pycnometer instrument for density measurement.	26
Figure 3.4	Ankom 200 fiber analyzer used for determining the chemical composition of raffia palm fibers.	27
Figure 3.5	Image showing (a) frozen raffia palm fibers in liquid nitrogen and (b) Leica CM1950 cryostat machine.	28
Figure 3.6	Bruker Vertex 70v Interferometer / Hyperion 3000 IR Microscope.	29
Figure 3.7	Picture showing schematic drawing of a single raffia palm fiber prepared for tensile test.	30
Figure 3.8	Humidity generator used for moisture absorption measurement.	32
Figure 3.9	Images of sodium hydroxide solution (a) before treatment and (b) after treatment	34
Figure 3.10	Images of sulfuric acid solution (a) before treatment and (b) after treatment.	34
Figure 3.11	HunterLab spectrophotometer used for colour measurements.	35
Figure 3.12	Renishaw Raman inVia Reflex microscope.	36
Figure 3.13	Flowchart for raffia palm fiber reinforced high density polyethylene composite processing and characterization.	37
Figure 3.14	Processing chart showing the mixing of untreated, alkaline and acidic treated raffia palm fibers with high density polyethylene to make raffia palm fiber reinforced high density polyethylene composites. $M_1 = 5$ wt.%, $M_2 = 10$ wt.%, $M_3 = 20$ wt.%, $M_4 = 30$ wt.% of fiber, NT = no treatment of the fiber, $T_1 =$ treatment with 10% w/v aqueous NaOH solution at 60°C for 5 h, $T_2 =$ treatment with 0.6 M H_2SO_4 solution at 100°C for 2 h.	38

Figure 3.15	Twin screw extrusion machine for producing extrudates required for composites manufacture.	39
Figure 3.16	Images of (a) water bath and (b) cooling strand pelletizer.	39
Figure 3.17	Retsch knife grinding mill.	40
Figure 3.18	Images of the (a) mold, mold releasing agent and molding plates and (b) compression molding machine.	40
Figure 3.19	Images of composites plates from extruded pellets showing surface porosity.	41
Figure 3.20	Images of composites plates from ground extruded pellets (no surface porosity).	42
Figure 3.21	Apparatus used for measuring densities of compression molded composites and high-density polyethylene.	43
Figure 3.22	Dog-bone shaped specimens for tensile test.	44
Figure 3.23	Instron™ tensile machine equipped with a clip-on extensometer for determining Young's modulus of test specimens.	44
Figure 3.24	A picture showing a typical flexural test on a sample of 10% composites.	45
Figure 3.25	Charpy impact testing machine used in this study.	47
Figure 3.26	Broaching machine used in notching the charpy impact samples.	47
Figure 3.27	Charpy impact test samples.	48
Figure 3.28	Water absorption tests on composites.	49
Figure 3.29	A photograph of the scanning electron microscope used for microstructural investigations.	49
Figure 4.1	Scanning electron micrographs showing transverse cross-section of (a) untreated, (b) alkaline treated and (c) acidic treated raffia palm fibers.	53
Figure 4.2	Scanning electron micrograph showing enlarged view of the inner section (lumen) of raffia palm fiber (transverse section).	54
Figure 4.3	Scanning electron micrograph showing enlarged view of the middle section (cortex) of raffia palm fiber (transverse section).	55
Figure 4.4	Scanning electron micrographs showing the longitudinal surface of untreated raffia palm fibers.	56
Figure 4.5	Scanning electron micrographs showing the longitudinal surface of raffia palm fibers treated with NaOH.	56

Figure 4.6	Scanning electron micrographs showing the longitudinal surface of raffia palm fibers treated with sulphuric acid.	57
Figure 4.7	Moisture adsorption behaviour of untreated raffia palm fiber at 50% relative humidity and 23°C.	58
Figure 4.8	Water absorption behaviour of untreated raffia palm fiber.	59
Figure 4.9	Water absorption behaviour of alkali and acidic treated raffia palm fiber.	60
Figure 4.10	A typical stress-strain curve obtained for a raffia palm fiber at room temperature.	61
Figure 4.11	Variation of fiber strength to fiber length.	61
Figure 4.12	Variation of percentage elongation to fracture of raffia palm fibers with fiber length.	63
Figure 4.13	Variation of tensile strength of raffia palm fibers with the crosshead speed.	63
Figure 4.14	Synchrotron based Fourier transform infrared spectra of untreated raffia palm fiber.	68
Figure 4.15	Synchrotron base Fourier transform infrared spectromicroscopy imaging of the transverse section of untreated raffia palm fiber showing (a) the map region of interest and chemical distribution of (b) cellulose (1165 cm ⁻¹), (c) lignin (1503 cm ⁻¹) and (d) pectin (1750 cm ⁻¹).	69
Figure 4.16	Synchrotron base Fourier transform infrared spectromicroscopy imaging of the lower left region of untreated raffia palm fiber showing (a) the map region of interest and chemical distribution of (b) cellulose (1165 cm ⁻¹), (c) lignin (1503 cm ⁻¹) and (d) pectin (1750 cm ⁻¹).	71
Figure 4.17	Fourier transform infrared spectra of untreated, alkali and acid treated raffia palm fibers.	72
Figure 4.18	Raman spectra of (a) untreated, (b) alkali and (c) acidic treated raffia palm fibers.	73
Figure 4.19	Result of X-ray diffraction analysis on untreated, alkaline and acidic treated raffia palm fibers.	74
Figure 4.20	Differential scanning calorimetry thermograms obtained for untreated (a) air-dried at 23°C and (b) oven-dried raffia palm fibers at 60°C.	76
Figure 4.21	Differential scanning calorimetry thermograms obtained for alkaline treated raffia palm fiber.	77
Figure 4.22	Differential scanning calorimetry thermograms obtained for acidic treated raffia palm fiber.	78

Figure 4.23	Effect of fiber content and chemical treatment on the bulk density of raffia palm fiber reinforced high density polyethylene composites.	80
Figure 4.24	A comparison of the bulk densities of untreated raffia palm fiber reinforced high density polyethylene composites obtained from measurements and those determined from the rule of mixture.	81
Figure 4.25	A comparison of the bulk densities of NaOH treated raffia palm fiber reinforced high density polyethylene composites obtained from measurements and those determined from the rule of mixture.	82
Figure 4.26	A comparison of the bulk densities of H ₂ SO ₄ treated raffia palm fiber reinforced high density polyethylene composites obtained from measurements and those determined from the rule of mixture.	82
Figure 4.27	Effect of fiber content and chemical treatment on tensile strength of raffia palm fiber reinforced high density polyethylene composites.	83
Figure 4.28	Effect of fiber content and chemical treatment on Young's modulus of raffia palm fiber reinforced high density polyethylene composites.	84
Figure 4.29	SEM micrographs of fracture surfaces of tensile specimens of high density polyethylene composites reinforced with (a) 5 wt.% untreated, (b) 30 wt.% untreated, (c) 5 wt.% NaOH treated, (d) 30 wt.% NaOH treated, (e) 5 wt.% H ₂ SO ₄ treated and (f) 30 wt.% H ₂ SO ₄ treated raffia palm fibers.	86
Figure 4.30	Effect of fiber content and fiber treatment on flexural strength of raffia palm fiber reinforced high density polyethylene matrix composites.	88
Figure 4.31	Effect of fiber content and fiber treatment on flexural modulus of raffia palm fiber reinforced high density polyethylene matrix composites.	88
Figure 4.32	Effect of fiber content on the impact energy absorbed of high density polyethylene composites reinforced with untreated raffia palm fibers.	90
Figure 4.33	Effect of fiber content on the impact energy absorbed of high density polyethylene composites reinforced with NaOH treated raffia palm fibers.	90
Figure 4.34	Effect of fiber content on the impact energy absorbed of high density polyethylene composites reinforced with H ₂ SO ₄ treated raffia palm fibers.	91
Figure 4.35	Scanning electron micrographs of charpy impact fracture surfaces at room temperature of high density polyethylene composites reinforced with (a) 5	92

wt.% untreated, (b) 30 wt.% untreated, (c) 5 wt.% NaOH treated, (d) 30 wt.% NaOH treated, (e) 5 wt.% H₂SO₄ treated and (f) 30 wt.% H₂SO₄ treated raffia palm fibers.

- Figure 4.36 Effect of fiber content and fiber treatment on melting temperature of raffia palm fiber reinforced high density polyethylene matrix composites. 93
- Figure 4.37 Effect of fiber content and fiber treatment on crystallization temperature of raffia palm fiber reinforced high density polyethylene matrix composites. 94
- Figure 4.38 Effect of fiber content and fiber treatment on fractional crystallinity of raffia palm fiber reinforced high density polyethylene matrix composites. 95
- Figure 4.39 Effect of fiber content on the water absorption behaviour of high density polyethylene composites reinforced with untreated raffia palm fibers. 97
- Figure 4.40 Effect of fiber content on the water absorption behaviour of high density polyethylene composites reinforced with of NaOH treated raffia palm fibers. 97
- Figure 4.41 Effect of fiber content on the water absorption behaviour of high density polyethylene composites reinforced with H₂SO₄ treated raffia palm fibers. 98
- Figure 4.42 Typical scanning electron micrograph showing the presence of pores in high density polyethylene compression molded samples. 99

LIST OF ABBREVIATIONS AND SYMBOLS

ABBREVIATIONS

a^*	Chromacity coordinates (green to red)
ADF	Acid detergent fiber
ADL	Acid detergent lignin
b	Flexural sample width (mm)
b^*	Chromacity coordinates (blue to yellow)
BG	Between groups
CI	Crystallinity index
CMC	Ceramics matrix composite
d	Flexural sample thickness (mm)
D	Deflection of flexural sample (mm)
Df	Degree of freedom
DMB	Dry matter basis
DSC	Differential scanning calorimeter
E	Young's modulus (GPa)
E_f	Flexural modulus (GPa)
E_i	Impact energy (J)
FRP	Fiber reinforced polymer or Fiber reinforce plastic
FRPC	Fiber reinforced polymer composite
FTIR	Fourier transform infrared
FTIRS	Fourier transform infrared spectroscopy
HDPE	High density polyethylene
L	Length of support span (mm)
L^*	Chromacity coordinates (white to black)
L_o	Gauge length (mm)
m	Slope of the load-deflection curve
MMC	Metal matrix composite
MS	Mean square
MSDC	Modulated differential scanning calorimeter
NDF	Neutral detergent fiber

NF	Natural fiber
NFRP	Natural fiber reinforced polymer
NT	Non-treated
P	Flexural load (N)
PMC	Polymer matrix composite
r	Maximum flexural strain
R	Crosshead speed (mm/min)
RH	Relative humidity
RPF	Raffia palm fiber
RT	Room temperature (23°C)
SEM	Scanning electron microscope
SF	Synthetic fiber
SS	Sum of squares
T_m	Melting temperature (°C)
WG	Within groups
XRD	X-ray Diffraction
Z	Rate of straining of the outer fiber (mm/min)

SYMBOLS

ΔE	Colour index
ρ_c	Density of composite (gcm ⁻³)
ρ_f	Density of fiber (gcm ⁻³)
ρ_l	Density of liquid (gcm ⁻³)
σ_f	Flexural strength (MPa)
σ_t	Tensile strength (MPa)

CHAPTER 1

INTRODUCTION

1.1 Overview

A composite is a multi-component material consisting of two or more different components that are chemically dissimilar and separated by a distinct interface. The properties of composite materials are functions of the properties of two constituent materials: the continuous material called matrix and the discrete material used in reinforcing the matrix, i.e. the reinforcement. The dispersed reinforcing materials are usually stiffer and stronger than the matrix [1]. The properties of a composite depend on the properties of its constituents as well as the volume fraction, geometry and distribution of the reinforcing component. Most composite materials are developed to achieve optimum combinations of mechanical properties such as strength, stiffness and toughness [2].

The mechanical properties of polymers are inadequate for many structural purposes, particularly their strength and stiffness which are lower than those of ceramics and metals [3]. This difficulty is commonly overcome by reinforcing polymers with other materials such as ceramics, glasses, metals and carbon-based materials. Reinforcing polymers with these materials gives rise to improved mechanical properties and widens their structural applications. Synthetic fibers (SFs), whiskers and particles are used to reinforce polymers for a variety of applications in automobiles, sporting goods, household appliances, boats, as well as construction and packaging materials [4]. However, it is equally recognized that composites made from synthetic reinforcements pose severe environmental pollution problems [5]. Hence, there exist an increasing interest in the use of natural fibers (NFs) for making polymer matrix composites (PMCs). Natural fibers are sourced mostly from plants. As a result, they are inexpensive, renewable and biodegradable. Some NFs have mechanical properties comparable to those of some synthetic fibers [6]. NF composites with thermoplastic and thermoset matrices have been embraced by European car manufacturers and suppliers for door panels, seat backs, headliners, package trays, dashboards, and interior parts [7]. Natural fibers derived from flax, sisal, and hemp plants have been used in making these products [9].

Although NFs have some attractive qualities, they have some shortcomings which limits their use in several structural applications. They have high variability in properties [8]. They have high

affinity to water which is caused by cellulose and hemicellulose of NFs. This results in poor bonding and swelling in NF-reinforced PMCs and, consequently, poor mechanical performance. The use of chemical treatments and coupling agents could be effective in enhancing bonding with polymers. In composites fabrication, if the coupling between the reinforcement and the matrix is poor, a coupling agent will be needed for good mechanical properties.

Although several studies have been carried out to investigate the use of natural fibers such as flax [8–11], sisal [12–14], hemp [15–17], jute [18–20], kenaf [16,21–23], abaca [24–26], banana [3,20,27], coir [28–30] and ramie [31–33] in making PMCs, very little attention has been given to the potential use of raffia palm fiber in these composites [5]. Raffia palm fiber is a natural vegetable fiber like sisal, banana and abaca, which are extracted from the leaflets of raffia palm tree – *Raphia farinifera* (Fig. 1.1b).

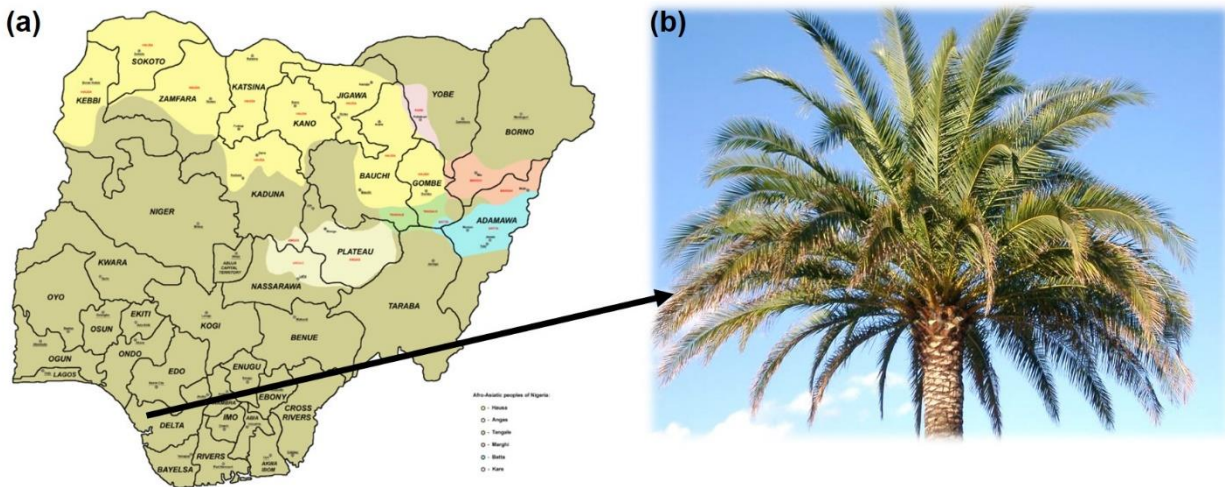


Figure 1.1. Photo showing (a) the location of raffia palm tree [34] and (b) raffia palm tree [35].

Raffia palm tree are grown in the tropical region of Africa, Madagascar and South America [36,37]. There are about 28 different species of raffia fibers grown in the tropics, and they have different properties [38]. The entire raffia palm tree is used for various purposes: from its nuts, one extracts edible and cosmetic oil; from its sap, a white sweet alcoholic liquid is collected, known as palm wine. The fibers extracted from the leaves are used for making dresses, carpets, blankets, ligatures for grafting and as construction materials [5,39]. To date, there has been few studies on the microstructure, chemical properties and characterization of raffia fibers and raffia fibers reinforced polymer composite. Sandy and Bacon [39] studied the tensile properties of raw *Raphia*

farinifera from Madagascar. Anike *et al.* [40] investigated the effects of alkali treatments on the tensile and hardness properties of raffia palm fiber reinforced polyester resin composite. Elenga *et al.* [5,38,41] reported on the microstructure, physical and tensile properties of raw and alkali treated *Raphia textilis*. Different characterization techniques such as scanning electron microscope (SEM), X-ray diffraction (XRD), Fourier transform infrared spectroscopy (FTIRS) and Instron testing machine were used. However, the effects of reinforcing HDPE with varying weight fractions of raw, alkaline and sulphuric acid treated *Raphia farinifera* (from Nigeria) are yet to be studied.

1.2 Objectives

The long-term goal of the present research is to develop and characterize raffia palm fiber reinforced polymer composites using high density polyethylene as the matrix for structural application. To realize this goal, the following specific objectives were pursued:

1. Optimization of the surface chemistry of raffia palm fibers (RPFs) for enhanced interfacial adhesion with polymers.
2. Determination of the effects of surface modification on mechanical and physical properties of RPFs reinforced high density polyethylene.

After the realization of my objectives, my major research contributions to knowledge are:

1. The use of synchrotron Mid-IR to understand the spatial distribution and concentration of chemical compositions of raffia palm fibers.
2. The effects of chemical treatments on the water absorption behaviour of raffia palm fibers.

1.3 Thesis Organization

This thesis consists of five chapters. An overview of the project and research objectives are presented in Chapter 1. A review of previous work relevant to the research topic is provided in Chapter 2. Experimental materials and procedures including composite synthesis and characterization are discussed in Chapter 3. Chapter 4 presents and discusses the research results obtained from tests conducted in Chapter 3. The conclusions drawn from the analysis of the tests results and recommendations for future work are provided in Chapter 5.

CHAPTER 2

LITERATURE REVIEW

This chapter reviews the different characterization techniques associated with NFs, different technique used in manufacturing NFs reinforced polymer matrix composites. It also includes some techniques used in characterizing NFs reinforced polymer matrix composites and its applications.

2.1 Composites Materials

The aim of combining different materials in a composite is to produce a superior and unique material that combines the desired properties of the constituent materials while retaining their identities in the new product [42]. The driving force behind the development of most existing composites is their capability to be designed to provide the targeted material behavior [43]. Development of new composites materials has continued to attract attention in the manufacturing industry, as it offers opportunity to use weak materials with other desirable properties by simply strengthening them with stronger and stiffer reinforcing components such as fibers, whiskers or particles.

2.2 Classification of Composite Materials

Depending on the matrix material, a composite may be classified as metal, polymer, or ceramic matrix composite. In general, metals and polymers are reinforced with fibers, whiskers or particles to increase strength or stiffness or both. For ceramic-matrix composites, the reinforcing component is added mostly to improve fracture toughness [2]. For fiber-reinforced composites, the matrix material binds the fibers together and acts as the medium through which an externally applied stress is transmitted and distributed to the fibers through the interface while only a very small proportion of the applied load is carried by the matrix material [2]. The matrix also protects the individual fibers from surface damage due mechanical abrasion or chemical attack from the environment. The strength of the interface between the matrix and reinforcing component generally controls the mechanical properties of a composite [44].

2.2.1 Metal Matrix Composites (MMCs)

A metal matrix composites (MMCs) consists of a metal matrix that is reinforced by a ceramic fibers or particles to enhance stiffness and strength. Most MMCs commonly produced are based on light metal alloy matrices, especially magnesium, aluminum and titanium alloys. High temperature cobalt and nickel-based alloys are also reinforced with ceramic particles to create a class of MMCs called cermets. [45]. Reinforcing A359 aluminum alloy with 20 vol.% ceramic silicon carbide particles resulted in the production of car brake discs with high wear resistance and good mechanical strength [45]. Ceramic fiber reinforced aluminum alloys have been developed for making propeller shafts used in automobile. This resulted in a 50% weight reduction in comparison to the conventional steel shafts, and reduced number of applied bearings [45]. Lee and Sue [46] studied the effect of dynamic impact on carbon fiber reinforced 7075 Al matrix composites. It was found that the dynamic strength of the composite increased by 35%. Plasma electrolytic oxidation (PEO) method was used to make aluminum alloy 383- SiO₂ particle composites for use in the production of engine block cylinder liners [47]. This reduced weight and manufacturing cost, while wear resistance increased by 85%.

2.2.2 Ceramics Matrix Composites (CMCs)

Ceramics have certain attractive properties such as high stiffness, hardness, compressive strength and relatively low density [48]. However, they are brittle and have low fracture toughness. CMCs are developed to retain the desirable properties of ceramics while compensating for their weaknesses in term of low tensile strength and poor fracture toughness. Matrices used for CMCs include alumina (Al₂O₃), boron carbide (B₄C), and boron nitride (BN) while the reinforcements are secondary materials which are usually ceramic fibers, whiskers or particles. The main reason for developing CMCs is to achieve substantial increases in toughness [49]. Short fibers have been successfully used in reinforcing CMCs. These reinforcements impede the propagation of cracks in the brittle ceramic matrix. [48]. TiC fiber reinforced alumina (Al₂O₃) composites have been commercially produced by hot pressing. TiC reinforced alumina composites exhibit excellent wear resistance [50].

2.2.3 Polymer Matrix Composites (PMCs)

Polymers have low density and good chemical resistance compared to metallic materials. This makes them choice materials for aerospace applications especially in the fabrication of the fuselage and wings [42]. However, low strength and poor stiffness of polymers limits their structural applications in most cases. The poor mechanical properties of polymers are overcome by reinforcement with suitable particles, whiskers or fibers. Most polymer matrix composites (PMCs) consist of thermosetting or thermoplastic polymer matrix reinforced with particles, short or long fibers. In addition, the matrix often determines the maximum service temperature because it softens, melts, or degrades at a much lower temperature than the reinforcing component [2]. When two or more reinforcements are combined in a PMC composite, it is called a hybrid composite. Advantages of hybrids over conventional PMCs include balanced strength and stiffness, improved toughness and impact resistance, and reduced weight [48]. Fiber reinforced polymers (FRPs) find wide application in aerospace structures (control surfaces, etc., in airplanes, for the rotor assembly in helicopters), sports equipment (shafts for golf clubs, handles of rackets), marine structures and in automobile (racing cars) among others [49].

2.3 Type of Reinforcements

Composites are also classified as particle reinforced, fiber reinforced or whisker reinforced composite depending whether fiber, whiskers or particles are used as reinforcement.

2.3.1 Particles

Some of the particles commonly used in reinforcing a metal matrix composite include aluminum oxide (Al_2O_3), titanium carbide (TiC), and silicon carbide (SiC) [51–53]. The particles can be spherical, disk-shaped, rod shaped, and plate shaped. The difference between particles and other reinforcing materials is in the aspect ratio. Particles have an aspect ratio close to unity [54]. Several studies have reported increase in hardness and wear resistance of composite materials when particles are used as reinforcements [52,55,56]. However, a decrease in the tensile strength of the material was also reported by some of these authors [52,55].

2.3.2 Whiskers

Whiskers are monocrystalline material with extremely high strength. They have diameters similar to fibers, yet they are short and have low length-to-diameter (l/d) ratio i.e. aspect ratio compared to fibers [57]. The use of whiskers in reinforcing either metal, ceramic or polymer matrices results in strength improvement of the matrices [58]. However, whiskers are not used extensively as reinforcement in composites due to their high production cost.

2.3.3 Fibers

Fiber is a thin thread of natural or artificial material, generally circular in cross-section. It is a material whose length is many times greater than its diameter, having an aspect ratio greater than 100, and can be either continuous or discontinuous [59,60]. Fiber reinforcement is used to enhance both the strength and stiffness of composites [48]. In fiber-reinforced composites, the fiber is often considered to be the principal constituent since it carries the major share of the load. Materials that are classified as fibers are either polycrystalline or amorphous, and have small diameters [2]. There are two types of fibers namely: natural fibers and man-made or synthetic fibers.

2.3.3.1 Synthetic Fibers (SFs)

Synthetic fibers are man-made fibers such as carbon fibers, aramid fibers, and glass fibers. They have been used in reinforcing polymers and metals producing high performance materials for structural applications [42]. Although composites reinforced with synthetic fibers possess superior mechanical properties, they have some severe drawbacks that include high cost, poor recyclability and non-biodegradability [6].

2.3.3.2 Natural Fibers (NFs)

Natural fibers are gaining increasing attention as alternative to synthetic fibers because they are renewable, abundantly available and environmental friendly. NFs are classified based on their origin (Fig. 2.1). They are sourced from animals (wool and silk), minerals (asbestos) and plants.

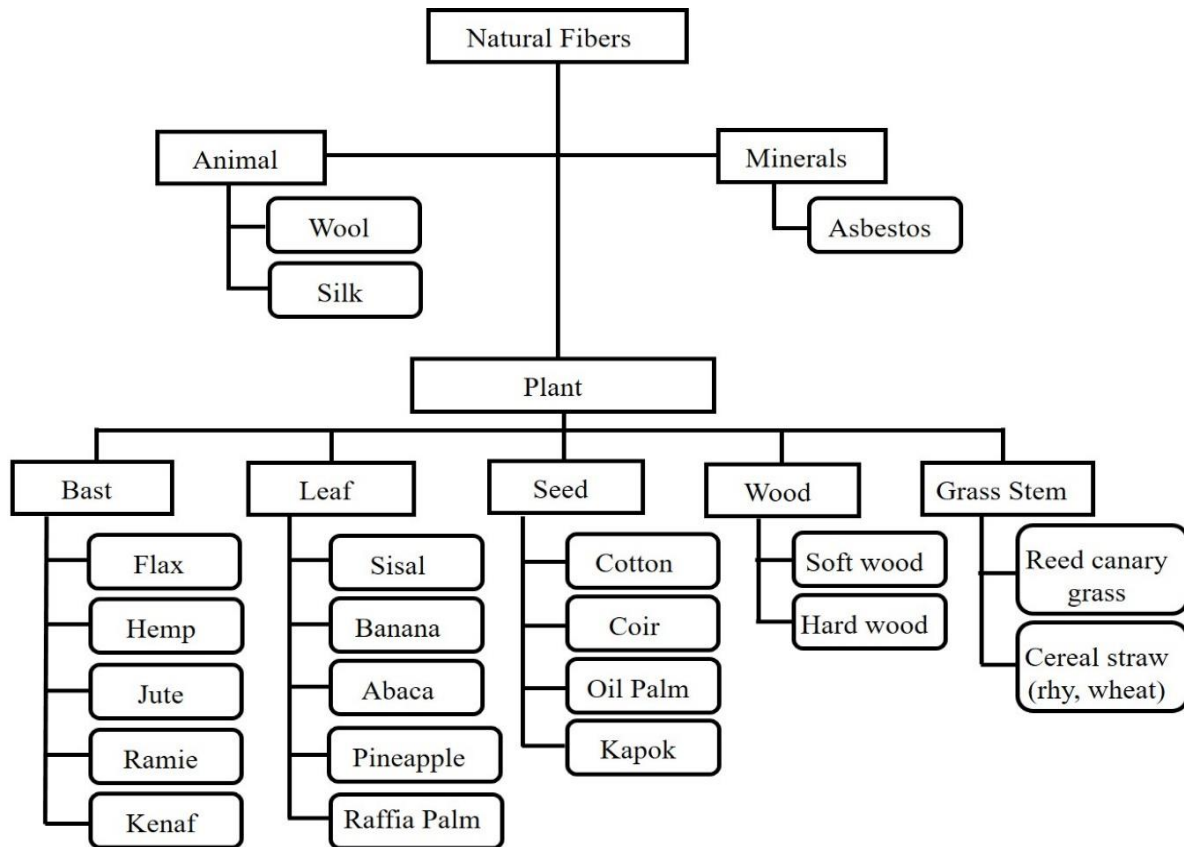


Figure 2.1 Classification of natural fibers according to origin [61].

The extraction part of a plant is the main difference between bast and leaf vegetable fibers. Bast fibers are extracted from the stem of a plant, while leaf fibers are gotten from the leaflets of a plant [62]. The use of NFs as reinforcing materials in both thermoplastic and thermoset matrix composites provides positive environmental benefits with respect to ultimate disposability and sustainability [63]. The mechanical properties of these composites depend mainly on (i) the properties of the fiber, (ii) the properties of the polymer and (iii) the nature and strength of the fiber-matrix interface [2].

2.4 Chemical Composition of Natural Fibers

Natural fibers are composed mainly of cellulose, hemicellulose, lignin, wax, pectin, and other materials. Among these, cellulose, hemicellulose and lignin are the basic components of NFs accounting for mechanical properties [64]. Cellulose is the major components in NFs. It is a natural occurring polymer consisting of D-glucopyranose or D-glucose units ($C_6H_{12}O_6$), which are linked

together by β -1, 4-glycosidic bonds [64–66]. Hence, the repeating units in cellulose is referred to as anhydro-cellulobiose, having a linear structure [64]. Cellulose is highly crystalline, with little amorphous region [65]. Hemicellulose consist of branched, short chains groups of polysaccharides with a lower degree of polymerization than cellulose [65]. The branch structured nature makes hemicellulose highly amorphous, hence, their mechanical properties are lower in comparison to cellulose [64,66]. The changes in fiber dimension with regards to environmental conditions is mostly attributed to hemicellulose swelling due to the water absorbed [66]. Lignin has a complex 3-dimensional polymer structure and it is amorphous [65]. Guaiacyl, syringyl, and p-hydroxyphenyl moieties are the three basic building blocks for lignin, and it is distributed throughout secondary cell wall, having high concentration in the middle lamella [65,66]. Both hemicellulose and lignin acts as the glue that holds the cell wall of each individual fibers in a fiber bundle together [66].

The chemical composition (cellulose, hemicellulose, and lignin contents) of NFs before and after treatment can be determined using different techniques. The use of crude fiber analysis by the Association of Official Analytical Chemists (AOAC) standard [67,68] in determining the chemical compositions of NFs has been reported by several authors [69–73]. Also the use of detergent fiber analysis developed by Peter Van Soest with the aid of Ankom 200 Fiber AnalyzerTM machine has been reported by several authors [28,74–77] to be efficient in determining the chemical compositions of NFs. One of the limitations of detergent fiber analysis is that it cannot quantify the amount of pectin present in NFs. The standard acid detergent fiber (ADF) method 5 [78], neutral detergent fiber (NDF) method 6 [79] and acid detergent lignin (ADL) method 8 [80] procedures were followed (details are provided in Appendix A). The percentages of cellulose, hemicellulose and lignin content are determined from the following equations:

$$\text{Lignin (\% dry matter)} = \text{ADL}$$

$$\text{Cellulose (\% dry matter)} = \text{ADF} - \text{ADL}$$

$$\text{Hemicellulose (\% dry matter)} = \text{NDF} - \text{ADF}$$

Table 2.1 shows the range of the average chemical constituents for a wide variety plant fiber. Their chemical compositions vary depending on the origin of the fiber [81].

Table 2.1. Chemical composition of some natural fibers [82].

Fiber	Cellulose (wt.%)	Hemicellulose (wt.%)	Lignin (wt.%)	Waxes (wt.%)
Bagasse	55.2	16.8	25.3	-
Bamboo	26 – 43	30	21 – 31	-
Flax	71	18.6 – 20.6	2.2	1.5
Kenaf	72	20.3	9	-
Jute	61 – 71	14 – 20	12 – 13	0.5
Hemp	68	15	10	0.8
Ramie	68.6 – 76.2	13 – 16	0.6 – 0.7	0.3
Abaca	56 – 63	20 – 25	7 – 9	3
Sisal	65	12	9.9	2
Coir	32 – 43	0.15 – 0.25	40 – 45	-
Oil palm	65	-	29	-
Pineapple	81	-	12.7	-
Curaua	73.6	9.9	7.5	-
Wheat straw	38 – 45	15 – 31	12 – 20	-
Rice husk	35 – 45	19 – 25	20	14 – 17
Rice straw	41 – 57	33	8 – 19	8 – 38

Climatic conditions, age and processing method influences not only the structure of fibers but also the chemical composition [83]. The variation occurs from plant to plant and within different parts of the same plant. The properties of NFs are closely related to the nature of its cellulose content and its crystallinity. Fibers with higher cellulose content possess higher mechanical properties [84].

2.5 Characterization of Natural Fibers

Generally, the mechanical properties of NFs are lower than those of synthetic fibers. The mechanical properties of some common natural and synthetic fibers are compared with those E-glass and carbon in Table 2.2.

Table 2.2. Mechanical properties of some natural and synthetic fibers.

Fiber	Density (gcm ⁻³)	Tensile strength (MPa)	Elastic modulus (GPa)	Elongation at break (%)	Reference
Jute	1.46	200 – 450	20 – 55	2.0 – 3.0	[20,81,85]
Sisal	1.45	349 – 635	9.4 – 22	2.0 – 2.5	[86–88]
Flax	1.5	345 – 1035	27.6	1.1 – 2.5	[66,88,89]
Hemp	1.47	690	70	2.0 – 4.0	[66,88]
Banana	1.30	529 – 914	7.7 – 32	1.0 – 3.0	[20,66]
Pineapple	1.52	170 – 1627	6.2	1.6	[66,90]
Kenaf	1.20	785	40	1.9	[91]
<i>Raffia textilis</i>	0.75*	148 – 660	28 – 32	2 – 4	[5]
E-glass	2.55	3400	71	4.5 – 4.9	[81,88]
Carbon	1.4	4000	230 - 240	1.4 – 1.8	[88]

* Not clear if the value was obtained through particle or bulk density measurements.

2.5.1 Moisture Adsorption

Many NFs adsorb moisture by instantaneous surface adsorption on exposure to humid air [92]. The rate at which they attain the equilibrium moisture adsorption is determined by their thickness and the ambient temperature. Moisture sensitivity is a major concern when NFs are used to reinforce polymer in composites because they swell and rot through fungal attack [93]. Thus, there is a need to measure the amount of moisture a fiber can adsorb after drying before being used to reinforce polymer. Moisture adsorption test is conducted by weight measurements, whereby samples are weighed, dried in an oven, and reweighed at different time intervals following ASTM D2495-07 standard [94]. Asim [95] conducted the moisture adsorption test on hemp fibers by conditioning the fibers in a desiccator conditioned at 23°C and 50% relative humidity and recording the weight change with time following ASTM D2987-11 standard [96]. Moisture adsorption test is also conducted using the humidity generator [97]. In this case, temperature and relative humidity affecting the moisture adsorbed are computer controlled, while the samples are weighed at different time intervals.

2.5.2 Water Absorption

As mentioned previously in Section 1.1, NFs are highly hydrophilic in nature and are permeable to water. Water uptake in these fibers depends greatly on the morphology and chemical structures [98,99]. Bio-fibers are primarily composed of cellulose, hemicellulose, lignin, and waxy particles. Among these components hemicellulose is primarily responsible for the water absorption behaviour of NFs [10,11,100]. Ana *et al.* [101] reported that the lignin component which is a hydrophobic compound, has little or no effect on the water absorption capacity of NFs. Studies have also indicated that penetration of water into the fibers occurs through the micro pores present on the fiber surface [102,103].

2.5.3 Thermal Conductivity

Thermal conductivity describes a material's ability to transport heat from high to low temperature region [104]. NFs used in reinforcing polymer matrices have low thermal conductivity and are good insulators. Different methods have been employed in measuring thermal conductivity of NFs, such as transient line-source [105,106], transient plane source (TPS) [107–109], laser flash [109–112] and steady-state heat transfer [113–116]. Li *et al.* [106] measured the thermal conductivity of flax fibers with the use of the line-source method. He reported the thermal conductivity of flax fibers used in reinforcing HDPE to be 0.119 W/m°C. Alausa *et al.* [114] reported that the thermal conductivity of *Raphia hookeri* using steady state heat transfer to be 0.056 W/mK. Damfeu *et al.* [116] studied the thermal conductivity of different NFs using steady-state heat transfer. He observed that the thermal conductivities of kapok, coconut and rattan fibers are 0.045 W/mK, 0.055 W/mK, and 0.07 W/mK respectively.

2.5.4 Thermal Analysis of Natural Fibers

The melting temperature (T_m) of a solid is the temperature at which it changes from solid to liquid state. Thus, thermal stability of fibers is very important in processing NFs reinforced composites. Since natural fibers are ligno-cellulosic and consist mainly of lignin, hemicellulose and cellulose, their cell walls undergo decomposition with increasing processing temperature [100]. Thermal stability of NFs was studied by several authors [95,117–120] with the aid of differential scanning calorimetry (DSC) and/or thermogravimetric analysis (TGA). Asim [95] studied the thermal

properties of hemp fibers using a Perkin-Elmer Simultaneous Thermal Analyzer 6000 equipment at a heating rate of 10°C/min from room temperature to 450°C. A small peak around 50°C was observed corresponding to loss of moisture. Two other broad exothermic peaks were observed at about 270°C and 360°C, which were attributed to decomposition of hemicellulose and cellulose respectively. Oliveira and D'Almeida [117] studied the thermal properties of tururi fibers using a Perkin-Elmer, model Pyris Diamond equipment, from 20 to 200°C under inert (N₂) atmosphere at a heating rate of 10°C/min. Three main peaks were observed. A broad endothermic peak occurred around 110°C which was associated with dehydration of water. Two exothermic peaks were identified at approximately 270°C and 360°C. These were associated with thermal decompositions of hemicellulose and cellulose, respectively. Ananda [120] studied the thermal properties of flax fibers using a DSC model Q2000, TA Instruments at a heating rate of 20°C from 20 to 400°C. An endothermic peak at around 107°C attributed to water evaporation from flax fibers was observed. Two exothermic peaks at around 349°C and 381°C were attributed to the degradation temperature of lignin and cellulose respectively.

2.5.5 FTIR and Raman Spectroscopy

Chemical treatments can alter the surface chemistry of NFs. Quantitative evaluation of some of these changes can be studied using Fourier Transform Infrared (FTIR) and Raman spectroscopy. These spectroscopic techniques help in identifying the different functional groups present in the fibers before and after chemical treatments [72]. Reduction in the intensity of some functional groups peak, shift in the spectra and disappearance of some functional groups aid in ascertaining the alterations that occur during chemical treatments of the fibers [121].

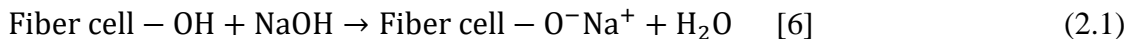
2.6 Chemical Treatment of Natural Fibers

The use of natural fibers in reinforcing polymer is not without its own challenges. The major challenges include poor interfacial adhesion, and poor compatibility between the hydrophilic fiber and the hydrophobic matrix causing fiber swelling within the matrix. There is also the difficulty in homogenous mixing the NFs and polymers. Due to the difference in chemical structure between fibers and polymer, obtaining a strong bonding between these fibers and polymer matrices can be very challenging. A weak fiber matrix bond will lead to ineffective stress transfer throughout the fiber-matrix interface. Therefore, chemical treatment of NFs is required to improved bonding and

therefore enhanced composite performance. These treatments are usually based on the use of reagents with functional groups that can react with the fibers and change their surface chemistry. The commonly used chemical treatments in modifying the surface chemistry of NFs and improving their compatibility with hydrophobic polymers include, sodium hydroxide, silane, sulphuric acid, benzoylation, permanganate and peroxide treatment among others. Surface treatment of fibers is used to reduce their tendency for moisture absorption and thereby facilitates greater compatibility with the polymer matrix [103].

2.6.1 Sodium Hydroxide (NaOH) Treatment

Mercerization is an economical and effective method used for improving the interfacial incompatibility between the matrix and the fiber. It has also proven to reduce water uptake of fibers. It improves the adhesive characteristics of the fiber surface by removing natural waxy materials, hemicellulose and artificial impurities, and produce good surface topography [102]. During this chemical treatment, the surface of the fibers are cleaned to ensure the removal of impurities, which reduces the fiber surface roughness and water absorption capacity via the removal of hydroxyl groups present on the fiber structure [6,93] as shown in equation 2.1.



The effect of NaOH treatment depends on the concentration of the alkaline solution, its temperature and the treatment time duration. Optimum conditions for mercerization increases the degree of bonding at the polymer-fiber interface [93]. Anike *et al.* [40] studied the effect of alkali treatment on mechanical properties of raffia palm fiber reinforced polyester matrix composite. After alkali treatment of the fiber, two of its components (i.e. hemicellulose and the lignin) were removed. This improved the tensile strength as well as the modulus of elasticity of the composite produced with the treated fiber, in comparison with those containing untreated fibers. Elenga *et al.* [41] studied the effects of alkali treatment on the surface chemistry and properties of raffia fiber by treating the fiber with different concentrations (2.5, 5 and 10 wt.%) of sodium hydroxide (NaOH) so as to preserve the cellulose part of the fiber but dissolving the hemicellulose and the lignin portions. The results showed that higher concentration of sodium hydroxide attacked the cellulose, leading to fiber weakening. The use of sodium hydroxide in treating NFs increases the fiber surface area for good adhesion with the matrix. Good adhesion between the matrix and the fiber is needed for improved mechanical properties.

2.6.2 Sulphuric Acid (H₂SO₄) Treatment

Treatment of NFs with dilute acids is widely used and it is reported to be effective in hydrolyzing hemicellulose from NFs, thereby exposing their cellulose content [122]. Dilute acid treatment is also effective in modifying the surface chemistry of NFs by removing almost 100% of hemicellulose from cellulose and lignin [123]. Treatment with sulphuric acid (H₂SO₄) is most commonly used, while other acids such as hydrochloric acid (HCl), phosphoric acid (H₃PO₄), and nitric acid (HNO₃) have also been used [124]. Process parameters such as temperature, acid concentration, exposure time, and solid-to-liquid ratio determine the product yield during acid treatment. Soleimani *et al.* [69] pretreated oat hull fiber with 0.1 N of H₂SO₄ at 130°C for 40 min. They reported that more than 95% of the hemicellulose was hydrolyzed. Grewal *et al.* [123] pretreated oat hull fibers with 1.2 N of H₂SO₄ at 99°C for 80 min under continuous stirring at an agitation speed of 300 rpm with a solid-liquid ratio of 1:10 (w/w). They also reported that more than 95% of the hemicellulose was extracted.

2.6.3 Silane Treatment

The use of silane in chemically modifying NFs has been reported in several studies to have been effective in enhancing the interface between the fibers and polymer matrix composites [125–128]. Zhou *et al.* [126] studied the effect of silane treatment on the microstructure of sisal fibers. 0.2 mol/L of 3 – aminopropyltri-ethoxysilane (APS) and N – (2 – aminoethyl) – 3 – aminopropyltri-methoxysilane (AAPTS) coupling agent were used in modifying sisal fibers at room temperature for 72 h. 1 g of sisal fibers per 100 mL of silane solution was maintained. After treatment, the fibers were washed several times in an 80/20 (v/v) ethanol/water mixture. Thereafter, the fibers were subjected to a Soxhlet extraction in ethanol to remove unreacted silane molecules and dried at room temperature. After treatment they observed non-cellulosic components of the fibers were removed from FTIR results. They also observed new absorption bands in the region from 800 to 1800 cm⁻¹ which corresponds to silane coupling agents. The presence of this band is an indication that silane was successfully grafted on to the fiber surface, enhancing a stronger interface when used in reinforcing polymers. Gonzalez *et al.* [127,128] investigated the effect of chemical treatments on the mechanical properties of henequen fibers reinforced HDPE matrix composite. The fibers were treated with 2% (w/v) NaOH solution at room temperature for 1 h denoted as

FIBNA. After treatment, the fibers were washed and dried at 60°C for 24 h. The fibers were also treated with 0.033% (w/w) vinyltris (2 – methoxy – ethoxy) silane solution at room temperature for 1 h denoted as FIBSIL. The pH of the solution was kept at 3.5. After treatment, the fibers were washed and dried at 60°C for 24 h. Also, after washing of the fibers which were treated with 2% NaOH, they were further immersed in 0.033% silane solution. This fiber was denoted as FIBNASIL. From FTIR and adsorption isotherm analysis, they observed that the amount of silane adsorbed onto the FIBNASIL fibers and removal of non-cellulosic components was higher in comparison to FIBSIL fibers. They attributed the increase in silane adsorbed in the FIBNASIL fiber to the fact that pre-treatment of fibers in alkali solution gave a larger amount of exposed cellulose on the fiber prior to silane treatment. They observed an increase in tensile properties of the composite when the fibers were pre-treated with alkali solution and finally with a silane coupling agent.

2.7 Processing Techniques for Natural Fiber Reinforced Composites

Polymer matrix composite materials are formed into shape using different processing technologies such as extrusion, compression, rotational, and injection molding techniques. Processing of NF reinforced polymer composites is based on mixing of short NFs and polymer matrix followed by subsequent molding [115]. Thermoplastics offer many advantages over thermosets. Thermoplastics offer design flexibility and ease of molding complex parts [100]. The two common methods for processing NF-reinforced polymer composites are injection molding and compression molding. Both are usually preceded by extrusion molding to attain a uniform dispersion of fibers in the melted polymer.

2.7.1 Extrusion Molding and Extrusion Compounding

Extrusion is a molding process where a melted material (polymer) is forced to go through a die orifice, providing a long and continuous product, whose cross-section is determined by the shape of the die [48]. Extrusion compounding is a molding process where polymer melts with other additives (i.e. fibers) are extruded through the die, and the final product is known as a compound or composite [54]. In operating the extrusion compounding machine, mixture of materials (powder polymers and ground fibers) are fed into the extrusion barrel through the hopper, and conveyed through the barrel by rotating screw. Electrical heaters placed around the barrel ensures total melt

of the material. The heaters are set at varying temperature to help melt the material gradually. The rotating screw aside from pushing the melted material through the die orifice also serves several functions as divided into sections. In the feed section, the rotating screw help convey the material from the hopper through the barrel. As the material is heated and transformed into liquid, the rotating screw helps removed any entrapped air in the barrel by compressing the melted material. In the metering section, the rotating screw helps in homogenizing the material while providing sufficient pressure in pushing the melted material through the die opening [48]. The extrudates are cooled by the surrounding air and with the use of a water-bath, which is attached to the end of the die orifice.

Most composites consisting of natural fibers and thermoplastics are produced by extrusion. During this process, the processing temperature is considered a limiting factor especially when it concerns the use of natural fibers [129]. Above 160°C and in the presence of oxygen, the fibers can undergo thermal oxidation resulting in darkening and, at higher temperatures, mechanical degradation will occur. Thus, the temperature in the extruder should be high enough to ensure the melting of the polymer and low enough to avoid burning of the fiber [74]. Therefore, the use of twin screw extruders has been preferred for the direct incorporation of short natural fibers and polymer matrix as against a single screw extruder [115]. It allows the possibility of controlling the energy introduction via screw configuration and processing conditions, in such a way that a lower process temperature can be reliably ensured. The purpose of this equipment is to provide adequate impregnation and homogenization of the polymer matrix and natural fibers mixture.

Li *et al.* [9] produced flax fiber reinforced high density polyethylene (HDPE) composites samples using both the extrusion and injection molding machines. A mixture of the fiber and HDPE was fed through a large hopper into the twin-screw extruder. The controlled extruder parameters were the screw speed and temperature. The twin-screw was rotated to convey, melt, mix and pump the material out, while the screw speed was maintained at 150 rpm. The extrusion barrel zone temperature was set to different temperatures (90, 120, 130, 140, and 160°C) for gradual melting of the polymer in order to ensure uniform mixing with the fibers [48]. The extrudate (pellets) taking the geometry of the die (i.e. six hole die with a diameter of 3 mm each) were produced, which were further processed using the conventional molding techniques [130].

2.7.2 Compression Molding

In this molding process, pellets of the composite produced via an extruder are transferred into a mold cavity, where a compressed plate taking the shape of the mold cavity is produced. In operating the compression-molding machine both the upper, lower compression plates (platen) and mold are preheated. Preheating the compression plates and mold reduces molding time and pressure, and produces a more homogeneous finished piece [2]. Afterwards, the material is placed in the mold and closed, after which heat, and pressure are applied to melt the material causing the material to become viscous taking the shape of the mold geometry.

El-Shekeil *et al.* [23,131] studied the mechanical properties of kenaf fibers reinforced polyurethane composite plates production via compression molding. The blend of intermediate materials was placed into the mold, where heat and pressure were applied to form the composite plates. Prior to full press, specimens were pre-heated for 7 min at 190°C. The contact with the hot mold plasticizes the materials, which takes the form of the mold cavity with the aid of the applied pressure [132]. Hot pressing was then carried out at a temperature around 190°C for 10 min and the mixture was cooled under pressure to room temperature.

2.7.3 Injection Molding

The injection molding is also an important molding technique used in composite molding. Injection molding can manufacture geometrically complex components with accurate dimensions [74]. It has high production cycle when the mold contains more than one cavity so that multiple parts are produced per cycle [48]. The working operation of the injection molding machine is much like the extrusion molding machine. It has a barrel that conveys the material from the hopper to the die, while heating and mixing the material. A non-return valve is mounted near the tip of the screw, which prevents the melted material from flowing backward along the screw threads. Aside from the injection unit, the whole machine also has a clamping unit whose functions are to: hold the two halves of the mold in proper alignment with one another; open and close the mold at the appropriate time in the molding cycle; and keeping the mold closed during injection [48].

Ramadevi *et al.* [133] studied the mechanical properties of abaca fiber reinforced polypropylene composite plates produced with the use of injection molding machine. A blend of mixture of the ground fibers and polymer were dried up at 80°C for 24 h. The mixture was then poured into the injection machine and molding was carried out at a temperature range of 150 – 180°C and a pressure of 20 kN/mm². The temperature of the mold was kept constant at 80°C for 24 h. Li *et al.* [134] studied the effect of injection molding processing parameters on the mechanical properties of flax fiber reinforced polyethylene composites. During injection molding, two set of temperature range (168 – 188°C and 177 – 200°C) and pressure (4.8 and 6.9 MPa) were varied respectively with different fiber weight composite. The highest tensile and flexural strength were found in the 30% weight fraction processed at low injection temperature (168 – 188°C) and pressure (4.8 MPa).

2.8 Characterization of Natural Fiber Reinforced Polymer Matrix Composites

The properties of natural fiber reinforced polymer matrix composites depend on those of the individual components and their interfacial compatibility. Stress transfer and load distribution efficiency at the interface is determined by the degree of adhesion between the components [93].

2.8.1 Water Absorption

Water absorption is a major challenge posed when NFs are used to reinforce polymer matrices. It causes breakdown of the fiber-matrix interface resulting in swelling of the fibers, loss in the efficiency of load transfer between the matrix and the fibers, and ultimately to reduction in strength and stiffness of the composites [135]. The rate of water uptake by NFs reinforce polymer composites depends on factors such as temperature, fiber volume fraction, fiber orientation, fiber type, area of exposed surfaces, interfacial bonding, and porosity [136]. A general method following ASTM D570-98 standard [137] has been used in determining the water absorption capacity of NFs reinforced polymer composites. Water absorption measurement is used to shed light into which material is responsible for water absorbed in the composite and its effects on the mechanical, thermal, and dimensional properties of the composite [138,139]. It is therefore important that the challenge posed by water absorption is addressed so that NFs may be considered as a viable reinforcement in composite manufacture [140].

One way to reduce water absorption in NFs is using compatibilizers which enhance interfacial adhesion between fibers and polymer matrices. Examples of compatibilizers used in composite manufacturing are maleic anhydride grafted polypropylene (PP-g-MA), maleic anhydride grafted SEBS (SEBS-g-MA), and maleated polypropylene (MAH-g-PP). The use of chemical treatment on NFs has also been reported to reduce their water absorption capacity and to maintain the integrity of the interface in case of exposure of the natural fiber reinforced polymer to water. Arbelaiz *et al.* [10] investigated the use of maleic anhydride-polypropylene copolymer (MAPP) as compatibilizer in the water absorption properties of flax fiber reinforced polypropylene composites. They observed that the use of MAPP reduced the rate of water absorption in the modified composites in comparison to composites without MAPP. They reported that reduction in the rate of water absorption in composites modified using MAPP is due to the improved interfacial adhesion. They observed that the rate of water absorption in the composites was linear for a period until it attained saturation. Maya *et al.* [102] evaluated the water absorption characteristics of sisal and oil palm composites treated with varying concentrations of sodium hydroxide (NaOH). They reported that the composites containing fibers treated with 0.5% NaOH showed the highest water uptake, while those treated with 4% NaOH samples exhibited the minimum water uptake. It was observed that as the concentration of NaOH increases, the adhesion between the fiber and the matrix increases, and the uptake of water decreases. They also observed that hydrophilic character of NFs was responsible for water uptake in the composites, and as the volume percent of fibers increase, there was a corresponding increase in the rate of water absorption [102]. They also reported a two-stage water saturation level, which was due to prolonged exposure of the swollen samples in water [102].

2.8.2 Thermal Properties

The fact that NFs are mixed with molten polymers during processing influences the final thermal (melting temperature, crystallization temperature and thermal conductivity) properties of the composites. The thermal properties (melting and crystallization temperature) of NFs reinforced polymer composites was studied by several authors [9,106,119,141,142] with the aid of differential scanning calorimetry (DSC) and/or thermogravimetric analysis (TGA). Li *et al.* [9,106] investigated the addition of flax fiber on the melting temperature of high density polyethylene (HDPE). The test was performed using a TG-DSC 111 machine from room temperature to 250°C

at a heating rate of 5°C/min. They reported the melting point of HDPE to be 139.3°C, which was found to decrease with the addition of flax fibers. It was reported that the decrease in melting temperature of the composites is because flax fiber requires low energy to be heated up in comparison to HDPE. They also investigated the effect of fiber addition on the thermal conductivity of HDPE [106]. The transient line source method at temperature of between 170 and 200°C was used. The thermal conductivity observed for HDPE was 0.4281 W/m°C. It was reported that with the addition of flax fibers and as the fiber content increased, there was a corresponding decrease in the thermal conductivity of the composite. It was reported that the decrease in thermal conductivity of the composites is due to a lower thermal conductivity of the flax fiber compared to that of HDPE. Tajvidi and Takemura [141] studied the effect of kenaf fibers addition on the thermal degradation of polypropylene (PP) using DSC from room temperature to 200°C at a heating rate of 20°C/min. Approximately, 10 mg of the ground composite was heated in aluminum pan, while an empty pan of the same material was used as the reference. They observed a slight reduction and increase in the melting and crystallization temperatures, respectively. It was reported that kenaf fibers acts as a nucleating agent, thereby increasing the crystallization temperature of the composites.

2.8.3 Mechanical Properties

The mechanical properties of NF reinforced polymer matrix composites depend on a number of factors such as volume fraction of the fibers, fiber–matrix adhesion, stress transfer at the interface, and orientation of the fibers [100]. The tensile properties of PMCs depend on the interfacial strength achieved between the fibers and polymer matrix since fibers have much higher strength and stiffness values than those of the matrices [143]. El-Shekeil *et al.* [23] studied the influence of kenaf fiber addition on the tensile and flexural properties of polyurethane thermoplastics according to ASTM D-638 [144] and ASTM 790 [145] standards respectively. They reported that low fiber loading resulted in low tensile strength. This was attributed to inefficient transfer of load from the matrix to the fibers through the interface. Maximum strength of kenaf fiber reinforced polyurethane composite (i.e. 33.5 MPa) was reached with 30 wt.% fiber loading. At high fiber loading of 40 and 50 wt.% there was a decrease in the tensile strength of the composite, due to high agglomeration and ineffective stress transfer. They reported an increase in the Young's modulus of the composites as the fiber content increased. They observed that as the fiber content

in the composite increase, there was a corresponding increase in both the flexural strength and modulus. Li *et al.* [9] studied the influence of flax fiber addition on the mechanical properties of high density polyethylene (HDPE). They reported that flax fiber reinforced HDPE containing 30 wt.% fiber gave the highest flexural strength and modulus, which are 51% and 128% respectively over that of pure HDPE. The tensile strength of HDPE composite containing 5 wt.% fiber increased by 1%, while a 17% increase in the strength was reported for HDPE composite containing 30 wt.% fiber.

2.9 Application of Natural Fiber Reinforced Polymer Matrix Composites

The applications of natural fiber reinforced polymer matrix composites are growing rapidly in many engineering fields. These composites find use in various industrial and structural applications, such as aircraft, automotive, sporting goods, marine, infrastructure, electronics, furniture and building construction industries as shown in Fig 2.2 [92,146].

Natural fiber reinforced polymer matrix composites are used in the production various parts of an automobile [6]. The manufacturing process for making parts to be used in industrial applications requires good finishes, which can be achieved with compression molding. Examples of compression molded automotive parts using natural fiber reinforced polymer matrix composites include, bumper covers, roof frames, door frames, door panels, engine valve covers, dash boards and truck car mats [92].

2.10 Summary

The literature review shows that the use of NFs as a potential substitute to synthetic fibers in reinforcing polymer matrices has increased in recent years due to environmental concerns. This chapter reviewed the chemical, physical, mechanical and thermal properties of NFs as well as the composites. Among the reviews on NFs, there were missing comprehensive study on the chemical composition, spatial distribution and concentration of the chemical compositions, water absorption behaviour and thermal properties of raffia palm fibers. Also, there are no comprehensive studies on the effect of chemical treatments and varying fiber contents on the physical, mechanical and thermal properties of raffia palm fiber reinforced HDPE composites using extrusion and

compression molding techniques. These missing research gaps gave the motivation to fully study the properties of raffia fibers and its use in composite manufacturing.

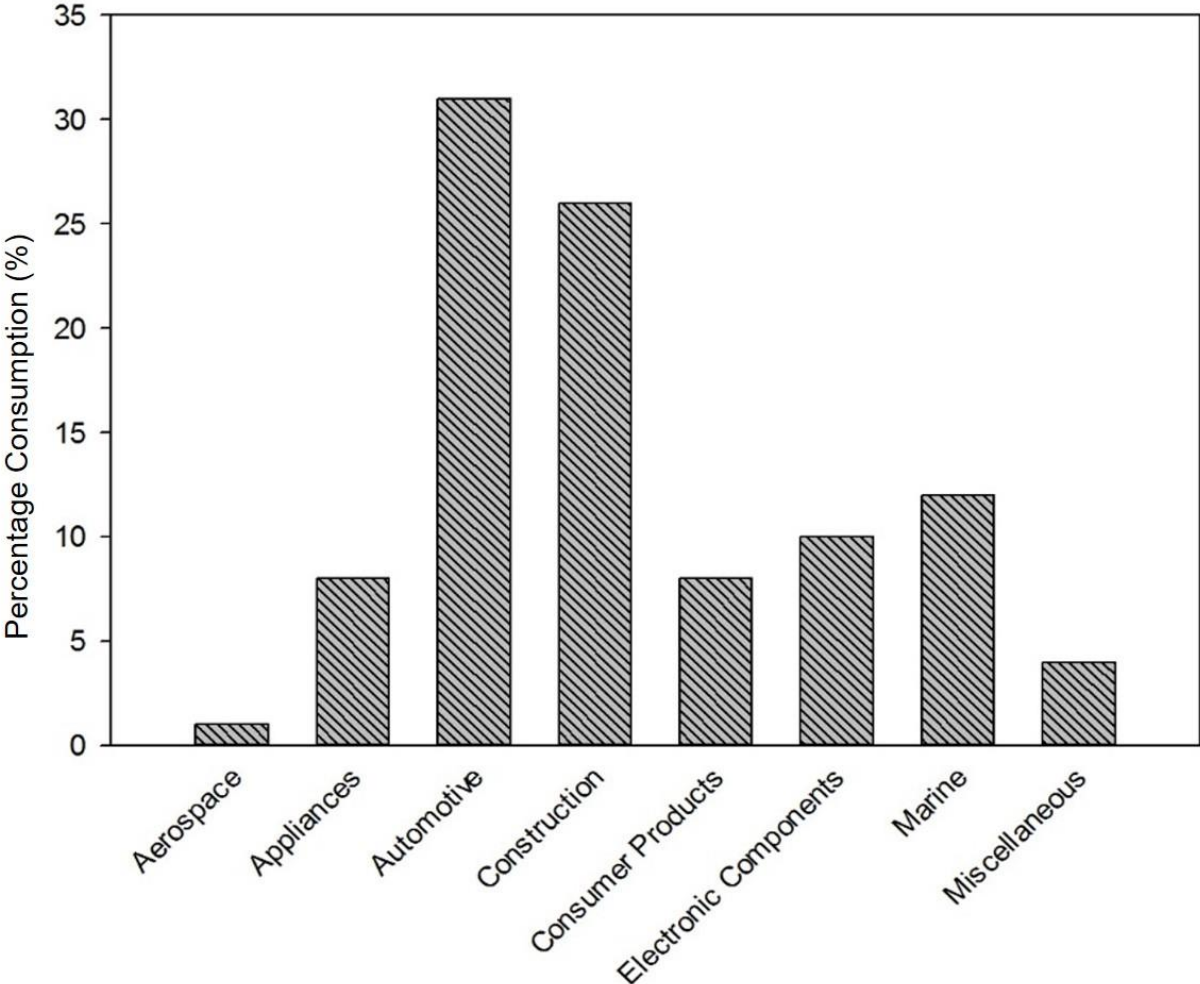


Figure 2.2. Applications of natural fiber reinforced polymer matrix composites [147].

CHAPTER 3

MATERIALS AND EXPERIMENTAL METHODS

This chapter presents and discusses the experimental materials used and procedures followed to achieve the objectives of this research mention in Section 1.2 of Chapter 1.

3.1 Materials

The raw raffia palm fibers (RPFs) used in this study were obtained from southern Nigeria. For ease of processing and characterization, the remnant binders were manually removed, and the resulting raw fibers were subsequently cleaned in 2% detergent to remove oily substances and other impurities on the fiber surface. After cleaning, the fibers were dried in an oven at 70°C for 24 h and subsequently air-cooled to room temperature. Figure 3.1 shows the images of raffia palm fibers before and after cleaning.

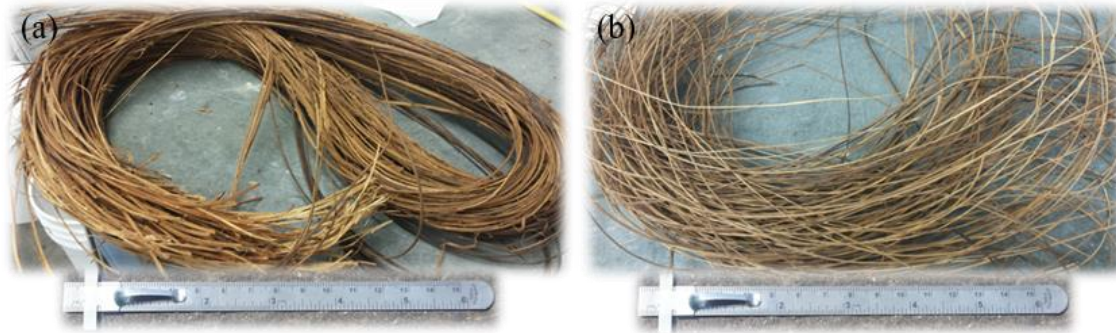


Figure 3.1. Photographs of raffia palm fiber (a) before cleaning and (b) after washing and drying.

The diameter of the cleaned RPFs was determined using a micrometer screw gauge. Twenty-eight fibers were chosen at random and diameter measurements were taken at ten locations along the fiber length. The average diameter obtained was 1.53 ± 0.29 mm. Figure 3.2 shows the flow chart for raffia palm fiber processing, treatment and characterization.

The high-density polyethylene (HDPE) used as the matrix for this study was supplied in powder form by Nova Chemicals Corporation, Calgary, AB. HDPE was selected as the matrix material due to its low melting point, availability, low cost, and ease of processing at temperature below the degradation temperature of natural fibers.

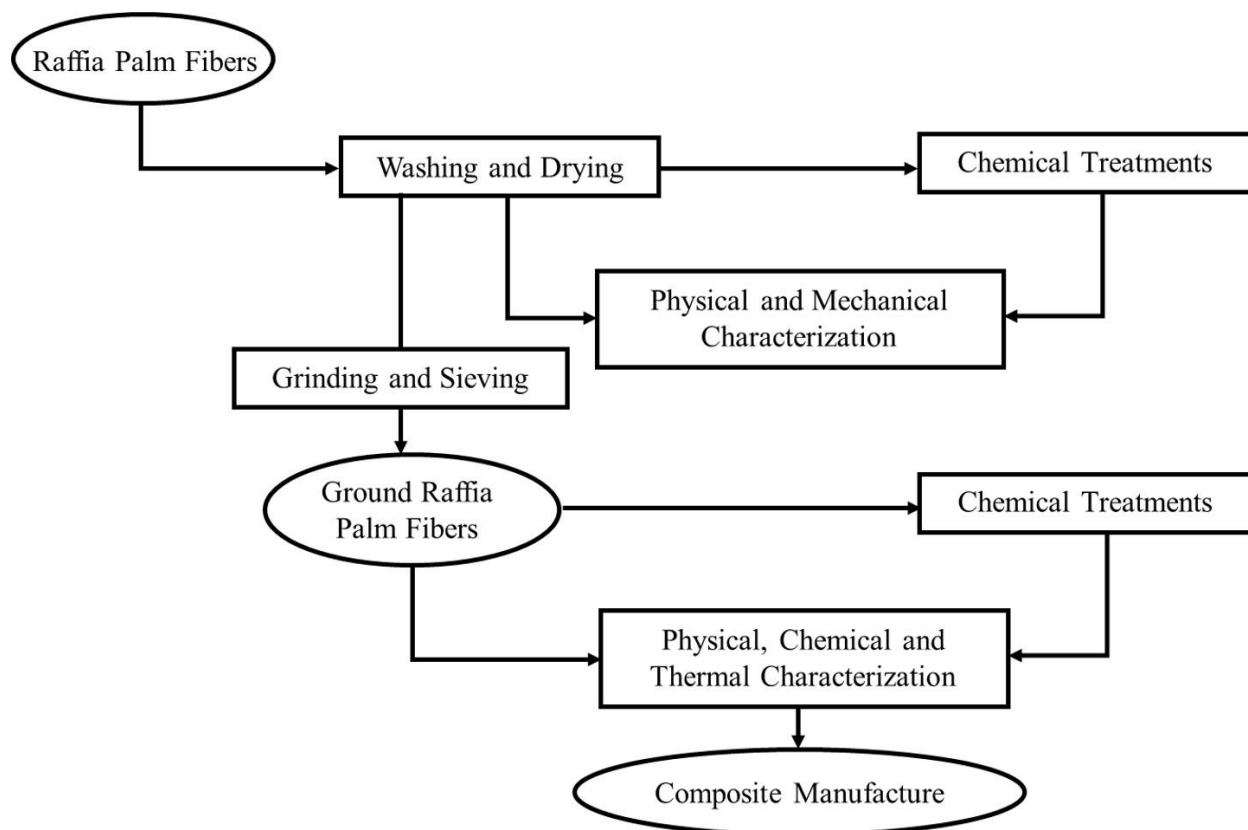


Figure 3.2. Flowchart for raffia palm fiber processing, treatment and characterization.

3.2 Characterization of Raffia Palm Fibers

To fully understand the behavior of RPFs, different physical, thermal, chemical and mechanical tests were carried out. These include diameter measurement, XRD analysis, thermal analysis, chemical analysis, tensile test, moisture adsorption and water absorption measurements.

3.2.1 Length Measurement

The fibers were ground and sieved using a 1.7 mm screen size. After sieving, 26 ground fibers were randomly chosen, and their length measured with an optical microscope interfaced with a PAX-It image analysis software. The average fiber length obtained was 1.63 ± 0.46 mm.

3.2.2 Density Measurement

The particle density (gcm^{-3}) is defined as the dry weight per unit volume of ground RPFs. The mass of the ground RPFs was measured using the weighing scale shown in Fig. 3.3a. The volume of the samples was measured using a nitrogen gas operated pycnometer shown in Fig. 3.3b.



Figure 3.3. Images of (a) weighing instrument for ground raffia palm fibers and (b) gas pycnometer instrument for density measurement.

In operating the gas pycnometer, the volume of the cell and reference gas chambers were calibrated using a solid spherical stainless-steel material. After calibration, ground fibers were placed in a steel cup, which was inserted into the gas pycnometer instrument. The cell and reference gas chambers were set at 0.0000 cm³. The reference gas valve was then turned on, allowing pressure between 16 – 17 psi to build up in the device as recommended by the manufacturer. After the reference gas chamber pressure was recorded, it was switched off. The cell gas valve was switched on, to record its pressure. The volume of the ground RPFs was then calculated using equation 3.1.

$$V_p = V_C - V_R \left(\frac{P_1}{P_2} - 1 \right) \quad 3.1$$

where P_1 = pressure in the reference gas chamber, P_2 = pressure in the cell gas chamber, V_p = volume of ground fibers, V_R = volume of spherical stainless-steel material in the reference chamber (90.53 cm³) and V_C = volume of spherical stainless-steel material in the cell chamber (147.63 cm³).

The fiber particle density was determined from the obtained mass and volume of fiber sample using equation 3.2.

$$\rho_f = \frac{mass}{volume} (gcm^{-3}) \quad 3.2$$

The procedure was repeated twice to ensure consistency in value, and the average value was taken to be the particle density of RPFs. The average particle density obtained was $1.50 \pm 0.01 \text{ g/cm}^3$. This value was found to be consistent with the density data for other vegetable fibers presented in Table 2.2.

3.2.3 Determination of Chemical Composition of RPFs

The chemical composition (cellulose, hemicellulose, and lignin contents) of RPFs before and after treatment was determined by acid digestion using Ankom 200 Fiber AnalyzerTM as shown in Fig. 3.4. The standard acid detergent fiber (ADF), neutral detergent fiber (NDF) and acid detergent lignin (ADL) analysis were carried out using Ankom 200 Method 5, Method 6 and Method 8, respectively. 0.5 g of ground fibers was used for each analysis. The analysis was repeated three times, and the reported value are the averages. The percentages of cellulose, hemicellulose and lignin content were determined from the following equations:

$$\text{Lignin (\% dry matter)} = \text{ADL}$$

$$\text{Cellulose (\% dry matter)} = \text{ADF} - \text{ADL}$$

$$\text{Hemicellulose (\% dry matter)} = \text{NDF} - \text{ADF}$$

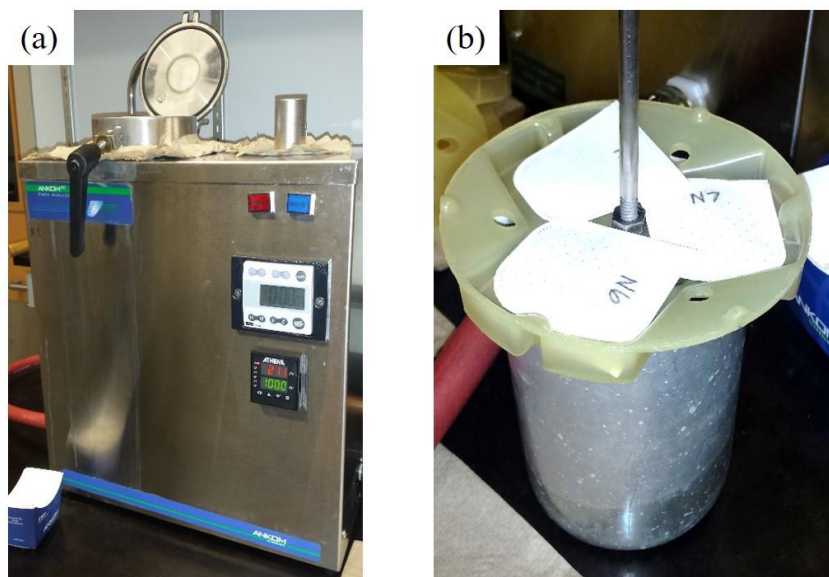


Figure 3.4. Ankom 200 fiber analyzer used for determining the chemical composition of raffia palm fibers.

3.2.4 Sample Preparation for Microscopy

RPFs were cold mounted for polishing using acrylic resin. The cold-mounted samples were pre-ground using 320 (46 μm), 500 (30 μm) and 1200 (15 μm) SiC grit emery papers and finally, fine ground using 2000 (10 μm) and 4000 (5 μm) SiC grit emery papers. Final polishing to obtain very smooth surface finish was done using 1 μm MD-Nap cloth with 1 μm MD-Nap suspension. Microstructural examination of both untreated, alkaline and acid treated fibers was conducted using a Hitachi FE-SEM SU8010 scanning electron microscope. All the samples were first gold coated using an Edwards S150B sputter coater before being examined in the SEM. Images were taken with an accelerating voltage of 3 kV.

3.2.5 Mid Infrared Spectromicroscopy (Mid – IRS)

Synchrotron based Fourier transform infrared spectromicroscopy (SB – FTIRS) has been known to be an extremely valuable analytical tool in determining the spatial distribution of chemical composition of biological and natural samples [148,149]. Thin section of untreated RPFs was prepared through cryogenic sectioning, using Leica CM1950 cryostat machine (Fig. 3.5). The samples were sliced to 8 μm thick and were placed on CaF_2 Polished Disc of 25 mm x 2 mm.

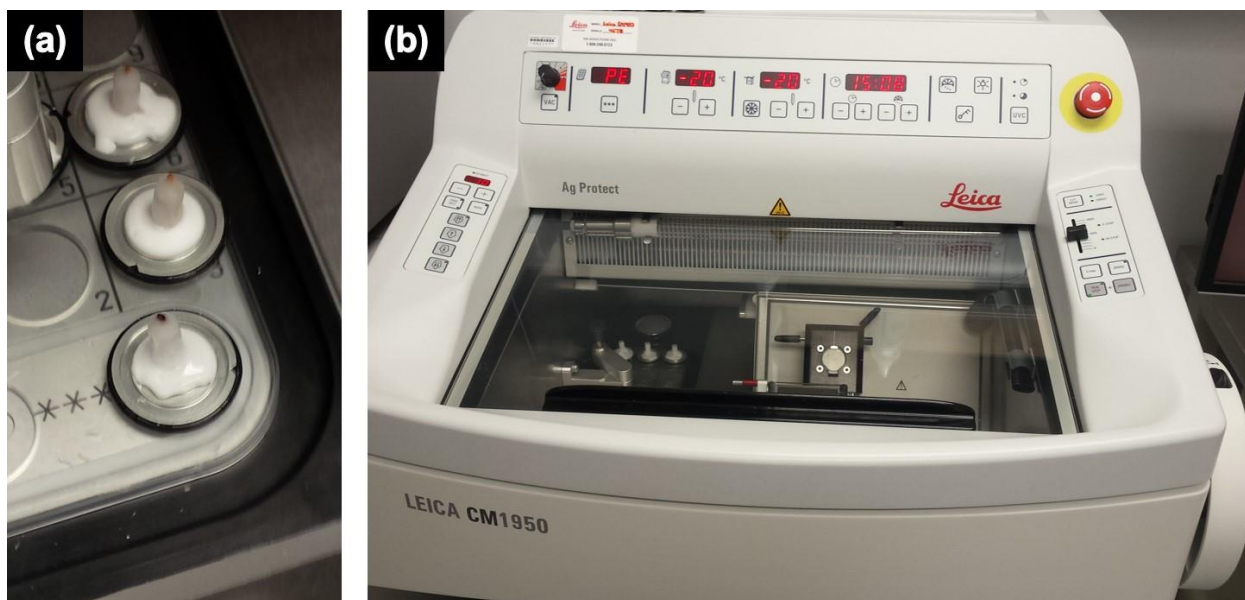


Figure 3.5. Image showing (a) frozen raffia palm fibers in liquid nitrogen and (b) Leica CM1950 cryostat machine.

Images were collected using the Bruker Vertex 70v Interferometer Hyperion 3000 IR Microscope (Fig. 3.6). The synchrotron radiation Fourier transform infrared spectroscopic technique was used with the microscope, equipped with a focal plane array (FPA) detector at the mid-Infrared beamline (01B1-1), Canadian Light Source Saskatoon.



Figure 3.6. Bruker Vertex 70v Interferometer / Hyperion 3000 IR Microscope.

A tile of 170 X 170 μm step size having 4,096 data points was mapped in both the x and y directions of the fiber. A complete IR spectrum was collected at each spot ($400\text{-}4000\text{ cm}^{-1}$) with a resolution of 4 cm^{-1} in transmission mode. For the background spectrum, 128 scans were collected and averaged. At each sampling point, 256 scans were collected and averaged. The data collected were analyzed using OPUS software (Bruker, Version 7.0).

3.2.6 Tensile Test

The tensile properties of cleaned fibers were determined according to ASTM D3822-14 standard [150] using a 5 kN capacity Instron™ Universal testing machine (model 3366) at a crosshead speed of 1 mm/min and using fiber length of 45 mm. The tensile test was conducted at ambient temperature of 27°C and relative humidity of 35%. The diameters and cross-sectional area of each fiber used in the test were measured and recorded. The fibers were mounted individually into the grips of the tensile testing machine with the help of brown tissue papers. The cellophane tape was used to fasten the tissue paper to the fibers to prevent slippage and fracture of the fiber in the grips. The fiber lengths were measured from one end of the tensile grip to the other as shown in Fig. 3.7.

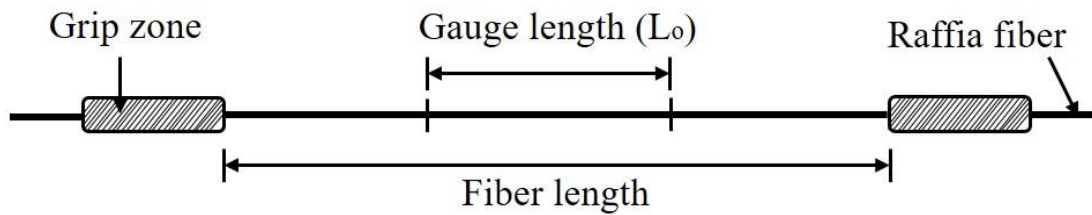


Figure 3.7. Picture showing schematic drawing of a single raffia palm fiber prepared for tensile test.

To study the effect of fiber length on the tensile properties of RPF, five different fiber lengths (45, 70, 95, 120 and 145 mm) were used. Ten RPFs were tested at each length with a gauge length of 25 mm. The effect of fiber length on the percent elongation was also investigated. In this test, a fixed gauge length of 25 mm was used while the fiber length varied. Seven different fiber lengths (45, 50, 55, 60, 65, 70, and 75 mm) were evaluated. Five fibers were tested at each length. Furthermore, the effect of cross head speed on mechanical properties of RPF was investigated. Four cross head speeds (0.5, 1.0, 1.5 and 2.0 mm/min) were used while the fiber length was fixed at 50 mm. For each test speed, ten RPFs were tested and the reported data are averages of the tests.

3.2.7 Statistical Analysis

Statistical analysis was performed using analysis of variance (ANOVA) with the aid of SigmaPlot 13. ANOVA was used with a level of significance of 0.05, which is a confidence level of 95%. ANOVA was done to determine if statistically significant differences exists between breaking strength of fibers for different fiber lengths. ANOVA was also used to determine if the breaking strength of the fibers is significantly influenced by strain rate.

3.2.8 Moisture Adsorption of RPFs

The objective of this test was to determine the moisture adsorption capability of dry RPFs on exposure to a humid environment. The pieces of equipment used in this test included an oven, a weighing and a desiccator. Five samples of 0.50 g each were used. The fibers were dried in the oven at 70°C over 60 hours. At different time intervals, the fibers were taken out of the furnace and weighed to assess if they were fully dried. To avoid moisture adsorption after drying, the fibers were kept in a desiccator before being placed in a 1200 mini humidity generator (Fig. 3.8), manufactured by thunder scientific corporation, Albuquerque, NM, USA. The setup parameters used for humidity measurement are shown in Table 3.1. The parameters were set based on the manual of operation to simulate a real-life scenario.

Table 3.1. Humidity generator setup parameters.

	Set Point	Actual Point	+/-
% Relative Humidity @ P _c T _c (%)	50.00	50.01	0.30
Saturation Pressure (PsiA)	27.68	27.67	0.05
Chamber Pressure (PsiA)		13.88	0.05
Saturation Temperature (°C)	23.00	23.00	0.05
Chamber Temperature (°C)		23.09	0.05
Mass Flow Rate (L/min)	10.00	10.00	

After fully drying the samples (i.e., there was no further change in mass no matter how long they were kept in the oven), they were placed in humidity generator which was set at 50% relative humidity. Sample weight readings were taken at different time intervals (5, 10, 26, 34, 46, 58, 70, 82, 106, 130 and 142 h). The moisture content of the fibers (in %) was computed using equation 3.3:

$$M_t (\text{wt.}\%) = \frac{W_t - W_o}{W_o} \times 100 \quad 3.3$$

where W_o and W_t denote the dry weight of raffia fibers and weight of the fibers after a specific time t , respectively.



Figure 3.8. Humidity generator used for moisture absorption measurement.

3.2.9 Water Absorption of RPFs

The objective of this test was to determine the water absorption capability of dry raffia fibers when immersed in water. The apparatus and material used in this test included an oven, and a weighing balance. Five samples of 0.50 g each were used in this experiment. The fibers were dried for up to 60 hours in an oven maintained at 70°C. After drying and the final weight noted, the fibers were immersed in distilled water at room temperature. The fibers were removed from the water bath at different times, the surface water was cleaned and weighed immediately. The weight was recorded as a function of time until saturation was reached. The water content of the fibers (in wt.%) was computed using equation 3.3.

3.2.10 X-ray Diffraction (XRD)

X-ray diffraction measurement of RPFs was carried out using a PANalytical Empyrean X-ray diffractometer with a Co target, rotating stage and goniometer in 2θ configuration (manufactured by PANalytical Inc. Westborough MA, United States). The wavelength of Co radiation is 0.179 nm. The generator was utilized at 40 kV and 45 mA. The intensities were measured from 5° to 110° at 2θ with step size of 0.0167° and a scan speed of 0.015 deg/sec. The radiation used was full spectrum Co ($K_{\alpha 1}$, $K_{\alpha 2}$) with the K_{β} filtered out with a diffracted side Fe filter. The results were analyzed using PANalytical X'Pert HighScore software. The empirical equation 3.4, proposed by

Sarikanat *et al.* [151,152], was used to estimate the degree of crystallinity (crystallinity index, *CI*) of ground RPF from the XRD results.

$$CI(\%) = \frac{I_{002} - I_{am}}{I_{002}} \times 100 \quad 3.4$$

where I_{002} corresponds to the (002) lattice reflection peak (the maximum intensity) at an angle of 2θ , around 22° . I_{am} corresponds to height of the minimum peak position between 002 and the 110 peaks and is attributed to the amorphous fraction (minimum intensity), located at about 18° .

3.2.11 Chemical Treatment of RPFs

Good raffia fiber-matrix adhesion is necessary for transfer of load from the matrix to the reinforcement at the interface. Poor adhesion will lead to debonding as load is transferred from the matrix to the fiber resulting in poor mechanical properties. To improve RPF-matrix adhesion, two chemical treatments were carried out to alter their surface chemistry: alkaline (NaOH) and acidic (H_2SO_4) treatments.

Two aqueous solutions of NaOH with different concentrations (5% and 10% by weight) were prepared by dissolving sodium hydroxide pellets in distilled water. These concentrations were chosen to preserve the cellulose part of the fiber [41]. Ground RPFs were immersed in the 5% w/v and 10% w/v aqueous NaOH solution at room temperature (RT) for different lengths of time (5 h, 10 h and 20 h) with a solution-to-fiber ratio of 10 ml to 1 g [153]. Similarly, ground RPFs was immersed in 10% w/v aqueous NaOH solution at $60^\circ C$ for 5 h, with a solution to fiber ratio of 10 ml to 1 g. Fig. 3.9 shows a typical image of the sodium hydroxide solution before and after chemical treatments of ground RPFs.

After the immersion, the fibers were initially washed in laboratory water and finally in distilled water to ensure that no NaOH was left. Subsequently, the fibers were dried at $60^\circ C$ for 24 h. Similarly, two different aqueous solutions of H_2SO_4 with different concentrations were prepared (0.3 and 0.6 molar) by diluting 99.9% pure sulphuric acid with distilled water. Ground RPFs were immersed separately in the two solutions at $100^\circ C$ for 2 h, with a solution to fiber ratio of 10 ml to 1 g. Fig. 3.10 shows a typical image of the sulphuric acid solution before and after chemical

treatments of ground RPFs. After the immersion, the fibers were washed in laboratory water and then in distilled water. Subsequently, they were dried at 60°C for 24 h.

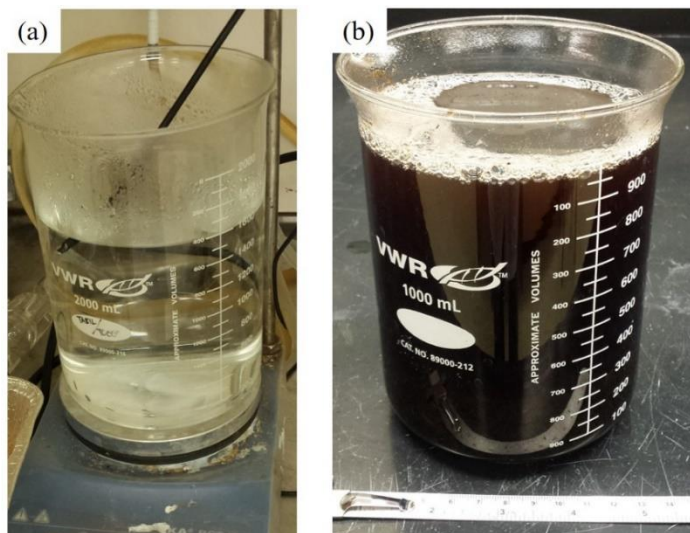


Figure 3.9. Images of sodium hydroxide solution (a) before treatment and (b) after treatment.

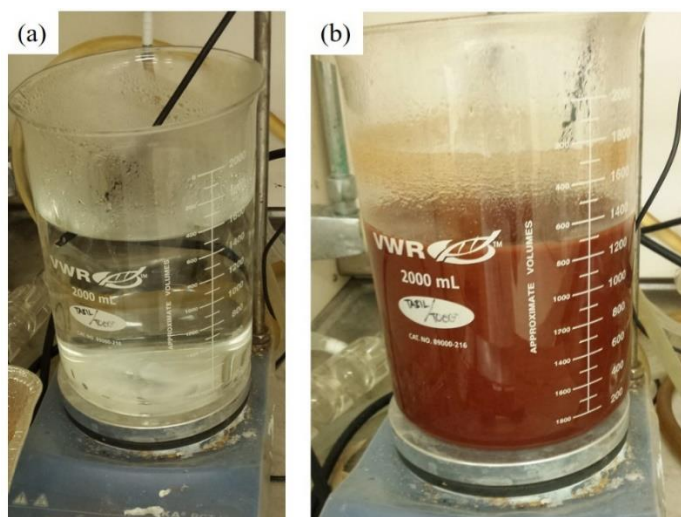


Figure 3.10. Images of sulfuric acid solution (a) before treatment and (b) after treatment.

3.2.12 Colour Measurement

A physical change accompanying the chemical treatments of RPFs is the colour. Therefore, after alkaline and acidic treatments of RPFs, colour measurements were carried out to ascertain the variation in colour between non-treated and treated RPFs. A HunterLab™ spectrophotometer (Fig. 3.11) with a port size of 30 mm in diameter was used for the measurement. Approximately 2 g of

fibers was used to determine the Hunter L^* , a^* , and b^* coordinates. The value of L^* coordinate represents the whiteness component (0 = black, and 100 = white); the a^* coordinate represents greenness to redness ($-a^*$ = green, and $+a^*$ = red); and b^* coordinate represents blueness to yellowness ($-b^*$ = blue, and $+b^*$ = yellow).



Figure 3.11. HunterLab spectrocolorimeter used for colour measurements.

Thus, an increase in L^* , a^* , and b^* denotes more white, red and yellow colours, respectively. The variation of colour (ΔE) was estimated in comparison to the raw fiber using equation 3.5 [48].

$$\Delta E = \left[(L_t^* - L^*)^2 + (a_t^* - a^*)^2 + (b_t^* - b^*)^2 \right]^{0.5} \quad 3.5$$

where the coordinates with subscript t are for treated RPFs, while those without subscripts are for untreated RPFs. The whiteness (L^*) and chromacity coordinates (a^* and b^*) for each sample were measured in 10 replicates and the average values of the results are presented.

3.2.13 Differential Scanning Calorimetry (DSC)

Thermal analysis of NFs yield information about their thermal stability [63]. Thermal analysis study was carried out using a 2910 V4.4E (TA instruments, USA) modulated differential scanning calorimeter (MDSC). Each scan was performed in an open aluminum pan under argon gas from room temperature to 390°C at a heating rate of 5 °C/min. Approximately 10 mg of ground RPFs was used.

3.2.14 FTIR and Raman Spectroscopy

Fourier transform infra-red (FTIR) and Raman spectroscopic techniques were used to determine chemical changes associated with chemical treatment of RPFs. These techniques provide complementary information on the chemical changes associated with chemical treatment of RPF [154,155]. The major difference between the two techniques is that, FTIR relies on absorbance or transmittance of infrared light on the sample, while a monochromatic scattered light of high intensity on the sample can be used i.e. UV, visible or IR are used in Raman [154]. Also, weak bands in IR spectra corresponds to strong bands in Raman and vice versa [155,156]. The study was carried out using a Renishaw Raman inVia Reflex Microscope (Fig. 3.12). In the macroscopic mode, a sample area of 100 μm diameter was examined using a low laser power of approximately 50 mW to minimize sample degradation. Raman spectra were recorded over the range of 3500–200 cm^{-1} at a scan rate of 32 cm^{-1} . The microscope has a Smith's IlluminantIR IITM accessory that allows Fourier transform Infrared spectroscopy (FTIRS) spectra to be acquired using an all reflective objective (ARO) and a diamond attenuated total reflection (ATR) objective. The mercuric cadmium telluride (MCT) detector on the IlluminantIR IITM spectrometer was cooled with liquid nitrogen. The spectra were obtained with an accumulation of 512 scans with a resolution of 4 cm^{-1} .



Figure 3.12. Renishaw Raman inVia Reflex microscope.

3.3 Manufacture of Raffia Palm Fiber Reinforced High Density Polyethylene Composites

Figure 3.13 shows the flow chart for raffia palm fibers reinforced high density polyethylene processing and characterization. Prior to use in composites manufacture, the fibers were dried at 60°C for 24 h to eliminate moisture. After drying, 5%, 10%, 20%, and 30% by mass of untreated, alkaline and acidic treated RPFs were mixed with HDPE. Figure 3.14 illustrates the processing chart used.

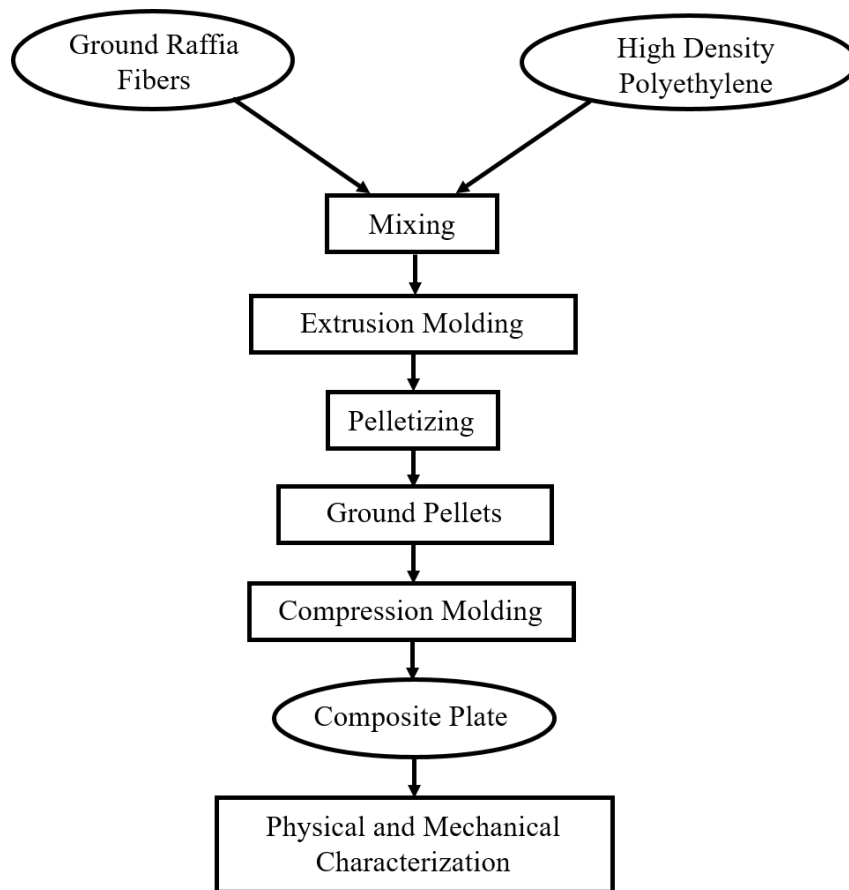


Figure 3.13. Flowchart for raffia palm fiber reinforced high density polyethylene composite processing and characterization.

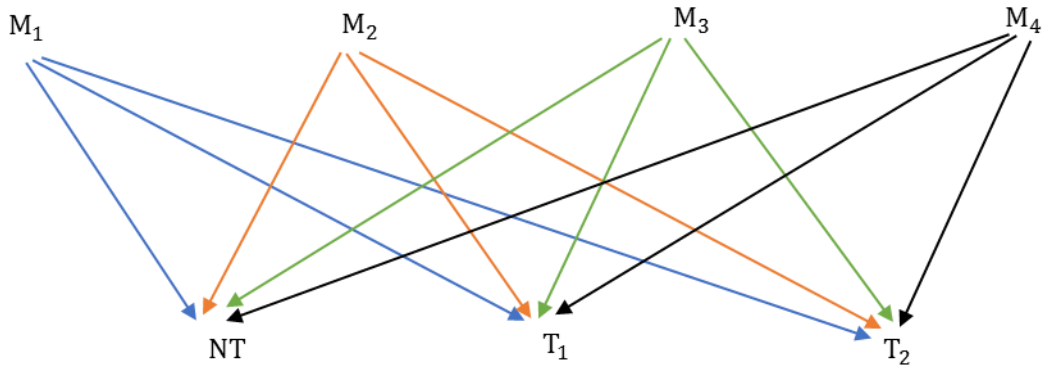


Figure 3.14. Processing chart showing the mixing of untreated, alkaline and acidic treated raffia palm fibers with high density polyethylene to make raffia palm fiber reinforced high density polyethylene composites. $M_1 = 5$ wt.%, $M_2 = 10$ wt.%, $M_3 = 20$ wt.%, $M_4 = 30$ wt.% of fiber, NT = no treatment of the fiber, T_1 = treatment with 10% w/v aqueous NaOH solution at 60°C for 5 h, T_2 = treatment with 0.6 M H_2SO_4 solution at 100°C for 2 h.

3.3.1 Extrusion Machine and Process of Mixture

After mixing the ground fibers with the polymer, the blend was fed into a parallel twin-screw extruder (model SHJ-35) machine shown in Fig. 3.15, where uniformly mixed extrudates measuring 2 mm in diameter and length of 50 to 100 m were produced.

The processing parameters used were: motor current = 6.5 A, melt pressure = 0.1 MPa, screw speed = 319 rpm and feeder speed = 22 rpm. The extrusion screw inside the barrel zone conveyed the material into the heated zones, where melting, mixing, and pushing of the polymer/fiber mixture take place from zone 1 to zone 10. The barrel zone temperature was varied in the following sequential order 145–150–155–160–165–170–170–170–170–175°C. The molten mixture was forced through a long needle-shaped die and solidified by subsequent cooling in a water bath (see Fig. 3.16a). After each composite formulation was extruded, pure HDPE polymer was used to clean the extrusion machine barrel before extruding the next composite formulation. The resulting cooled extrudates were pelletized into small cylindrical pellets using a cooling strand pelletizer (model LQ-60) shown in Fig. 3.16b.

After pelletizing, the pellets were oven-dried at 70°C for 48 h to eliminate any moisture remaining. They were subsequently ground using a Retsch knife grinding mill (SM 2000) with a sieve size of 4 mm. A photograph of the Retsch knife grinding mill used in this study is presented in Fig. 3.17.



Figure 3.15. Twin-screw extrusion machine used for producing extrudates required for composites manufacture.

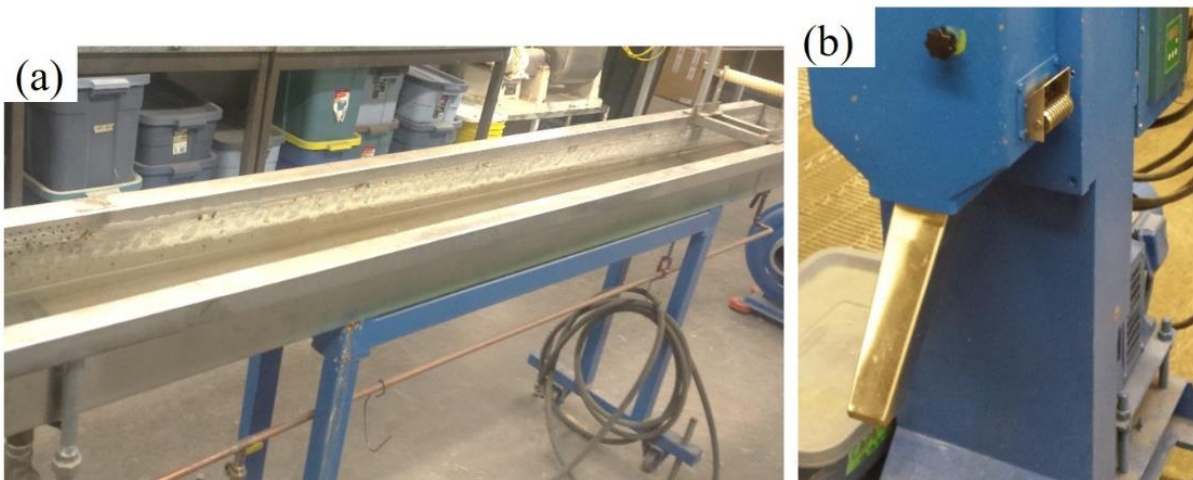


Figure 3.16. Images of (a) water bath and (b) cooling strand pelletizer.



Figure 3.17. Retsch knife grinding mill.

3.3.2 Compression Molding Equipment and Process

Compression molding technique was used in forming the ground extruded pellets into composite plates of predetermined thickness. The mold was coated with mold release agents for easy removal of the composite plate from the mold (Fig. 3.18) and then preheated.

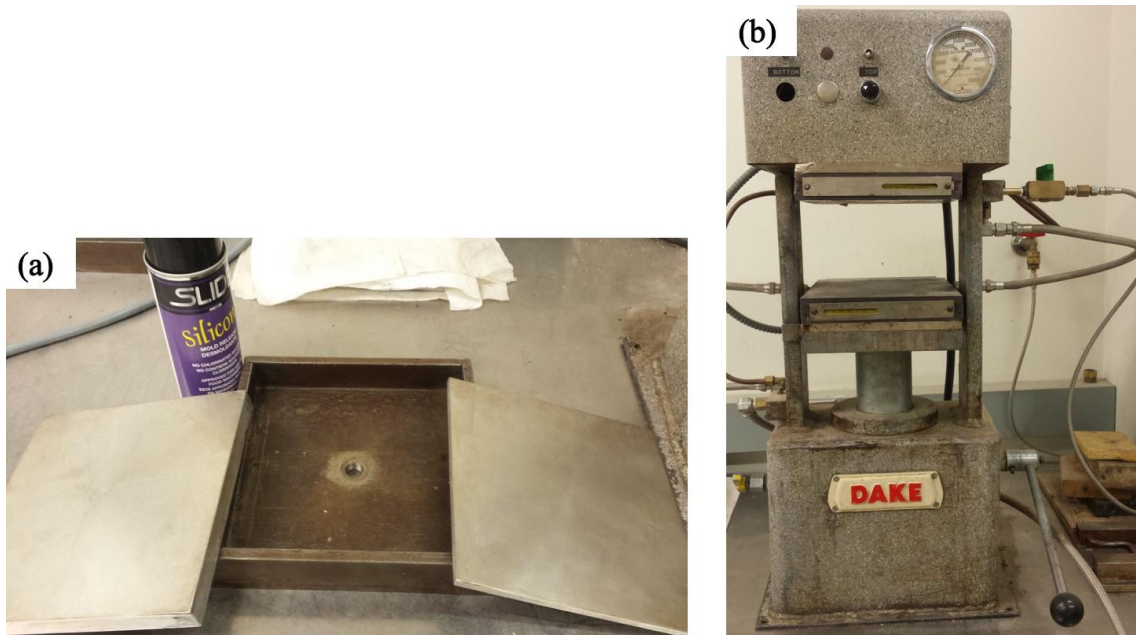


Figure 3.18. Images of the (a) mold, mold releasing agent and molding plates and (b) compression molding machine.

Composite plates of dimensions 200 mm × 200 mm × 3.2 mm were prepared by preheating 130 g of ground extruded composites pellets for 10 min at 170°C under an applied pressure of 2.0 MPa to ensure the melted material assume the shape of the mold cavity. The applied pressure was subsequently increased to 6.5 MPa while keeping the temperature constant for 5 min to eliminate any void in the composite plates before solidification. Finally, the machine was switched off while the water gauge was switched on for cooling while keeping the pressure constant at 6.5 MPa for 25 min to ensure dimensional stability. The test specimens for, tensile, flexural and density tests were cut from the molded composite plates according to the relevant testing standard. To achieve the desired thickness for the Charpy impact test, 300 g of ground pellets was compressed.

Figure 3.19 shows the image of compressed plate made using extruded pellets, while Fig. 3.20 shows the image of compressed plate with the use of ground extruded pellets. The presence of pores was observed in compressed plate with the use of extruded pellets, which were significantly reduced when ground extruded pellets were used in compression. Since the porosity of composites made from unground pellets plates were high, all compression molded plates used for making specimens of RPF reinforced HDPE composites for further testing were made using ground pellets.

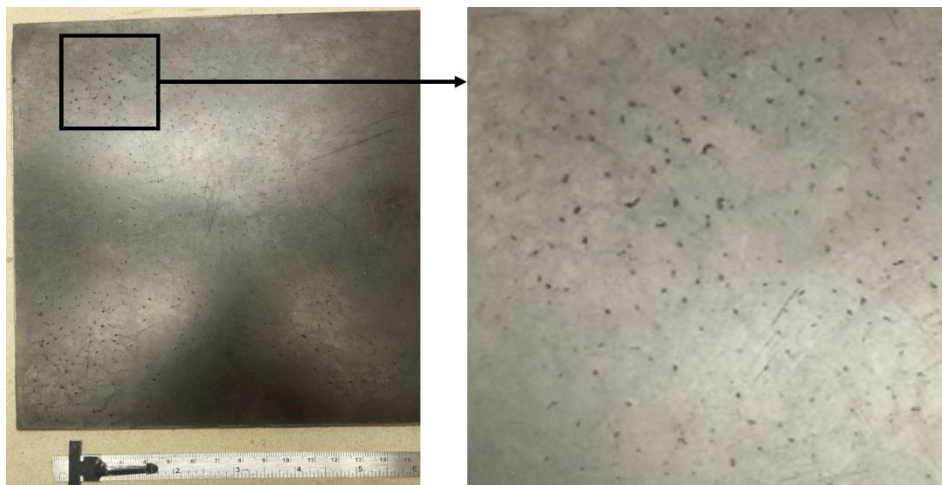


Figure 3.19. Images of composites plates from extruded pellets showing surface porosity.

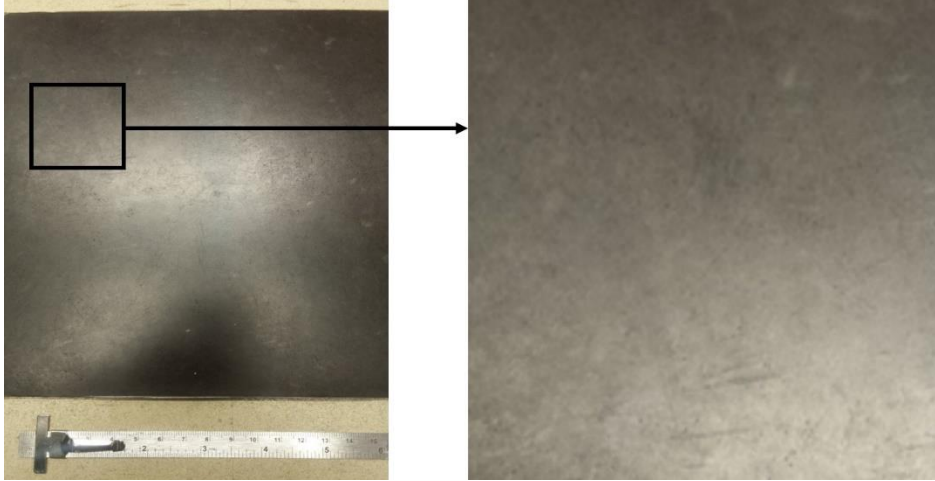


Figure 3.20. Images of composites plates from ground extruded pellets (no surface porosity).

3.4 Characterization of RPF Reinforced HDPE Composites

The mechanical and physical properties of the RPFs reinforced HDPE matrix composites developed in this study were determined by conducting several tests. Microstructure of fractured surfaces of specimens after mechanical testing was examined using scanning electron microscopes.

3.4.1 Density Measurement

Samples measuring 12.5 mm × 12.5 mm × 3.2 mm were used for density measurement. Figure 3.21 shows the apparatus used. The specimens were weighed first in air (M_1) and reweighed while immersed in a liquid (ethanol) of known density (M_2). The density of the specimen was calculated using equation 3.6:

$$\rho_c = \frac{M_1}{M_1 - M_2} \times \rho_l \quad 3.6$$

where ρ_c and ρ_l are the densities of the specimen and liquid, respectively. The density of ethanol is 0.789 g/cm³.

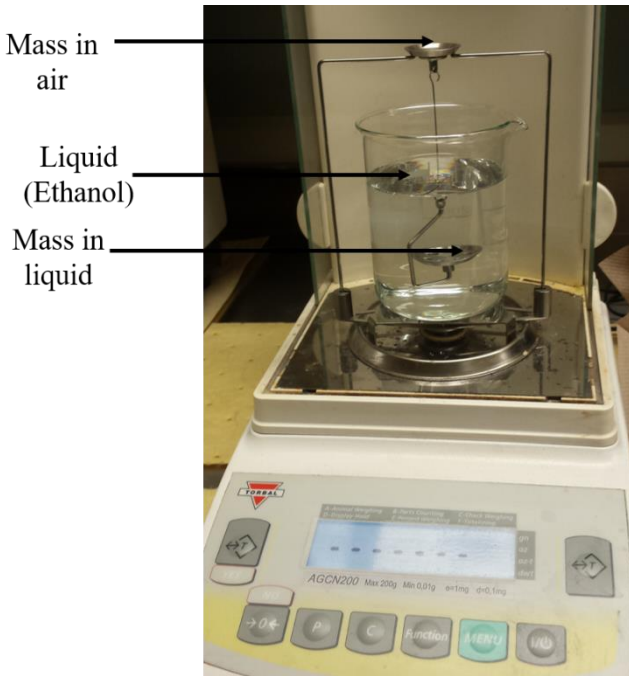


Figure 3.21. Apparatus used for measuring densities of compression molded composites and high-density polyethylene.

3.4.2 Tensile Test of Composites

Tensile test was conducted using a Instron™ (model 5500R) machine according to ASTM D638 standard [144]. The test was conducted at ambient temperature (23°C) and 20% relative humidity. The test specimens were cut into dog-bone shape of dimension 150 mm × 20 mm × 3.2 mm using a hydraulic cutter. Fig. 3.22 shows typical tensile test specimens. Five specimens were tested for each composite formulation with a load cell of 5 kN and crosshead speed of 5 mm/min. An extensometer with a 50-mm gauge length was attached to the test specimens as shown in Fig 3.23 to obtain stress-strain measurements for Young's modulus determination.

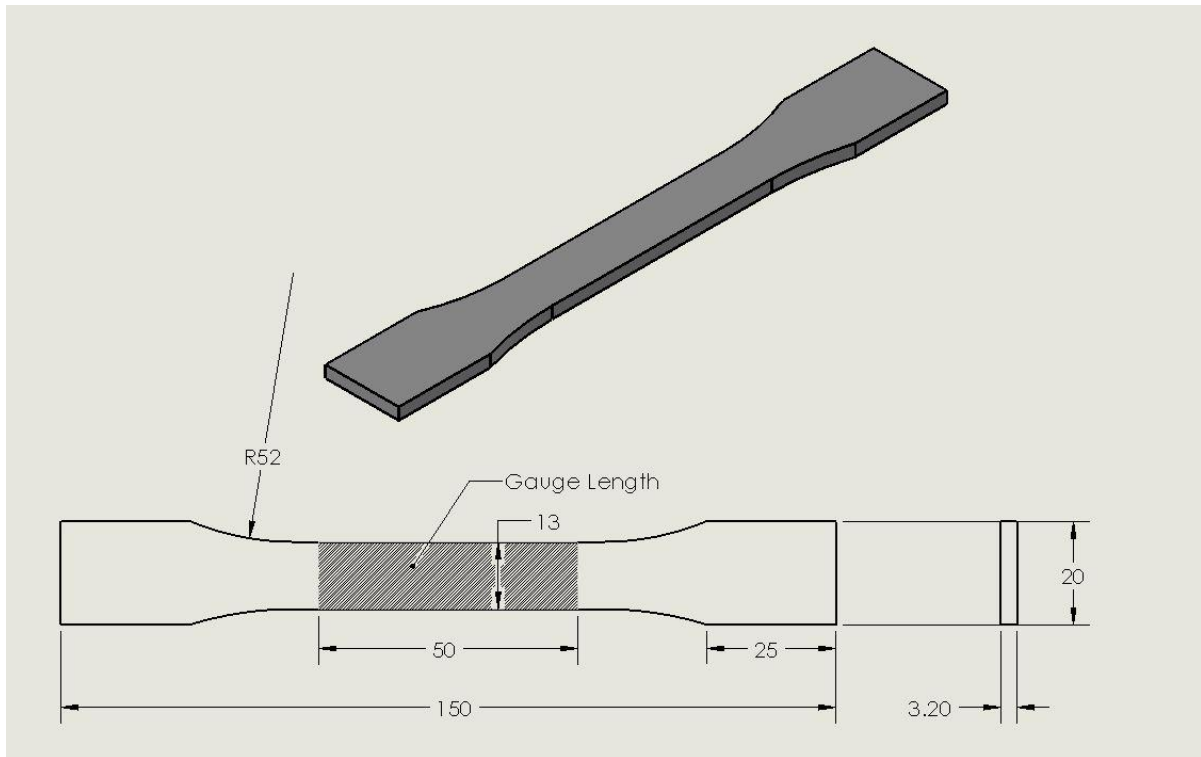


Figure 3.22. Dog-bone shaped specimens for tensile test.



Figure 3.23. Instron™ tensile machine equipped with a clip-on extensometer for determining Young's modulus of test specimens.

3.4.3 Flexural Test of Composites

Three-point bending test was performed using an Instron™ (model 5500R) machine (Fig. 3.24) according to ASTM D790-15 standard [145]. Samples measuring 127 mm × 12.7 mm × 3.2 mm were tested at a crosshead speed of 4 mm/min, which was determined using equation 3.7 [145].

$$R = \frac{ZL^2}{6d} \quad 3.7$$

where Z which is a constant, is the rate of straining of the outer fiber (0.01 mm/min), while L and d are the support span (87 mm) and the thickness of the sample (3.2 mm), respectively.

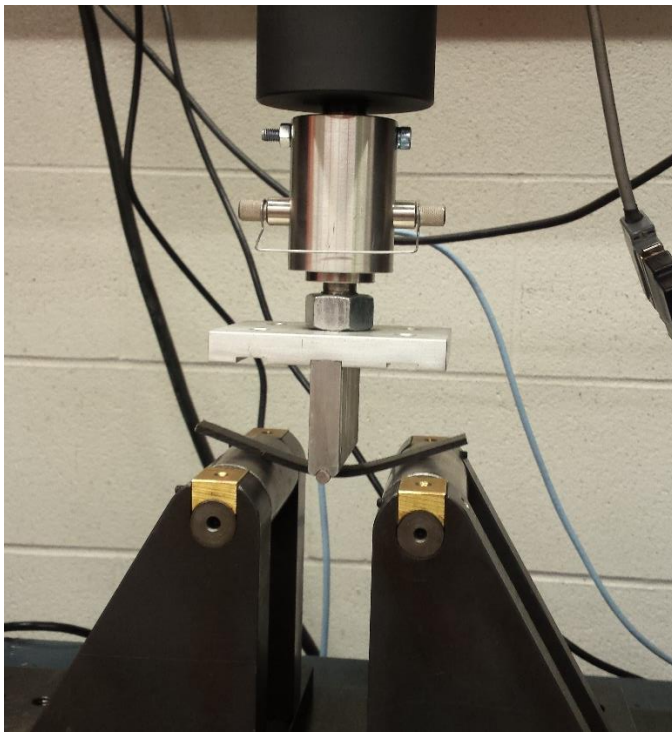


Figure 3.24. A picture showing a typical flexural test on a sample of 10% composites.

The flexural stress was calculated using equation 3.8, which is used when the support span-to-depth ratios is greater than 16 [145].

$$\sigma_f = \left[\frac{3PL}{2bd^2} \right] \left[1 + 6 \left(\frac{D}{L} \right)^2 - 4 \left(\frac{d}{L} \right) \left(\frac{D}{L} \right) \right] \quad 3.8$$

where σ_f , P , b , and D are the stress in the outer fiber at midpoint (MPa), the load at given point on the load-deflection curve (N), the width of the beam tested (12.7 mm), and the maximum deflection (mm), respectively.

The flexural modulus was calculated using equation 3.9 [145]:

$$E_f = \frac{L^3 m}{4bd^3} \quad 3.9$$

where E_f , and m are the flexural modulus and the slope of the initial straight-line portion of the load-deflection curve, respectively. Five samples were tested for the matrix material and each formulation of the composite materials. Therefore, the bending test results presented in this thesis are the averages obtained for the ten tests.

3.4.4 Charpy Impact Test of Composites

Toughness of a polymeric materials can be determined by measuring the impact properties of such material. The higher the impact energy of the material, the higher the toughness. Charpy impact test was performed using an Instron impact tester (Fig. 3.25) on both unreinforced HDPE and RPFs reinforced HDPE. The tests were carried out according to ASTM D 6110-10 standard [157].

Test samples measuring 55 mm (length) x 7.5 mm (thickness) x 10 mm (width) were notched using a broaching machine as shown in Fig. 3.26. Figure 3.27 shows the dimension of the charpy test samples with a notched depth, radius and angle of 1.75 mm, 0.25 mm and 22.5° respectively. Five specimens tested for each composite formulation were conditioned in a chiller to attain 0°C, -20°C and -40°C respectively. The energy absorbed per unit area (E_i) was calculated using equation 3.10 [158] and the reported energy absorbed per unit area (E_i) are the average values.

$$E_i = \frac{E_a}{b \times d} \quad 3.10$$

where E_a , b and d are the energy absorbed, width and thickness of each sample were measured and recorded, respectively.



Figure 3.25. Charpy impact testing machine used in this study.



Figure 3.26. Broaching machine used in notching the charpy impact samples.

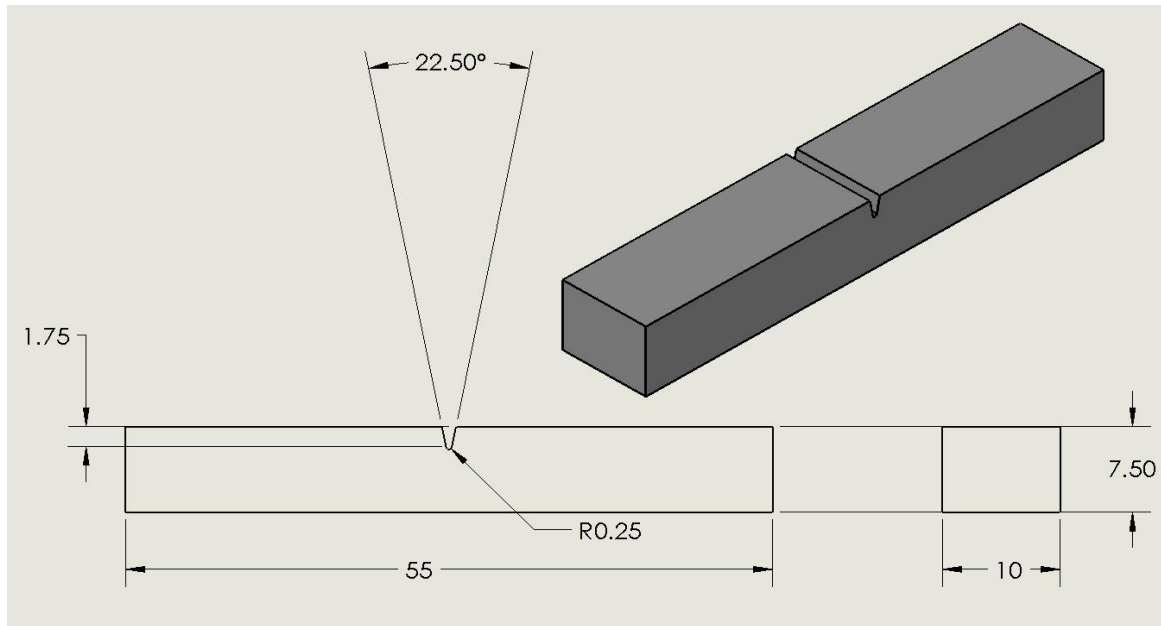


Figure 3.27. Charpy impact test samples.

3.4.5 Water Absorption

The water absorption behaviour of the composites was determined by immersing samples measuring 28 mm (length) x 7.5 mm (thickness) x 10 mm (width) in distilled water at room temperature. Three samples per composite formulations were used (see Fig. 3.28). The samples were weighed before immersing in distilled water at room temperature following ASTM D570-98 standard [137]. At a regular time, interval (every 24 h), the samples were removed, and the surface moisture was wiped, and then weighed. This process was repeated until the samples reached their saturation limit. The percentage water absorbed was determined using equation 3.3.

3.4.6 Thermal Analysis

Thermal analysis (melting and crystallization temperature) of RPF reinforced polymer composites was carried out using Q20 V4.5A (TA instruments, USA) differential scanning calorimeter (DSC). Each scan was performed in an aluminum pan under argon gas from room temperature to 250°C at a heating rate of 10°C/min. Approximately 7.5 mg of ground composites was used for each composite formulation.

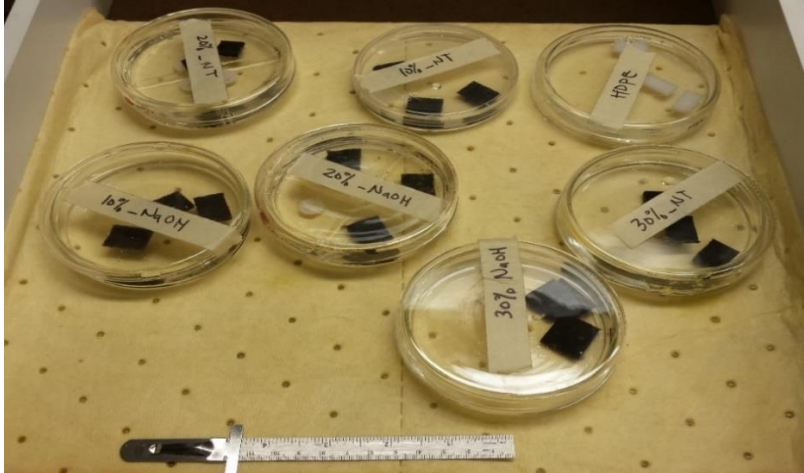


Figure 3.28. Water absorption tests on composites.

3.4.7 Microscopic Investigations of Composites

Microstructural evaluation of fractured test samples was conducted using a Hitachi FE-SEM SU8010 scanning electron microscope (Fig 3.29). The samples were first gold coated using an Edwards S150B sputter coater before being examined with the SEM. An accelerating voltage of 3 kV was used.

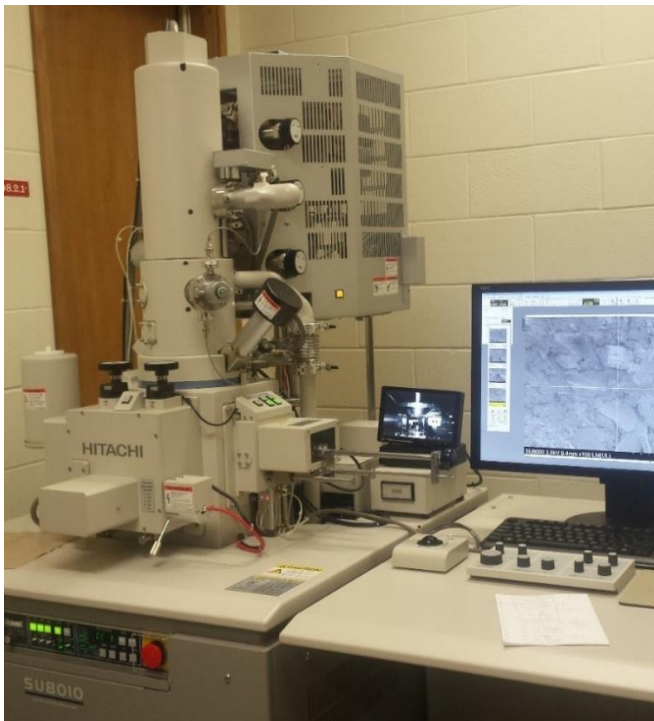


Figure 3.29. A photograph of the scanning electron microscope used for microstructural investigations.

CHAPTER 4

RESULTS AND DISCUSSION

The results obtained from the experimental investigations in Chapter 3 are presented and discussed in this chapter. It contains two major sections, the first of which focuses on characterization of raffia fibers. The second section contains results of characterization of the composites developed using raffia palm fibers and HDPE.

4.1 Characterization of Raffia Palm Fiber (RPF)

Characterization of RPF include the determination of its chemical composition, mechanical and thermal properties, crystallinity, water and moisture absorption behaviour, among others.

4.1.1 Chemical Composition of RPF

The results of compositional analysis in the “as-received” basis of RPF before and after chemical treatment with varying concentrations of NaOH and H₂SO₄ is presented in Table 4.1. Table 4.2 shows the results of chemical composition of RPF in the “dry matter” basis. The “dry matter” basis indicates the composition levels in a sample based on its dry matter content, excluding the presence of moisture. Hence, it eliminates the dilution effect of the water, thereby providing the essential common basis for a direct comparison of the chemical composition contents of NFs. The dry matter basis (DMB) chemical composition was calculated from the as-received using equation 4.1 [159].

$$DMB (\%) = \left[\frac{As - received\ content (\%)}{100\% - \% moisture} \right] \times 100 \quad 4.1$$

An increase (average value of $19 \pm 3\%$) in the cellulose content was recorded after NaOH treatment. However, only a slight change (average value of $4 \pm 8\%$) in the hemi-cellulose content in relation to non-treated RPFs was recorded. The cellulose content of the fiber is very important because it provides strength and stability. Mechanical properties of NFs depend on it [24,88,98]. Of all NaOH treated fibers, it was observed that the fibers treated with 10% NaOH solution at 60°C for 5 h exhibit the highest cellulose content. Therefore, this formulation was used in modifying the surface chemistry of RPFs for composite fabrication.

H₂SO₄ treatment resulted in a 27 ± 2 % increase in the cellulose content while the hemi-cellulose content reduced by 81 ± 13 %. For acid treatment, RPF exposure to 0.6 M H₂SO₄ solution at 100°C for 2 h was selected for use in modifying the surface chemistry of RPFs because it yields a higher cellulose content.

Table 4.1. Chemical composition (as received basis) of raffia palm fibers.

Fiber	Soaking time (h)	Cellulose (wt. %)	Hemicellulose (wt. %)	Lignin (wt. %)	Others (wt. %)	Dry Matter (wt. %)	Moisture (wt. %)
Untreated fiber	0	50.1	11.7	22.3	15.8	93.9	6.1
5% NaOH at RT	5	58.3	11.7	22.1	7.9	93.0	7.0
5% NaOH at RT	10	58.0	11.9	22.8	7.2	93.4	6.6
5% NaOH at RT	20	59.3	10.5	22.1	8.1	93.0	7.0
10% NaOH at RT	5	59.9	13.5	22.3	4.3	96.2	3.8
10% NaOH at RT	10	60.4	12.5	22.6	5.4	96.1	3.9
10% NaOH at RT	20	60.9	12.8	21.7	4.6	96.2	3.8
10% NaOH at 60°C	5	62.1	12.0	20.8	5.0	95.2	4.8
0.3 M H ₂ SO ₄ at 100°C	2	63.0	3.2	29.1	4.6	98.7	1.3
0.6 M H ₂ SO ₄ at 100°C	2	64.5	1.0	31.5	2.9	98.6	1.4

Table 4.2. Chemical composition (dry matter basis) of raffia palm fibers.

Fiber	Soaking time (h)	Cellulose (wt. %)	Hemicellulose (wt. %)	Lignin (wt. %)	Others (wt. %)
Untreated fiber	0	53.4	12.3	23.8	10.5
5% NaOH at RT	5	62.7	12.6	23.7	0.9
5% NaOH at RT	10	62.1	12.8	24.4	0.6
5% NaOH at RT	20	63.8	11.3	23.8	1.1
10% NaOH at RT	5	62.3	14.0	23.2	0.5
10% NaOH at RT	10	62.8	13.0	23.5	0.6
10% NaOH at RT	20	63.3	13.3	22.5	0.8
10% NaOH at 60°C	5	65.3	12.7	21.9	0.2
0.3 M H ₂ SO ₄ at 100°C	2	63.0	3.5	29.1	4.4
0.6 M H ₂ SO ₄ at 100°C	2	65.2	0.3	31.3	3.1

4.1.2 Microstructure of RPF

Figure 4.1(a) shows typical SEM micrographs of the transverse section of an untreated RPF. The section has an oval shape with an average diameter of 1.53 mm. The micrograph indicates three distinct regions: an inner region (lumen) labeled 1, a middle region (cortex) labeled 2 and an outer surface (epidermis) labeled 3. Between the outer surface and the inner core, there are two radial pathways labeled 4, which probably serve as conduits for water/moisture exchange between the core of the fiber and the environment. After chemical treatments, the microstructure of the transverse sections of alkali and acidic treated RPFs were relatively the same in shape and morphology as shown in Fig. 1(b and c) in comparison to untreated fiber (Fig. 1a).

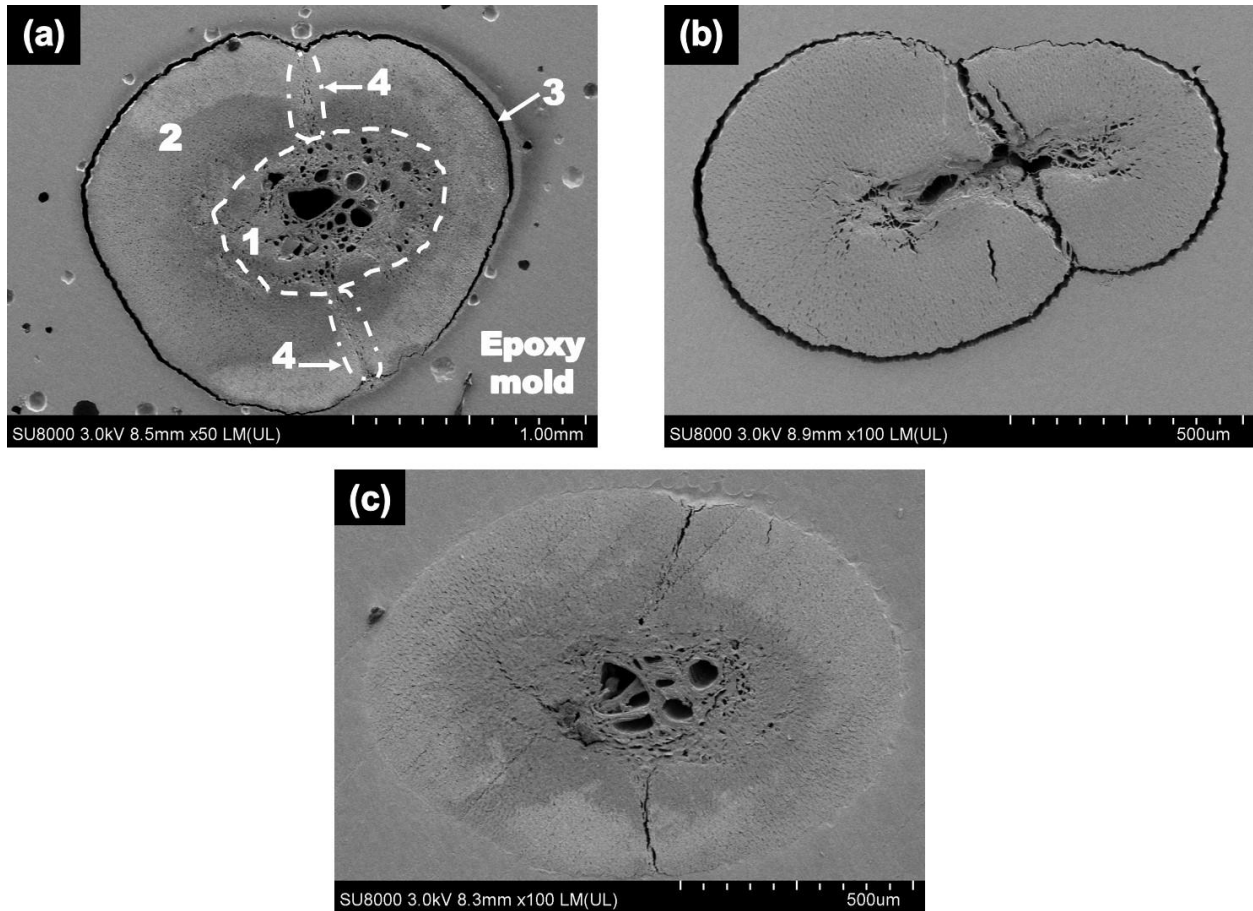


Figure 4.1. Scanning electron micrographs showing transverse cross-section of (a) untreated, (b) alkaline treated and (c) acidic treated raffia palm fibers.

The SEM micrograph in Fig. 4.2 shows the enlarged view of the inner region of an untreated RPF. Observably, RPF is a hollow fiber with some large holes, called lumens located at the inner region. As shown in Fig. 4.3 RPF is a bundle of fiber made up of several elementary fibers having its own lumen located at the inner region. The lumen has been found to be discontinuous in the fiber and remain inside every individual elementary fiber [160]. The middle lamella (Fig. 4.3) glues the elementary fibers together and they are made up of lignin and hemicellulose [86,161]. It can be seen from Figs. 4.2 and 4.3 that the size of the lumens in the inner region are larger in size compared to the ones located in middle region for each elemental fiber. The cross-sectional structure of RPF is similar to the reported structure of coir fiber [160], sisal fiber [86], and abaca fiber [162]. The structure of these fibers was found to have an inner or center region with some varying sizes of holes called the lumen. At higher magnification, it was reported that these fibers comprise of several elemental fibers united by the middle lamella.

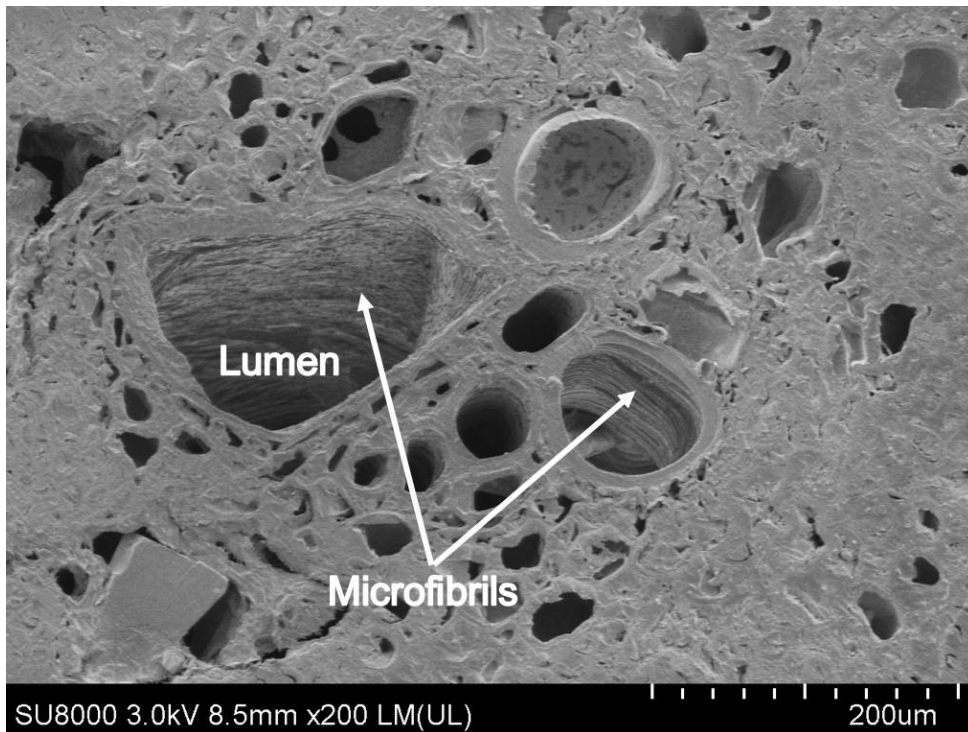


Figure 4.2. Scanning electron micrograph showing enlarged view of the inner section (lumen) of raffia palm fiber (transverse section).

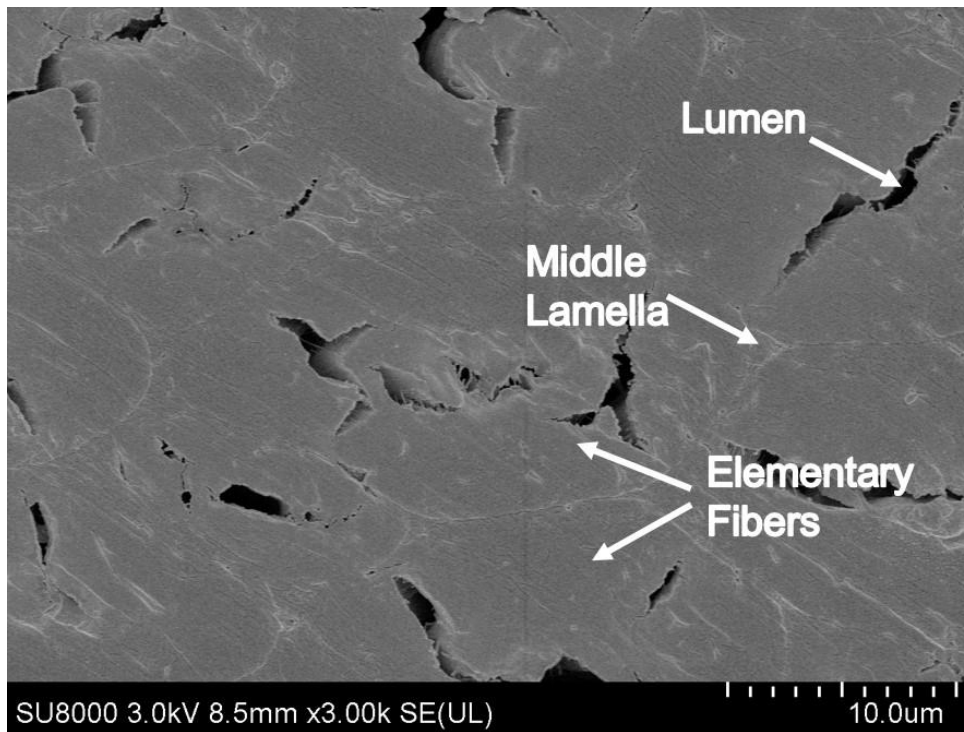


Figure 4.3. Scanning electron micrograph showing enlarged view of the middle section (cortex) of raffia palm fiber (transverse section).

Scanning electron micrographs of untreated RPF (Fig. 4.4) shows the presence of longitudinal cracks on the surface of the fibers. Such type of cracks has been reported to affect the fracture behavior of natural fibers [8]. Chinga *et al.* [8] reported that defect such as kinks present in flax fibers resulted in a longitudinal splitting of the fiber over a large area. They observed that the fiber starts to fracture where a large defect is located and continue to split until it encounters the next defect along the fiber length. Silva *et al.* [163] reported that due to the flaws present in sisal fiber, an increase in the susceptibility of sisal fibers to fracture were observed. The fracture occurred at location of flaws which was due to the collapse of weak fiber cell wall and delamination between the elementary fibers. The surfaces of alkali and sulphuric acid treated RPFs are much cleaner than those of untreated fibers as shown in Figs. 4.5 and 4.6. This suggests that these chemicals removed wax, oil and other impurities from the surfaces of the fibers. It was reported that the use of chemical treatment led to the removal of non-cellulosic components and also resulted in changes in both surface chemistry and thermal properties natural fibers [127,164]. The removal of these materials is expected to promote strong bonding between the fibers and the polymer matrix when used in composite manufacture [103].

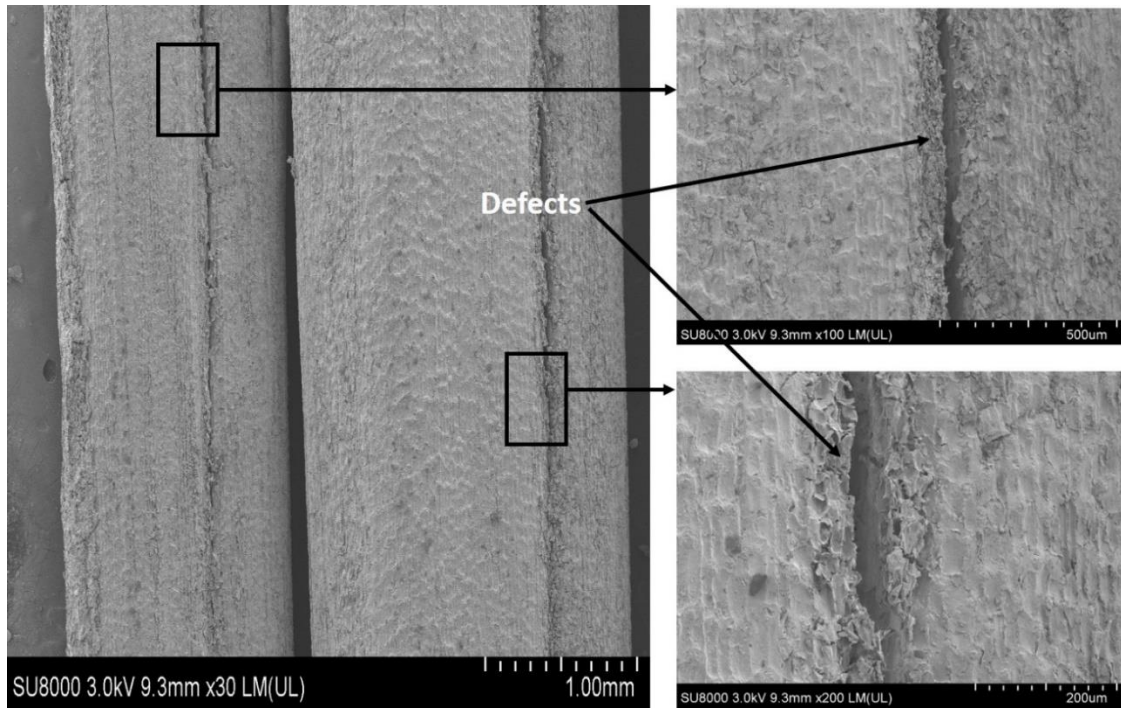


Figure 4.4. Scanning electron micrographs showing the longitudinal surface of untreated raffia palm fibers.

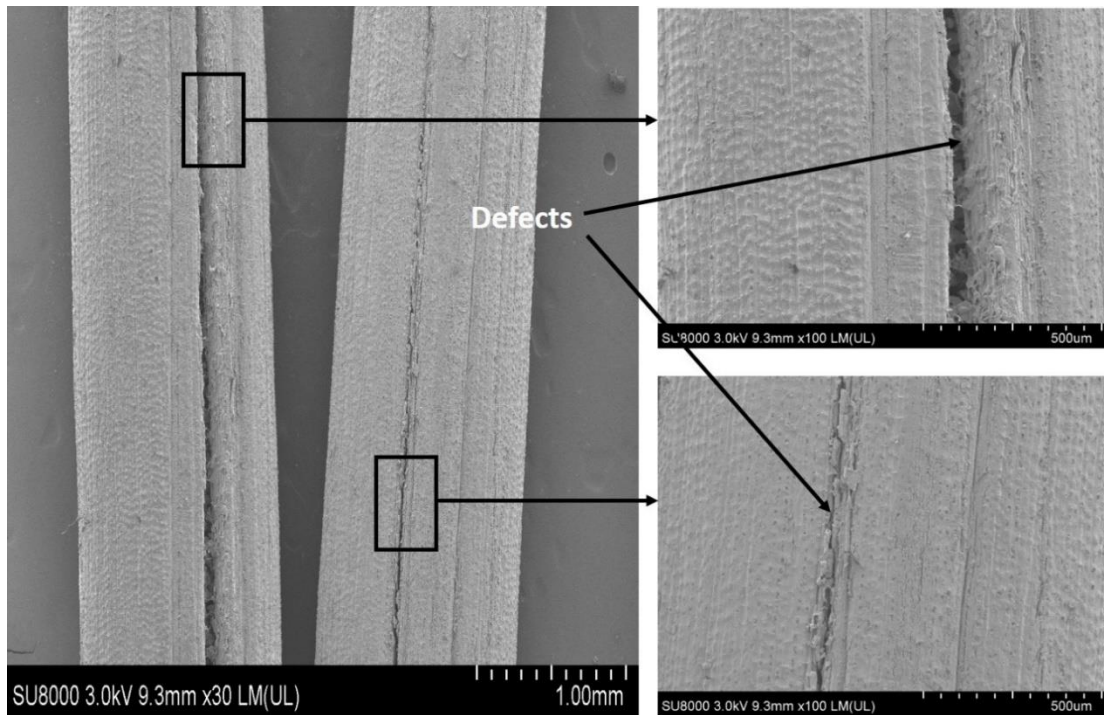


Figure 4.5. Scanning electron micrographs showing the longitudinal surface of raffia palm fibers treated with NaOH.

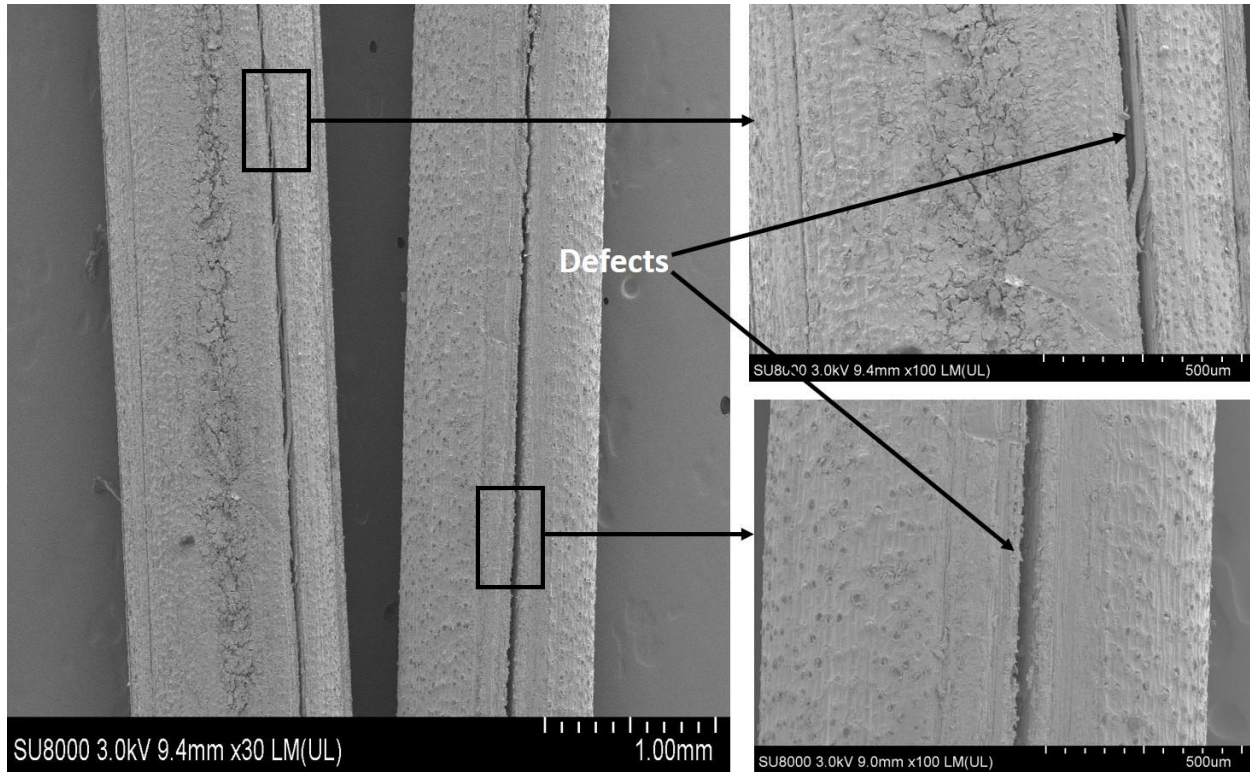


Figure 4.6. Scanning electron micrographs showing the longitudinal surface of raffia palm fibers treated with sulphuric acid.

4.1.3 Moisture Adsorption and Water Absorption

A typical plot showing the variation of % moisture adsorbed by untreated raffia palm fibers as a function of time at room temperature is shown in Fig. 4.7. The data plotted represent the average values for five fiber specimens. All the samples showed similar moisture adsorption behaviour. The specimens adsorbed moisture very rapidly during the first 24 h of exposure after which a saturation stage is reached, whereby the change in adsorbed moisture remained constant with further increase in exposure time. The average moisture adsorbed obtained for RPFs at 50% relative humidity and 23°C after 24 h is therefore 6.52 wt.%. Fangueiro and Rana [165] obtained similar result by measuring the equilibrium moisture content of different NFs at 23°C and 50% relative humidity for a week. The equilibrium moisture content absorbed for flax, ramie, jute and sisal fiber was 10.6, 10.2, 9.4 and 9.5 wt.% respectively.

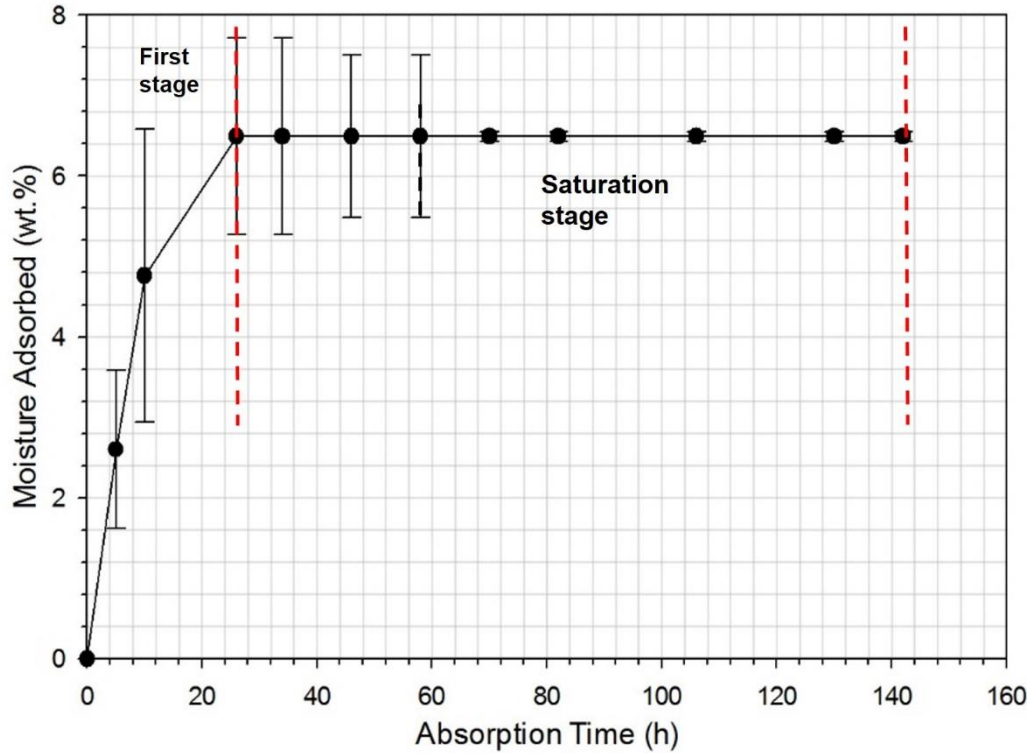


Figure 4.7. Moisture adsorption behaviour of untreated raffia palm fiber at 50% relative humidity and 23°C.

The variation of water uptake as a function of exposure time at room temperature is presented in Fig. 4.8. A close inspection of the wt.% water absorbed vs time curve shows that the fibers experienced a two-stage saturation during exposure. The first saturation occurred between 130 and 202 hours and the second occurred between 274 and 494 hours. During the first stage of water absorption, the lumen of the RPFs as seen in Figs. 4.1 and 4.2 facilitated the rapid absorption of water by capillary action [102]. The continued exposure of the samples to water, after the first saturation stage, permitted water absorption through the smaller internal pores in the elemental fibers. This resulted in the second saturation stage. The average percentage of water absorbed at the first and second saturation stages are 56 wt.% and 62 wt.%, respectively. As of now, only a one-stage saturation of water absorption has been reported in the literature. Kannan *et al.* [166] and Sampathkumar *et al.* [167] reported a 73 wt.% and 78.5 wt.% maximum water absorbed for sisal and areca fibers respectively. They observed an increase in the percentage of water absorbed initially until it reaches a maximum saturation point. The presence of lumen in NFs generates

pathways for diffusion of water into the fiber from the environment. The greater the amount and size of lumen in NFs, the greater the amount of water absorbed from the environment [167].

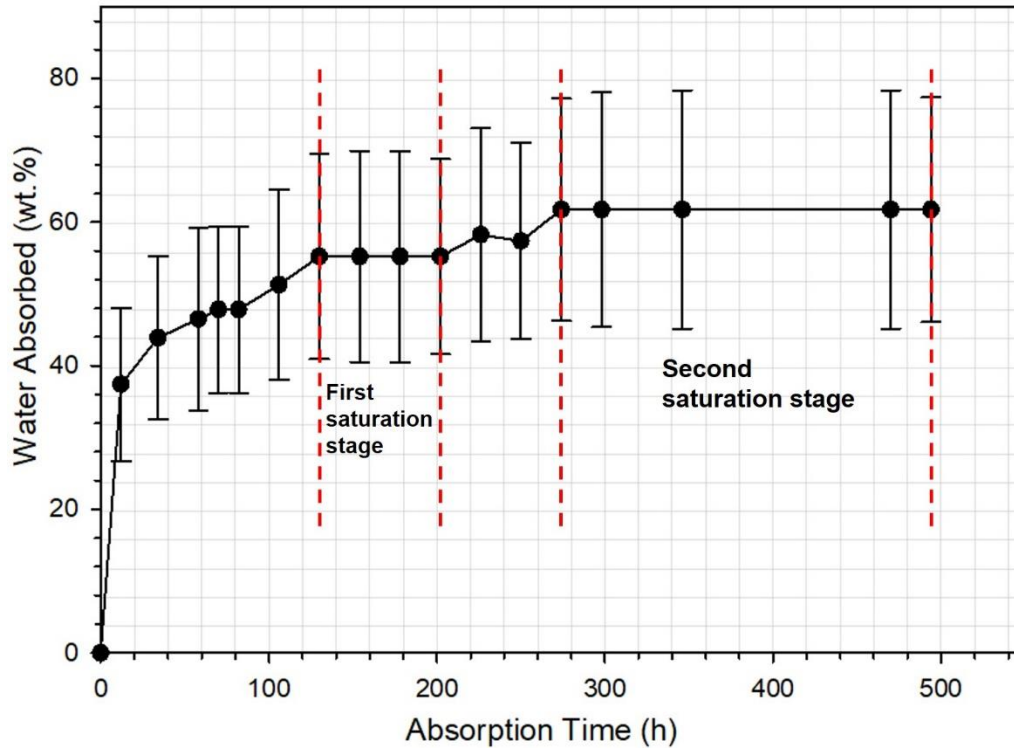


Figure 4.8. Water absorption behaviour of untreated raffia palm fiber.

Figure 4.9 shows the effect of chemical treatment on water absorption behaviour of RPFs. A two-stage water absorption behaviour can also be observed in both alkali and acidic treated RPFs as observed for non-treated fibers (Fig. 4.8). There is also a general decrease in water absorbed in the fibers as a result of chemical treatment, which is believed to be due to the removal of the hydroxyl groups of hemicellulose [167]. The maximum % water absorbed for the alkali and acidic treated fibers are 44 wt.% and 35 wt.%, respectively. Thus, there is a decrease of 29 wt.% and 44 wt.% in the maximum % water absorbed for the alkali and acidic treated fibers, respectively, in comparison with the non-treated fiber.

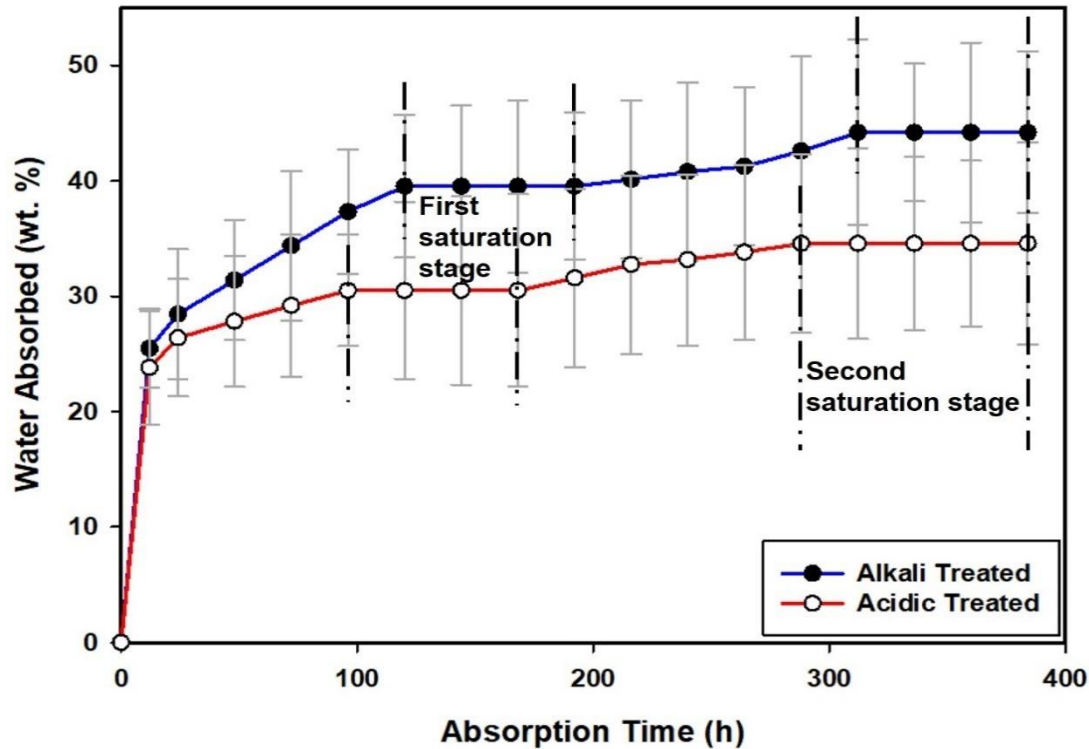


Figure 4.9. Water absorption behaviour of alkali and acidic treated raffia palm fibers.

4.1.4 Mechanical Properties

A typical stress-strain curve obtained for cleaned untreated RPF (cross head speed = 1 mm/min, gauge length = 25 mm) is shown in Fig. 4.10. RPF initially deformed inelastically after which it deformed elastically until the maximum stress. Similar result was reported by Cai *et al.* [162], Silva *et al.* [163], Mathura and Cree [28] for abaca, sisal and Trinidad coir fibers, respectively. The non-linear deformation behaviour was reported to a collapse of the weak primary cell walls and delamination between the elemental fibers in the fiber bundle [163].

The average fracture strength obtained for 10 fiber specimens was 236 ± 46 MPa. Figure 4.11 shows the variation of fiber fracture strength with fiber length. It is found to decrease with increasing fiber length. This can be attributed to an increase in the number of defects as the length increased [28,163,168,169]. The greater the fiber length, the greater is the possibility of having more or critical-sized defects leading to failure in the tested fiber, which can result in a decrease in tensile strength [161].

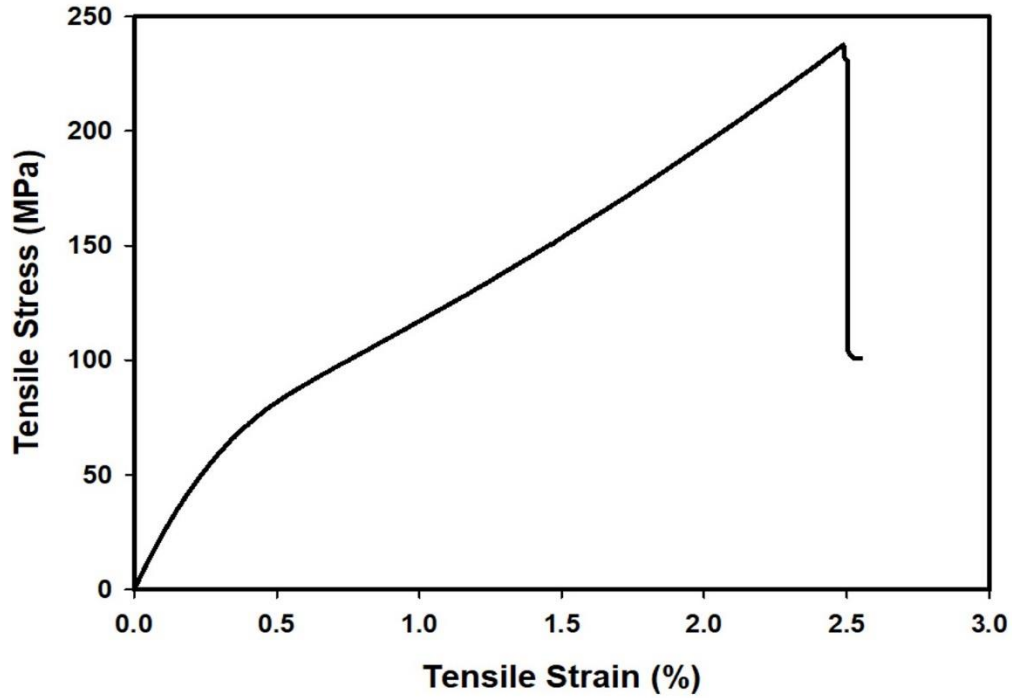


Figure 4.10. A typical stress-strain curve obtained for a raffia palm fiber at room temperature.

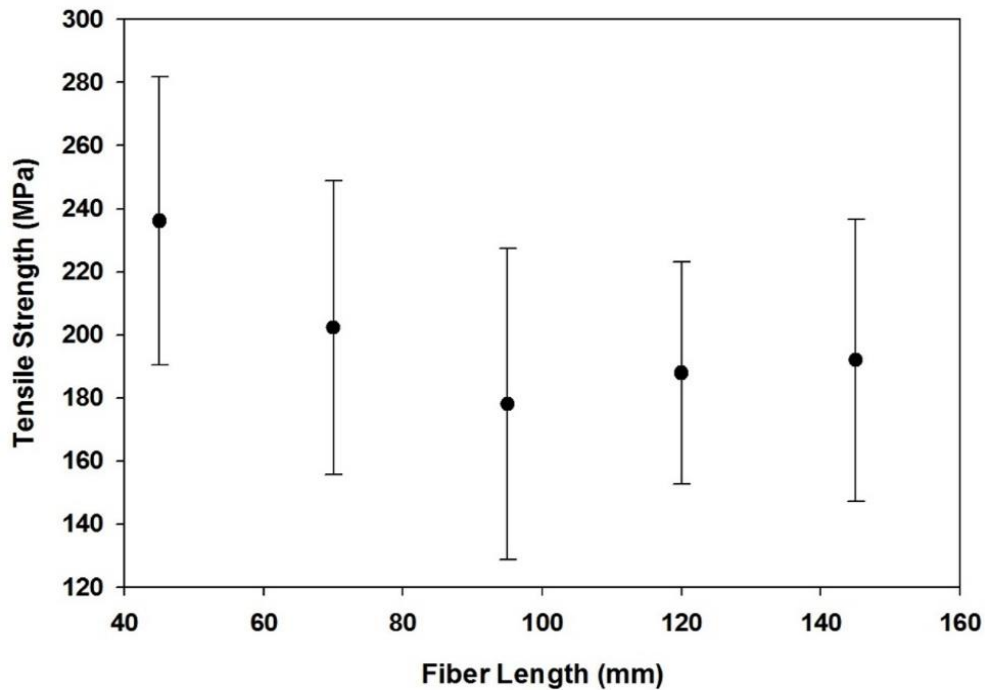


Figure 4.11. Variation of fiber strength to fiber length.

The average fracture strength value obtained in this study is quite different to the breaking strength value reported for *Raphia textilis* by Elenka *et al.* (average value of 500 ± 97 MPa) [5] obtained

from Congo, and *Raphia farinifera* by Sandy and Bacon (average value of 500 ± 80 MPa) [39] gotten from Madagascar. The difference in the species and location of raffia fibers investigated by the authors in reference [5,39] in comparison to raffia palm fiber in this study could be the reason for the difference in the reported average strengths.

The effect of fiber length on the percentage elongation to fracture under tensile loading is summarized in Fig. 4.12, while Fig. 4.13 shows the variation of fracture strength at a fixed fiber length with increasing crosshead speed. There appears to be no appreciable influence of fiber length on percentage elongation to fracture. Mukherjee and Satyanarayana [168] reported that under applied stress, as the length of sisal fiber increases, there were little or no changes in the % elongation of the fiber. This behaviour was attributed to the stiff nature of NFs [170]. Similarly, crosshead speed does not have any remarkable effect on the fracture strength of the fibers. Mukherjee and Satyanarayana [168] and Tomczak *et al.* [169] investigated the effect of varying strain on the tensile strength of Sisal and Curaua fibers respectively. They reported that NFs having a crystallinity index above 50% subjected to high testing speed (between 2 and 50 mm/min) will behave like a viscoelastic material with crystalline region bearing most of the applied stress resulting in increased strength. However, at low speeds, the fibers will behave like a viscous liquid while the amorphous region bears a major portion of the applied load resulting in little or no remarkable effect on the fracture strength. This is in agreement with the results of the effects of crosshead speed on fracture strength obtained in this study.

The effect of chemical treatment on the tensile properties of RPFs is presented in Table 4.3. The tensile strength of alkaline and sulfuric acid treated fibers reduced by 47% and 89%, respectively,. This may be due to the concentration of solutions and exposure time used. Edeerozey *et al.* [21] reported that increasing alkali concentration from 6 to 9% resulted in significant reduction in the tensile strength of kenaf fibers (from 239 to 165 MPa). Similar result was reported by Mahjoub *et al.* [91] on the tensile properties of kenaf fibers. He reported a decrease in the tensile strength and modulus of kenaf fiber due to increasing concentration (5, 7, 10 and 15%) of NaOH solution and immersion time.

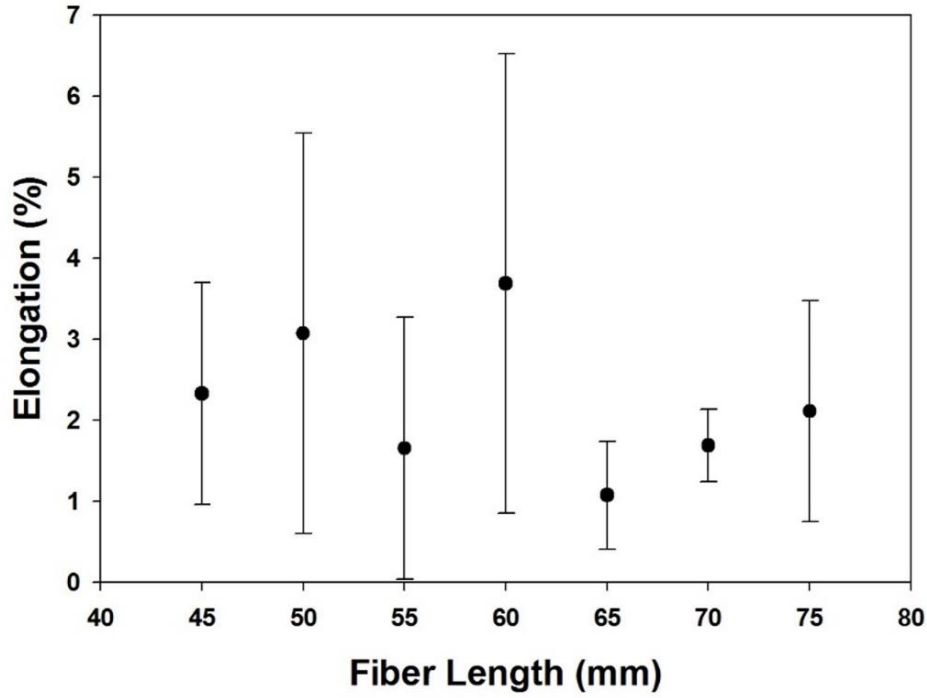


Figure 4.12. Variation of percentage elongation to fracture of raffia palm fibers with fiber length.

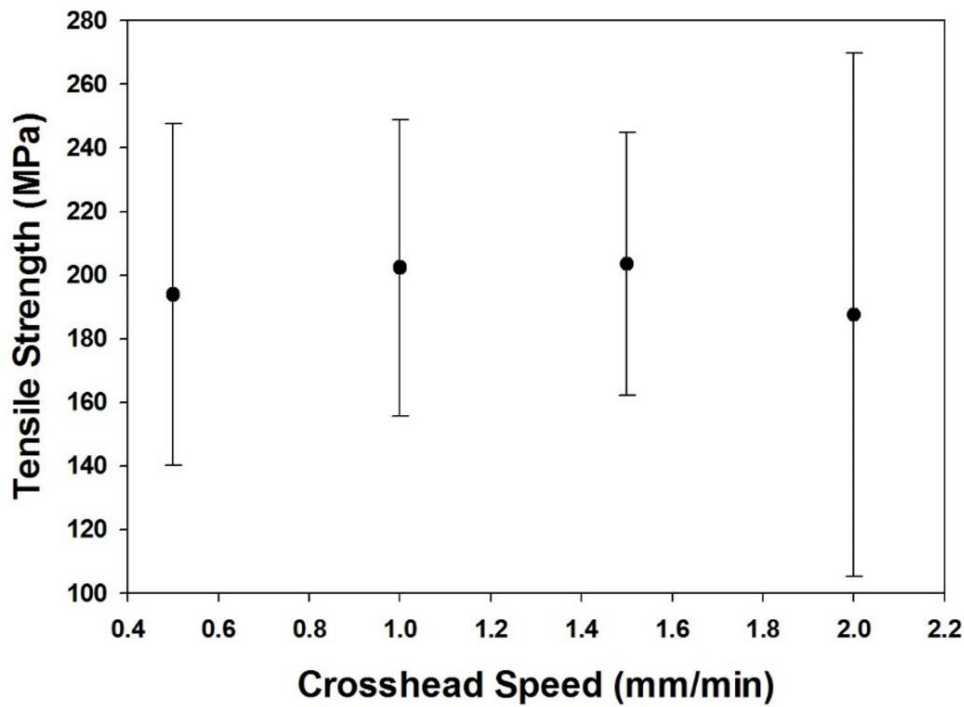


Fig. 4.13. Variation of tensile strength of raffia palm fibers with the crosshead speed.

Table 4.3. Mechanical properties of chemically treated raffia palm fibers.

Fiber	Tensile Strength (MPa)	Elongation at break (%)
Untreated fiber	236.1 ± 45.7	2.5 ± 1.9
Alkaline treated fiber	129.3 ± 31.4	2.1 ± 0.8
Acidic treated fiber	26.9 ± 4.9	2.4 ± 0.6

4.1.5 Statistical Analysis

The results of analysis of variance (ANOVA) tests on the obtained tensile data for the RPFs are presented in Tables 4.4 – 4.6. The F-test and the *p*-value determines if statistically significant differences exist between groups. If F is greater than F_{crit} and *p*-value is less than 0.05, the null hypothesis is rejected, and the results are said to have a statistically significant difference in their mean values. If F is less than F_{crit} and *p*-value is greater than 0.05, the null hypothesis cannot be rejected and there is no statistically significant difference in the mean values.

Although it can be inferred from Fig. 4.11 that fracture strength generally decreases with increase in length of the fiber, however, the results of ANOVA (Table 4.4) suggest that the decrease in tensile strength with increasing fiber length is statistically insignificant since *p*-value is greater than 0.05. It should be noted that these ANOVA are only true within the range of variables tested in this study.

Table 4.4. ANOVA test results for tensile strength of raffia palm fibers with varying fiber lengths of 45, 70, 95, 120 and 145 mm.

Source of variation	Df	SS	MS	F	<i>p</i> -value	Fcrit
Between Groups	4	20023.342	5005.836	2.518	0.054	2.579
Within Groups	45	89461.444	1988.032			
Total	49	109484.786				

Table 4.5. ANOVA test results for %elongation at 25 mm gauge length of raffia palm fibers with varying fiber lengths of 45, 50, 55, 60, 65, 70 and 75 mm.

Source of variation	Df	SS	MS	F	<i>p</i> -value	Fcrit
Between Groups	6	24.112	4.019	1.329	0.277	2.445
Within Groups	28	84.643	3.023			
Total	34	108.755				

Table 4.6. ANOVA test results for tensile strength at 50 mm gauge length of raffia palm fibers with varying crosshead speed of 0.5, 1, 1.5 and 2 mm/min.

Source of variation	Df	SS	MS	F	<i>p</i> -value	Fcrit
Between Groups	3	1698.793	566.264	0.167	0.918	2.866
Within Groups	36	122031.742	3389.771			
Total	39	123730.534				

DF = degree of freedom, SS = sum of squares, MS = mean square, *p*-value = calculated probability, F = F-test statistic, and F_{crit} = critical F value.

The results of ANOVA for % elongation to fracture for gauge length of 25 mm and tensile strength for fiber with gauge length of 50 mm deformed at different cross head speed are presented in Tables 4.5 and 4.6, respectively. The ANOVA result shows that there are no statistically significant differences in % elongation to fracture for different fiber gauge lengths. Similarly, no statistically significant difference in tensile strength is obtained for the case where the deformation crosshead speed was varied between 0.5 and 2 mm/min. It should be noted that these ANOVA are only true within the range of variables tested in this study. Also, statistical analysis (Table 4.7) showed that there is a statistically significant difference in fiber strength for different fiber treatments. However, no statistically significant difference (Table 4.8) in % elongation of the fiber for different fiber treatments was obtained. This indicated that chemical treatments of the fiber significantly affected its tensile strength.

Table 4.7. ANOVA test results of fiber treatments on the tensile strength at 45 mm fiber length of raffia palm fibers.

Source of variation	Df	SS	MS	F	<i>p</i> -value	Fcrit
Between Groups	2	170182.85	85091.42	70.4	0.0000000002	3.42
Within Groups	23	27799.67	1208.68			
Total	25	197982.51				

Table 4.8. ANOVA test results of fiber treatments on % elongation at 25 mm gauge length of raffia palm fibers.

Source of variation	Df	SS	MS	F	<i>p</i> -value	Fcrit
Between Groups	2	1.02	0.51	0.28	0.76	3.42
Within Groups	23	42.26	1.84			
Total	25	43.28				

4.1.6 Colour Measurement of RPFs

One of the physical changes accompanying the chemical treatment of RPF is colour change. The results of colour measurements which were obtained using the Hunter L^* , a^* , and b^* coordinates are presented in Table 4.9. The value of L^* coordinate represents the whiteness component (0 = black, and 100 = white); the a^* coordinate represents greenness to redness ($-a^*$ = green, and $+a^*$ = red); and b^* coordinate represents blueness to yellowness ($-b^*$ = blue, and $+b^*$ = yellow). The result shows that the fiber became 23% darker after alkali treatment. Also, there was a 27% and 14% reduction in redness and yellowness, respectively, in comparison to the untreated fiber.

Table 4.9. Variation of raffia palm fiber colour with NaOH and H₂SO₄ treatment.

Fiber	ΔL^*	Δa^*	Δb^*	ΔE^*
Untreated Fiber	51.73 ± 0.55	9.76 ± 0.38	20.98 ± 0.71	0
Alkaline treated fiber	39.86 ± 1.44	7.13 ± 0.13	18.10 ± 0.62	12.49
Acidic treated fiber	37.38 ± 0.41	11.40 ± 0.08	15.30 ± 0.12	15.52

After acidic treatment, the fibers became 28% darker with 17% increase in the red pigment and 27% reduction in the yellow pigment in comparison to untreated fiber. Elenga et al. [41] reported that alkali treatment *Raphia textilis* fiber became darker by 13%.

RPFs subjected to acidic treatment were 6% lower in brightness compared to those subjected to alkaline treatment. The red pigment of acid treated fibers was 60% higher in comparison with those of alkaline treated fibers. However, the yellow pigment for acid treated fibers was 15% lower in comparison to the alkaline treated fibers. The decrease in colour of alkali and acidic treated RPFs is due mainly to the removal of non-cellulosic materials (like waxy substances, and oil) which has been found to be responsible for the natural colours of natural fibers [73,171]. Statistical analysis (Tables B.1 in Appendix B) showed that there is a statistically significant difference between the L*, a* and b* colour variations of untreated fiber to treated fibers. This suggest that chemical treatments significantly affected the colour variation of the fibers.

4.1.7 Synchrotron Based Fourier Transform Infrared Spectromicroscopy (SB – FTIRS)

Using synchrotron FTIR spectromicroscopy, the spatial distribution and relative concentration of the chemical compositions associated with RPFs structure (cellulose, lignin and pectin) were mapped. The peak around 1165 cm⁻¹, 1503 cm⁻¹, 1750 cm⁻¹ bands (Figs. 4.14) were integrated to determine the distribution and relative concentration of the cellulose, lignin and pectin chemical compositions respectively across the fiber [15,149,172,173]. The hemicellulose component of raffia palm fiber located around the 1045 cm⁻¹ peak, was too noisy which made it difficult a consistent map. The infrared images were taken from the region of the visible outlined by the rectangle area. The size of the rectangle area in the visible image was 170 μm × 170 μm.

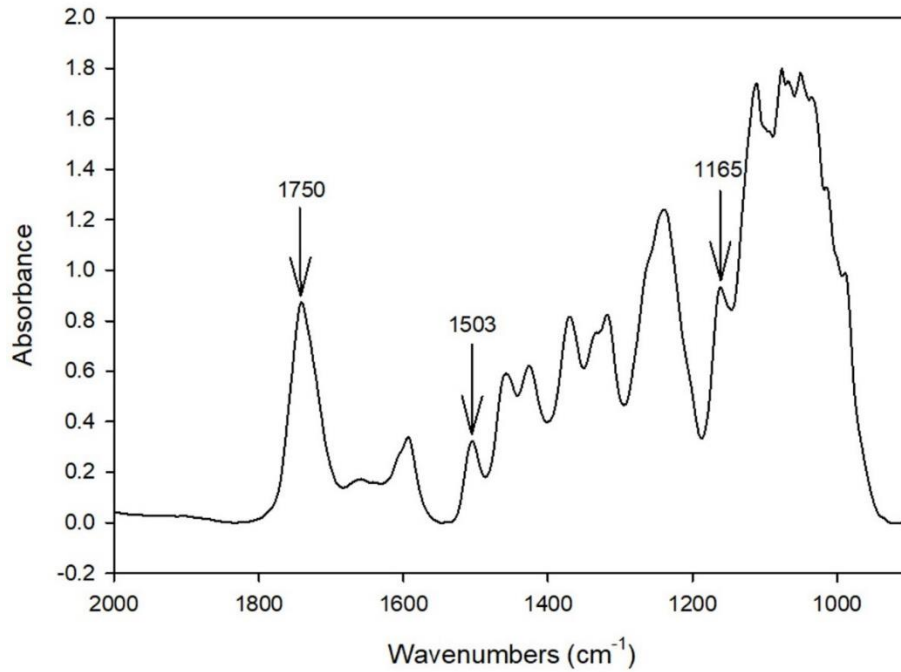
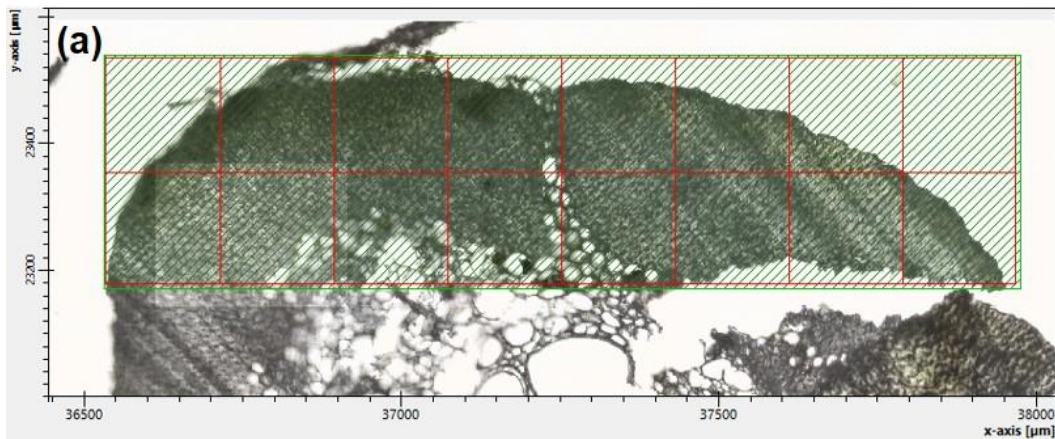


Figure 4.14. Synchrotron based Fourier transform infrared spectra of untreated raffia palm fiber.

As observed in Figs 4.15, the inner region of the fiber has relatively little or no chemical composition, majorly due to the presence of lumen which are big in size in the inner region. The infrared colour blue intensity further supports that there is no presence of cellulose or pectin in the inner region of RPF, although little traces of the presence of lignin was observed. It was observed that the chemical compositions were mainly concentrated in the middle region (cortex) of the fiber, which comprises of several elemental fibers as seen in Fig 4.3.



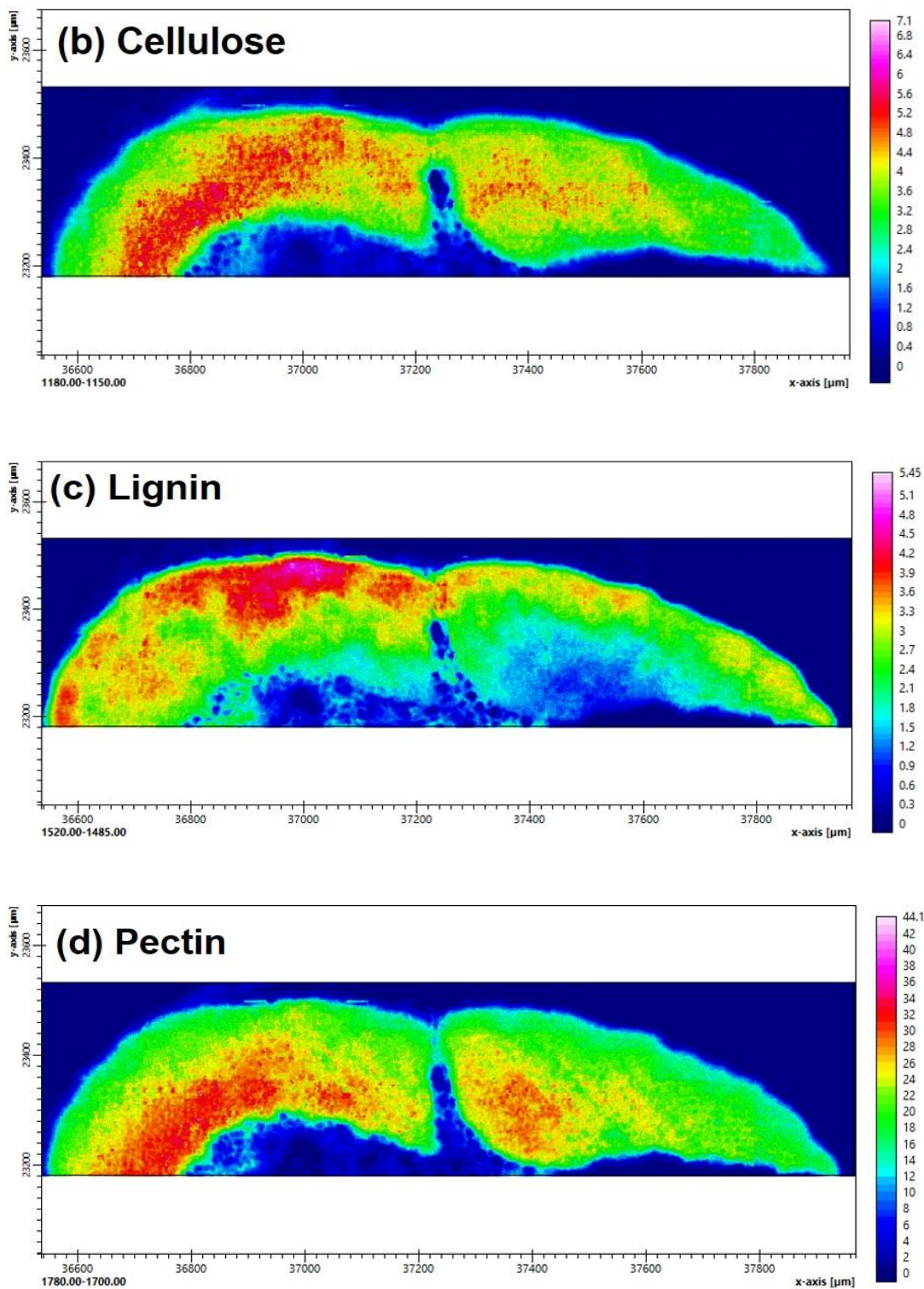
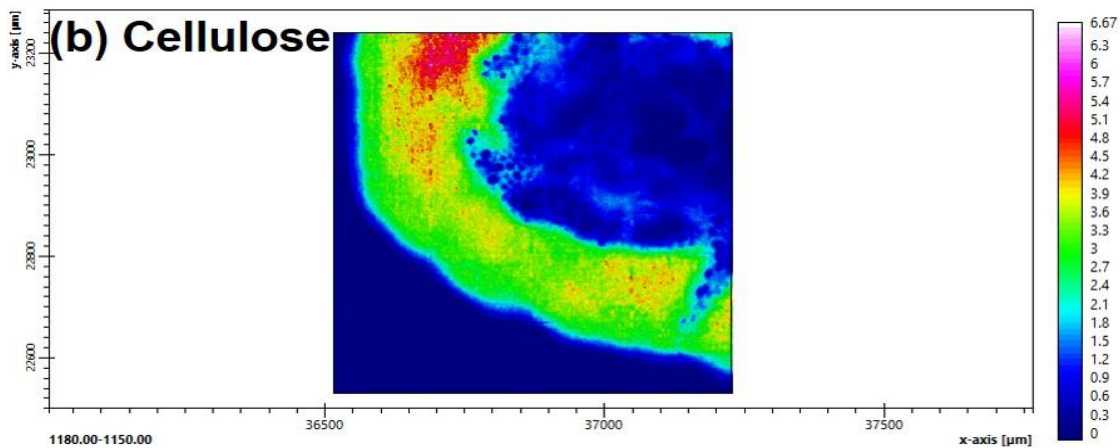
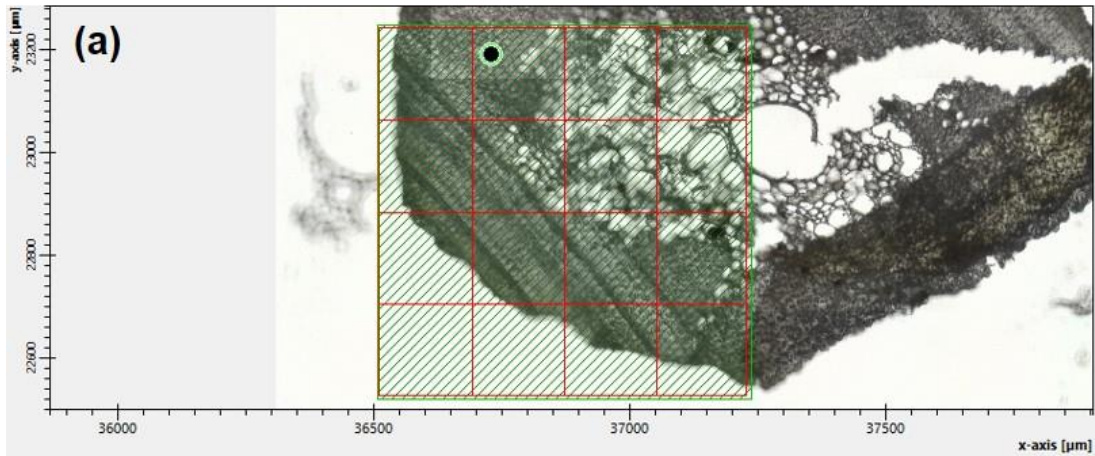


Figure 4.15. Synchrotron based Fourier transform infrared spectromicroscopy imaging of transverse section of untreated raffia palm fiber showing (a) the map region of interest and chemical distribution of (b) cellulose (1165 cm^{-1}), (c) lignin (1503 cm^{-1}) and (d) pectin (1750 cm^{-1}).

Although, the presence of cellulose, lignin and pectin was detected to be present in the middle region and at the epidermis of the fiber, the presence of red and yellow infrared colours shows that the concentration of cellulose is more in the middle region of the fiber. The presence of red, yellow and pink infrared colours shows that lignin was more distributed in the middle region and at the epidermis of the fiber. The presence of green infrared colours shows that there were traces of lignin in the inner region of the fiber as seen in Fig 4.15. The presence of green infrared colours (Fig. 4.16c) in the inner region of the fiber also confirms that there little traces of lignin. The presence of red and yellow infrared colours shows that pectin was more distributed in the middle region of the fiber and close to the inner region of the fiber.



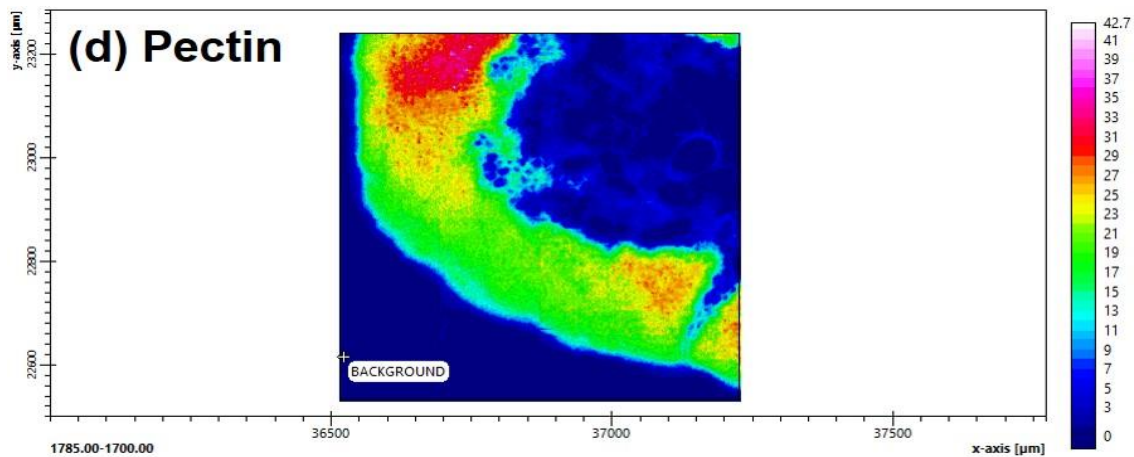
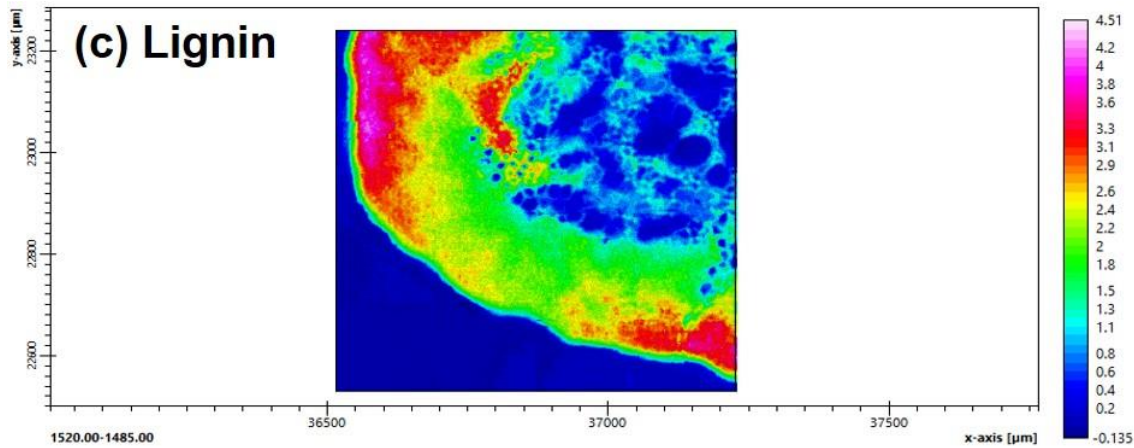


Figure 4.16. Synchrotron base Fourier transform infrared spectromicroscopy imaging of transverse lower left section of untreated raffia palm fiber showing (a) the map region of interest and chemical distribution of (b) cellulose (1165 cm^{-1}), (c) lignin (1503 cm^{-1}) and (d) pectin (1750 cm^{-1}).

4.1.8 FT-Infrared and Raman Spectroscopy

The extent of chemical changes associated with the use of alkali and acid treatments of RPFs was analyzed using Fourier transform infrared spectroscopy (FTIRS). Typical spectra obtained from this test are presented in Fig. 4.17 for both the untreated and treated fibers. The absorbance peaks of interest are clearly marked in the spectra.

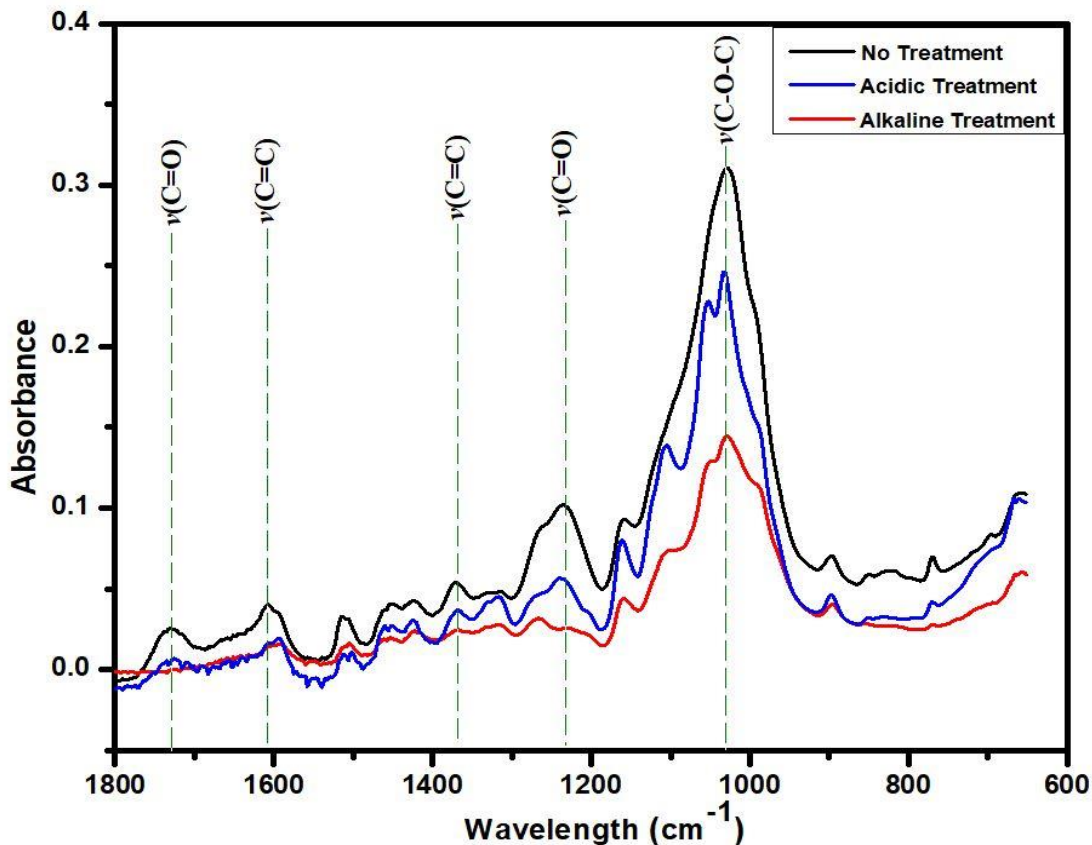


Figure 4.17. Fourier transform infrared spectra of untreated, alkali and acid treated raffia palm fibers.

In general, the spectra of the treated RPFs are similar to that of the untreated fiber. However, after NaOH and H₂SO₄ treatments, there were reductions in the intensity of certain peaks in comparison with those of the untreated fiber. The absorption peak at 1733 cm⁻¹ is attributed to $\nu(\text{C}=\text{O})$ stretching of methyl ester and carboxylic acid in pectin [15]. The presence of this band at 1733 cm⁻¹ before NaOH and H₂SO₄ treatments indicates the presence of pectin which disappears after alkali treatment. The absorbance peak of NFs in the region of 1610 cm⁻¹ indicates the presence of fatty acids [174,175] and is attributed to $\nu(\text{C}=\text{C})$ stretching. This peak disappeared after alkali and acidic treatments, thus confirming the removal of any traces of oils. The untreated fiber spectra also exhibit weak absorption peak at 1378 cm⁻¹, which indicates the presence of lignin [174] and is attributed to $\nu(\text{C}=\text{C})$ stretching. The disappearance of the peak around 1230 cm⁻¹ is attributed to the $\nu(\text{C}=\text{O})$ stretching after alkali and acidic treatments. This indicates a significant reduction in hemicellulose content of the fiber [174]. A significant reduction in absorption peak at 1025 cm⁻¹

is attributed to $\nu(\text{C-O-C})$ stretching band, and it is believed to be caused by degradation of the hemicellulose in alkali and acidic treated RPFs [176].

Raman spectroscopy was also used to provide information on the impact of alkali and acidic chemical treatments on the surface chemistry of natural fibers [121]. Typical spectra obtained from this test are presented in Fig. 4.18 for both the untreated and treated fibers. The absorbance peaks of interest are clearly marked in the spectra. The shift in Raman spectra of NaOH treated fiber and a reduction in the H_2SO_4 treated fiber intensity was observed. The peak at 891 cm^{-1} correspond to $\nu(\text{C-H})$ stretching, which indicates the presence of hemi-cellulose for untreated fibers [177]. After alkaline treatment, a reduction and a shift in these peaks were observed. The disappearance of this peak in the acidic treated fiber was also observed.

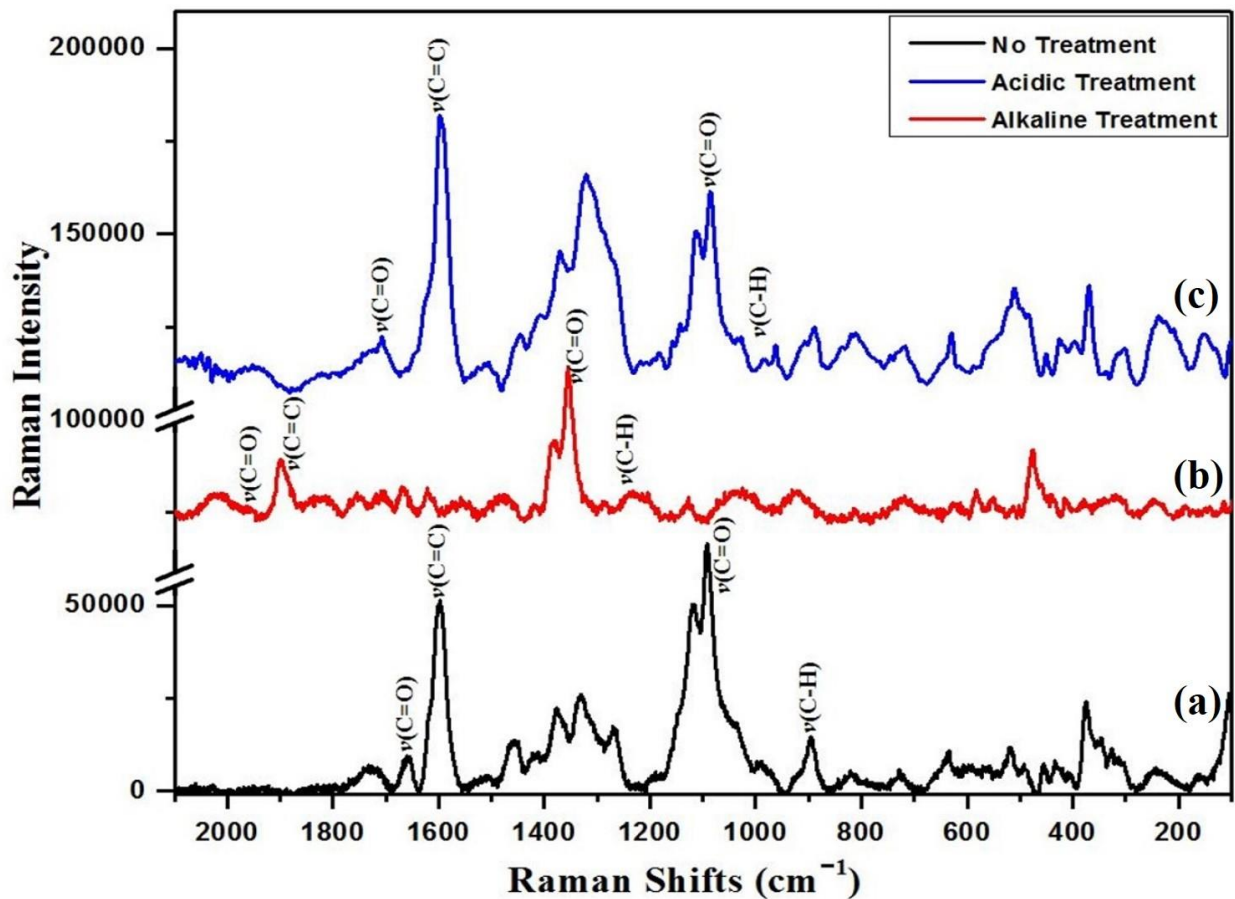


Figure 4.18. Raman spectra of (a) untreated, (b) alkali and (c) acidic treated raffia palm fibers.

The Raman peak detected around 1085 cm^{-1} is attributed to $\nu(\text{C}=\text{O})$ stretching of cellulose in the untreated fiber [178]. The presence of these peak was found to remain in both the treated fiber. The Raman peak detected around 1587 cm^{-1} is attributed to $\nu(\text{C}=\text{C})$ aryl stretching of lignin [173]. A reduction and shift in this peak were observed after alkali treatment. This peak was found to increase in the acidic treated fiber, which is in agreement with the chemical composition result presented in Table 4.1. Also, the peak at 1737 cm^{-1} which indicates the presence of waxes and fatty acids ester [173] attributed to $\nu(\text{C}=\text{O})$ vibrations was also observed. The presence of this peak was found to be removed and reduced in the alkali and acidic treated fibers respectively.

4.1.9 X-ray Diffraction

The XRD diffractogram (Fig. 4.19) of untreated, alkaline and acidic treated RPF shows three intense peaks, which are peculiar to natural fibers. The presence of the diffraction peaks indicates that RPF is semi-crystalline in nature.

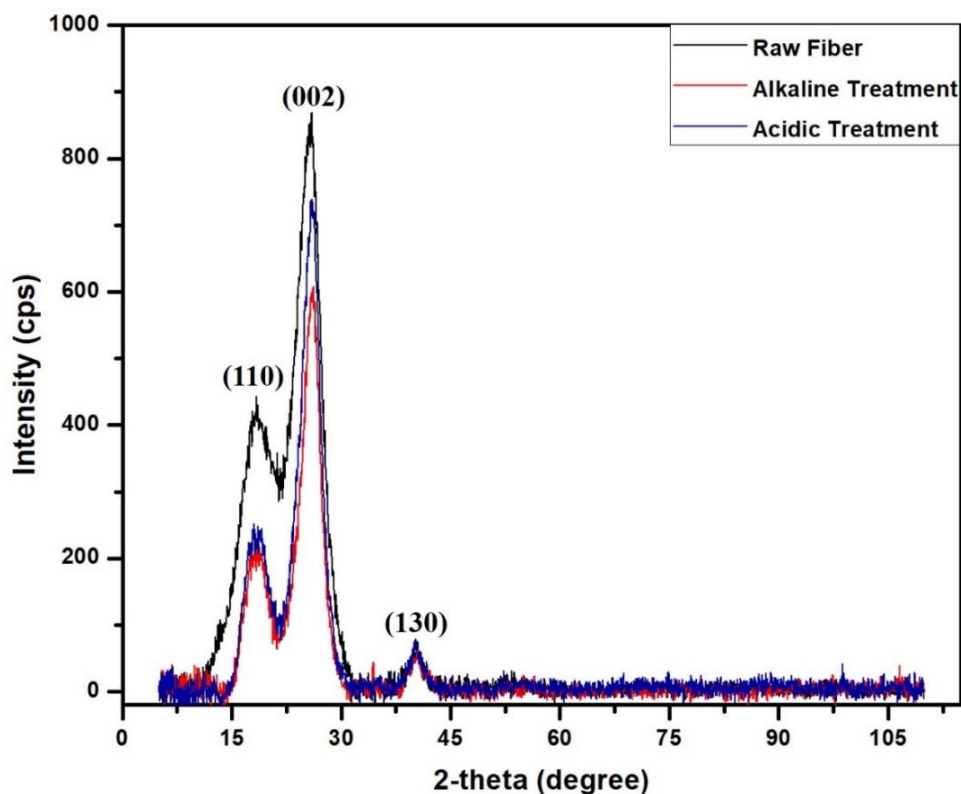


Figure 4.19. Result of X-ray diffraction analysis on untreated, alkaline and acidic treated raffia palm fibers.

The most prominent peaks appeared at scattering angles (2Θ) of 18.4° , 26.1° , and 40.5° which correlates to the reflections from (110), (002) and (130) crystallographic planes respectively [41,152]. The crystallinity index (CI) of the untreated RPF is estimated to be 66.6%. Elenga *et al.* [5] reported the CI of *Raphia textilis* fiber to be 64%, which is higher than that of *Wrightia tinctoria* seed fibers (49.2%) and ramie (58%), but close to that of cotton (60%) and smaller than that of sisal (71%), jute (71%), flax (80%) and hemp (88%). Low crystallinity means that the fibers will have relatively high amorphous regions. These amorphous regions increases the amount of moisture absorbed in natural fibers [73]. Interestingly, the degree of crystallinity of treated RPFs increased after NaOH and H₂SO₄ treatment. After alkali and acidic treatment of RPFs, the crystallinity index was estimated to be 87.2% and 89.7% respectively. The increase in crystallinity index of treated RPF is an indication that the cellulose crystals in treated RPFs are better oriented in comparison to untreated fiber. This is due to the removal of non-crystalline materials from the fibers, including amorphous hemicelluloses and other non-cellulosic material as seen in section 4.1.8 [24,179].

4.1.10 DSC Measurements

The results of thermal analysis on non-treated RPFs using differential scanning calorimetry (DSC) are presented in Fig. 4.20. The fibers exhibit a thermal behaviour comparable to those of other natural fibers commonly used in the manufacture of polymeric composites. The DSC curve for non-treated RPFs shows an endothermic peak at temperature in the range of 110°C to 140°C , which is attributed to evaporation of water. Exothermic peaks are observed at higher temperatures, which can be attributed to decomposition of hemicellulose and cellulose [180].

To understand drying effect on thermal properties of RPFs, DSC analysis was carried on two untreated fiber samples. The untreated fibers conditioned at 50% relative humidity and 23°C was denoted as air-dried RPFs. The untreated fibers dried at 60°C in the oven was denoted as oven-dried RPFs. Significant reduction in the heat absorbed (from 148 to 60 J/g), due to evaporation of water in the endothermic peaks of oven-dried fibers compared to the air-dried fibers is evident as shown in Fig. 4.20. The moisture absorbed from the surrounding and the internal moisture content of the fiber is the reason why air-dried RPF absorbed higher heat in comparison to oven-dried RPF.

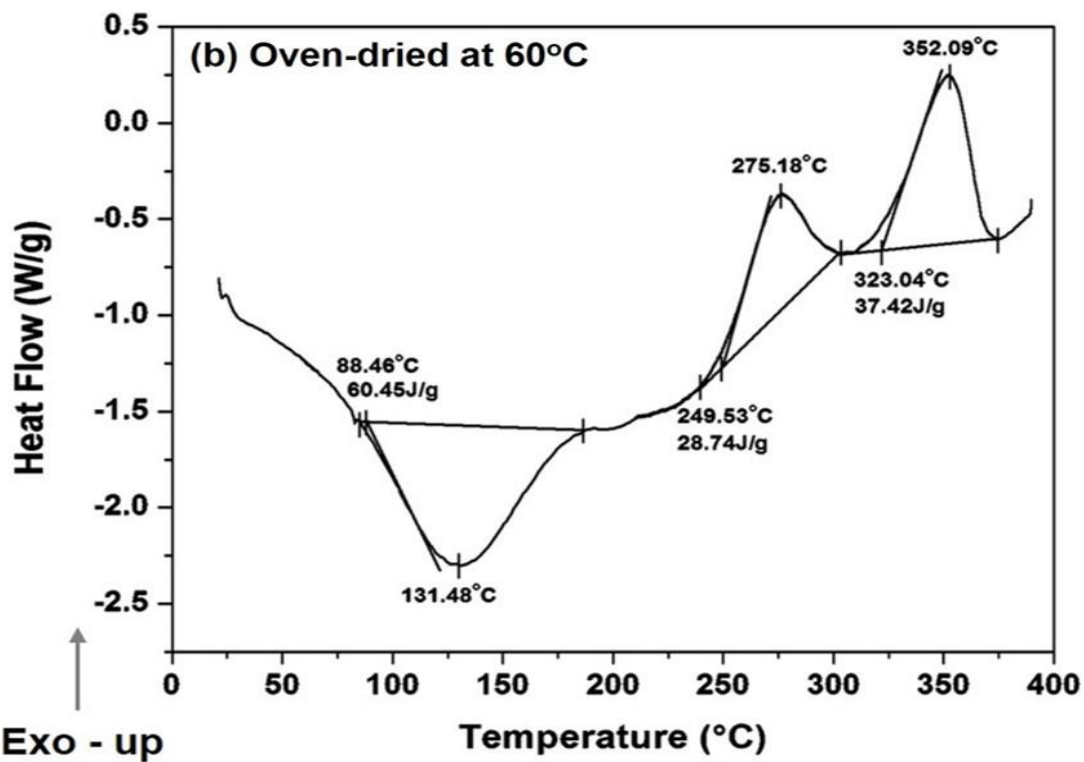
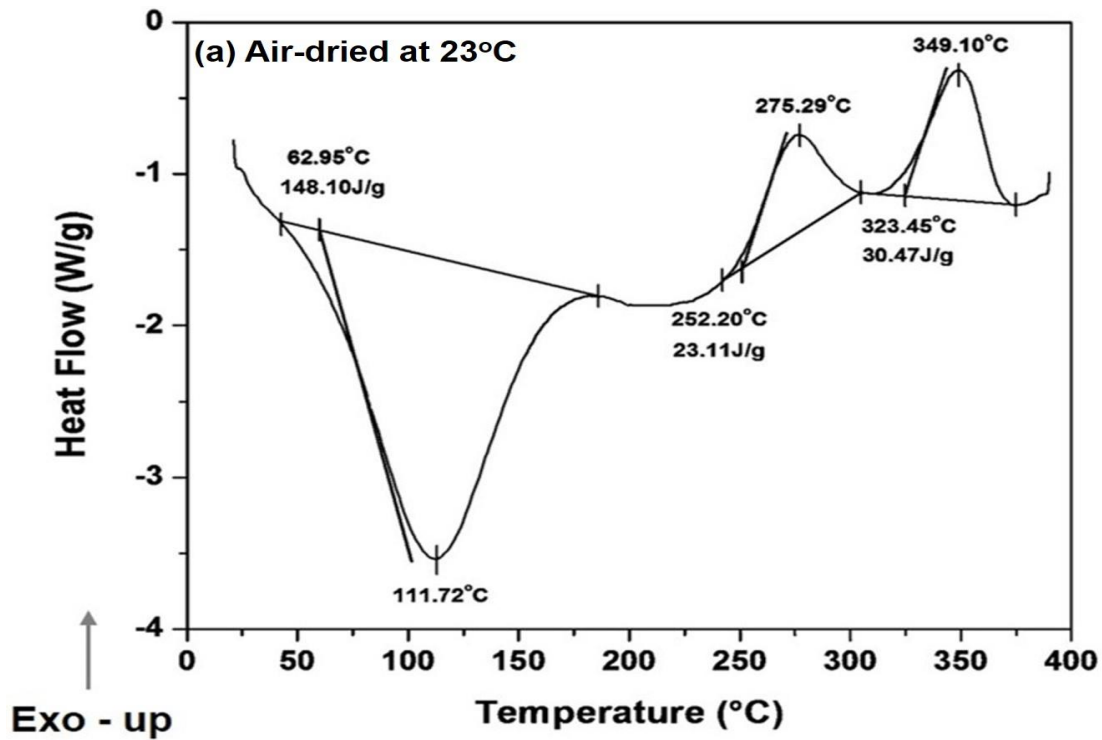


Figure 4.20. Differential scanning calorimetry thermograms obtained for untreated (a) air-dried at 23°C and (b) oven-dried raffia palm fibers at 60°C.

Furthermore, to understand the effect of fiber treatment on its thermal properties, both the alkali and acidic treated RPFs were oven-dried at 60°C for 24 h. The DSC curves as shown in Figs. 4.21 and 4.22 reveals that there was an overall increase in the amount of heat generated, T_g value, degradation temperature of hemicellulose and cellulose for the alkali and acidic treated fibers. A previous study using FT-IR and Raman spectroscopy [15] indicated that structural changes in natural fiber due to chemical treatments are likely to have direct effect on their thermal degradation characteristics.

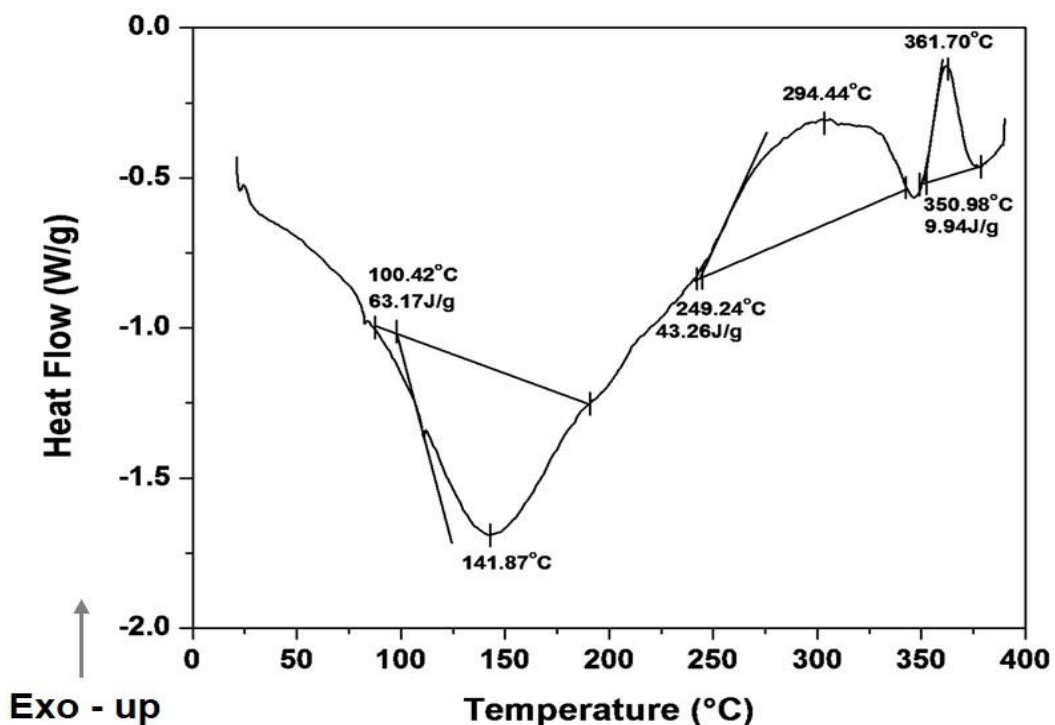


Figure 4.21. Differential scanning calorimetry thermogram obtained for alkaline treated raffia palm fiber.

The removal of non-cellulosic components and increase in cellulose content after chemical treatments leads to increase in the enthalpy values and degradation temperature of RPFs as presented in Table 4.10. Similar results of an increase in the decomposition temperature of cellulose from 357°C – 367°C for hemp fiber was reported by Hao [181]. The increase in the amount of heat absorbed and degradation temperature of both hemi-cellulose and cellulose of alkaline and acidic treated RPFs corresponds with the disappearance of the C=O band in the FTIR spectra of the treated fibers. From FTIR and Raman results, it is apparent that this band's

disappearance significantly affected the thermal degradation of the RPFs. This is probably because more non-cellulosic materials were removed resulting in high degree of crystalline structural order, which requires a higher degradation temperature [15].

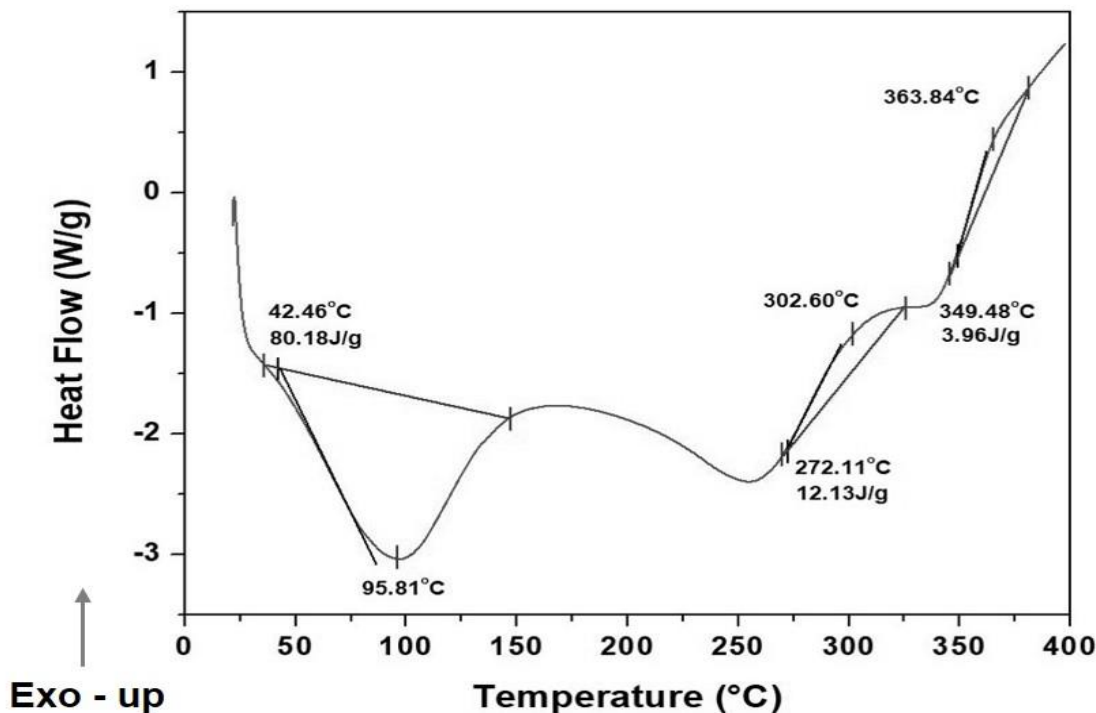


Figure 4.22. Differential scanning calorimetry thermogram obtained for acidic treated raffia palm fiber.

Initial degradation of RPFs started at 130°C and 96°C for alkali and acidic treated fibers respectively, with a broad endotherm that indicates the evaporation of water molecules in the fiber [182]. It also suggests that the fibers experienced glass transition stage at this peak temperatures [181]. The second decomposition stage (i.e. the two exothermic peaks) is due to the degradation of cellulosic substances such as hemi-cellulose and cellulose respectively [183]. The degradation process involves two distinct stages. The low temperature decomposition (first exothermic peak) observed in the temperature range 250°C - 300°C, can be attributed to the thermal degradation of the hemicelluloses – the least thermally stable lignocellulosic component. The second decomposition process (second exothermic peak) is observed in the temperature range 300°C – 400°C and can be attributed to the decomposition of cellulose [141]. The degradation temperature of hemicellulose and cellulose obtained in this study is in agreement with the results published by

Oliveira and D’Almeida [117]. They observed the presence of a broad endothermic peak between 110°C and 171°C which is due to the dehydration of water molecules in ubucu (*manicaria saccifera*) fiber. They also observed two exothermic peaks at 270°C and 360°C which was attributed to the thermal decomposition of hemicellulose and cellulose respectively.

Table 4.10. Thermal properties of untreated and treated raffia palm fibers obtained from differential scanning calorimetry analysis.

Sample	Enthalpy for the endothermic temperature (J/g)	Endothermic temperature (°C)	Hemi-cellulose degradation temperature (°C)	Cellulose degradation temperature (°C)
Untreated Fiber	60.45	131.48	275.18	352.09
NaOH Treated Fiber	63.17	141.87	294.44	361.70
H ₂ SO ₄ Treated Fiber	80.18	95.81	302.60	363.84

Deepa *et al.* [119] obtained similar results from the investigation of thermal properties of banana fiber; the degradation of the hemi-cellulose occurred at between 280°C and 290°C, followed by decomposition of cellulose around 340°C – 360°C. Aziz and Ansell [16] reported that chemical treatment increases the thermal stability of both kenaf and hemp fibers. It can be concluded from the results obtained in this study that the thermal stability of RPFs increased after the chemical treatment. The DSC results proved that RPFs have enhanced T_g, degradation temperature of hemi-cellulose and cellulose, making them less prone to degradation during composite processing at higher temperatures compared to non-treated fibers.

4.2 Characterization of RPF Reinforced Polymer Composite

To fully understand the behaviour of the composites containing different fiber weight fractions mechanical, physical and thermal tests were performed on the developed composites.

4.2.1 The Effect of Fiber Addition on the Density of High Density Polyethylene

The effects of the addition of non-treated and treated RPFs on the density of the HDPE matrix are presented in Fig. 4.23 (and Table C.1 in Appendix C). The addition of RPFs increased the density of HDPE slightly. For instance, a 2% increase in density was observed when HDPE was reinforced with 5 wt.% untreated RPFs, while an increase of 6% was obtained when 30 wt.% fiber was added.

Irrespective of whether the raffia palm fibers were chemically treated or not, the density of the composite increased as the fiber weight fraction in the composite increased. The increase in the density of HDPE composites for all fiber wt.% is due to the higher density of the untreated fiber (1.50 g/cm^3), alkali treated fiber (1.53 g/cm^3) and H_2SO_4 treated fiber (1.52 g/cm^3) compared to HDPE (0.96 g/cm^3). However, statistical results (Table C.2 in Appendix C) shows that the effect of various levels of fiber wt.% depends on the treatment that was done. It also reveals that there is a statistically significant interaction between the different fiber wt.% and treatment done on the density of the composite.

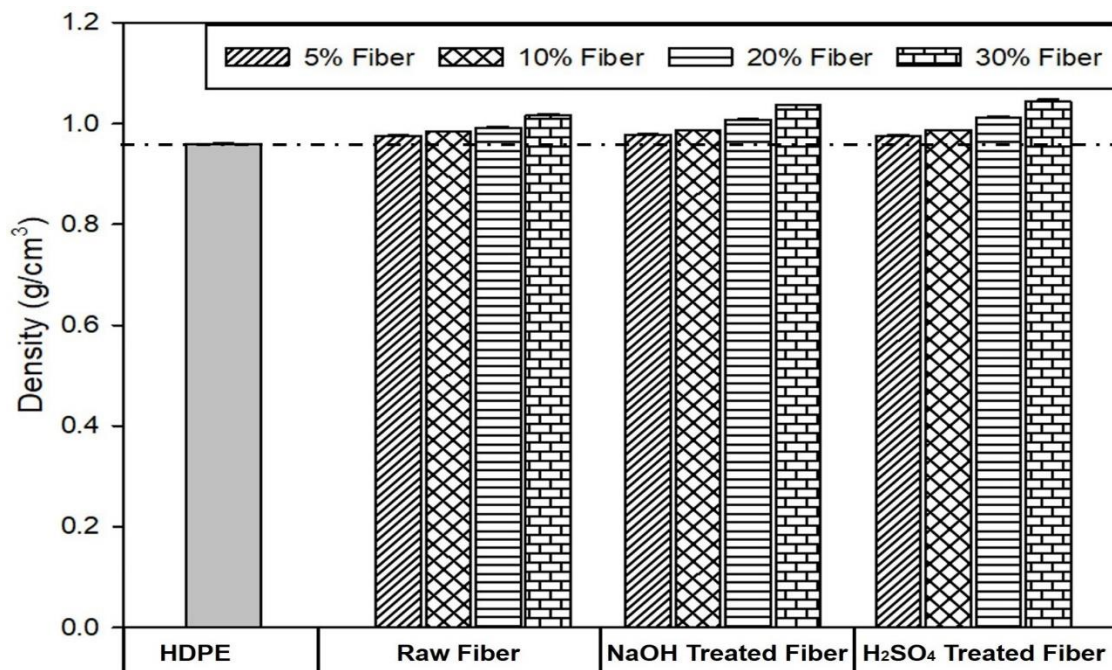


Figure 4.23. Effect of fiber content and chemical treatment on the bulk density of raffia palm fiber reinforced high density polyethylene composites.

Applying the rule of mixture, the weight fractions of the fiber was converted into volume fraction using equation 4.2 [184]. It is believed that the individual materials contribute independently to the overall density of the composite, in proportion to its volume fraction. Therefore, the density of the composite was calculated using equation 4.3 [2]:

$$V_F = \frac{W_F}{W_F + (1 - W_F) \frac{\rho_F}{\rho_m}} \quad 4.2$$

$$\rho_C = \rho_m V_m + \rho_F V_F \quad 4.3$$

Where W_F is the weight fraction of the fiber, ρ_C , ρ_m , ρ_F are the densities of the composite, matrix and fiber respectively, and V_m , V_F are volume fraction of the matrix and fibers respectively.

In Figs. 4.24 – 4.26, the experimentally obtained density of the composites and those calculated using the rule of mixture model (theoretical) are compared.

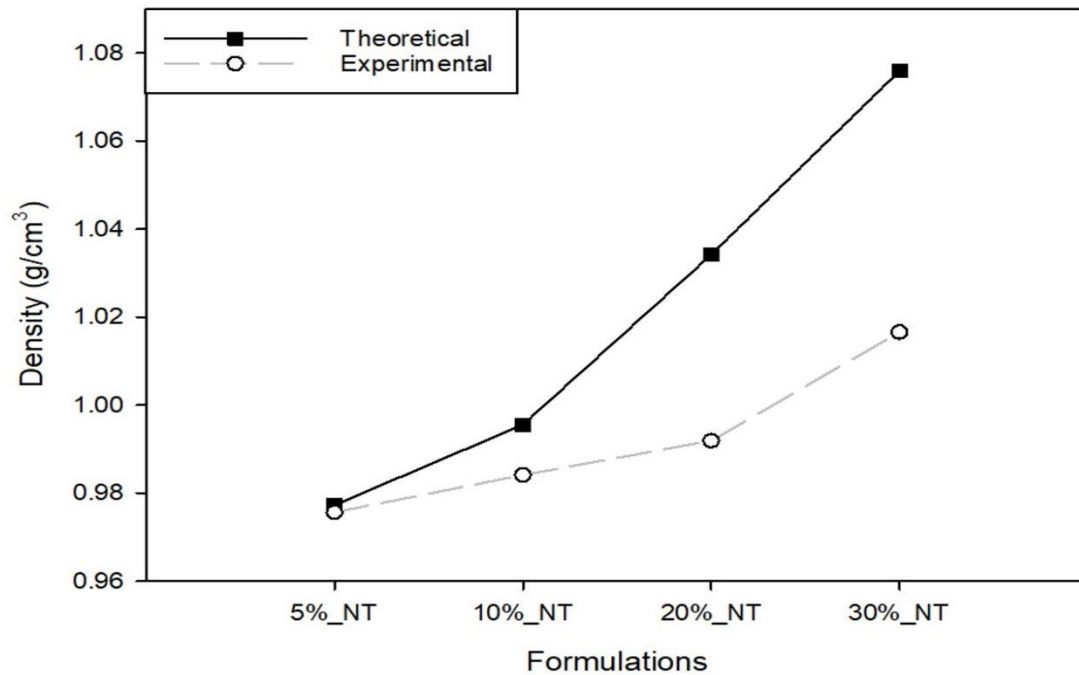


Figure 4.24. A comparison of the bulk densities of untreated raffia palm fiber reinforced high density polyethylene composites obtained from measurements and those determined from the rule of mixture.

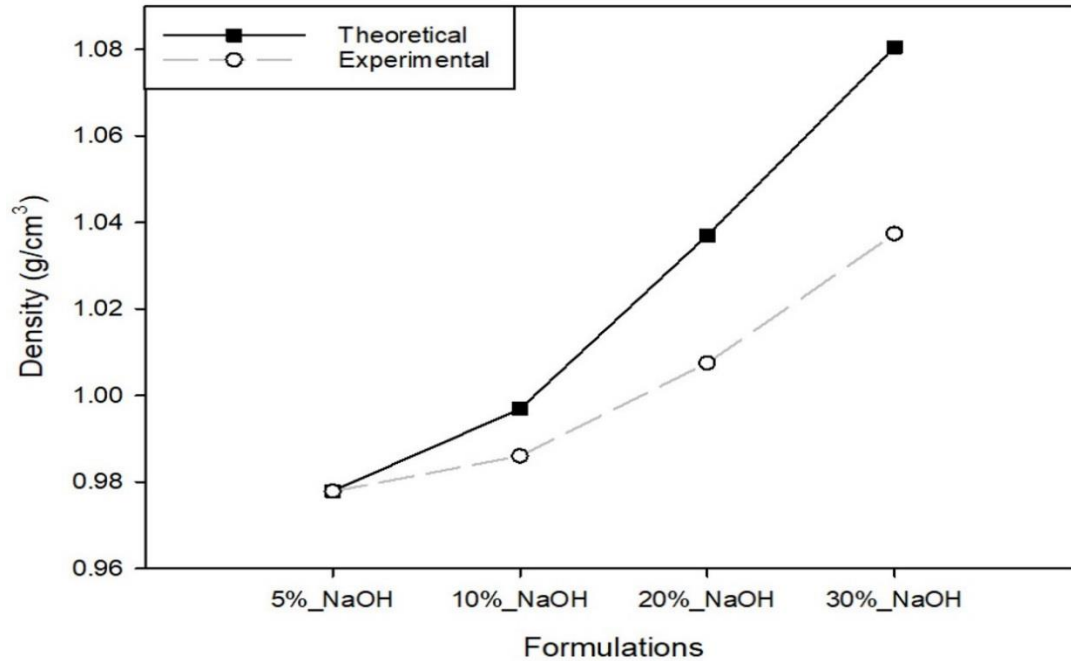


Figure 4.25. A comparison of the bulk densities of NaOH treated raffia palm fiber reinforced high density polyethylene composites obtained from measurements and those determined from the rule of mixture.

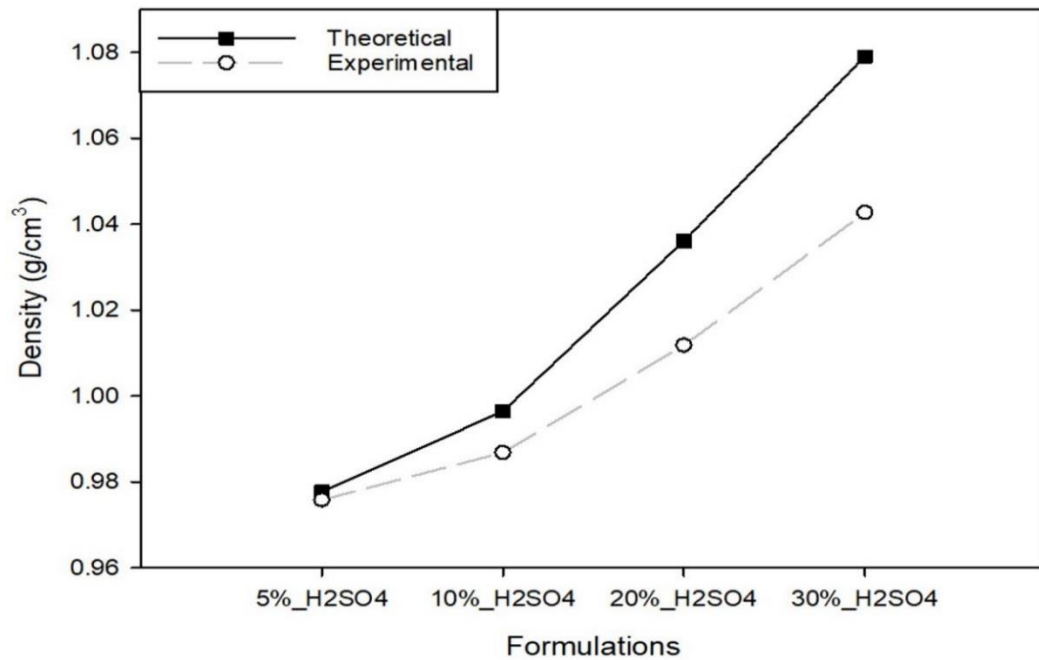


Figure 4.26. A comparison of the bulk densities of H₂SO₄ treated raffia palm fiber reinforced high density polyethylene composites obtained from measurements and those determined from the rule of mixture.

The rule of mixture predicts a larger increase in the density of the composites as fiber volume increased than that obtained from the experimental data.

4.2.2 Tensile Properties of Raffia Palm Fiber Reinforced HDPE

The results of the tensile test on the unreinforced and RPF reinforced HDPE are presented in Figs. 4.27 and 4.28 (and Table D.1 in Appendix D). The tensile strength of HDPE composites decreased with increasing amount of untreated and treated RPFs reinforcements. The reduction in tensile strength observed with fiber addition in this study is in agreement with the results published by Soleimani *et al.* [69] who reported a decreased in the tensile strength of a bio fiber (oat hull) reinforced PLA composites. Also, a reduced tensile strength was reported in flax fibers reinforced PLA and hemp fiber reinforced PP composites by Oksman *et al.* [185] and Hargitai *et al.* [186] respectively.

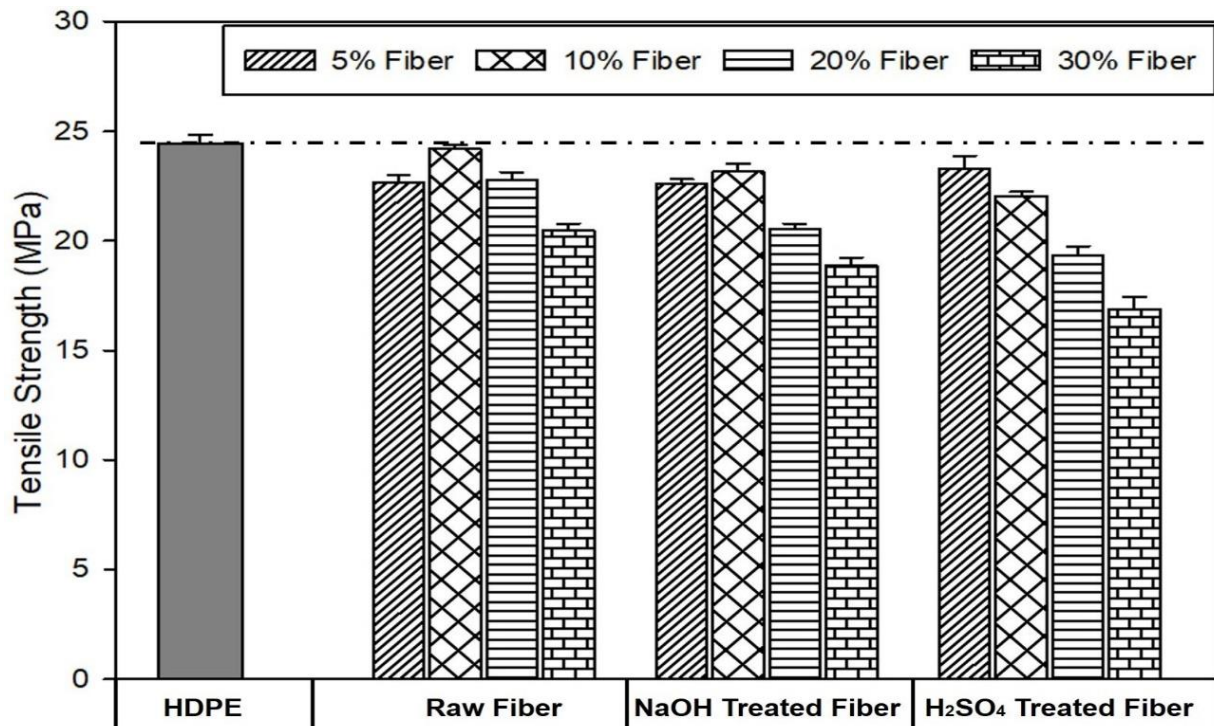


Figure 4.27. Effect of fiber content and chemical treatment on tensile strength of raffia palm fiber reinforced high density polyethylene composites.

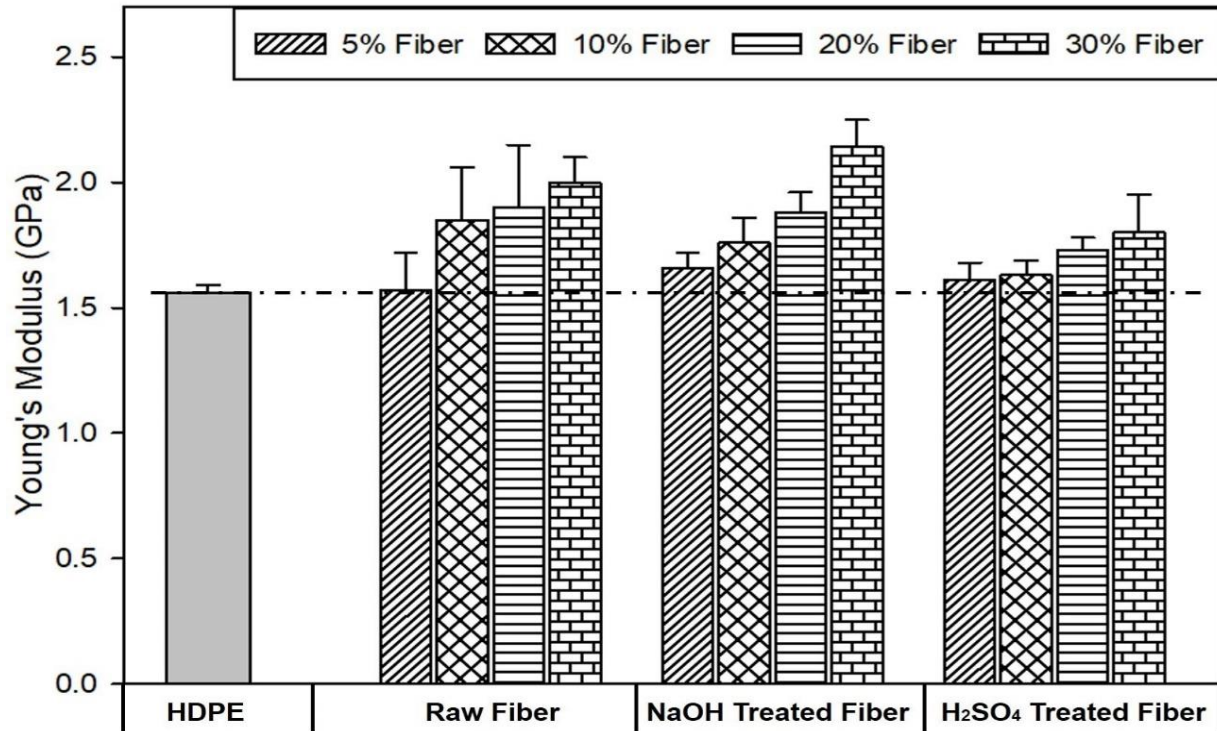


Figure 4.28. Effect of fiber content and chemical treatment on Young's modulus of raffia palm fiber reinforced high density polyethylene composites.

The decrease in tensile strength of the reinforced HDPE composites could be as a result of weak interface between the fibers and the polymer matrix, resulting in inefficient stress transfer from the matrix to the fibers [187]. It could also be due to weakening of fiber strength during fabrication of the composites at the processing temperature of 170°C.

Although the tensile strength of HDPE composites decreased with the addition of untreated and treated RPFs, a modest increase in the stiffness was observed (Figs. 4.24 – 4.25). Also, increase in the stiffness of HDPE composite was observed as both the untreated and treated fiber weight fraction was increased from 5 to 30 %. The increase in the stiffness of the composites as the fiber content increased can be attributed to the stiffness of the fibers [170]. The high stiffness of untreated and treated RPFs can be attributed to the high cellulose content, crystallinity index and low percent elongation of the fibers [151,160,188]. Thus, as the fiber content increases, a corresponding increase in stiffness of the composite is observed. Statistical analysis results (Tables D.2 and D.3 in Appendix D) shows that the effect of various levels of fiber wt.% depends on the

treatment that was done. It also reveals that there is a statistically significant interaction between the different fiber wt.% and treatment done on the tensile strength and Young's modulus of the composite. A similar study by Arrakhiz *et al.* [189] on the mechanical properties of LDPE composites shows that the addition of doum fibers enhanced the stiffness of the polymer matrix while the tensile strength decreased. Also, Hargitai *et al.* [186] reported an increase in the stiffness of polypropylene (PP) when reinforced with hemp fiber in comparison to unreinforced PP.

4.2.3 Fractography of Failed Tensile Specimens

SEM micrographs showing the fracture surfaces of the composites subjected to tensile loads are presented in Fig. 4.29. The failure modes included fiber pull-out, fiber splitting, debonding, and fiber fracture. The SEM micrograph (Figs. 29 a - b) shows that there are gaps between the polymer and untreated fibers which is an indication of poor bonding between the matrix and the fiber. As reported earlier (section 4.1.4), chemical treatments reduced the tensile strength of RPFs which led to weaker fibers. Therefore, the decrease in tensile strength of treated RPFs reinforced HDPE composites could be as a result of the low tensile strength reported for the treated fibers. Due to the low tensile strength of the treated fibers, the fracture failure [as shown in Figs. 4.29 (c-e)] of the treated fibers reinforced HDPE composite was mainly due to fiber fracture and splitting. Also at higher fiber content, the decrease in the tensile strength of HDPE composites could be as a result of inefficient stress transfer due to fiber agglomeration in the matrix [180].

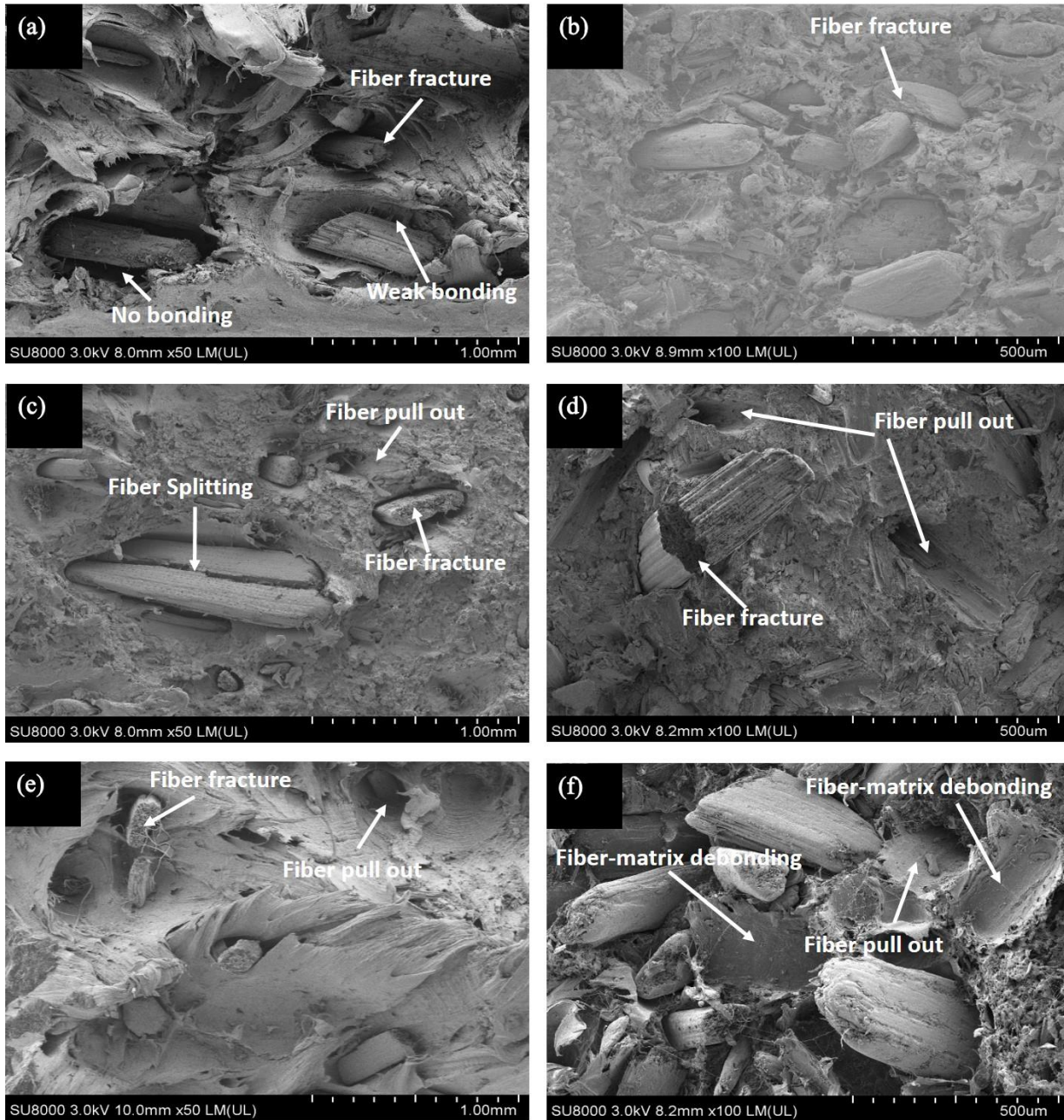


Figure 4.29. Scanning electron micrographs of fracture surfaces of tensile specimens of high density polyethylene composites reinforced with (a) 5 wt.% untreated, (b) 30 wt.% untreated, (c) 5 wt.% NaOH treated, (d) 30 wt.% NaOH treated, (e) 5 wt.% H₂SO₄ treated and (f) 30 wt.% H₂SO₄ treated raffia palm fibers.

4.2.4 The Effect of Fiber Reinforcement on the Flexural Properties of HDPE

The effect of RPFs reinforcement on the flexural strength and modulus of HDPE are presented in Figs. 4.30 and 4.31 (and Table E.1 in Appendix E). It can be observed that both flexural strength and modulus of HDPE increased by an average of 13% and 26%, respectively, when reinforced with 5 wt.% RPFs. The highest increase in flexural strength was obtained for composites containing 5 wt.% raffia palm fibers. On the other hand, an increase in the flexural modulus was observed as fiber content increased from 5 to 30 wt.% for both treated and untreated fibers. Statistical analysis results (Tables E.2 and E.3 in Appendix E) shows that the effect of various levels of fiber wt.% depends on the treatment that was done. It also reveals that there is a statistically significant interaction between the different fiber wt.% and treatment done on the flexural strength and modulus of the composite. Similar studies have shown that the flexural strength and modulus of polymers are enhanced with the addition of NFs. Yousif *et al.* [22] reported that both the flexural strength and modulus of epoxy increased by an average of 25% and 70% respectively with the addition of kenaf fibers. Also, Bledzki *et al.* [25] reported an increase in the flexural strength and modulus of PP reinforced with abaca fibers. Similar result was reported by Herrera-Franco and Valadez-Gonzalez [190] on henequen fiber reinforced HDPE composite. They reported an increase in the flexural strength and modulus as henequen fiber was added to the polymer.

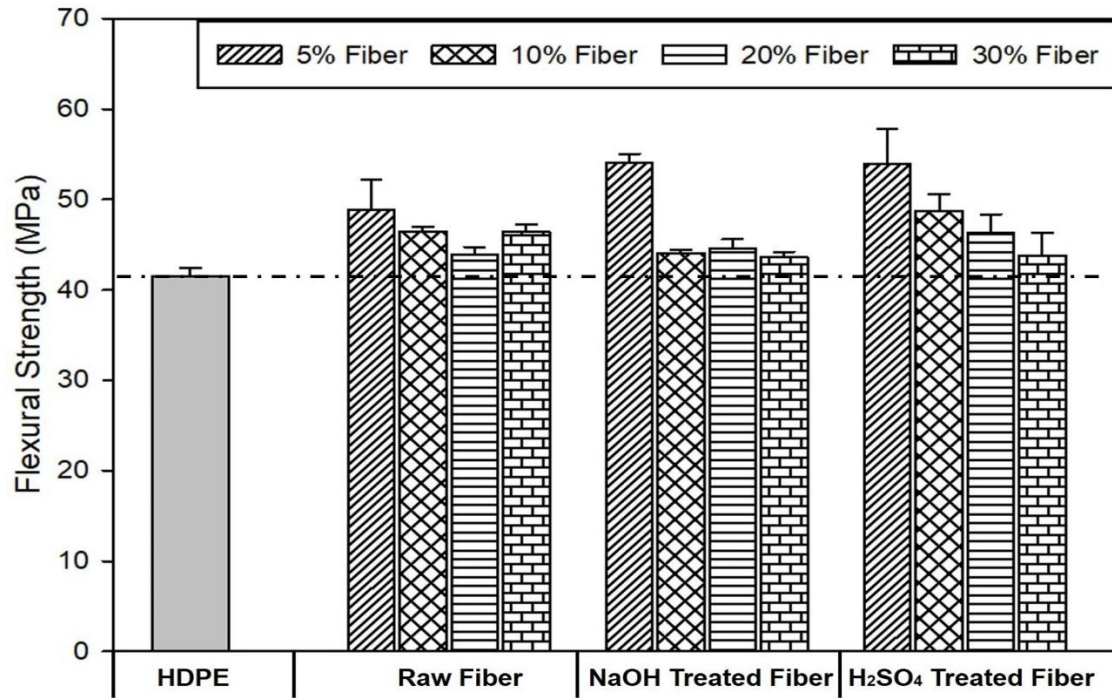


Figure 4.30. Effect of fiber content and fiber treatment on flexural strength of raffia palm fiber reinforced high density polyethylene matrix composites.

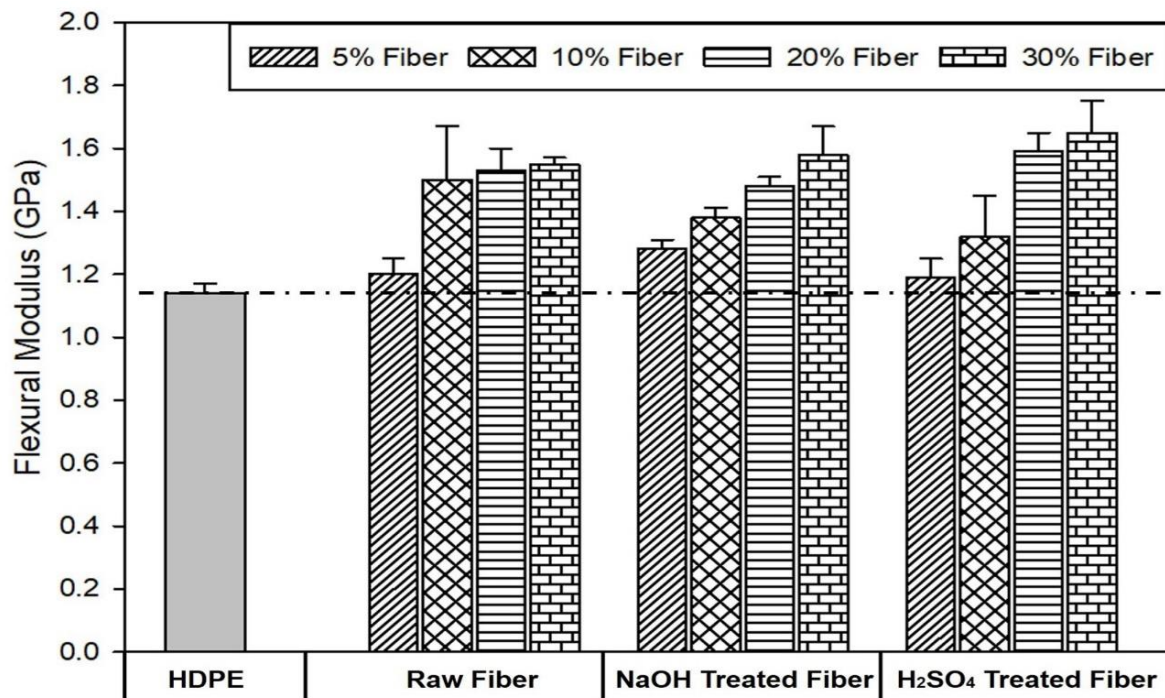


Figure 4.31. Effect of fiber content and fiber treatment on flexural modulus of raffia palm fiber reinforced high density polyethylene matrix composites.

4.2.5 The Effect of Fiber Addition on the Energy Absorbed of HDPE

The results of Charpy impact test on the unreinforced and RPF reinforced HDPE at room temperature, 0°C, -20°C, and -40°C are presented in Figs. 4.32 - 4.34 (and Table F.1 in Appendix F). The impact energy absorbed by the unreinforced HDPE and reinforced HDPE composites generally decreased with temperatures. For the composites, the impact energy absorbed also decreased with increasing fiber content at all test temperatures. Similar result of a decrease in the Charpy impact strength of flax fiber reinforced PLA composite was reported by Oksman *et al.* [185]. However, other studies have shown an increase in the impact strength of NFs reinforced polymer composites [14,25,26,69]. Soleimani *et al.* [69] reported that the impact strength of NFs reinforced polymer composite could be improved with the use of an impact modifier. They reported an increase in the impact strength of oat hull reinforced PLA composite with the use of polyurethane-based elastomer (21.5 kJ/m²) in comparison to unreinforced PLA (13 kJ/m²). At lower temperatures the composite material became more brittle, thereby absorbing low energy before fracture [25]. However, statistical results (Table F.2 in Appendix F) reveals that the effect of various levels of fiber wt.% does not depend on the treatment that was done. This shows that there is no statistically significant interaction between the different fiber wt.% and treatment done on the impact energy absorbed by the composite. It also reveals that the effect of various levels of fiber wt.% depends on the temperature. Therefore, there is a statistically significant interaction between the different fiber wt.% and temperature. Similarly, it also reveals that the effect of various treatments done on the fiber depends on the temperature. Therefore, there is a statistically significant interaction between the treatments performed on the fiber and temperature on the impact energy absorbed by the composite.

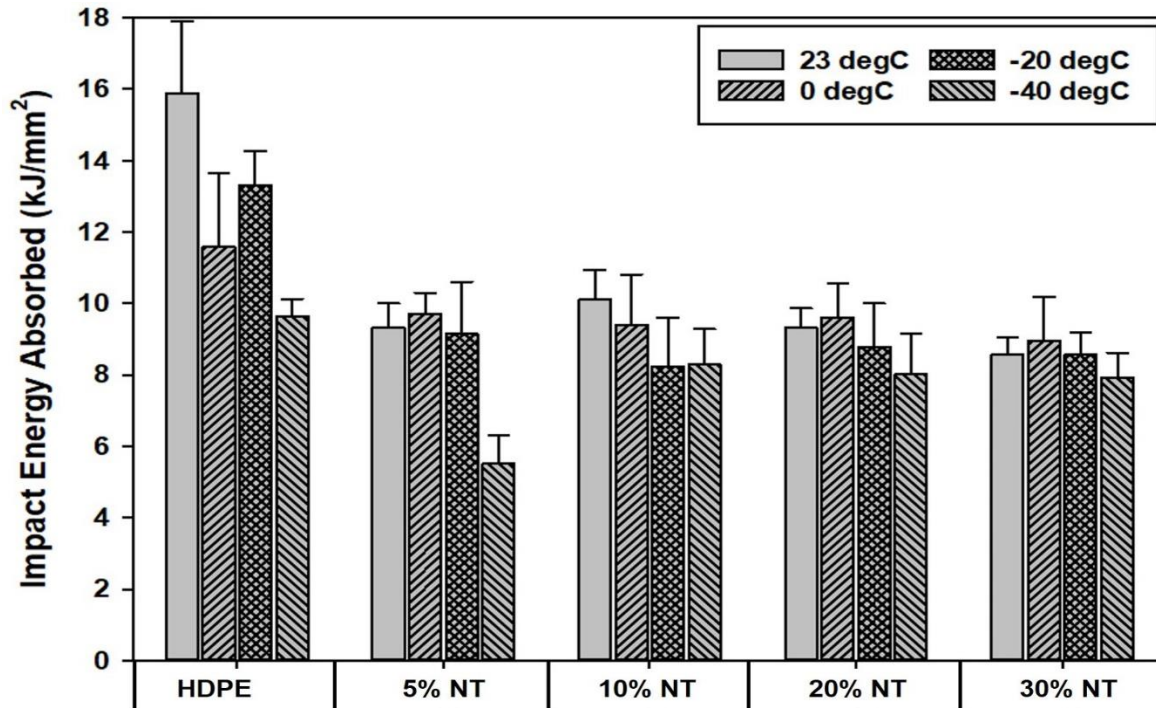


Figure 4.32. Effect of fiber content on the impact energy absorbed of high density polyethylene composites reinforced with untreated raffia palm fibers.

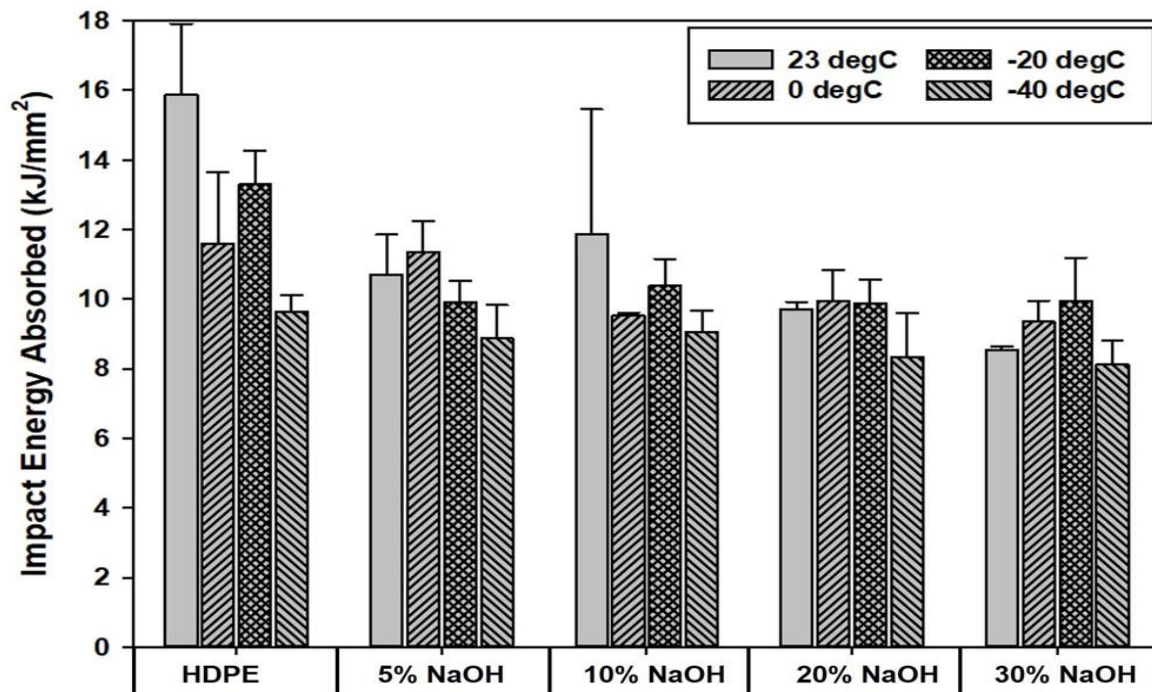


Figure 4.33. Effect of fiber content on the impact energy absorbed of high density polyethylene composites reinforced with NaOH treated raffia palm fibers.

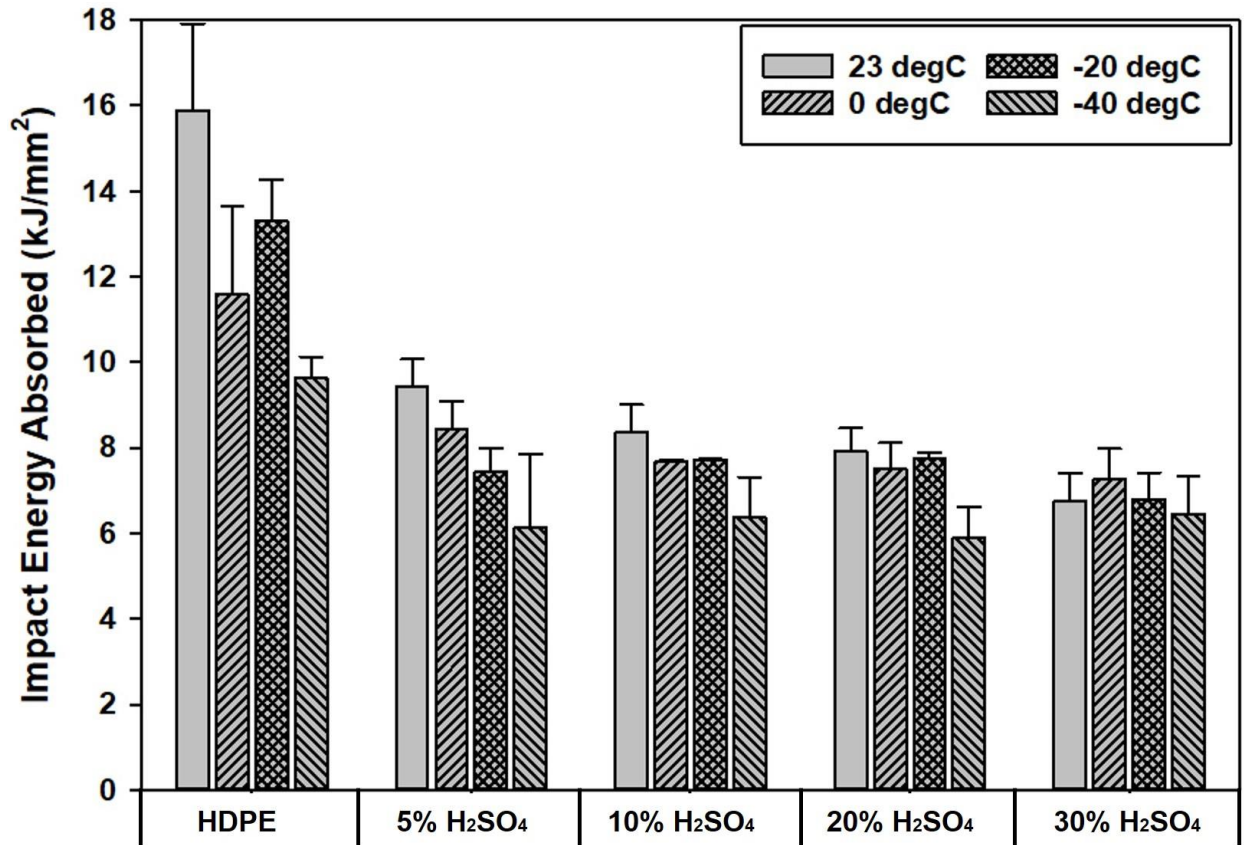


Figure 4.34. Effect of fiber content on the impact energy absorbed of high density polyethylene composites reinforced with H₂SO₄ treated raffia palm fibers.

4.2.6 SEM Analysis of Fractured Charpy Impact Samples

SEM micrographs showing the fracture surfaces of composites after fracturing during Charpy impact test at room temperature are presented in Fig. 4.35. Fiber pull-out from the matrix can be observed in the fractography. Meanwhile, as the fiber content increased, more fiber pull-out was observed. Fiber delamination and debonding from HDPE matrix were also observed (Fig. 4.35 c - f) in the composite reinforced with alkali and acid treated fibers. Similarly, as the fiber content increased to 30 wt.%, fiber breakages and debonding from HDPE matrix became more pronounced (Fig. 4.35 d and f). The increase in fiber pull-out and debonding in the composites containing high fiber content agrees with the low impact strength (Table F.1 in Appendix F) in comparison with the composite containing 5 wt.% fiber.

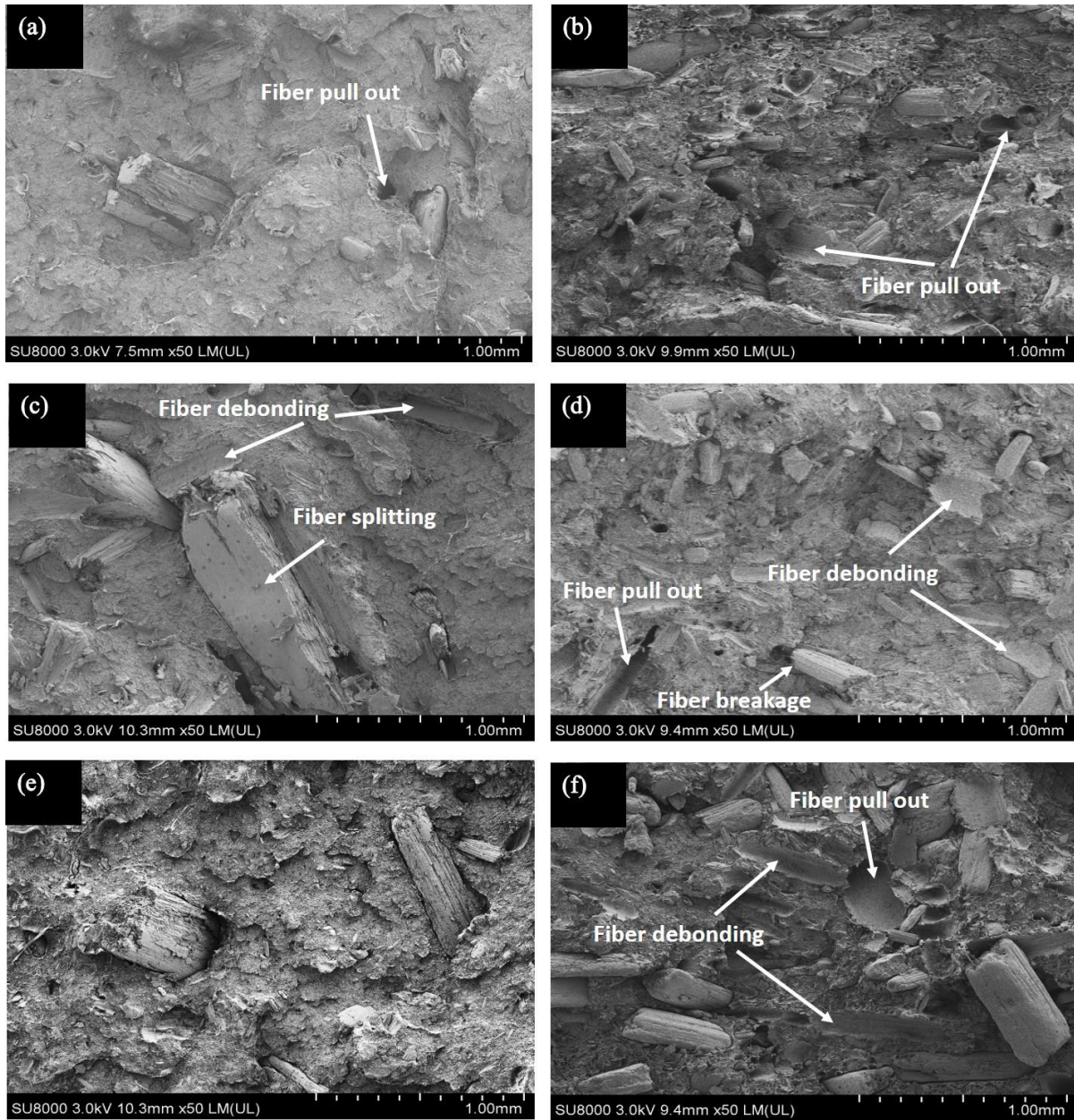


Figure 4.35. Scanning electron micrographs of charpy impact fracture surfaces at room temperature of high density polyethylene composites reinforced with (a) 5 wt.% untreated, (b) 30 wt.% untreated, (c) 5 wt.% NaOH treated, (d) 30 wt.% NaOH treated, (e) 5 wt.% H₂SO₄ treated and (f) 30 wt.% H₂SO₄ treated raffia palm fibers.

4.2.7 The Effect of Fiber Addition on Thermo-Physical Properties of HDPE

The results of thermal analysis of RPF reinforced HDPE composites using the DSC method are presented in Figs. 4.36 – 4.38 (and Table G.1 in Appendix G).

The addition of RPFs, whether treated or not, reduced the melting temperature of HDPE as shown in Fig 4.36. The reduction in melting temperature observed with fiber addition in this study is in agreement with the results published by Tajvidi and Takemura [191]. They reported a decrease in the melting temperature of kenaf fibers reinforced PP composites. Also, a reduction in the melting temperature was reported in flax fibers reinforced HDPE composites by Li *et al.* [9,74]. They reported the melting temperature of HDPE to be 139.3°C, which was found to decrease with the addition of flax fibers. The decrease in melting temperature of flax fibers reinforced HDPE composites was attributed to the fact that flax fiber requires low energy to be heated up in comparison to HDPE [106].

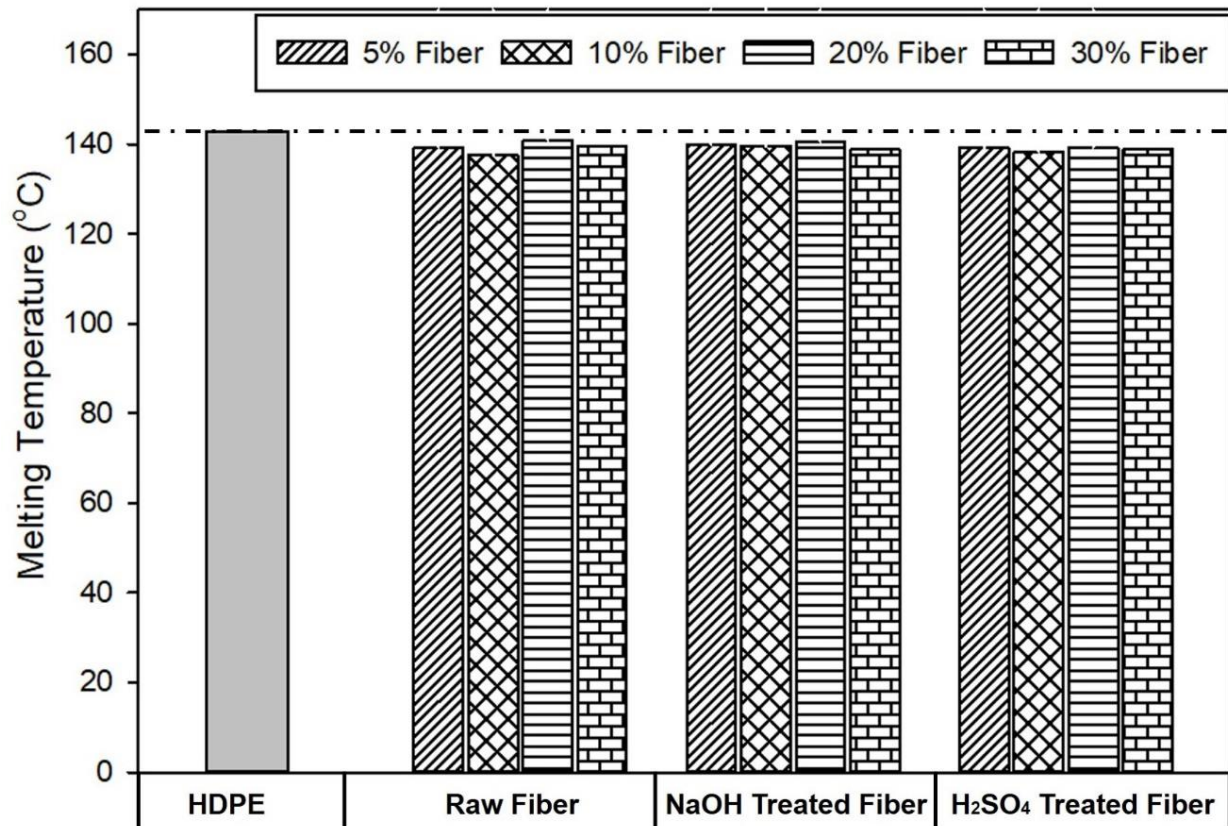


Figure 4.36. Effect of fiber content and fiber treatment on melting temperature of raffia palm fiber reinforced high density polyethylene matrix composites.

Although the addition of untreated and treated RPFs lowered the melting temperature of HDPE, there was a slight increase in the crystallization temperature in all cases as shown in Fig. 4.37. The increase in crystallization temperature obtained in this study is in agreement with the result

published by Arias *et al.* [192]. They reported an increase in the crystallization temperature of PLA with the addition of flax fibers. Crystallization peaks are due to re-arrangement of crystals in the polymer composites [193]. Since crystallization of molten polymers occurs by nucleation and growth processes [2], studies have shown that NFs are effective nucleation agents, thereby accelerating the crystallization process in polymer composites [191–194]. Heterogeneous nucleation sites are created in the composite material, which further increases the crystallization temperature of reinforced HDPE with the NFs acting as nucleating agents [195].

The effect of fiber addition on the fractional crystallinity (X_c) of unreinforced HDPE was also evaluated. The value of X_c was estimated using Equation 4.4 [141]:

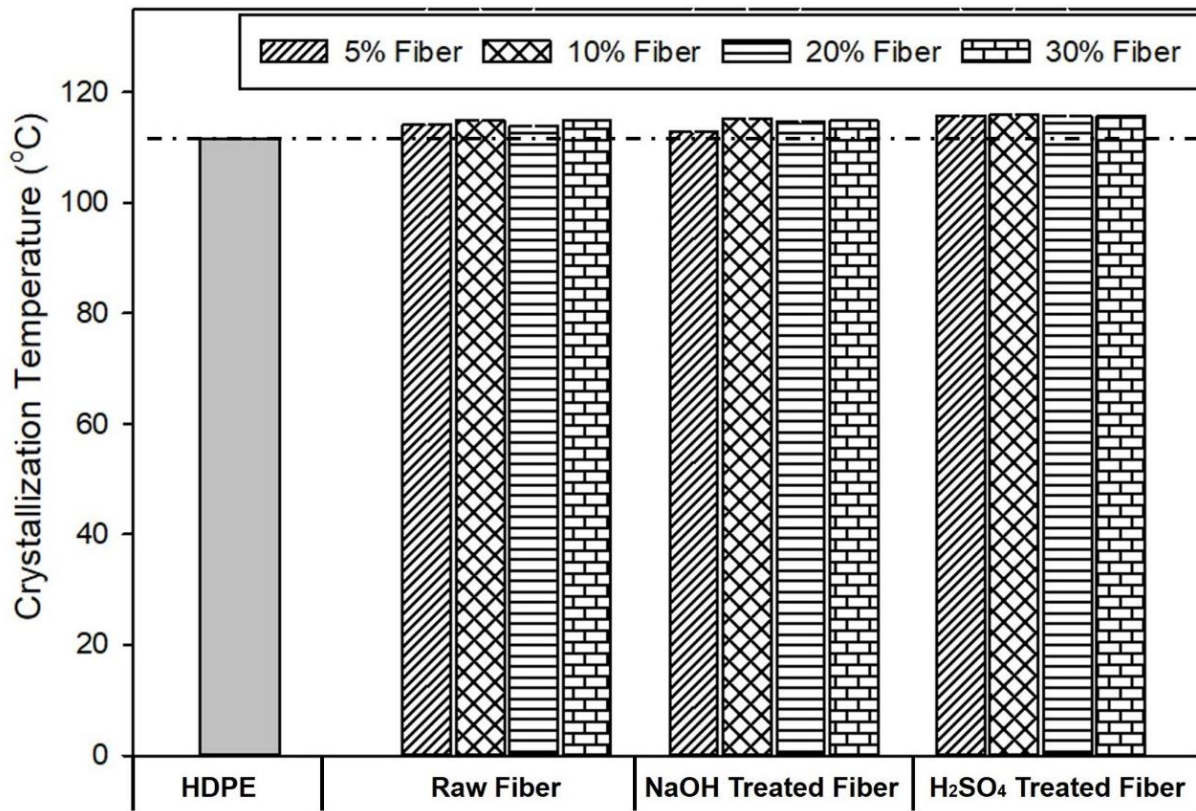


Figure 4.37. Effect of fiber content and fiber treatment on crystallization temperature of raffia palm fiber reinforced high density polyethylene matrix composites.

$$X_c(\%) = \frac{\Delta H_f}{\Delta H_{100} \times m} \times 100 \quad 4.4$$

where ΔH_f , m , ΔH_{100} , are respectively the heat of fusion of the sample, mass fraction of polymer in the composites and heat of fusion of 100% crystalline polymer. The ΔH_{100} value of HDPE is 290 J/g [196]. The heats of fusion of the samples were determined by integrating the areas under their respective melting peaks.

It was found that as the amount of RPFs increased, there was a slight increase in the crystallinity of the reinforced HDPE (Fig. 4.38). Due to the creation of heterogeneous nucleation sites, which resulted in an increase in the crystallization temperature of HDPE composites with the addition NFs, an increase in the crystallinity of the polymer was reported in other studies [197,198]. The increase in crystallinity obtained in this study agrees with the result published by Tajvidi and Takemura [191]. They reported an increase in the crystallinity of HDPE with the addition of kenaf fibers. Also, an increase in the crystallinity of PP with the addition of sisal fibers was reported by Ibrahim *et al.* [14].

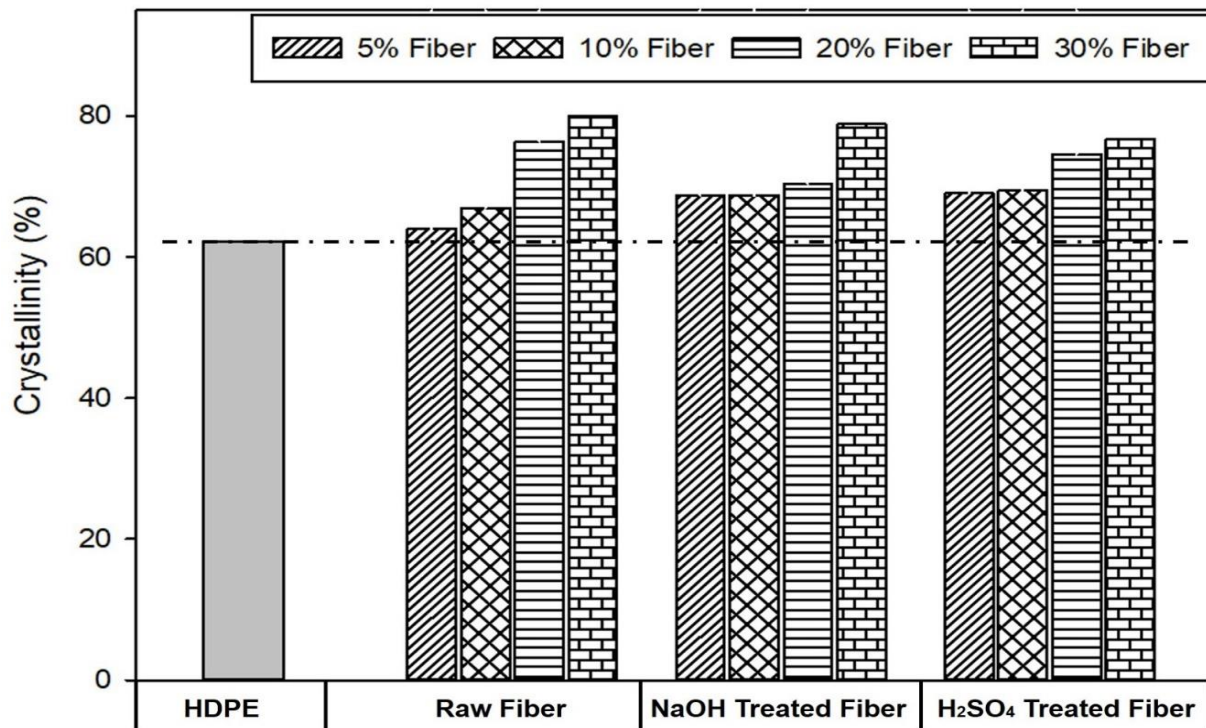


Figure 4.38. Effect of fiber content and fiber treatment on fractional crystallinity of raffia palm fiber reinforced high density polyethylene matrix composites.

4.2.8 The Influence of Fiber Addition on the Water Absorption Capacity of HDPE

The results of the investigation into water absorption of HDPE reinforced with untreated and treated RPFs are presented in Figs. 4.39 – 4.41 (and Table H.1 in Appendix H). It can be observed that the previous finding of a two-stage water saturation behaviour for non-treated (Fig. 4.8) and treated (Fig. 4.9) fibers also occurred in all composites specimens. The molded HDPE did not show a two-stage water saturation behaviour indicating that the water absorption behavior of the composites was controlled by the fibers. The first saturation level is practically the same for composites containing 5 – 20 wt.% untreated fibers. Water absorption at the second saturation stage also increased with increasing fiber content for composites reinforced with treated and untreated fibers. Previous studies have also shown that water uptake for NF reinforced thermoplastic composites increased with fiber content [10,99,101,102,199]. The amount of water absorbed in HDPE composites containing alkali and acidic treated fibers was lower than that of untreated fiber. A maximum value of 0.41, 0.36, and 0.31 wt.% water absorbed was observed for reinforced untreated, alkaline and acidic treated fibers HDPE composites respectively. The decrease in the amount of water absorbed in HDPE composite containing alkali and acidic treated fibers is due to the removal of hydroxyl groups in the hemicellulose of RPF after chemical treatments [29]. Jacob *et al.* [102] also observed that apart from the removal of non-cellulosic component in natural rubber composite reinforced with 4% NaOH chemically modified sisal fibers, increase in crystallinity of the treated fibers reduced the level of water absorbed by the composites. Chawla [57] also reported that increase in the degree crystallinity of the NF reinforced composites lowered the amount of water absorbed. The findings from these authors with the increase in fractional crystallinity of HDPE composites (section 4.2.8) agrees with the low water absorbed in HDPE composites containing treated fibers in comparison to untreated fibers.

Statistical analysis result (Table H.2 in Appendix H) shows that the effect of various levels of fiber wt.% depends on the treatment that was done. It also reveals that there is a statistically significant interaction between the different fiber wt.% and treatment done on the water absorption behaviour of the composite.

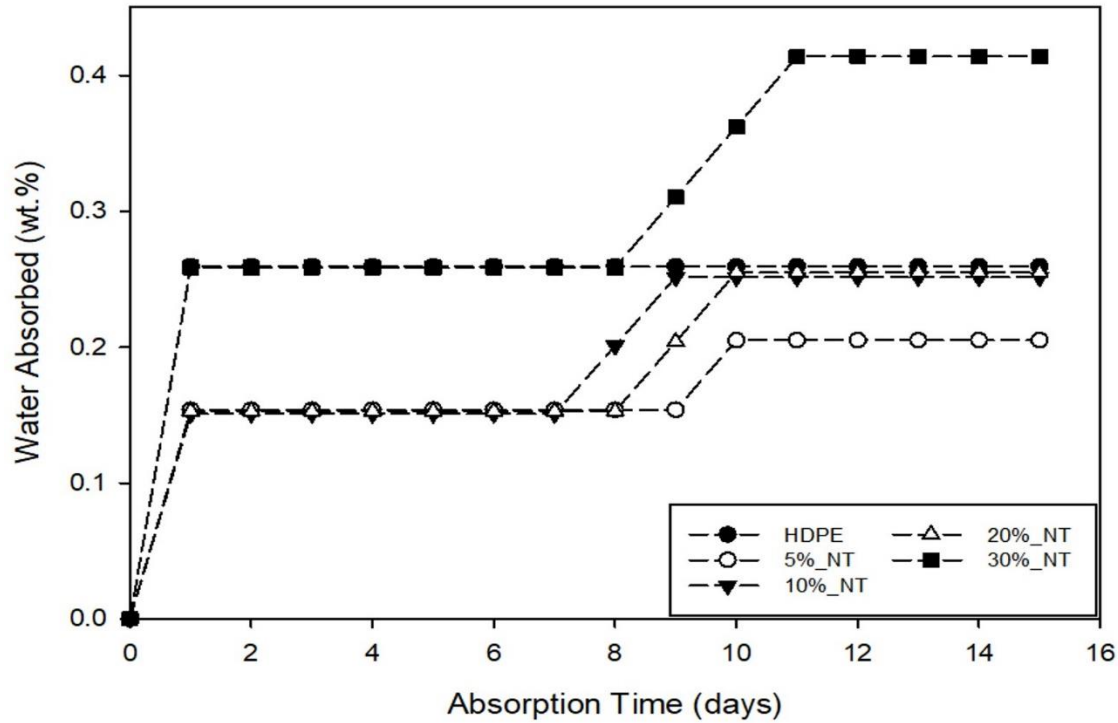


Figure 4.39. Effect of fiber content on the water absorption behaviour of high density polyethylene composites reinforced with untreated raffia palm fibers.

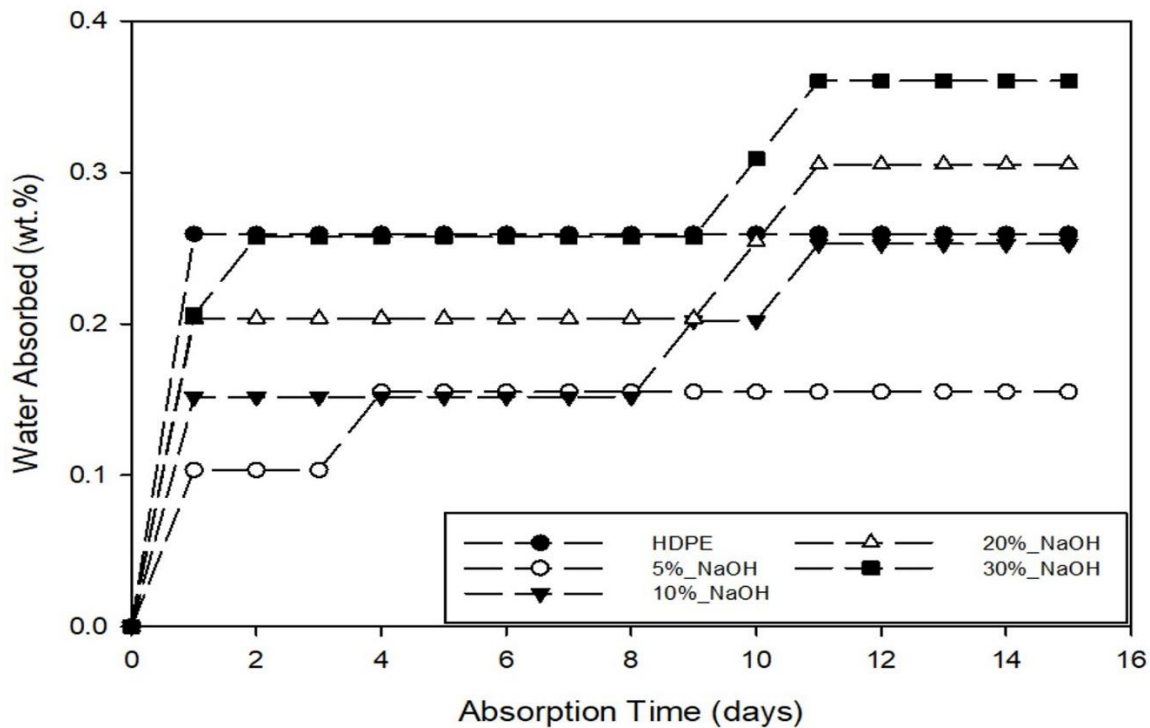


Figure 4.40. Effect of fiber content on the water absorption behaviour of high density polyethylene composites reinforced with of NaOH treated raffia palm fibers.

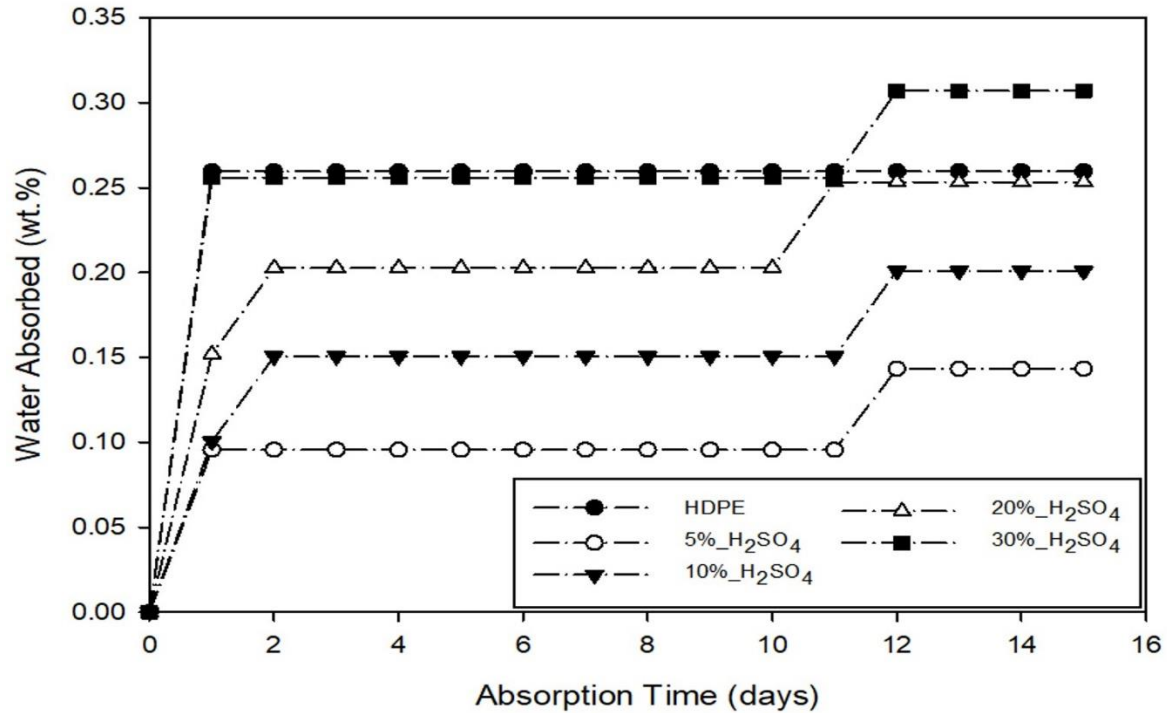


Figure 4.41. Effect of fiber content on the water absorption behaviour of high density polyethylene composites reinforced with H₂SO₄ treated raffia palm fibers.

It was also found (Figs. 4.39 – 4.41 and Table H.1) that HDPE absorbed more water than composites reinforced with 5%, 10% and 20% untreated and treated fibers. To ascertain why HDPE absorbed more water than 5%, 10% and 20% untreated and treated RPF reinforced HDPE composites, an unreinforced HDPE specimen was observed in the scanning electron microscope (Fig 4.42). As can be seen in Fig. 4.42, there are pores in the molded unreinforced HDPE plates. The presence of these pores could have increase the amount of water absorbed in unreinforced HDPE.

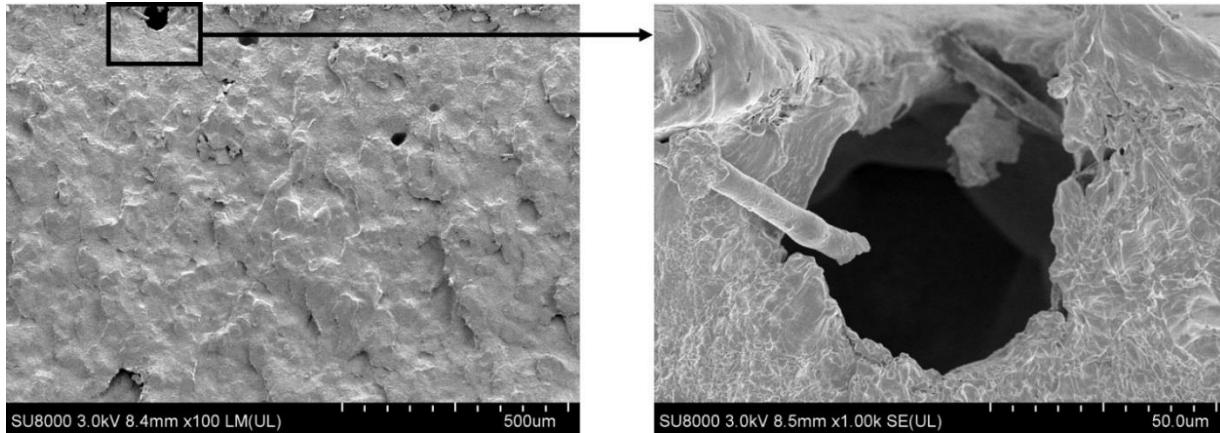


Figure 4.42. Typical scanning electron micrograph showing the presence of pores in high density polyethylene compression molded samples.

4.3 Summary

In this study, raffia palm fibers (RPFs) were characterized and chemically modified using alkaline and sulphuric acid treatment. The fibers were successfully incorporated into the HDPE polymer matrix while varying the weight percent of the fibers. The different formulation of HDPE/fiber mixtures were extruded using a twin-screw extruder for better dispersion of fiber into the polymer matrix, and then compression molded. The physical, mechanical and thermal properties of manufactured composites such as density, water absorption, tensile strength, Young's modulus, flexural strength, flexural modulus and charpy-impact strength were studied.

Scanning electron microscopic investigations of the fibers before and after treatment were carried out. The fiber microstructure features include central voids (lumens) and other fiber defect such as longitudinal cracks. RPFs have non-homogenous cross sections along the length of the fibre, and the variable fiber cross section accounts for the large variation in the determined tensile properties of the fibers. Also, the variable size and location of defects in the fiber cell wall affected the fracture behaviour of these fibers under tension.

Chemical analysis of alkaline treated fibers indicated an increase in the weight fraction of cellulose content in the fibers. Dilute sulfuric acid treatment eliminated the hemi-cellulose content which resulted in an increase in the weight fraction of the cellulose and lignin contents. Also, the chemically modified fibers address the major shortcoming in the use of RPFs in reinforcing

polymer matrix composite. It was observed that the water absorption of reinforced HDPE composites was influenced by the addition of fibers. Also, composites reinforced with sulphuric acid treated fibers showed the lowest water absorbed, in comparison to composites reinforced with alkali treated and non-treated fibers. The mechanical properties of HDPE reinforced composites (especially Young's modulus, flexural strength and flexural modulus) are higher than that of unreinforced HDPE.

CHAPTER 5

CONCLUSIONS AND RECOMMENDATIONS

In this research work, fiber reinforced polymer matrix composites were developed from raffia palm fibers and high-density polyethylene (HDPE) using extrusion and compression molding techniques. The mechanical and physical properties related to both the fiber and composites were investigated.

5.1 Conclusions

The following conclusions are made based on the experimental results and analysis of the data:

1. Chemical treatment of raffia palm fibers with NaOH and H₂SO₄ changed both the morphological and chemical properties of the fiber. The surfaces of the treated fiber are much cleaner than those of untreated fibers which suggests the removal of removed wax, oil and impurities from the surfaces of the fibers by the chemicals.
2. Structural changes occur in the non-cellulosic components of RPFs after alkali and acidic treatments as revealed by FTIRS and Raman. Certain chemical groups were removed upon chemical treatment, thereby rendering fewer hydroxyl groups in the fiber available for reactions.
3. The crystallinity index of the RPFs increase by chemical treatment. The highest crystallinity index of 89.7% was observed for the acid treated fiber.
4. DSC results showed an increase in the thermal degradation temperature of RPFs chemical composition in the treated fibers in comparison to untreated fiber.
5. An increase in the density of the composites was observed for both untreated, alkaline and acidic treated fibers. As the fiber content of the composites increased, there was a corresponding increase in the density of the composites. A 2% increase in density was observed when HDPE was reinforced with 5wt. % untreated RPFs, while an increase of 6% was obtained when 30 wt.% fiber was added.
6. Young's modulus, flexural strength, flexural modulus, water absorption capacity, and fractional crystallinity of HDPE composites increases as the fiber content of the composites is increased. In contrast, the tensile strength, charpy-impact strength and melting temperature of the composites decreased when compared with unreinforced HDPE.

5.2 Recommendations for Future Work

For future research work, the following recommendations are suggested:

1. NaOH and H₂SO₄ chemical treatments were used in this study to modify the surface chemistry of the fiber. Other treatments such as silane, acetylation, sodium chlorite, and the use of coupling agents such as maleic anhydride-polypropylene (MAPP), maleic anhydride grafted polyethylene (MA-g-PE) may also be considered. These treatments and couplings can further improve the interfacial adhesion in the composite.
2. Optimizing the processing conditions in extrusion molding technique may be investigated in future work, for example investigating the effect of extrusion screw speed between 120 and 170 rpm on composites performance.
3. Investigation the use of synchrotron Mid-IR to map the hemicellulose component of raffia palm fiber.

REFERENCES

1. Brigante, D. New Composite Materials: Selection, Design and Application. *Springer Int. Publ. Switz.* **2014**, 1–179, doi:10.1007/978-3-319-01637-5.
2. William D. Callister, J.; Rethwisch, D. G. Materials Science and Engineering: An Introduction 9E. *John Wiley Sons, Inc* **2014**, 9, 266–267.
3. J. Santhosh; N. Balanarasimman; R. Chandrasekar; Raja, S. Study of Properties of Banana Fiber Reinforced Composites. *Int. J. Res. Eng. Technol.* **2014**, 3, 144–150.
4. Thiruchitrambalam, M.; Athijayamani, A.; Sathiyamurthy, S.; Thaheer, A. S. A. A Review on the Natural Fiber-Reinforced Polymer Composites for the Development of Roselle Fiber-Reinforced Polyester Composite. *J. Nat. Fibers* **2010**, 7, 307–323.
5. Elenga, R. G.; Dirras, G. F.; Goma Maniongui, J.; Djemia, P.; Biget, M. P. On the microstructure and physical properties of untreated raffia textilis fiber. *Compos. Part A Appl. Sci. Manuf.* **2009**, 40, 418–422.
6. Mohammed, L.; Ansari, M. N. M.; Pua, G.; Jawaid, M.; Islam, M. S. A Review on Natural Fiber Reinforced Polymer Composite and Its Applications. *Int. J. Polym. Sci.* **2015**, doi:10.1155/2015/243947.
7. Holbery, J.; Houston, D. Natural-fibre-reinforced polymer composites in automotive applications. *Jom* **2006**, 58, 80–86.
8. Chinga-carrasco, G.; Aslan, M.; Sørensen, B. F.; Madsen, B. Strength variability of single flax fibres. *J. Mater. Sci.* **2011**, 46, 6344–6354.
9. Li, X.; Tabil, L. G.; Panigrahi, S.; Crerar, W. J. The Influence of Fiber Content on Properties of Injection Molded Flax Fiber-HDPE Biocomposites. *CSBE/SCGAB, Edmonton, AB Canada*, **2006**, doi:10.13031/2013.22101.
10. Arbelaz, A.; Fernández, B.; Ramos, J. A.; Retegi, A.; Llano-Ponte, R.; Mondragon, I. Mechanical properties of short flax fibre bundle/polypropylene composites: Influence of matrix/fibre modification, fibre content, water uptake and recycling. *Compos. Sci. Technol.* **2005**, 65, 1582–1592.
11. Aslan, M. Characterisation of Flax Fibres and Flax Fibre Composites: being cellulose based sources of materials. *Phd Thesis; Tech. Univ. Denmark* **2012**, 18–45.
12. Joseph, K.; Thomast, S.; Pavithran, C. Effect of chemical treatment on the tensile properties of short sisal fibre-reinforced polyethylene composites. *Polym.* **1996**, 37, 5139–5149.

13. Li, Y.; Mai, Y.-W.; Ye, L. Sisal fibre and its composites: a review of recent developments. *Compos. Sci. Technol.* **2000**, *60*, 2037–2055.
14. Ibrahim, I. D.; Jamiru, T.; Sadiku, R. E.; Kupolati, W. K.; Agwuncha, S. C. Dependency of the Mechanical Properties of Sisal Fiber Reinforced Recycled Polypropylene Composites on Fiber Surface Treatment, Fiber Content and Nanoclay. *J. Polym. Environ.* **2017**, *25*, 427–434.
15. Ouajai, S.; Shanks, R. A. Composition, structure and thermal degradation of hemp cellulose after chemical treatments. *Polym. Degrad. Stab.* **2005**, *89*, 327–335.
16. Aziz, S. H.; Ansell, M. P. The effect of alkalization and fibre alignment on the mechanical and thermal properties of kenaf and hemp bast fibre composites: Part 1 - polyester resin matrix. *Compos. Sci. Technol.* **2004**, *64*, 1219–1230.
17. Elkhaoulani, A.; Arrakhiz, F. Z.; Benmoussa, K.; Bouhfid, R.; Qaiss, A. Mechanical and thermal properties of polymer composite based on natural fibers: Moroccan hemp fibers/polypropylene. *Mater. Des.* **2013**, *49*, 203–208.
18. Khan, F.; Ahmad, S. R. Chemical modification and spectroscopic analysis of jute fibre. *Polym. Degrad. Stab.* **1996**, *52*, 335–340.
19. Corrales, F.; Vilaseca, F.; Llop, M.; Girones, J.; Mendez, J. A.; Mutje, P. Chemical modification of jute fibers for the production of green-composites. *J. Hazard. Mater.* **2007**, *144*, 730–735.
20. Pujari, S.; Ramakrishna, A.; Kumar, M. S. Comparison of Jute and Banana Fiber Composites : A Review. *Int. J. Curr. Eng. Technol.* **2014**, 121–126, doi:10.14741/ijcet/spl.2.2014.22.
21. Edeerozey, A. M. M.; Akil, H. M.; Azhar, A. B.; Ariffin, M. I. Z. Chemical modification of kenaf fibers. *Mater. Lett.* **2007**, *61*, 2023–2025.
22. Yousif, B. F.; Shalwan, A.; Chin, C. W.; Ming, K. C. Flexural properties of treated and untreated kenaf/epoxy composites. *Mater. Des.* **2012**, *40*, 378–385.
23. El-Shekeil, Y. A.; Sapuan, S. M.; Abdan, K.; Zainudin, E. S. Influence of fiber content on the mechanical and thermal properties of Kenaf fiber reinforced thermoplastic polyurethane composites. *Mater. Des.* **2012**, *40*, 299–303.
24. Cai, M.; Takagi, H.; Nakagaito, A. N.; Li, Y.; Waterhouse, G. I. N. Effect of alkali treatment on interfacial bonding in abaca fiber-reinforced composites. *Compos. Part A Appl. Sci.*

- Manuf.* **2016**, *90*, 589–597.
25. Bledzki, A. K.; Mamun, A. A.; Faruk, O. Abaca fibre reinforced PP composites and comparison with jute and flax fibre PP composites. *Express Polym. Lett.* **2007**, *1*, 755–762.
 26. Punyamurthy, R.; Sampathkumar, D. Abaca Fiber Reinforced Epoxy Composites : Evaluation of Impact Strength. *Int. J. Sci. Basic Appl. Res.* *4531*, 305–317.
 27. Ronald Aseer, J.; Sankaranarayananasamy, K.; Jayabalan, P.; Natarajan, R.; Priya Dasan, K. Morphological, Physical, and Thermal Properties of Chemically Treated Banana Fiber. *J. Nat. Fibers* **2013**, *10*, 365–380.
 28. Mathura, N.; Cree, D. Characterization and mechanical property of Trinidad coir fibers. *J. Appl. Polym. Sci.* **2016**, 1–9, doi:10.1002/app.43692.
 29. Mir, S. S.; Hasan, M.; Hasan, S. M. N.; Hossain, M. J.; Nafsin, N. Effect of Chemical Treatment on the Properties of Coir Fiber Reinforced Polypropylene and Polyethylene Composites. *Polym. Compos.* **2015**, 1259–1265, doi:10.1002/pc.
 30. S, J.; Deka, H.; Varghese, T. O.; Nayak, S. K. Recent Development and Future Trends in Coir Fiber-Reinforced Green Polymer Composites: Review and Evaluation. *Polym. Compos.* **2016**, *37*, 3296–3309.
 31. Lavoratti, A.; Romanzini, D.; Amico, S. C.; Zattera, A. J. Influence of Fibre Treatment on the Characteristics of Buriti and Ramie Polyester Composites. *Polym. Polym. Compos.* **2017**, *25*, 247–256.
 32. Zhang, Y.; Wen, B.; Cao, L.; Li, X.; Zhang, J. Preparation and properties of unmodified ramie fiber reinforced polypropylene composites. *J. Wuhan Univ. Technol. Sci. Ed.* **2015**, *30*, 198–202.
 33. Barkoula, N. M.; Alcock, B.; Cabrera, N. O.; Peijs, T. Fatigue properties of highly oriented polypropylene tapes and all-polypropylene composites. *Polym. Polym. Compos.* **2008**, *16*, 101–113.
 34. File:Afro asiatic peoples nigeria.png - Wikimedia Commons Available online: https://commons.wikimedia.org/wiki/File:Afro_asiatic_peoples_nigeria.png (accessed on Nov 28, 2017).
 35. Free Stock Photo 117-palm_trees_2928.JPG | freeimageslive Available online: https://www.freeimageslive.co.uk/free_stock_image/palmtrees2928jpg (accessed on Nov 28, 2017).

36. The map of Nigeria Available online: <https://thesheet.ng/at-last-apc-bows-to-pressure-to-setup-committee-on-restructuring-nigeria-look/> (accessed on Oct 23, 2017).
37. Kocak, D.; Merdan, N.; Evren, O. B. Research into the specifications of woven composites obtained from raffia fibers pretreated using the ecological method. *Text. Res. J.* **2015**, *85*, 302–315.
38. Elenga, R. G.; Dirras, G. F.; Maniongui, J. G.; Mabilia, B. Thin-layer drying of *Raffia textilis* fiber. *BioResources* **2011**, *6*, 4135–4144.
39. Sandy, M.; Bacon, L. Tensile testing of raffia. *J. Mater. Sci. Lett.* **2001**, *20*, 529–530.
40. Anike, D.; Onuegbu, T.; Ogbu, I.; Alaekwe, I. The Effect of Alkali Treatment on the Tensile Behaviour and Hardness of *Raffia Palm Fibre Reinforced Composites*. *Am. J. Polym. Sci.* **2014**, *4*, 117–121.
41. Elenga, R. G.; Djemia, P.; Tingaud, D.; Chauveau, T.; Maniongui, J. G.; Dirras, G. Effects of Alkali Treatment on the Microstructure, Composition, and Properties of the *Raffia textilis* Fiber. *Bioresour. Peer-reviewed online J.* **2013**, *8*, 2934–2949.
42. Saba, O. S. Manufacture and Characterization of Fiber Reinforced Epoxy for Application in Cowling Panels of Recreational Aircraft. *MSc. Thesis; Univ. Saskatchewan, Saskatoon, Canada* **2014**, 116.
43. Harrigan, W. C. Commercial processing of metal matrix composites. *Mater. Sci. Eng. A* **1998**, *244*, 75–79.
44. Pickering, K. L. Properties and Performance of Natural Fibre Composites. *Woodhead Maney Publ. Limited, Cambridge, England, UK* **2011**.
45. Kaczmar, J. W.; Pietrzak, K.; Wlosinski, W. The production and application of metal matrix composite materials. *J. Mater. Process. Technol.* **2000**, *106*, 58–67.
46. Lee, W. S.; Sue, W. C. Dynamic Impact and Fracture Behaviour of Carbon Fiber Reinforced 7075 Aluminum Metal Matrix Composite. *J. Compos. Mater.* **2000**, *34*, 1821–1841.
47. Zhang, P.; Nie, X.; Henry, H.; Zhang, J. Preparation and tribological properties of thin oxide coatings on an Al383/SiO₂ metallic matrix composite. *Surf. Coatings Technol.* **2010**, *205*, 1689–1696.
48. Groover, M. P. Fundamentals of Modern Manufacturing: Materials, Processes, and Systems. *John Wiley Sons, Inc. Danvers, Massachusetts, USA* **2010**, *4*, 1025.
49. Lee, W. B.; Ralph, B.; Yuen, H. C. Materials Processing Technology The processing of

- metal matrix composites - an overview. *J. Mater. Process. Technol.* **1997**, *63*, 339-353.
50. Ralph, B.; Yuen, H. C.; Lee, W. B. The processing of metal matrix composites — an overview. *J. Mater. Process. Technol.* **1997**, *63*, 339–353.
 51. Sayuti, M.; Sulaiman, S.; Vijayaram, T. R.; Baharudin, B. T. H. T.; Arifin, M. K. A. Chapter 18: Manufacturing and Properties of Quartz (SiO₂) Particulate Reinforced Al-11.8% Si Matrix Composites. *Intech, Rijeka, Croat.* **2012**, 411–430, doi 10.5772/48095.
 52. Sulaiman, S.; Sayuti, M.; Samin, R. Mechanical properties of the as-cast quartz particulate reinforced LM6 alloy matrix composites. *J. Mater. Process. Technol.* **2008**, *201*, 731–735.
 53. Ejiiofor, J. U.; Reddy, R. G. Developments in the processing and properties of particulate Al-Si composites. *JOM* **1997**, *49*, 31–37.
 54. Salit, M. S.; Jawaid, M.; Bin, N.; Hoque, E. Manufacturing of Natural Fibre Reinforced Polymer Composites. *Springer Int. Publ. Cham, Switz.* **2015**, 393, doi:10.1007/978-3-319-07944-8.
 55. H.L. Rizkalla and A. Abdulwahed Some mechanical properties of metal-non metal Al-SiO₂ particulate composites. *J. Mater. Process. Technol.* **1996**, *56*, 398–403.
 56. Ertürk, A. T.; Şahin, M.; Aras, M. Tribological Behavior of SiC Particulate Reinforced AA5754 Matrix Composite Under Dry and Lubricated Conditions. *Trans. Indian Inst. Met.* **2017**, *70*, 1233–1240.
 57. Chawla, K. K. Composite Materials: Science and Engineering. *Springer Sci. New York, USA* **2013**, *3*, 533.
 58. Yang, J. S.; Park, Y. H.; Park, B. G.; Park, I. M.; Park, Y. H. Microstructure and mechanical properties of Alborex + SiC p / AS52 hybrid metal matrix composites. *Int. J. Cast Met. Res.* **2008**, *21*, 231–235.
 59. Campbell, F. C. Manufacturing Processes for Advanced Composites. *Elsevier Adv. Technol. Oxford, UK* **2003**.
 60. B. Terry and G. Jones Metal matrix composites. *Elsevier Adv. Technol. Mayf. House, Oxford UK* **1990**.
 61. Zhu, J.; Zhu, H.; Njuguna, J.; Abhyankar, H. Recent development of flax fibres and their reinforced composites based on different polymeric matrices. *Materials (Basel).* **2013**, *6*, 5171–5198.
 62. Jain, A.; Rastogi, D.; Chanana, B. Bast and leaf fibres : A comprehensive review. *Int. J.*

- Home Sci.* **2016**, 2, 313–317.
63. A. S. Singha and V. K. Thakur Mechanical properties of natural fibre reinforced polymer composites. *Indian Acad. Sci.* **2006**, 31, 1–6.
 64. Bledzki, A. K.; Gassan, J. Composites reinforced with cellulose based fibers. *Prog. Polym. Sci.* **1999**, 24, 221–274.
 65. Rowell, R.; Pettersen, R.; Tshabalala, M. Handbook of Wood Chemistry and Wood Composites: Cell Wall Chemistry. *CRC Press. Taylor Fr. Group, Boca Raton, Florida, USA* **2012**, 35–74, doi:10.1201/b12487-5.
 66. Chang Hong, R. wood A Review on Natural Fibre- Based Composites-Part I: Structure, Processing and Properties of Vegetable Fibres. *J. Nat. Fibers* **2004**, 1, 37–41.
 67. Möller, J. Gravimetric Determination of Acid Detergent Fiber and Lignin in Feed: Interlaboratory Study. *J. AOAC Int.* **2009**, 92, 74–90.
 68. Fay, J. P.; Guaita, M. S.; Danelón, J. L.; Chifflet, S.; Wawrzkievicz, M.; Fernández, H. M.; Ross, D. A. Evaluation of Two Procedures to Determine Acid and Neutral Detergent Fibers in Ruminant Feeds of the Temperate Region of Argentina. *J. AOAC Int.* **2005**, 88, 995–997.
 69. Soleimani, M.; Tabil, L. G.; Oguocha, I.; Fung, J. Interactive Influence of Biofiber Composition and Elastomer on Physico-Mechanical Properties of PLA Green Composites. *J. Polym. Environ.* **2017**, 1–11, doi:10.1007/s10924-017-0967-8.
 70. Fiore, V.; Scalici, T.; Valenza, A. Characterization of a new natural fiber from *Arundo donax* L. as potential reinforcement of polymer composites. *Carbohydr. Polym.* **2014**, 106, 77–83.
 71. Grewal, R. K. Investigations on biocomposites from oat hull and biodegradable polymers. *MSc. Thesis; Univ. Saskatchewan, Saskatoon, Canada* **2015**, 1–55.
 72. Tibolla, H.; Pelissari, F. M.; Menegalli, F. C. Cellulose nanofibers produced from banana peel by chemical and enzymatic treatment. *LWT - Food Sci. Technol.* **2014**, 59, 1311–1318.
 73. Reddy, N.; Yang, Y. Structure and properties of natural cellulose fibers obtained from sorghum leaves and stems. *J. Agric. Food Chem.* **2007**, 55, 5569–5574.
 74. Li, X. Development of Flax Fiber Reinforced Polyethylene Biocomposites by Injection Molding. *Phd Thesis; Univ. Saskatchewan, Saskatoon, Canada* **2008**, 241.
 75. Soleimani, M.; Tabil, L.; Panigrahi, S.; Opoku, A. The effect of fiber pretreatment and compatibilizer on mechanical and physical properties of flax fiber-polypropylene

- composites. *J. Polym. Environ.* **2008**, *16*, 74–82.
76. Fadele, O.; Oguocha, I. N.; Odeshi, A.; Soleimani, M. (067) The effect of alkalization on properties of raffia palm fiber. *Proc. 26th CANSAM* **2017**, 6–9.
 77. Jin, W.; Singh, K.; Zondlo, J. Pyrolysis Kinetics of Physical Components of Wood and Wood-Polymers Using Isoconversion Method. *Agriculture* **2013**, *3*, 12–32.
 78. Ankom Technology Acid Detergent Fiber in Feeds - Filter Bag Technique. *Method 5* **2000**, 6–7.
 79. Ankom Technology Neutral Detergent Fiber in Feeds - Filter Bag Technique. *Method 6* **2011**, 10–11.
 80. Ankom Technology Determining Acid Detergent Lignin in Beakers. *Method 8* **2013**, 11–12.
 81. Buitrago, B.; Jaramillo, F.; Gomez, M. Some Properties of Natural Fibers (Sisal, Pineapple, and Banana) in Comparison to Man-Made Technical Fibers (Aramide, Glass, Carbon). *J. Nat. Fibers* **2015**, *12*, 357–367.
 82. Faruk, O.; Bledzki, A. K.; Fink, H. P.; Sain, M. Biocomposites reinforced with natural fibers: 2000-2010. *Prog. Polym. Sci.* **2012**, *37*, 1552–1596.
 83. Bledzki, A. K.; Gassan, J. Composites reinforced with cellulose based fibres. *Prog. Polym. Sci.* **1999**, *24*, 221–274.
 84. Tan, B.; Ching, Y.; Poh, S.; Abdullah, L.; Gan, S. A Review of Natural Fiber Reinforced Poly(Vinyl Alcohol) Based Composites: Application and Opportunity. *Polymers (Basel)*. **2015**, *7*, 2205–2222.
 85. Roe, P. J.; Ansell, M. P. Jute-reinforced polyester composites. *J. Mater. Sci.* **1985**, *20*, 4015–4020.
 86. Ernestina, M.; Fidelis, A.; Vitorino, T.; Pereira, C.; Dias, R.; Filho, T. The effect of fiber morphology on the tensile strength of natural fibers. *J. Mater. Res. Technol.* **2013**, *2*, 149–157.
 87. Bisanda, E. T. N.; Ansell, M. P. Properties of sisal-CNSL composites. *J. Mater. Sci.* **1992**, *27*, 1690–1700.
 88. Bledzki, A. K.; Gassan, J. Composites reinforced with cellulose based fibres. *Prog. Polym. Sci.* **1999**, *24*, 221–274.
 89. Charlet, K.; Jernot, J. P.; Gomina, M.; Bréard, J.; Morvan, C.; Baley, C. Influence of an

- Agatha flax fibre location in a stem on its mechanical, chemical and morphological properties. *Compos. Sci. Technol.* **2008**, *69*, 1399–1403.
90. Devi, L. U.; Bhagawan, S. S.; Thomas, S. Dynamic Mechanical Properties of Pineapple Leaf Fiber Polyester Composites. *Polym. Polym. Compos.* **2011**, *32*, 1741–1750.
 91. Mahjoub, R.; Yatim, J. M.; Mohd Sam, A. R.; Hashemi, S. H. Tensile properties of kenaf fiber due to various conditions of chemical fiber surface modifications. *Constr. Build. Mater.* **2014**, *55*, 103–113.
 92. Mallick, P. K. Fiber Reinforced Composites: Materials, Manufacturing and Design. *CRC Press. Florida, USA* **2008**, *3*, 619.
 93. Wallenberger, F. T.; Weston, N. Natural Fibers, Plastics and Composites. *Kluwer Acad. Publ. Massachusetts, USA* **2004**, 370.
 94. ASTM D2495-07 Standard Test Method for Moisture in Cotton by Oven-Drying. *ASTM Int. U.S.A* **2007**.
 95. Shahzad, A. A Study in Physical and Mechanical Properties of Hemp Fibres. *Adv. Mater. Sci. Eng.* **2013**, 1–10, doi: 10.1155/2013/325085.
 96. ASTM D2987/D2987M-11 Standard Test Method for Moisture Content of Asbestos Fiber. *ASTM Int. U.S.A* **2012**.
 97. Corporation, T. S. Model 1200 Humidity Generator. *Thunder Sci. New Mex.* **2017**.
 98. Reddy, N.; Yang, Y. Biofibers from agricultural byproducts for industrial applications. *Trends Biotechnol.* **2005**, *23*, 22–27.
 99. Mulinari, D. R.; Voorwald, H. J. C.; Cioffi, M. O. H.; Rocha, G. J.; Da Silva, M. L. C. P. Surface modification of sugarcane bagasse cellulose and its effect on mechanical and water absorption properties of sugarcane bagasse cellulose/ HDPE composites. *BioResources* **2010**, *5*, 661–671.
 100. Nabi, S. D.; Jog, J. P. Natural Fiber Polymer Composites : A Review. *Adv. Polym. Technol.* **1999**, *18*, 351–363.
 101. Espert, A.; Vilaplana, F.; Karlsson, S. Comparison of water absorption in natural cellulosic fibres from wood and one-year crops in polypropylene composites and its influence on their mechanical properties. *Compos. Part A Appl. Sci. Manuf.* **2004**, *35*, 1267–1276.
 102. Jacob, M.; Varughese, K. T.; Thomas, S. Water sorption studies of hybrid biofiber-reinforced natural rubber biocomposites. *Biomacromolecules* **2005**, *6*, 2969–2979.

103. Kabir, M. M.; Wang, H.; Lau, K. T.; Cardona, F. Chemical treatments on plant-based natural fibre reinforced polymer composites: An overview. *Compos. Part B Eng.* **2012**, *43*, 2883–2892.
104. T. Behzad; Sain, M. A Short Review on Rubber / Clay Nanocomposites With Emphasis on Mechanical Properties. *Polym. Eng. Sci.* **2007**, *47*, 21–25.
105. ASTM D5930-16 Standard Test Method for Thermal Conductivity of Plastics by Means of a Transient. *ASTM Int. U.S.A* **2017**.
106. Li, X.; Tabil, L. G.; Oguocha, I. N.; Panigrahi, S. Thermal diffusivity, thermal conductivity, and specific heat of flax fiber-HDPE biocomposites at processing temperatures. *Compos. Sci. Technol.* **2008**, *68*, 1753–1758.
107. Kalaprasad, G.; Pradeep, P.; Mathew, G.; Pavithran, C.; Thomas, S. Thermal conductivity and thermal diffusivity analyses of low-density polyethylene composites reinforced with sisal, glass and intimately mixed sisal/glass fibres. *Compos. Sci. Technol.* **2000**, *60*, 2967–2977.
108. Mangal, R.; Saxena, N. S.; Sreekala, M. S.; Thomas, S.; Singh, K. Thermal properties of pineapple leaf fiber reinforced composites. *Mater. Sci. Eng. A* **2003**, *339*, 281–285.
109. Loong, T. T.; Salleh, H. A review on measurement techniques of apparent thermal conductivity of nanofluids. *IOP Conf. Ser. Mater. Sci. Eng.* **2017**, *226*, doi:10.1088/1757-899X/226/1/012146.
110. Jiang, L.; Lu, Y. J.; Tang, K.; Wang, Y. D.; Wang, R.; Roskilly, A. P.; Wang, L. Investigation on heat and mass transfer performance of novel composite strontium chloride for sorption reactors. *Appl. Therm. Eng.* **2017**, *121*, 410–418.
111. Leena, M.; Srinivasan, S. A comparative study on thermal conductivity of TiO₂/ethylene glycol–water and TiO₂/propylene glycol–water nanofluids. *J. Therm. Anal. Calorim.* **2017**, 1–12, doi:10.1007/s10973-017-6616-6.
112. Zhang, D.; Zhao, Z.; Wang, B.; Li, S.; Zhang, J. Investigation of a new type of composite ceramics for thermal barrier coatings. *Mater. Des.* **2016**, *112*, 27–33.
113. Mounika, M.; Ramaniah, K.; Ratna Prasad, A. V.; Rao, K. M.; Hema Chandra Reddy, K. Thermal conductivity characterization of bamboo fiber reinforced polyester composite. *J. Mater. Environ. Sci.* **2012**, *3*, 1109–1116.
114. Alausa, S. K.; Oyesiku, O. O.; Aderibigbe, J. O.; Akinola, O. S. Thermal properties of

- Calamus deerratus , Raphia hookeri and synthetic board in building design in Southwestern Nigeria. *African J. Plant Sci.* **2011**, *5*, 281–283.
115. Kim, S. W.; Lee, S. H.; Kang, J. S.; Kang, K. H. Thermal conductivity of thermoplastics reinforced with natural fibers. *Int. J. Thermophys.* **2006**, *27*, 1873–1881.
 116. Damfeu, J. C.; Meukam, P.; Jannot, Y. Modeling and measuring of the thermal properties of insulating vegetable fibers by the asymmetrical hot plate method and the radial flux method: Kapok, coconut, groundnut shell fiber and rattan. *Thermochim. Acta* **2016**, *630*, 64–77.
 117. Oliveira, A. K. F.; d’Almeida, J. R. M. Characterization of ubuçu (*Manicaria saccifera*) natural fiber mat. *Polym. from Renew. Resour.* **2014**, *5*, 13–28.
 118. Rwawiire, S.; Tomkova, B. Morphological, Thermal, and Mechanical Characterization of *Sansevieria trifasciata* Fibers. *J. Nat. Fibers* **2015**, *12*, 201–210.
 119. Deepa, B.; Abraham, E.; Cherian, B. M.; Bismarck, A.; Blaker, J. J.; Pothan, L. A.; Leao, A. L.; de Souza, S. F.; Kottaisamy, M. Structure, morphology and thermal characteristics of banana nano fibers obtained by steam explosion. *Bioresour. Technol.* **2011**, *102*, 1988–1997.
 120. Tripathy, A. C. Characterization of Flax Fibres and the Effect of Different Drying Methods for Making Biocomposites. *MSc. Thesis; Univ. Saskatchewan, Saskatoon, Canada* **2009**, 124.
 121. Jähn, A.; Schröder, M. W.; Fütting, M.; Schenzel, K.; Diepenbrock, W. Characterization of alkali treated flax fibres by means of FT Raman spectroscopy and environmental scanning electron microscopy. *Spectrochim. Acta - Part A* **2002**, *58*, 2271–2279.
 122. Abril, D.; Abril, A. Ethanol from lignocellulosic biomass techno-economic.pdf. *Cienc. e Investig. Agrar.* **2009**, *36*, 177–190.
 123. Grewal, R. K.; Soleimani, M.; Tabil, L. G. Investigations on biocomposites from oat hull and biodegradable polymers. *Can. Soc. Bioeng.* **2015**, *15*, 1–9.
 124. Taherzadeh, M. J.; Karimi, K. *Pretreatment of lignocellulosic wastes to improve ethanol and biogas production: A review. Int J of Pol Sci*; 2008; *9*; doi: 10.3390/ijms9091621.
 125. Wang, B.; Panigrahi, S.; Tabil, L.; Crerar, W.; Sokansanj, S.; Braun, L. Modification of flax fibres by chemical treatment. *Can. Soc. Eng. Agric. Food Biol. Syst.* **2003**, *3*, 6–9.
 126. Zhou, F.; Cheng, G.; Jiang, B. Effect of silane treatment on microstructure of sisal fibers.

- Appl. Surf. Sci.* **2014**, 292, 806–812.
127. Gonzalez, A. V; Cervantes-Uc, J. M.; Olayo, R.; Herrera-Franco, P. J. Effect of fiber surface treatment on the fiber-matrix bond strength of natural fiber reinforced composites. *Compos. Part B Eng.* **1999**, 30, 309–320.
 128. Valadez-Gonzalez, A.; Cervantes-Uc, J.; Olayo, R.; Herrera-Franco, P. . Chemical modification of henequén fibers with an organosilane coupling agent. *Compos. Part B Eng.* **1999**, 30, 321–331.
 129. Paulo Aparecido dos Santos, J. C. G.; Amarasekera, J.; Moraes, G. Natural Fibers Plastic Composites for Automotive Applications. *SABIC Innov. Plast.* **2006**, 6, 1–9.
 130. Bürkle, E.; Scheel, G.; Darnedde, L. Energy-efficient processing of natural fiber-reinforced plastics. *Kunststoffe Int.* **2009**, 99, 25–29.
 131. S.M. Sapuan Y.A. El-Shekeil Fei-ling Pua, F. M. A.-O.; Sapuan, S. M.; Pua, F.; El-Shekeil, Y. A.; AL-Oqila, F. M. Mechanical properties of soil buried kenaf fibre reinforced thermoplastic polyurethane composites. *Mater. Des.* **2013**, 50, 467–470.
 132. Biron, M. Thermosets and Composites: Material Selection. Applications, Manufacturing and Cost Analysis. *Elsevier Publ. House, Oxford, UK* **2014**.
 133. Punyamurthy, R.; Sampathkumar, D.; Ranganagowda, R. P. G.; Bennehalli, B.; Srinivasa, C. V. Mechanical properties of abaca fiber reinforced polypropylene composites: Effect of chemical treatment by benzenediazonium chloride. *J. King Saud Univ. - Eng. Sci.* **2015**, 29, 289–294.
 134. Satya Panigrahi; Xue Li; Lope Tabil Injection moulding processing of flax fibre- reinforced polyethylene biocomposites. *Int. Conf. Flax Other Bast Plants* **2008**, 83, 399–407.
 135. Bagherpour, S. Chapter 6: Fibre Reinforced Polyester Composites. *Intech, Rijeka, Croat.* **2012**, 135–166, doi:10.5772/2748.
 136. Deng, H.; Reynolds, C. T.; Cabrera, N. O.; Barkoula, N.-M.; Alcock, B.; Peijs, T. The water absorption behaviour of all-polypropylene composites and its effect on mechanical properties. *Compos. Part B Eng.* **2010**, 41, 268–275.
 137. ASTM D570-98 ASTM D570 – 98 – Standard Test Method for Water Absorption of Plastics. *ASTM Int. U.S.A* **2014**.
 138. Susskind, L.; Jain, R. *Fiber Reinforced Polymer (FRP) Composites for Infrastructure Applications*; 2013; 55; ISBN 08956308.

139. Wang, W.; Sain, M.; Cooper, P. A. Study of moisture absorption in natural fiber plastic composites. *Compos. Sci. Technol.* **2006**, *66*, 379–386.
140. Dhakal, H. N.; Zhang, Z. Y.; Richardson, M. O. W. Effect of water absorption on the mechanical properties of hemp fibre reinforced unsaturated polyester composites. *Compos. Sci. Technol.* **2007**, *67*, 1674–1683.
141. Tajvidi, M.; Takemura, A. Thermal Degradation of Natural Fiber-reinforced Polypropylene Composites. *J. Thermoplast. Compos. Mater.* **2010**, *23*, 281–298.
142. Aydin, M.; Tozlu, H.; Kemaloglu, S.; Aytac, A.; Ozkoc, G. Effects of Alkali Treatment on the Properties of Short Flax Fiber-Poly (Lactic Acid) Eco-Composites. *J. Polym. Environ.* **2011**, *19*, 11–17.
143. Ku, H.; Wang, H.; Pattarachaiyakoop, N.; Trada, M. A review on the tensile properties of natural fiber reinforced polymer composites. *Compos. Part B Eng.* **2011**, *42*, 856–873.
144. ASTM D638-14 Standard Test Method for Tensile Properties of Plastics. *ASTM Int. U.S.A* **2014**.
145. ASTM D790-15 Standard Test Methods for Flexural Properties of Unreinforced and Reinforced Plastics and Electrical Insulating Materials. *ASTM Int. U.S.A* **2017**.
146. Mohammed, L.; Ansari, M. N. M.; Pua, G.; Jawaid, M.; Islam, M. S. A Review on Natural Fiber Reinforced Polymer Composite and Its Applications. *Int. J. Polym. Sci.* **2015**, doi:10.1155/2015/243947.
147. Mohanty, A. K.; Misra, M.; Drzal, L. T. *Natural Fibers, Biopolymers, and Biocomposites*; 2005; ISBN 978-0-8493-1741-5.
148. Dumas, P.; Miller, L. The use of synchrotron infrared microspectroscopy in biological and biomedical investigations. *Vib. Spectrosc.* **2003**, *32*, 3–21.
149. Yu, P.; McKinnon, J. J.; Christensen, C. R.; Christensen, D. A. Imaging molecular chemistry of pioneer corn. *J. Agric. Food Chem.* **2004**, *52*, 7345–7352.
150. ASTM D3822/D3822M-14 Standard Test Method for Tensile Properties of Single Textile Fibers. *ASTM Int. U.S.A* **2015**.
151. Sarikanat, M.; Seki, Y.; Sever, K.; Durmuşkahya, C. Determination of properties of *Althaea officinalis* L. (Marshmallow) fibres as a potential plant fibre in polymeric composite materials. *Compos. Part B Eng.* **2014**, *57*, 180–186.
152. Park, S.; Baker, J. O.; Himmel, M. E.; Parilla, P. A.; Johnson, D. K. Cellulose crystallinity

- index: measurement techniques and their impact on interpreting cellulase performance. *Biotechnol. Biofuels* **2010**, doi:10.1186/1754-6834-3-10.
153. Mohanta, N.; Acharya, S. Fiber surface treatment: Its effect on structural, thermal, and mechanical properties of *Luffa cylindrica* fiber and its composite. *J. Compos. Mater.* **2015**, doi:10.1177/0021998315615654.
 154. Turunen, M. J.; Saarakkala, S.; Rieppo, L.; Helminen, H. J.; Jurvelin, J. S.; Isaksson, H. Comparison between infrared and raman spectroscopic analysis of maturing rabbit cortical bone. *Appl. Spectrosc.* **2011**, *65*, 595–603.
 155. Schrader, B. *Infrared and Raman Spectroscopy: Methods and Applications*. VCH Publ. Inc., New York, USA **1995**, ISBN 3-527-26446-9.
 156. Blackwell, J.; Vasko, P. D.; Koenig, J. L. Infrared And Raman Spectra Of Native Cellulose From Cell Wall Of *Valonia Ventricosa*. *J. Appl. Phys.* **1970**, *41*, 4375–4379.
 157. ASTM D6110-10 Standard Test Method for Determining the Charpy Impact Resistance of Notched Specimens of Plastics. *ASTM Int. U.S.A* **2010**.
 158. Al-Bahadly, E. A. The Mechanical Properties of Natural Fiber Composites. *Phd Thesis; Swinburne Univ. Technol. Melbourne, Aust.* **2013**, 1–228.
 159. Jurgens, M. H.; Bregendahl, K. *Animal Feeding and Nutrition*. Kendall Hunt Publ. Co. **2007**, *10*, 100–105.
 160. Tran, L. Q. N.; Minh, T. N.; Fuentes, C. A.; Chi, T. T.; Van Vuure, A. W.; Verpoest, I. Investigation of microstructure and tensile properties of porous natural coir fibre for use in composite materials. *Ind. Crops Prod.* **2015**, *65*, 437–445.
 161. Wang, F.; Shao, J.; Keer, L. M.; Li, L.; Zhang, J. The effect of elementary fibre variability on bamboo fibre strength. *Mater. Des.* **2015**, *75*, 136–142.
 162. Cai, M.; Takagi, H.; Nakagaito, A. N.; Katoh, M.; Ueki, T.; Waterhouse, G. I. N.; Li, Y. Influence of alkali treatment on internal microstructure and tensile properties of abaca fibers. *Ind. Crops Prod.* **2015**, *65*, 27–35.
 163. Silva, F. de A.; Chawla, N.; Filho, R. D. de T. Tensile behavior of high performance natural (sisal) fibers. *Compos. Sci. Technol.* **2008**, *68*, 3438–3443.
 164. Cicala, G.; Cristaldi, G.; Latteri, A. Composites Based on Natural Fibre Fabrics. *Woven Fabr. Eng.* **2010**, 317–342, doi:10.5772/10465.
 165. Fangueiro, R.; Rana, S. *Natural Fibres : Advances in Science and Technology Towards*

- Industrial Applications. *Springer Nat.* **2015**, *12*, 37–43.
166. Kannan, R.; Anand, A. V.; Hariprasad, V.; Singh, R. A.; Jayalakshmi, S.; Arumugam, V. Effect of Cashew Nut Shell Oil (Cardanol) on Water Absorption and Mechanical Characteristics of Sisal Fibers. *Proc. Int. Conf. Recent Innov. Prod. Eng. MIT* **2017**, 91–92, ISBN: 978-93-86256-65-2.
 167. Sampathkumar, D.; Punyamurth, R.; Venkateshappa, S. C. Effect of Chemical Treatment on Water Absorption of Areca Fiber. *J. Appl. Sci. Res.* **2012**, *8*, 5298–5305.
 168. Mukherjee, P. S.; Satyanarayana, K. G. Structure and properties of some vegetable fibres. *J. Mater. Sci.* **1984**, *19*, 3925–3934.
 169. Tomczak, F.; Satyanarayana, K. G.; Sydenstricker, T. H. D. Studies on lignocellulosic fibers of Brazil : Part III – Morphology and properties of Brazilian curaua fibers. *Compos. Part A Appl. Sci. Manuf.* **2007**, *38*, 2227–2236.
 170. Obasi, H. C. Properties of raphia palm interspersed fibre filled high density polyethylene. *Adv. Mater. Sci. Eng.* **2013**, 2–6, doi:10.1155/2013/932143.
 171. Rokbi, M.; Osmani, H.; Imad, A.; Benseddiq, N. Effect of chemical treatment on flexure properties of natural fiber-reinforced polyester composite. *Procedia Eng.* **2011**, *10*, 2092–2097.
 172. Yu, P. Molecular chemistry imaging to reveal structural features of various plant feed tissues. *J. Struct. Biol.* **2005**, *150*, 81–89.
 173. Edwards, H. G.; Farwell, D. W.; Webster, D. FT Raman microscopy of untreated natural plant fibres. *Spectrochim. acta. Part A* **1997**, *53*, 2383–2392.
 174. Mwaikambo, L. Y.; Ansell, M. P. Chemical modification of hemp, sisal, jute, and kapok fibers by alkalization. *J. Appl. Polym. Sci.* **2002**, 2222–2234, doi:10.1002/app.10460.
 175. Chan, C. H.; Chia, C. H.; Zakaria, S.; Ahmad, I.; Dufresne, A. Production and characterisation of cellulose and nano- crystalline cellulose from kenaf core wood. *BioResources* **2013**, *8*, 785–794.
 176. Udoetok, I. A.; Wilson, L. D.; Headley, J. V Quaternized Cellulose Hydrogels as Sorbent Materials and Pickering Emulsion Stabilizing Agents. *Materials (Basel)*. **2016**, *9*, 1-16.
 177. Himmelsbach, D. S.; Akin, D. E. Near-infrared Fourier-transform Raman spectroscopy of flax (*Linum usitatissimum* L.) stems. *J. Agric. Food Chem.* **1998**, *46*, 991–998.
 178. Gierlinger, N.; Schwanninger, M.; Reinecke, A.; Burgert, I. Molecular changes during

- tensile deformation of single wood fibers followed by Raman microscopy. *Biomacromolecules* **2006**, *7*, 2077–2081.
179. Kaushik, V. K.; Kumar, A.; Kalia, S. Effect of Mercerization and Benzoyl Peroxide Treatment on Morphology, Thermal Stability and Crystallinity of Sisal Fibers. *Int. J. Text. Sci.* **2012**, *1*, 101–105.
 180. Martins, M. A.; Pessoa, J. D. C.; Gonçalves, P. S.; Souza, F. I.; Mattoso, L. H. C. Thermal and mechanical properties of the acai fiber/natural rubber composites. *J. Mater. Sci.* **2008**, *43*, 6531–6538.
 181. Hao, A. Mechanical and Thermal Properties of Kenaf Polypropylene Nonwoven Composites. *Phd Thesis; Univ. Texas, Texas, USA* **2013**, 19–30.
 182. Saravanakumar, S. S.; Kumaravel, A.; Nagarajan, T.; Sudhakar, P.; Baskaran, R. Characterization of a novel natural cellulosic fiber from *Prosopis juliflora* bark. *Carbohydr. Polym.* **2013**, *92*, 1928–1933.
 183. Wong, S.; Shanks, R.; Hodzic, A. Interfacial improvements in poly (3-hydroxybutyrate)-flax fibre composites with hydrogen bonding additives. *Compos. Sci. Technol.* **2004**, *64*, 1321–1330.
 184. Messiry, M. El Theoretical analysis of natural fiber volume fraction of reinforced composites. *Alexandria Eng. J.* **2013**, *52*, 301–306.
 185. Oksman, K.; Skrifvars, M.; Selin, J. F. Natural fibres as reinforcement in polylactic acid (PLA) composites. *Compos. Sci. Technol.* **2003**, *63*, 1317–1324.
 186. Hargitai, H.; Racz, I.; Anandjiwala, R. D. Development of HEMP Fiber Reinforced Polypropylene Composites. *J. Thermoplast. Compos. Mater.* **2008**, *21*, 165–174.
 187. George, J.; Sreekala, M.; Thomas, S. A review on interface modification and characterization of natural fiber reinforced plastic composites. *Polym. Eng. Sci.* **2001**, *41*, 1471–1485.
 188. Wang, B. Pre-treatment of Flax Fibers for use in Rotationally Molded Biocomposites. *MSc. Thesis; Univ. Saskatchewan, Saskatoon, Canada* **2004**, 447–463, doi:10.1177/0731684406072526.
 189. Arrakhiz, F. Z.; El Achaby, M.; Malha, M.; Bensalah, M. O.; Fassi-Fehri, O.; Bouhfid, R.; Benmoussa, K.; Qaiss, a. Mechanical and thermal properties of natural fibers reinforced polymer composites: Doum/low density polyethylene. *Mater. Des.* **2013**, *43*, 200–205.

190. Herrera-Franco, P. J.; Valadez-Gonzalez, A. A study of the mechanical properties of short natural-fiber reinforced composites. *Compos. Part B Eng.* **2005**, *36*, 597–608.
191. Tajvidi, M.; Takemura, A. Effect of Fiber Content and Type, Compatibilizer, and Heating Rate on Thermogravimetric Properties of Natural Fiber High Density Polyethylene Composites. *Polym. Compos. Compos.* **2009**, *16*, 101–113.
192. Arias, A.; Heuzey, M. C.; Huneault, M. A. Thermomechanical and crystallization behavior of polylactide-based flax fiber biocomposites. *Cellulose* **2013**, *20*, 439–452.
193. Johari, A. P.; Mohanty, S.; Kurmvanshi, S. K.; Nayak, S. K. Influence of Different Treated Cellulose Fibers on the Mechanical and Thermal Properties of Poly(lactic acid). *ACS Sustain. Chem. Eng.* **2016**, *4*, 1619–1629.
194. Dong, Y.; Ghataura, A.; Takagi, H.; Haroosh, H. J.; Nakagaito, A. N.; Lau, K. Composites : Part A Polylactic acid (PLA) biocomposites reinforced with coir fibres : Evaluation of mechanical performance and multifunctional properties. *Compos. Part A* **2014**, *63*, 76–84.
195. Bernland, K. M. Nucleating and clarifying polymers. *MSc. Thesis; Luleå Univ. Technol.* **2010**, 12–19.
196. Chen, C.; Xu, R.; Chen, X.; Xie, J. Influence of cocrystallization behavior on structure and properties of HDPE / LLDPE microporous membrane. *J. Polym. Res.* **2016**, 1–9, doi:10.1007/s10965-016-0935-3.
197. Mathot, V. B. F. Crystallization of polymers: A personal view on a lifetime in research. *J. Therm. Anal. Calorim.* **2010**, *102*, 403–412.
198. Macauley, N. J.; Harkin-Jones, E. M. A.; Murphy, W. R. The Influence of Nucleating Agents on the Extrusion and Thermoforming of Polypropylene. *Polym. Eng. Sci.* **1998**, *3*, 516–523.
199. Takemura, K. Effect of Water Absorption on Mechanical Properties of Hemp Fiber Reinforced Composite. *Key Eng. Mater.* **2009**, 161–164, doi:10.4028/www.scientific.net/KEM.417-418.161.

APPENDICES

APPENDIX A



ADF Method – Method 5

Acid Detergent Fiber in Feeds - Filter Bag Technique (for A200 and A200I)

Definition: This method determines Acid Detergent Fiber, which is the residue remaining after digesting with H₂SO₄ and CTAB. The fiber residues are predominantly cellulose and lignin.

Scope: This method is applicable to grains, feeds, forages, and all fiber-bearing material.

Apparatus

1. Analytical Balance – capable of weighing 0.1 mg.
2. Oven – capable of maintaining a temperature of $102 \pm 2^{\circ}\text{C}$.
3. Digestion instrument – capable of performing the digestion at $100 \pm 0.5^{\circ}\text{C}$ and maintaining a pressure of 10 – 25 psi. The instrument must be capable of creating a similar flow around each sample to ensure uniformity of extraction (ANKOM²⁰⁰ with 65 rpm agitation, ANKOM Technology).
4. Filter Bags – constructed from chemically inert and heat resistant filter media, capable of being heat sealed closed and able to retain 25-micron particles while permitting solution penetration (F57 and F58, ANKOM Technology).
5. Heat sealer – sufficient for sealing the filter bags closed to ensure complete closure (1915, ANKOM Technology).
6. Desiccant Pouch – collapsible sealable pouch with inside that enables the removal of air from around the filter bags (*Moisture Stop* weigh pouch, ANKOM Technology).
7. Marking pen – solvent and acid resistant (F08, ANKOM Technology).

Reagents

1. Acid Detergent Solution – Add 20 g cetyl trimethylammonium bromide (CTAB) to 1L 1.00 N H₂SO₄ previously standardized (premixed chemical solution available from ANKOM). Agitate and heat to aid solution.

CAUTION 1: Sulfuric acid is a strong acid and will cause severe burns. Protective clothing should be worn when working with this acid. Always add acid to water and not the reverse.

CAUTION 2: CTAB will irritate mucous membranes. A dust mask and gloves should be worn when handling this chemical.

Sample Preparation

Grind samples in a centrifugal mill with a 2mm screen or cutter type (Wiley) mill with a 1 mm screen. Samples ground finer may have particle loss from the filter bags and result in low values.

1. Use a solvent resistant marker to label the filter bags to be used in the analysis.
2. Weigh and record the weight of each empty filter bag (W_1) and zero the balance.
NOTE: Do not pre-dry filter bags. Any moisture will be accounted for by the blank bag correction.

3. Place 0.45 – 0.50g of prepared sample in up to 23 of the bags and record the weight (W_2) of each. Avoid placing the sample in the upper 4mm of the bag.
4. Include at least one empty bag in the run to determine the blank bag correction (C_1).

NOTE: A running average blank bag correction factor (C_1) should be used in the calculation of fiber. The inclusion of at least one blank bag in each run is mainly used as an indicator of particle loss. A C_1 larger than 1.0000 indicates that sample particles were lost from filter bags and deposited on the blank bag during the extraction. Any fiber particle loss from the filter bags will generate erroneous results. If particle loss is observed then the grinding method needs to be evaluated.

5. Using a heat sealer, completely seal each filter bag closed within 4mm of the top to encapsulate the sample.

NOTE: Use sufficient heat to completely seal the filter bags and allow enough cool time (2 sec) before raising the heat sealer arm to remove each bag from the heat sealer.

6. **Pre-extract only samples containing > 5% fat:** Extract samples by placing bags with samples into a container with a top. Pour enough acetone into the container to cover the bags and secure the top.

CAUTION 3: Acetone is extremely flammable. Avoid static electricity and use a fume hood when handling. Shake the container 10 times and allow the bags to soak for 10 minutes. Repeat with fresh acetone. Pour out acetone and place bags on a wire screen to air-dry.

Exception – Roasted soybean: Due to the processing of roasted soy a modification to the extraction is required. Place roasted soy samples into a container with a top. Pour enough acetone into the container to cover the bags and secure the top. Shake the container 10 times and pour off the acetone. Add fresh acetone and allow samples to soak for twelve hours. After the soak time, pour out the acetone and place the bags on a wire screen to air-dry.

7. To eliminate sample clumping, spread the sample uniformly inside the filter bags by shaking and flicking the bags.
8. Place up to 3 bags on each of eight Bag Suspender Trays (maximum of 24 bags). Stack the trays on the center post of the Bag Suspender with each level rotated 120 degrees in relation to the tray below it. Place the empty 9th tray on top.

NOTE: All nine trays must be used regardless of the number of bags being processed.

9. Verify that the Exhaust Hose is connected to the instrument and securely positioned in the drain.
10. Turn the instrument Power Switch to the ON position.
11. Before inserting the Bag Suspender into the Vessel, read the Temperature Controller on the instrument. If the temperature is higher than room temperature, fill the Vessel with cold tap water. The temperature on the Controller will decrease. When the value on the Controller reaches its lowest number and starts to increase, open the Exhaust Valve and exhaust the water. Repeat this process until the number on the Temperature Controller equilibrates to room temperature.
12. Open the Vessel Lid and insert the Bag Suspender with bags into the Vessel and place the Bag Suspender Weight on top of the empty 9th tray to keep the Bag Suspender submerged.
13. When processing 24 sample bags, add 1900-2000 mL of ambient temperature AD solution to the fiber analyzer vessel. If processing less than 20 bags, add 100 mL/bag of AD solution (use minimum of 1500 mL to ensure Bag Suspender is covered).
14. Turn Agitate and Heat ON and confirm agitation.
15. Set the timer for 60 minutes and close the lid.
16. When the ADF extraction is complete, turn Agitate and Heat OFF.
17. Open the drain valve (slowly at first) and exhaust the hot solution before opening the Vessel Lid.

NOTE: The solution in the Vessel is under pressure. The exhaust valve needs to be opened to release the pressure and solution prior to opening the Vessel Lid.

18. After the solution has been exhausted, close the exhaust valve and open the Vessel Lid. Add 1900-2000 mL of 70-90°C rinse water. Turn Agitate on and rinse for 5 minutes. If the Heat is ON, the Vessel Lid should be closed. If the Heat is OFF, the Vessel Lid can be open. Repeat 5-minute hot water rinses 2 more times. Just before draining the 3rd rinse, test the water with pH paper. If acid is present repeat rinses until neutral.
19. After the rinsing procedures are complete, open the Vessel Lid and remove the filter bags. Gently press out excess water from the bags. Place bags in a 250ml beaker and add enough acetone to cover the bags and soak for 3-5 minutes.
20. Remove the filter bags from the acetone and place them on a wire screen to air-dry. Completely dry in an oven at $102 \pm 2^\circ\text{C}$. (In most ovens the filter bags will be completely dry within 2-4 hours.)
NOTE: Do not place bags in the oven until the acetone in the bags has completely evaporated.
21. Remove the filter bags from the oven and immediately place them directly into a collapsible desiccant pouch and flatten to remove any air. Cool to ambient temperature and weigh the filter bags (W_3). NOTE: Do not use a conventional desiccator container.

Calculations

$$\% \text{ ADF (as-received basis)} = \frac{100 \times (W_3 - (W_1 \times C_1))}{W_2}$$

Where:

W_1 = Bag tare weight

W_2 = Sample weight

W_3 = Dried weight of bag with fiber after extraction process

C_1 = Blank bag correction (running average of final oven-dried weight divided by original blank bag weight)

Neutral Detergent Fiber in Feeds - Filter Bag Technique (for A200 and A200I)

Definition: This method determines Neutral Detergent Fiber, which is the residue remaining after digesting in a detergent solution. The fiber residues are predominantly hemicellulose, cellulose, and lignin.

Scope: This method is applicable to grains, feeds, forages, and all fiber-bearing material.

Apparatus

1. Analytical Balance – capable of weighing 0.1 mg.
2. Oven – capable of maintaining a temperature of $102 \pm 2^\circ\text{C}$.
3. Digestion instrument – capable of performing the digestion at $100 \pm 0.5^\circ\text{C}$ and maintaining a pressure of 10 – 25 psi. The instrument must be capable of creating a similar flow around each sample to ensure uniformity of extraction (ANKOM²⁰⁰ with 65 rpm agitation, ANKOM Technology).
4. Filter Bags – constructed from chemically inert and heat resistant filter media, capable of being heat sealed closed and able to retain 25-micron particles while permitting solution penetration (F57 and F58, ANKOM Technology).
5. Heat sealer – sufficient for sealing the filter bags closed to ensure complete closure (1915, ANKOM Technology).
6. Desiccant Pouch – collapsible sealable pouch with inside that enables the removal of air from around the filter bags (*Moisture Stop* weigh pouch, ANKOM Technology).
7. Marking pen – solvent and acid resistant (F08, ANKOM Technology).

Reagents

1. Neutral Detergent Solution—Add 30g Sodium dodecyl sulfate (USP), 18.61g Ethylenediaminetetraacetic disodium salt (dehydrate), 6.81g Sodium borate, 4.56g Sodium phosphate dibasic (anhydrous), and 10.0ml Triethylene glycol to 1L distilled H₂O (premixed chemical solution available from ANKOM Technology). Check that pH is from 6.9 to 7.1. Agitate and heat to aid solution.

CAUTION 1: Powdered chemicals will irritate mucous membranes. A dust mask and gloves should be worn when handling these chemicals.

2. Alpha-amylase—Heat-stable bacterial alpha-amylase: activity = 17,400 Liquefon Units / ml (FAA, ANKOM Technology).
3. Sodium sulfite— Na_2SO_3 , anhydrous (FSS, ANKOM Technology).

Sample Preparation

Grind samples in a centrifugal mill with a 2-mm screen or cutter type (Wiley) mill with a 1 mm screen. Samples ground finer may have particle loss from the filter bags and result in low values.

1. Use a solvent resistant marker to label the filter bags to be used in the analysis.
2. Weigh and record the weight of each empty filter bag (W_1) and zero the balance. NOTE: Do not pre-dry filter bags. Any moisture will be accounted for by the blank bag correction.
3. Place 0.45 – 0.50g of prepared sample in up to 23 of the bags and record the weight (W_2) of each. Avoid placing the sample in the upper 4mm of the bag.
4. Include at least one empty bag in the run to determine the blank bag correction (C_1).

NOTE: A running average blank bag correction factor (C_1) should be used in the calculation of fiber. The inclusion of at least one blank bag in each run is mainly used as an indicator of particle loss. A C_1 larger than 1.0000 indicates that sample particles were lost from filter bags and deposited on the blank bag during the extraction. Any fiber particle loss from the filter bags will generate erroneous results. If particle loss is observed then the grinding method needs to be evaluated.

5. Using a heat sealer, completely seal each filter bag closed within 4mm of the top to encapsulate the sample. NOTE: Use sufficient heat to completely seal the filter bags and allow enough cool time (2 sec) before raising the heat sealer arm to remove each bag from the heat sealer.
6. **Pre-extract only samples containing > 5% fat:** Extract samples by placing bags with samples into a container with a top. Pour enough acetone into the container to cover the bags and secure the top.

CAUTION 2: Acetone is extremely flammable. Avoid static electricity and use a fume hood when handling. Shake the container 10 times and allow bags to soak for 10 minutes. Repeat with fresh acetone. Pour out acetone and place bags on a wire screen to air-dry.

Exception – Roasted soybean: Due to the processing of roasted soy a modification to the

extraction is required. Place roasted soy samples into a container with a top. Pour enough acetone into the container to cover the bags and secure the top. Shake the container 10 times and pour off the acetone. Add fresh acetone and allow samples to soak for twelve hours. After the soak time, pour out the acetone and place the bags on a wire screen to dry.

7. To eliminate sample clumping, spread the sample uniformly inside the filter bags by shaking and flicking the bags.
8. Place up to 3 bags on each of eight Bag Suspender Trays (maximum of 24 bags). Stack the trays on the center post of the Bag Suspender with each level rotated 120 degrees in relation to the tray below it. Place the empty 9th tray on top.

NOTE: All nine trays must be used regardless of the number of bags being processed.

9. Verify that the Exhaust Hose is connected to the instrument and securely positioned in the drain.
10. Turn the instrument Power Switch to the ON position.
11. Open the Vessel Lid and insert the Bag Suspender with bags into the Vessel and place the Bag Suspender weight on top of the empty 9th tray to keep the Bag Suspender submerged.
12. When processing 24 sample bags, add 1900-2000 mL of ambient temperature ND solution to the fiber analyzer vessel. If processing less than 20 bags, add 100 mL/bag of ND solution (use minimum of 1500 mL to ensure Bag Suspender is covered). Add 20 g (0.5 g per 50 mL of ND solution) of sodium sulfite and 4.0 mL of alpha-amylase to the solution in the vessel.
13. Turn Agitate and Heat ON and confirm agitation.
14. Set the timer for 75 minutes and close the lid.
15. When the NDF extraction is complete, turn Agitate and Heat OFF.
16. Open the drain valve (slowly at first) and exhaust the hot solution before opening the Vessel Lid. NOTE: The solution in the Vessel is under pressure. The exhaust valve needs to be opened to release the pressure and solution prior to opening the Vessel Lid.
17. After the solution has been exhausted, close the exhaust valve and open the Vessel Lid. Add 1900-2000 mL of 70-90°C rinse water and 4.0 mL of alpha-amylase to the first and second rinses. Turn Agitate on and rinse for 5 minutes. If the Heat is ON, the Vessel Lid should be closed. If the Heat is OFF, the Vessel Lid can be open. Repeat 5-minute hot water rinse 1 more time for a total of 3 rinses.

18. When the NDF extraction and rinsing procedures are complete, open the Vessel Lid and remove the filter bags. Gently press out excess water from the bags. Place bags in a 250ml beaker and add enough acetone to cover bags and soak for 3-5 minutes.
19. Remove the filter bags from the acetone and place them on a wire screen to air-dry. Completely dry in an oven at $102 \pm 2^\circ\text{C}$. (In most ovens the filter bags will be completely dry within 2-4 hours.) NOTE: Do not place bags in the oven until the acetone in the bags has completely evaporated.
20. Remove the filter bags from the oven and immediately place them directly into a collapsible desiccant pouch and flatten to remove any air. Cool to ambient temperature and weigh the filter bags (W_3). NOTE: Do not use a conventional countertop or cabinet desiccator.

Calculations

$$\% \text{ NDF (as-received basis)} = \frac{100 \times (W_3 - (W_1 \times C_1))}{W_2}$$

Where:

W_1 = Bag tare weight

W_2 = Sample weight

W_3 = Dried weight of bag with fiber after extraction process

C_1 = Blank bag correction (running average of final oven-dried weight divided by original blank bag weight)

Reagents

Sulfuric acid (72% by weight) – ANKOM Technology FSA72 or dilute reagent grade H₂SO₄ to a specific gravity of 1634 g/L at 20°C (24.00N) by adding 1200 g H₂SO₄ to 350 ml H₂O in a 1 L MCA volumetric flask with cooling. Standardize this solution to 1634 g/L at 20°C specific gravity by removing solution and adding H₂O or H₂SO₄ as required.

Safety Precautions

Acetone is highly flammable. Use fume hood when handling acetone and avoid inhaling or contact with skin. Ensure that all the acetone has evaporated before placing in the oven.

Wear rubber gloves and face shield when handling sulfuric acid.

Always add sulfuric acid to water. If acid contacts skin, wash with copious amounts of water.

Apparatus

- a) Filtration device – ANKOM Technology – F57 Filter Bags
- b) Impulse bag sealer – ANKOM Technology – 1915 Heat Sealer
- c) Desiccator – ANKOM Technology – Desiccant/Moisture Stop pouch – X45
- d) 2L & 3L Beaker

Procedure

- 1) Grind the sample to pass through a 1 mm screen (2mm screen when using a cyclone mill).
- 2) Weigh each Filter Bag (W₁), record the weight, and tare the balance.
- 3) Add 0.5 g (± 0.05 g) of air-dried sample (W₂) directly into each Filter Bag.
- 4) Weigh and seal one (1) blank bag and include it in the digestion to determine the blank bag correction (C₁).
- 5) Seal the bags closed 4 mm from the open edge using the heat sealer.
- 6) Spread the sample uniformly inside each filter bag by flicking the bag to eliminate clumping.
- 7) Perform ADF determinations using Fiber Analyzer (See ADF Procedure).

- 8) After performing ADF determinations, place dried bags with samples into a 3 L beaker and completely cover the bags with 72% H₂SO₄ (approximately 250 ml).

IMPORTANT: Bags must be completely dry and at ambient temperature before adding concentrate acid. If moisture (even ambient moisture) is present in the bags, heat generated by the H₂SO₄ and H₂O reaction will adversely affect the results.

- 9) Place a 2 L beaker inside the 3 L beaker to keep bags submerged. Agitate the bags at the start and at 30minute intervals by gently pushing and lifting the 2 L beaker up and down approximately 30 times.
- 10) After 3 hours pour off the H₂SO₄ and **rinse with tap water to remove all acid.**

IMPORTANT: If acid remains in the bags when they go into the oven, the samples will burn, resulting in values that are higher than they should be.

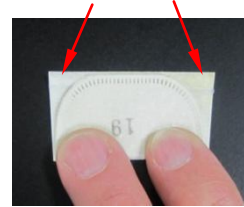
- 11) Repeat rinses until pH paper shows neutral color when touching the bags. Rinse with approximately 250 ml of acetone for 3 minutes to remove the water. **Handle the bags gently during rinsing. Fine lignin particles can exit the filter if not handled carefully.**



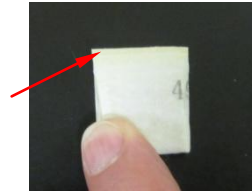
WARNING – Do NOT place bags in an oven until all acetone has evaporated.

- 13) Remove the bags from the oven and place them directly into Desiccant/Moisture Stop pouches and flatten to remove air. Cool to ambient temperature and weigh the bags (W₃).
- 14) Prepare each bag for the ash procedure.

14.1) Fold each bag from bottom to top. Because the bags are wider at the top than at the bottom, there will be a little extra material on each side after the first fold.



14.2) Fold each bag from right to left. The extra material now lines up on left side.



14.3) Heat seal the bag at the location of the extra material.



15) Ash the bags in pre-weighed crucibles (30 or 50 ml) at 525°C for 3 hours or until C-free. Cool and calculate weight loss (W_4).

16) Calculate blank bag ash correction (C_2) using weight loss upon ignition of a blank bag sequentially run through ADF and lignin steps.

17) Calculate percent ADL.

$$\text{ADL (as-received basis)} = \frac{(W_3 - (W_1 \times C_1)) \times 100}{W_2}$$

$$\text{ADL}_{\text{DM}} \text{ (DM basis)} = \frac{(W_3 - (W_1 \times C_1)) \times 100}{W_2 \times \text{DM}}$$

$$\text{ADL}_{\text{OM}} \text{ (DM basis)} = \frac{(W_4 - (W_1 \times C_2)) \times 100}{W_2 \times \text{DM}}$$

Where:

W_1 = Bag tare weight

W_2 = Sample weight

W_3 = Weight after extraction process

W_4 = Weight of Organic Matter (OM) (weight loss on ignition of bag and fiber residue)

C_1 = Blank bag correction (final oven-dried weight/original blank bag weight)

C_2 = Ash corrected blank bag (Loss of weight on ignition of bag/original blank bag)

DM = Dry Matter

APPENDIX B

Statistical Analysis of Variation of RPF Colour with Fiber Treatment

Table B.1. ANOVA results for colour variations of raffia palm fibers with fiber treatment.

Source of Variation	DF	SS	MS	F	P
Colour Co-ordinate	2	18198.987	9099.493	22674.572	<0.001
Treatment	2	712.705	356.352	887.977	<0.001
Colour Co-ordinate X Treatment	4	716.864	179.216	446.579	<0.001
Residual	81	32.506	0.401		
Total	89	19661.061	220.911		

Main effects cannot be properly interpreted if significant interaction is determined. This is because the size of a factor's effect depends upon the level of the other factor. The effect of various levels of colour co-ordinate depends on what level of treatment is present. There is a statistically significant interaction between colour co-ordinates and Treatment ($P = <0.001$).

All Pairwise Multiple Comparison Procedures (Bonferroni t-test):

Comparisons for factor: Colour co-ordinate

Comparison	Diff of Means	t	P	P<0.050
ΔL vs. Δa	33.559	205.171	<0.001	Yes
ΔL vs. Δb	24.860	151.987	<0.001	Yes
Δb vs. Δa	8.699	53.183	<0.001	Yes

Comparisons for factor: Treatment

Comparison	Diff of Means	t	P	P<0.050
Acidic vs. No Treatment	6.130	37.475	<0.001	Yes
Alkaline vs. No Treatment	5.795	35.431	<0.001	Yes
Alkaline vs. Acidic Treatment	0.334	2.044	0.133	No

Comparisons for factor: Treatment within ΔL

Comparison	Diff of Means	t	P	P<0.050
Acidic vs. No Treatment	14.343	50.627	<0.001	Yes
Alkaline vs. No Treatment	11.867	41.888	<0.001	Yes
Alkaline vs. Acidic Treatment	2.476	8.740	<0.001	Yes

Comparisons for factor: Treatment within Δa

Comparison	Diff of Means	t	P	P<0.050
Acidic vs. Alkaline Treatment	4.267	15.062	<0.001	Yes
Acidic vs. No Treatment	1.633	5.764	<0.001	Yes
Alkaline vs. No Treatment	2.634	9.297	<0.001	Yes

Comparisons for factor: Treatment within Δb

Comparison	Diff of Means	t	P	P<0.050
Acidic vs. No Treatment	5.679	20.046	<0.001	Yes
Alkaline vs. No Treatment	2.885	10.183	<0.001	Yes
Alkaline vs. Acidic Treatment	2.794	9.862	<0.001	Yes

Comparisons for factor: Colour co-ordinate within no treatment

Comparison	Diff of Means	t	P	P<0.050
ΔL vs. Δa	41.962	148.116	<0.001	Yes
ΔL vs. Δb	30.742	108.512	<0.001	Yes
Δb vs. Δa	11.220	39.604	<0.001	Yes

Comparisons for factor: Colour co-ordinate within alkaline treatment

Comparison	Diff of Means	t	P	P<0.050
ΔL vs. Δa	32.729	115.526	<0.001	Yes
ΔL vs. Δb	21.760	76.808	<0.001	Yes
Δb vs. Δa	10.969	38.718	<0.001	Yes

Comparisons for factor: Colour co-ordinate within acidic treatment

Comparison	Diff of Means	t	P	P<0.050
ΔL vs. Δa	25.986	91.725	<0.001	Yes
ΔL vs. Δb	22.078	77.930	<0.001	Yes
Δb vs. Δa	3.908	13.794	<0.001	Yes

APPENDIX C

Result and Statistical Analysis of the Effect of Fiber Content and Fiber Treatment on the Density of RPF reinforced HDPE

Table C.1. Effect of raffia palm fiber addition on the density of high density polyethylene composites.

Polymer	Fiber Content (wt.%)	Density of Molded Samples (g/cm ³)
HDPE	0	0.9597 ± 0.0014
Raw Fiber	5	0.9756 ± 0.0006
	10	0.9841 ± 0.0009
	20	0.9919 ± 0.0016
	30	1.0166 ± 0.0024
NaOH Treated Fiber	5	0.9778 ± 0.0010
	10	0.9860 ± 0.0014
	20	1.0075 ± 0.0009
	30	1.0374 ± 0.0005
H ₂ SO ₄ Treated Fiber	5	0.9758 ± 0.0007
	10	0.9868 ± 0.0003
	20	1.0118 ± 0.0017
	30	1.0427 ± 0.0051

Table C.2. SigmaPlot two-way analysis of variance of the effect of fiber content and fiber treatment on the density of raffia palm fiber reinforced high density polyethylene.

Source of Variation	DF	SS	MS	F	P
Fiber Load	3	0.0123	0.00408	1292.476	<0.001
Treatment	3	0.0153	0.00510	1613.653	<0.001
Fiber Load × Treatment	9	0.00488	0.000543	171.693	<0.001
Residual	32	0.000101	0.00000316		
Total	47	0.0325	0.000692		

Dependent Variable: Density (gcm⁻³).

Main effects cannot be properly interpreted if significant interaction is determined. This is because the size of a factor's effect depends upon the level of the other factor. The effect of various levels of fiber load depends on what level of treatment is present. There is a statistically significant interaction between fiber load and treatment ($P = <0.001$).

All Pairwise Multiple Comparison (Bonferroni t-test):

Comparisons for factor: Fiber load

Comparison	Diff of Means	t	P	P<0.050
30 wt.% vs. 5 wt.%	0.0419	57.715	<0.001	Yes
30 wt.% vs. 10 wt.%	0.0349	48.138	<0.001	Yes
30 wt.% vs. 20 wt.%	0.0214	29.466	<0.001	Yes
20 wt.% vs. 5 wt.%	0.0205	28.249	<0.001	Yes
20 wt.% vs. 10 wt.%	0.0135	18.672	<0.001	Yes
10 wt.% vs. 5 wt.%	0.00695	9.577	<0.001	Yes

Comparisons for factor: Treatment

Comparison	Diff of Means	t	P	P<0.050
Acidic Treatment vs. HDPE	0.0446	61.435	<0.001	Yes
Acidic vs. No Treatment	0.0122	16.823	<0.001	Yes
Acidic vs. Alkaline Treatment	0.00208	2.859	0.044	Yes
Alkaline Treatment vs. HDPE	0.0425	58.576	<0.001	Yes
Alkaline vs. No Treatment	0.0101	13.964	<0.001	Yes
No Treatment vs. HDPE	0.0324	44.612	<0.001	Yes

Comparisons for factor: Treatment within 5 wt.%

Comparison	Diff of Means	t	P	P<0.05
Alkaline Treatment vs. HDPE	0.0181	12.494	<0.001	Yes
Alkaline vs. No Treatment	0.00220	1.516	0.836	No
Alkaline vs. Acidic Treatment	0.00207	1.424	0.985	Do Not Test
Acidic Treatment vs. HDPE	0.0161	11.070	<0.001	Yes
Acidic vs. No Treatment	0.000133	0.0919	1.000	Do Not Test
No Treatment vs. HDPE	0.0159	10.978	<0.001	Yes

Comparisons for factor: Treatment within 10 wt.%

Comparison	Diff of Means	t	P	P<0.05
Acidic Treatment vs. HDPE	0.0271	18.695	<0.001	Yes
Acidic vs. No Treatment	0.00267	1.837	0.453	No
Acidic vs. Alkaline Treatment	0.000800	0.551	1.000	Do Not Test
Alkaline Treatment vs. HDPE	0.0263	18.144	<0.001	Yes
Alkaline vs. No Treatment	0.00187	1.286	1.000	Do Not Test
No Treatment vs. HDPE	0.0245	16.857	<0.001	Yes

Comparisons for factor: Treatment within 20 wt.%

Comparison	Diff of Means	t	P	P<0.05
Acidic Treatment vs. HDPE	0.0521	35.920	<0.001	Yes
Acidic vs. No Treatment	0.0200	13.757	<0.001	Yes
Acidic vs. Alkaline Treatment	0.00430	2.963	0.034	Yes
Alkaline Treatment vs. HDPE	0.0478	32.957	<0.001	Yes
Alkaline vs. No Treatment	0.0157	10.794	<0.001	Yes
No Treatment vs. HDPE	0.0322	22.163	<0.001	Yes

Comparisons for factor: Treatment within 30 wt.%

Comparison	Diff of Means	t	P	P<0.05
Acidic Treatment vs. HDPE	0.0830	57.187	<0.001	Yes
Acidic vs. No Treatment	0.0261	17.960	<0.001	Yes
Acidic vs. Alkaline Treatment	0.00527	3.629	0.006	Yes
Alkaline Treatment vs. HDPE	0.0777	53.558	<0.001	Yes
Alkaline vs. No Treatment	0.0208	14.331	<0.001	Yes
No Treatment vs. HDPE	0.0569	39.227	<0.001	Yes

Comparisons for factor: Fiber load within no treatment

Comparison	Diff of Means	t	P	P<0.05
30 wt.% vs. 5 wt.%	0.0410	28.249	<0.001	Yes
30 wt.% vs. 10 wt.%	0.0325	22.369	<0.001	Yes
30 wt.% vs. 20 wt.%	0.0248	17.064	<0.001	Yes
20 wt.% vs. 5 wt.%	0.0162	11.185	<0.001	Yes
20 wt.% vs. 10 wt.%	0.00770	5.305	<0.001	Yes
10 wt.% vs. 5 wt.%	0.00853	5.879	<0.001	Yes

Comparisons for factor: Fiber load within Alkaline Treatment

Comparison	Diff of Means	t	P	P<0.05
30 wt.% vs. 5 wt.%	0.0596	41.064	<0.001	Yes
30 wt.% vs. 10 wt.%	0.0514	35.414	<0.001	Yes
30 wt.% vs. 20 wt.%	0.0299	20.601	<0.001	Yes
20 wt.% vs. 5 wt.%	0.0297	20.463	<0.001	Yes
20 wt.% vs. 10 wt.%	0.0215	14.813	<0.001	Yes
10 wt.% vs. 5 wt.%	0.00820	5.650	<0.001	Yes

Comparisons for factor: Fiber load within acidic treatment

Comparison	Diff of Means	t	P	P<0.05
30 wt.% vs. 5 wt.%	0.0669	46.117	<0.001	Yes
30 wt.% vs. 10 wt.%	0.0559	38.492	<0.001	Yes
30 wt.% vs. 20 wt.%	0.0309	21.267	<0.001	Yes
20 wt.% vs. 5 wt.%	0.0361	24.850	<0.001	Yes
20 wt.% vs. 10 wt.%	0.0250	17.225	<0.001	Yes
10 wt.% vs. 5 wt.%	0.0111	7.625	<0.001	Yes

A result of "Do Not Test" occurs for a comparison when no significant difference is found between two means that enclose that comparison. For example, if you had four means sorted in order, and found no difference between means 4 vs. 2, then you would not test 4 vs. 3 and 3 vs. 2, but still test 4 vs. 1 and 3 vs. 1 (4 vs. 3 and 3 vs. 2 are enclosed by 4 vs. 2: 4 3 2 1). Note that not testing the enclosed means is a procedural rule, and a result of Do Not Test should be treated as if there is no significant difference between the means, even though one may appear to exist.

APPENDIX D

Result and Statistical Analysis of the Effect of Fiber Content and Fiber Treatment on the Tensile Properties of RPF reinforced HDPE

Tensile Strength

Table D.1. Effect of raffia palm fiber addition on the tensile properties of high density polyethylene composites.

Polymer	Fiber Content (wt.%)	Tensile Strength (MPa)	Young's Modulus (GPa)
HDPE	-	24.42 ± 0.40	1.56 ± 0.03
Raw Fiber	5	22.64 ± 0.38	1.57 ± 0.15
	10	24.22 ± 0.17	1.85 ± 0.21
	20	22.78 ± 0.37	1.90 ± 0.25
	30	20.48 ± 0.31	2.00 ± 0.10
	NaOH Treated	5	22.58 ± 0.24
Fiber	10	23.16 ± 0.35	1.76 ± 0.10
	20	20.53 ± 0.25	1.88 ± 0.08
	30	18.86 ± 0.37	2.14 ± 0.11
	H ₂ SO ₄ Treated	5	23.27 ± 0.62
Fiber	10	22.05 ± 0.19	1.63 ± 0.06
	20	19.35 ± 0.41	1.73 ± 0.05
	30	16.90 ± 0.57	1.80 ± 0.15

Table D.2. SigmaPlot two-way analysis of variance of the effect of fiber content and fiber treatment on the tensile strength of raffia palm fiber reinforced high density polyethylene.

Source of Variation	DF	SS	MS	F	P
Fiber Load	3	139.328	46.443	316.255	<0.001
Treatment	3	183.007	61.002	415.402	<0.001
Fiber Load × Treatment	9	76.036	8.448	57.531	<0.001
Residual	64	9.398	0.147		
Total	79	407.769	5.162		

Dependent Variable: Tensile strength (MPa).

Main effects cannot be properly interpreted if significant interaction is determined. This is because the size of a factor's effect depends upon the level of the other factor. The effect of various levels of fiber load depends on what level of treatment is present. There is a statistically significant interaction between fiber load and treatment ($P = <0.001$).

All Pairwise Multiple Comparison (Bonferroni t-test):

Comparisons for factor: Fiber load

Comparison	Diff of Means	t	P	P<0.050
10 wt.% vs. 30 wt.%	3.297	27.211	<0.001	Yes
10 wt.% vs. 20 wt.%	1.693	13.971	<0.001	Yes
10 wt.% vs. 5 wt.%	0.236	1.947	0.335	No
5 wt.% vs. 30 wt.%	3.061	25.264	<0.001	Yes
5 wt.% vs. 20 wt.%	1.457	12.023	<0.001	Yes
20 wt.% vs. 30 wt.%	1.605	13.240	<0.001	Yes

Comparisons for factor: Treatment

Comparison	Diff of Means	t	P	P<0.050
HDPE vs. Acidic Treatment	4.030	33.256	<0.001	Yes
HDPE vs. Alkaline Treatment	3.142	25.928	<0.001	Yes
HDPE vs. No Treatment	1.897	15.650	<0.001	Yes
No Treatment vs. Acidic	2.133	17.606	<0.001	Yes
No Treatment vs. Alkaline	1.245	10.278	<0.001	Yes
Alkaline vs. Acidic Treatment	0.888	7.328	<0.001	Yes

Comparisons for factor: Treatment within 5 wt.%

Comparison	Diff of Means	t	P	P<0.05
HDPE vs. Alkaline Treatment	1.846	7.617	<0.001	Yes
HDPE vs. No Treatment	1.786	7.369	<0.001	Yes
HDPE vs. Acidic Treatment	1.154	4.761	<0.001	Yes
Acidic vs. Alkaline Treatment	0.692	2.855	0.035	Yes
Acidic vs. No Treatment	0.632	2.608	0.068	No
No Treatment vs. Alkaline	0.0600	0.248	1.000	No

Comparisons for factor: Treatment within 10 wt.%

Comparison	Diff of Means	t	P	P<0.05
HDPE vs. Acidic Treatment	2.372	9.787	<0.001	Yes
HDPE vs. Alkaline Treatment	1.262	5.207	<0.001	Yes
HDPE vs. No Treatment	0.208	0.858	1.000	No
No Treatment vs. Acidic	2.164	8.929	<0.001	Yes
No Treatment vs. Alkaline	1.054	4.349	<0.001	Yes
Alkaline vs. Acidic Treatment	1.110	4.580	<0.001	Yes

Comparisons for factor: Treatment within 20 wt.%

Comparison	Diff of Means	t	P	P<0.05
HDPE vs. Acidic Treatment	5.072	20.927	<0.001	Yes
HDPE vs. Alkaline Treatment	3.894	16.067	<0.001	Yes
HDPE vs. No Treatment	1.648	6.800	<0.001	Yes
No Treatment vs. Acidic	3.424	14.127	<0.001	Yes
No Treatment vs. Alkaline	2.246	9.267	<0.001	Yes
Alkaline vs. Acidic Treatment	1.178	4.860	<0.001	Yes

Comparisons for factor: Treatment within 30 wt.%

Comparison	Diff of Means	t	P	P<0.05
HDPE vs. Acidic Treatment	7.522	31.036	<0.001	Yes
HDPE vs. Alkaline Treatment	5.566	22.965	<0.001	Yes
HDPE vs. No Treatment	3.944	16.273	<0.001	Yes
No Treatment vs. Acidic	3.578	14.763	<0.001	Yes
No Treatment vs. Alkaline	1.622	6.692	<0.001	Yes
Alkaline vs. Acidic Treatment	1.956	8.070	<0.001	Yes

Comparisons for factor: Fiber load within no treatment

Comparison	Diff of Means	t	P	P<0.05
10 wt.% vs. 30 wt.%	3.736	15.415	<0.001	Yes
10 wt.% vs. 5 wt.%	1.578	6.511	<0.001	Yes
10 wt.% vs. 20 wt.%	1.440	5.941	<0.001	Yes
20 wt.% vs. 30 wt.%	2.296	9.473	<0.001	Yes
20 wt.% vs. 5 wt.%	0.138	0.569	1.000	No
5 wt.% vs. 30 wt.%	2.158	8.904	<0.001	Yes

Comparisons for factor: Fiber load within alkaline treatment

Comparison	Diff of Means	t	P	P<0.05
10 wt.% vs. 30 wt.%	4.304	17.758	<0.001	Yes
10 wt.% vs. 20 wt.%	2.632	10.860	<0.001	Yes
10 wt.% vs. 5 wt.%	0.584	2.410	0.113	No
5 wt.% vs. 30 wt.%	3.720	15.349	<0.001	Yes
5 wt.% vs. 20 wt.%	2.048	8.450	<0.001	Yes
20 wt.% vs. 30 wt.%	1.672	6.899	<0.001	Yes

Comparisons for factor: Fiber load within acidic treatment

Comparison	Diff of Means	t	P	P<0.05
5 wt.% vs. 30 wt.%	6.368	26.274	<0.001	Yes
5 wt.% vs. 20 wt.%	3.918	16.166	<0.001	Yes
5 wt.% vs. 10 wt.%	1.218	5.025	<0.001	Yes
10 wt.% vs. 30 wt.%	5.150	21.249	<0.001	Yes
10 wt.% vs. 20 wt.%	2.700	11.140	<0.001	Yes
20 wt.% vs. 30 wt.%	2.450	10.109	<0.001	Yes

Young's Modulus

Table D.3. SigmaPlot two-way analysis of variance of the effect of fiber content and fiber treatment on the Young's modulus of raffia palm fiber reinforced high density polyethylene.

Source of Variation	DF	SS	MS	F	P
Fiber Load	3	0.795	0.265	20.485	<0.001
Treatment	3	1.127	0.376	29.051	<0.001
Fiber Load × Treatment	9	0.462	0.0514	3.971	<0.001
Residual	64	0.828	0.0129		
Total	79	3.212	0.0407		

Dependent Variable: Young's modulus (GPa).

Main effects cannot be properly interpreted if significant interaction is determined. This is because the size of a factor's effect depends upon the level of the other factor. The effect of various levels of fiber load depends on what level of treatment is present. There is a statistically significant interaction between fiber load and treatment ($P = <0.001$).

All Pairwise Multiple Comparison (Bonferroni t-test):

Comparisons for factor: Fiber load

Comparison	Diff of Means	t	P	P<0.050
30 wt.% vs. 5 wt.%	0.274	7.619	<0.001	Yes
30 wt.% vs. 10 wt.%	0.175	4.866	<0.001	Yes
30 wt.% vs. 20 wt.%	0.109	3.031	0.021	Yes
20 wt.% vs. 5 wt.%	0.165	4.588	<0.001	Yes
20 wt.% vs. 10 wt.%	0.0660	1.835	0.427	No
10 wt.% vs. 5 wt.%	0.0990	2.753	0.046	Yes

Comparisons for factor: Treatment

Comparison	Diff of Means	t	P	P<0.050
Alkaline Treatment vs. HDPE	0.298	8.272	<0.001	Yes
Alkaline vs. Acidic Treatment	0.166	4.616	<0.001	Yes
Alkaline vs. No Treatment	0.0285	0.792	1.000	No
No Treatment vs. HDPE	0.269	7.480	<0.001	Yes
No Treatment vs. Acidic	0.137	3.823	0.002	Yes
Acidic Treatment vs. HDPE	0.131	3.657	0.003	Yes

Comparisons for factor: Treatment within 5 wt.%

Comparison	Diff of Means	t	P	P<0.05
Alkaline Treatment vs. HDPE	0.0980	1.363	1.000	No
Alkaline vs. No Treatment	0.0860	1.196	1.000	Do Not Test
Alkaline vs. Acidic Treatment	0.0480	0.667	1.000	Do Not Test
Acidic Treatment vs. HDPE	0.0500	0.695	1.000	Do Not Test
Acidic vs. No Treatment	0.0380	0.528	1.000	Do Not Test
No Treatment vs. HDPE	0.0120	0.167	1.000	Do Not Test

Comparisons for factor: Treatment within 10 wt.%

Comparison	Diff of Means	t	P	P<0.05
No Treatment vs. HDPE	0.292	4.060	<0.001	Yes
No Treatment vs. Acidic	0.226	3.142	0.015	Yes
No Treatment vs. Alkaline	0.0940	1.307	1.000	No
Alkaline Treatment vs. HDPE	0.198	2.753	0.046	Yes
Alkaline vs. Acidic Treatment	0.132	1.835	0.427	No
Acidic Treatment vs. HDPE	0.0660	0.918	1.000	No

Comparisons for factor: Treatment within 20 wt.%

Comparison	Diff of Means	t	P	P<0.05
No Treatment vs. HDPE	0.336	4.672	<0.001	Yes
No Treatment vs. Acidic	0.170	2.364	0.127	No
No Treatment vs. Alkaline	0.0180	0.250	1.000	Do Not Test
Alkaline Treatment vs. HDPE	0.318	4.421	<0.001	Yes
Alkaline vs. Acidic Treatment	0.152	2.113	0.231	Do Not Test
Acidic Treatment vs. HDPE	0.166	2.308	0.145	No

Comparisons for factor: Treatment within 30 wt.%

Comparison	Diff of Means	t	P	P<0.05
Alkaline Treatment vs. HDPE	0.576	8.008	<0.001	Yes
Alkaline vs. Acidic Treatment	0.332	4.616	<0.001	Yes
Alkaline vs. No Treatment	0.140	1.946	0.336	No
No Treatment vs. HDPE	0.436	6.062	<0.001	Yes
No Treatment vs. Acidic	0.192	2.669	0.058	No
Acidic Treatment vs. HDPE	0.244	3.392	0.007	Yes

Comparisons for factor: Fiber load within no treatment

Comparison	Diff of Means	t	P	P<0.05
30 wt.% vs. 5 wt.%	0.424	5.895	<0.001	Yes
30 wt.% vs. 10 wt.%	0.144	2.002	0.297	No
30 wt.% vs. 20 wt.%	0.1000	1.390	1.000	Do Not Test
20 wt.% vs. 5 wt.%	0.324	4.505	<0.001	Yes
20 wt.% vs. 10 wt.%	0.0440	0.612	1.000	Do Not Test
10 wt.% vs. 5 wt.%	0.280	3.893	0.001	Yes

Comparisons for factor: Fiber load within alkaline treatment

Comparison	Diff of Means	t	P	P<0.05
30 wt.% vs. 5 wt.%	0.478	6.646	<0.001	Yes
30 wt.% vs. 10 wt.%	0.378	5.255	<0.001	Yes
30 wt.% vs. 20 wt.%	0.258	3.587	0.004	Yes
20 wt.% vs. 5 wt.%	0.220	3.059	0.019	No
20 wt.% vs. 10 wt.%	0.120	1.668	0.601	Do Not Test
10 wt.% vs. 5 wt.%	0.1000	1.390	1.000	Do Not Test

Comparisons for factor: Fiber load within acidic treatment

Comparison	Diff of Means	t	P	P<0.05
30 wt.% vs. 5 wt.%	0.194	2.697	0.054	No
30 wt.% vs. 10 wt.%	0.178	2.475	0.096	Do Not Test
30 wt.% vs. 20 wt.%	0.0780	1.084	1.000	Do Not Test
20 wt.% vs. 5 wt.%	0.116	1.613	0.670	Do Not Test
20 wt.% vs. 10 wt.%	0.100	1.390	1.000	Do Not Test
10 wt.% vs. 5 wt.%	0.0160	0.222	1.000	Do Not Test

A result of "Do Not Test" occurs for a comparison when no significant difference is found between two means that enclose that comparison. For example, if you had four means sorted in order, and found no difference between means 4 vs. 2, then you would not test 4 vs. 3 and 3 vs. 2, but still test 4 vs. 1 and 3 vs. 1 (4 vs. 3 and 3 vs. 2 are enclosed by 4 vs. 2: 4 3 2 1). Note that not testing

the enclosed means is a procedural rule, and a result of Do Not Test should be treated as if there is no significant difference between the means, even though one may appear to exist.

APPENDIX E

Result and Statistical Analysis of the Effect of Fiber Content and Fiber Treatment on the Flexural Properties of RPF reinforced HDPE

Flexural Strength

Table E.1. Effect of raffia palm fiber content on the flexural properties of high density polyethylene composites.

Polymer	Fiber Content (wt.%)	Flexural Strength (MPa)	Flexural Modulus (GPa)
HDPE	-	41.57 ± 0.89	1.14 ± 0.03
Raw Fiber	5	48.91 ± 3.32	1.20 ± 0.05
	10	46.51 ± 0.52	1.50 ± 0.17
	20	43.96 ± 0.81	1.53 ± 0.07
	30	46.42 ± 0.86	1.55 ± 0.02
	NaOH Treated	5	54.10 ± 0.96
Fiber	10	44.11 ± 0.41	1.38 ± 0.03
	20	44.57 ± 1.04	1.48 ± 0.03
	30	43.68 ± 0.55	1.58 ± 0.09
	H ₂ SO ₄ Treated	5	53.99 ± 3.84
Fiber	10	48.79 ± 1.82	1.32 ± 0.13
	20	46.36 ± 2.02	1.59 ± 0.06
	30	43.80 ± 2.55	1.65 ± 0.10

Table E.2. SigmaPlot two-way analysis of variance of the effect of fiber content and fiber treatment on the flexural strength of raffia palm fiber reinforced high density polyethylene.

Source of Variation	DF	SS	MS	F	P
Fiber Load	3	432.130	144.043	49.037	<0.001
Treatment	3	497.279	165.760	56.431	<0.001
Fiber Load × Treatment	9	287.335	31.926	10.869	<0.001
Residual	64	187.994	2.937		
Total	79	1404.739	17.782		

Dependent Variable: Flexural Strength (MPa).

Main effects cannot be properly interpreted if significant interaction is determined. This is because the size of a factor's effect depends upon the level of the other factor. the effect of various levels of fiber load depends on what level of treatment is present. there is a statistically significant interaction between fiber load and treatment ($P = <0.001$).

All Pairwise Multiple Comparison (Bonferroni t-test):

Comparisons for factor: Fiber load

Comparison	Diff of Means	t	P	P<0.050
5 wt.% vs. 30 wt.%	5.773	10.653	<0.001	Yes
5 wt.% vs. 20 wt.%	5.526	10.195	<0.001	Yes
5 wt.% vs. 10 wt.%	4.396	8.112	<0.001	Yes
10 wt.% vs. 30 wt.%	1.377	2.541	0.081	No
10 wt.% vs. 20 wt.%	1.129	2.083	0.247	Do Not Test
20 wt.% vs. 30 wt.%	0.248	0.458	1.000	Do Not Test

Comparisons for factor: Treatment

Comparison	Diff of Means	t	P	P<0.050
Acidic Treatment vs. HDPE	6.663	12.295	<0.001	Yes
Acidic vs. No Treatment	1.785	3.294	0.010	Yes
Acidic vs. Alkaline Treatment	1.622	2.994	0.023	Yes
Alkaline Treatment vs. HDPE	5.041	9.301	<0.001	Yes
Alkaline vs. No Treatment	0.163	0.301	1.000	No
No Treatment vs. HDPE	4.878	9.000	<0.001	Yes

Comparisons for factor: Treatment within 5 wt.%

Comparison	Diff of Means	t	P	P<0.05
Alkaline Treatment vs. HDPE	12.524	11.554	<0.001	Yes
Alkaline vs. No Treatment	5.184	4.782	<0.001	Yes
Alkaline vs. Acidic Treatment	0.110	0.101	1.000	No
Acidic Treatment vs. HDPE	12.414	11.452	<0.001	Yes
Acidic vs. No Treatment	5.074	4.681	<0.001	Yes
No Treatment vs. HDPE	7.340	6.771	<0.001	Yes

Comparisons for factor: Treatment within 10 wt.%

Comparison	Diff of Means	t	P	P<0.05
Acidic Treatment vs. HDPE	7.222	6.663	<0.001	Yes
Acidic vs. Alkaline Treatment	4.688	4.325	<0.001	Yes
Acidic vs. No Treatment	2.286	2.109	0.233	No
No Treatment vs. HDPE	4.936	4.554	<0.001	Yes
No Treatment vs. Alkaline	2.402	2.216	0.182	No
Alkaline Treatment vs. HDPE	2.534	2.338	0.135	No

Comparisons for factor: Treatment within 20 wt.%

Comparison	Diff of Means	t	P	P<0.05
Acidic Treatment vs. HDPE	4.792	4.421	<0.001	Yes
Acidic vs. No Treatment	2.404	2.218	0.181	No
Acidic vs. Alkaline Treatment	1.796	1.657	0.615	Do Not Test
Alkaline Treatment vs. HDPE	2.996	2.764	0.045	Yes
Alkaline vs. No Treatment	0.608	0.561	1.000	Do Not Test
No Treatment vs. HDPE	2.388	2.203	0.187	No

Comparisons for factor: Treatment within 30 wt.%

Comparison	Diff of Means	t	P	P<0.05
No Treatment vs. HDPE	4.848	4.472	<0.001	Yes
No Treatment vs. Alkaline	2.738	2.526	0.084	No
No Treatment vs. Acidic	2.622	2.419	0.111	Do Not Test
Acidic Treatment vs. HDPE	2.226	2.054	0.265	No
Acidic vs. Alkaline Treatment	0.116	0.107	1.000	Do Not Test
Alkaline Treatment vs. HDPE	2.110	1.947	0.336	Do Not Test

Comparisons for factor: Fiber load within no treatment

Comparison	Diff of Means	t	P	P<0.05
5 wt.% vs. 20 wt.%	4.952	4.568	<0.001	Yes
5 wt.% vs. 30 wt.%	2.492	2.299	0.149	No
5 wt.% vs. 10 wt.%	2.404	2.218	0.181	Do Not Test
10 wt.% vs. 20 wt.%	2.548	2.351	0.131	No
10 wt.% vs. 30 wt.%	0.0880	0.0812	1.000	Do Not Test
30 wt.% vs. 20 wt.%	2.460	2.269	0.160	Do Not Test

Comparisons for factor: Fiber load within alkaline treatment

Comparison	Diff of Means	t	P	P<0.05
5 wt.% vs. 30 wt.%	10.414	9.607	<0.001	Yes
5 wt.% vs. 10 wt.%	9.990	9.216	<0.001	Yes
5 wt.% vs. 20 wt.%	9.528	8.790	<0.001	Yes
20 wt.% vs. 30 wt.%	0.886	0.817	1.000	No
20 wt.% vs. 10 wt.%	0.462	0.426	1.000	Do Not Test
10 wt.% vs. 30 wt.%	0.424	0.391	1.000	Do Not Test

Comparisons for factor: Fiber load within acidic treatment

Comparison	Diff of Means	t	P	P<0.05
5 wt.% vs. 30 wt.%	10.188	9.399	<0.001	Yes
5 wt.% vs. 20 wt.%	7.622	7.032	<0.001	Yes
5 wt.% vs. 10 wt.%	5.192	4.790	<0.001	Yes
10 wt.% vs. 30 wt.%	4.996	4.609	<0.001	Yes
10 wt.% vs. 20 wt.%	2.430	2.242	0.171	No
20 wt.% vs. 30 wt.%	2.566	2.367	0.126	No

A result of "Do Not Test" occurs for a comparison when no significant difference is found between two means that enclose that comparison. For example, if you had four means sorted in order, and found no difference between means 4 vs. 2, then you would not test 4 vs. 3 and 3 vs. 2, but still test 4 vs. 1 and 3 vs. 1 (4 vs. 3 and 3 vs. 2 are enclosed by 4 vs. 2: 4 3 2 1). Note that not testing the enclosed means is a procedural rule, and a result of Do Not Test should be treated as if there is no significant difference between the means, even though one may appear to exist.

Flexural Modulus

Table E.3. SigmaPlot two-way analysis of variance of the effect of fiber content and fiber treatment on the flexural modulus of raffia palm fiber reinforced high density polyethylene.

Source of Variation	DF	SS	MS	F	P
Fiber Load	3	0.897	0.299	57.184	<0.001
Treatment	3	1.300	0.433	82.922	<0.001
Fiber Load × Treatment	9	0.456	0.0507	9.692	<0.001
Residual	64	0.335	0.00523		
Total	79	2.987	0.0378		

Dependent Variable: Flexural Modulus (GPa).

Main effects cannot be properly interpreted if significant interaction is determined. This is because the size of a factor's effect depends upon the level of the other factor. the effect of various levels of fiber load depends on what level of treatment is present. there is a statistically significant interaction between fiber load and treatment (P = <0.001).

All Pairwise Multiple Comparison (Bonferroni t-test):

Comparisons for factor: Fiber load

Comparison	Diff of Means	t	P	P<0.050
30 wt.% vs. 5 wt.%	0.275	12.029	<0.001	Yes
30 wt.% vs. 10 wt.%	0.145	6.342	<0.001	Yes
30 wt.% vs. 20 wt.%	0.0435	1.903	0.369	No
20 wt.% vs. 5 wt.%	0.232	10.126	<0.001	Yes
20 wt.% vs. 10 wt.%	0.102	4.440	<0.001	Yes
10 wt.% vs. 5 wt.%	0.130	5.686	<0.001	Yes

Comparisons for factor: Treatment

Comparison	Diff of Means	t	P	P<0.050
No Treatment vs. HDPE	0.302	13.188	<0.001	Yes
No Treatment vs. Alkaline	0.0150	0.656	1.000	No
No Treatment vs. Acidic	0.00700	0.306	1.000	Do Not Test
Acidic Treatment vs. HDPE	0.295	12.881	<0.001	Yes
Acidic vs. Alkaline Treatment	0.00800	0.350	1.000	Do Not Test
Alkaline Treatment vs. HDPE	0.286	12.532	<0.001	Yes

Comparisons for factor: Treatment within 5 wt.%

Comparison	Diff of Means	t	P	P<0.05
Alkaline Treatment vs. HDPE	0.140	3.062	0.019	Yes
Alkaline vs. Acidic Treatment	0.0940	2.056	0.263	No
Alkaline vs. No Treatment	0.0800	1.750	0.510	Do Not Test
No Treatment vs. HDPE	0.0600	1.312	1.000	No
No Treatment vs. Acidic	0.0140	0.306	1.000	Do Not Test
Acidic Treatment vs. HDPE	0.0460	1.006	1.000	Do Not Test

Comparisons for factor: Treatment within 10 wt.%

Comparison	Diff of Means	t	P	P<0.05
No Treatment vs. HDPE	0.352	7.698	<0.001	Yes
No Treatment vs. Acidic	0.172	3.762	0.002	Yes
No Treatment vs. Alkaline	0.118	2.581	0.073	No
Alkaline Treatment vs. HDPE	0.234	5.118	<0.001	Yes
Alkaline vs. Acidic Treatment	0.0540	1.181	1.000	No
Acidic Treatment vs. HDPE	0.180	3.937	0.001	Yes

Comparisons for factor: Treatment within 20 wt.%

Comparison	Diff of Means	t	P	P<0.05
Acidic Treatment vs. HDPE	0.442	9.667	<0.001	Yes
Acidic vs. Alkaline Treatment	0.102	2.231	0.175	No
Acidic vs. No Treatment	0.0520	1.137	1.000	Do Not Test
No Treatment vs. HDPE	0.390	8.529	<0.001	Yes
No Treatment vs. Alkaline	0.0500	1.094	1.000	Do Not Test
Alkaline Treatment vs. HDPE	0.340	7.436	<0.001	Yes

Comparisons for factor: Treatment within 30 wt.%

Comparison	Diff of Means	t	P	P<0.05
Acidic Treatment vs. HDPE	0.510	11.154	<0.001	Yes
Acidic vs. No Treatment	0.106	2.318	0.142	No
Acidic vs. Alkaline Treatment	0.0780	1.706	0.557	Do Not Test
Alkaline Treatment vs. HDPE	0.432	9.448	<0.001	Yes
Alkaline vs. No Treatment	0.0280	0.612	1.000	Do Not Test
No Treatment vs. HDPE	0.404	8.835	<0.001	Yes

Comparisons for factor: Fiber load within no treatment

Comparison	Diff of Means	t	P	P<0.05
30 wt.% vs. 5 wt.%	0.344	7.523	<0.001	Yes
30 wt.% vs. 10 wt.%	0.0520	1.137	1.000	No
30 wt.% vs. 20 wt.%	0.0140	0.306	1.000	Do Not Test
20 wt.% vs. 5 wt.%	0.330	7.217	<0.001	Yes
20 wt.% vs. 10 wt.%	0.0380	0.831	1.000	Do Not Test
10 wt.% vs. 5 wt.%	0.292	6.386	<0.001	Yes

Comparisons for factor: Fiber load within alkaline treatment

Comparison	Diff of Means	t	P	P<0.05
30 wt.% vs. 5 wt.%	0.292	6.386	<0.001	Yes
30 wt.% vs. 10 wt.%	0.198	4.330	<0.001	Yes
30 wt.% vs. 20 wt.%	0.0920	2.012	0.291	No
20 wt.% vs. 5 wt.%	0.200	4.374	<0.001	Yes
20 wt.% vs. 10 wt.%	0.106	2.318	0.142	No
10 wt.% vs. 5 wt.%	0.0940	2.056	0.263	No

Comparisons for factor: Fiber load within acidic treatment

Comparison	Diff of Means	t	P	P<0.05
30 wt.% vs. 5 wt.%	0.464	10.148	<0.001	Yes
30 wt.% vs. 10 wt.%	0.330	7.217	<0.001	Yes
30 wt.% vs. 20 wt.%	0.0680	1.487	0.851	No
20 wt.% vs. 5 wt.%	0.396	8.661	<0.001	Yes
20 wt.% vs. 10 wt.%	0.262	5.730	<0.001	Yes
10 wt.% vs. 5 wt.%	0.134	2.931	0.028	No

A result of "Do Not Test" occurs for a comparison when no significant difference is found between two means that enclose that comparison. For example, if you had four means sorted in order, and found no difference between means 4 vs. 2, then you would not test 4 vs. 3 and 3 vs. 2, but still test 4 vs. 1 and 3 vs. 1 (4 vs. 3 and 3 vs. 2 are enclosed by 4 vs. 2: 4 3 2 1). Note that

not testing the enclosed means is a procedural rule, and a result of Do Not Test should be treated as if there is no significant difference between the means, even though one may appear to exist.

APPENDIX F

Result and Statistical Analysis of the Effect of Fiber Content and Fiber Treatment on the Impact Strength of RPF reinforced HDPE

Table F.1. Impact properties of unreinforced and raffia palm fiber reinforced high density polyethylene at different temperatures.

Polymer	Fiber Content (wt.%)	Impact Energy Absorbed (kJ/mm ²)			
		23°C	0°C	-20°C	-40°C
HDPE	-	15.88 ± 2.04	11.59 ± 2.06	13.29 ± 0.98	9.65 ± 0.48
Raw	5	9.33 ± 0.67	9.71 ± 0.59	9.14 ± 1.47	5.51 ± 0.80
Fiber	10	10.11 ± 0.83	9.40 ± 1.42	8.24 ± 1.36	8.29 ± 0.99
	20	9.32 ± 0.54	9.61 ± 0.96	8.79 ± 1.21	8.03 ± 1.12
	30	8.57 ± 0.48	8.94 ± 1.24	8.58 ± 0.62	7.93 ± 0.69
NaOH	5	10.71 ± 1.14	11.37 ± 0.86	9.92 ± 0.61	8.88 ± 0.95
Treated	10	11.86 ± 3.60	9.54 ± 0.07	10.38 ± 0.78	9.06 ± 0.61
Fiber	20	9.71 ± 0.21	9.96 ± 0.87	9.86 ± 0.69	9.33 ± 1.28
	30	8.53 ± 0.12	9.35 ± 0.61	9.96 ± 1.23	8.12 ± 0.70
H ₂ SO ₄	5	9.43 ± 0.64	8.43 ± 0.67	7.44 ± 0.56	6.13 ± 1.72
Treated	10	8.36 ± 0.65	7.66 ± 0.05	7.73 ± 0.02	6.37 ± 0.94
Fiber	20	7.93 ± 0.54	7.51 ± 0.61	7.76 ± 0.11	5.88 ± 0.73
	30	6.74 ± 0.67	7.27 ± 0.71	6.79 ± 0.62	6.44 ± 0.89

Table F.2. SigmaPlot three-way analysis of variance of the effect fiber content, fiber treatment and temperature on the impact strength of raffia palm fiber reinforced high density polyethylene.

Source of Variation	DF	SS	MS	F	P
Fiber Load	3	18.536	6.179	4.664	0.003
Treatment	3	1185.069	395.023	298.155	<0.001
Temperature	3	348.631	116.210	87.713	<0.001
Fiber Load × Treatment	9	20.673	2.297	1.734	0.082
Fiber Load × Temperature	9	32.021	3.558	2.685	0.005
Treatment × Temperature	9	194.406	21.601	16.304	<0.001
Fiber Load × Treatment × Temperature	27	37.609	1.393	1.051	0.400
Residual	256	339.172	1.325		
Total	319	2176.117	6.822		

Dependent Variable: Impact Energy (KJ/mm²).

The main effects for fiber load cannot be properly interpreted since the size of the factor's effect depends upon the level of another factor.

The main effects for treatment cannot be properly interpreted since the size of the factor's effect depends upon the level of another factor.

The main effects for temperature cannot be properly interpreted since the size of the factor's effect depends upon the level of another factor.

The effect of various levels of fiber load does not depend on what level of treatment is present. There is not a statistically significant interaction between fiber load and treatment (P = 0.082).

The effect of various levels of fiber load depends on what level of temperature is present. There is a statistically significant interaction between fiber load and temperature (P = 0.005).

The effect of various levels of treatment depends on what level of temperature is present. There is a statistically significant interaction between treatment and temperature (P = <0.001).

All Pairwise Multiple Comparison (Bonferroni t-test):

Comparisons for factor: Fiber load

Comparison	Diff of Means	t	P	P<0.050
10 wt.% vs. 30 wt.%	0.616	3.385	0.005	Yes
10 wt.% vs. 20 wt.%	0.273	1.502	0.806	No
10 wt.% vs. 5 wt.%	0.0623	0.342	1.000	Do Not Test
5 wt.% vs. 30 wt.%	0.554	3.043	0.016	Yes
5 wt.% vs. 20 wt.%	0.211	1.160	1.000	Do Not Test
20 wt.% vs. 30 wt.%	0.343	1.883	0.365	No

Comparisons for factor: Treatment

Comparison	Diff of Means	t	P	P<0.050
HDPE vs. Acidic Treatment	5.238	28.783	<0.001	Yes
HDPE vs. No Treatment	3.889	21.366	<0.001	Yes
HDPE vs. Alkaline Treatment	2.884	15.849	<0.001	Yes
Alkaline vs. Acidic Treatment	2.354	12.934	<0.001	Yes
Alkaline vs. No Treatment	1.004	5.517	<0.001	Yes
No Treatment vs. Acidic Treat	1.350	7.417	<0.001	Yes

Comparisons for factor: Temperature

Comparison	Diff of Means	t	P	P<0.050
23 °C vs. -40 °C	2.908	15.977	<0.001	Yes
23 °C vs. 0 °C	1.197	6.577	<0.001	Yes
23 °C vs. -20 °C	1.029	5.652	<0.001	Yes
-20 °C vs. -40 °C	1.879	10.325	<0.001	Yes
-20 °C vs. 0 °C	0.168	0.925	1.000	No
0 °C vs. -40 °C	1.711	9.400	<0.001	Yes

Comparisons for factor: Temperature within 5 wt.%

Comparison	Diff of Means	t	P	P<0.050
23 °C vs. -40 °C	3.796	10.429	<0.001	Yes
23 °C vs. -20 °C	1.390	3.820	0.001	Yes
23 °C vs. 0 °C	1.063	2.921	0.023	Yes
0 °C vs. -40 °C	2.733	7.508	<0.001	Yes
0 °C vs. -20 °C	0.327	0.899	1.000	No
-20 °C vs. -40 °C	2.405	6.609	<0.001	Yes

Comparisons for factor: Temperature within 10 wt.%

Comparison	Diff of Means	t	P	P<0.050
23 °C vs. -40 °C	3.212	8.823	<0.001	Yes
23 °C vs. 0 °C	2.008	5.516	<0.001	Yes
23 °C vs. -20 °C	1.644	4.518	<0.001	Yes
-20 °C vs. -40 °C	1.567	4.306	<0.001	Yes
-20 °C vs. 0 °C	0.363	0.998	1.000	No
0 °C vs. -40 °C	1.204	3.307	0.006	Yes

Comparisons for factor: Temperature within 20 wt.%

Comparison	Diff of Means	t	P	P<0.050
23 °C vs. -40 °C	2.740	7.527	<0.001	Yes
23 °C vs. 0 °C	1.046	2.874	0.026	Yes
23 °C vs. -20 °C	0.807	2.217	0.165	No
-20 °C vs. -40 °C	1.933	5.311	<0.001	Yes
-20 °C vs. 0 °C	0.239	0.657	1.000	No
0 °C vs. -40 °C	1.694	4.654	<0.001	Yes

Comparisons for factor: Temperature within 30 wt.%

Comparison	Diff of Means	t	P	P<0.050
23 °C vs. -40 °C	1.884	5.175	<0.001	Yes
23 °C vs. 0 °C	0.671	1.844	0.398	No
23 °C vs. -20 °C	0.273	0.750	1.000	Do Not Test
-20 °C vs. -40 °C	1.610	4.425	<0.001	Yes
-20 °C vs. 0 °C	0.398	1.093	1.000	Do Not Test
0 °C vs. -40 °C	1.212	3.331	0.006	Yes

Comparisons for factor: Fiber load within 23 °C

Comparison	Diff of Means	t	P	P<0.05
10 wt.% vs. 30 wt.%	1.625	4.465	<0.001	Yes
10 wt.% vs. 20 wt.%	0.841	2.311	0.130	No
10 wt.% vs. 5 wt.%	0.216	0.593	1.000	Do Not Test
5 wt.% vs. 30 wt.%	1.409	3.872	<0.001	Yes
5 wt.% vs. 20 wt.%	0.625	1.718	0.522	Do Not Test
20 wt.% vs. 30 wt.%	0.784	2.154	0.193	No

Comparisons for factor: Fiber load within 0 °C

Comparison	Diff of Means	t	P	P<0.05
5 wt.% vs. 30 wt.%	1.017	2.794	0.034	Yes
5 wt.% vs. 10 wt.%	0.729	2.002	0.278	No
5 wt.% vs. 20 wt.%	0.608	1.671	0.576	Do Not Test
20 wt.% vs. 30 wt.%	0.409	1.124	1.000	No
20 wt.% vs. 10 wt.%	0.121	0.331	1.000	Do Not Test
10 wt.% vs. 30 wt.%	0.288	0.792	1.000	Do Not Test

Comparisons for factor: Fiber load within -20 °C

Comparison	Diff of Means	t	P	P<0.05
5 wt.% vs. 30 wt.%	0.292	0.802	1.000	No
5 wt.% vs. 20 wt.%	0.0418	0.115	1.000	Do Not Test
5 wt.% vs. 10 wt.%	0.0381	0.105	1.000	Do Not Test
10 wt.% vs. 30 wt.%	0.254	0.697	1.000	Do Not Test
10 wt.% vs. 20 wt.%	0.00361	0.00991	1.000	Do Not Test
20 wt.% vs. 30 wt.%	0.250	0.687	1.000	Do Not Test

Comparisons for factor: Fiber load within -40 °C

Comparison	Diff of Means	t	P	P<0.05
10 wt.% vs. 5 wt.%	0.800	2.198	0.173	No
10 wt.% vs. 20 wt.%	0.369	1.015	1.000	Do Not Test
10 wt.% vs. 30 wt.%	0.297	0.816	1.000	Do Not Test
30 wt.% vs. 5 wt.%	0.503	1.382	1.000	Do Not Test
30 wt.% vs. 20 wt.%	0.0724	0.199	1.000	Do Not Test
20 wt.% vs. 5 wt.%	0.431	1.183	1.000	Do Not Test

Comparisons for factor: Temperature within HDPE

Comparison	Diff of Means	t	P	P<0.050
23 °C vs. -40 °C	6.235	17.130	<0.001	Yes
23 °C vs. 0 °C	4.296	11.803	<0.001	Yes
23 °C vs. -20 °C	2.593	7.124	<0.001	Yes
-20 °C vs. -40 °C	3.642	10.006	<0.001	Yes
-20 °C vs. 0 °C	1.703	4.679	<0.001	Yes
0 °C vs. -40 °C	1.939	5.327	<0.001	Yes

Comparisons for factor: Temperature within no treatment

Comparison	Diff of Means	t	P	P<0.050
0 °C vs. -40 °C	1.933	5.310	<0.001	Yes
0 °C vs. -20 °C	0.698	1.918	0.337	No
0 °C vs. 23 °C	0.0551	0.151	1.000	Do Not Test
23 °C vs. -40 °C	1.878	5.158	<0.001	Yes
23 °C vs. -20 °C	0.643	1.767	0.471	Do Not Test
-20 °C vs. -40 °C	1.235	3.392	0.005	Yes

Comparisons for factor: Temperature within alkaline treatment

Comparison	Diff of Means	t	P	P<0.050
23 °C vs. -40 °C	1.605	4.408	<0.001	Yes
23 °C vs. -20 °C	0.187	0.512	1.000	No
23 °C vs. 0 °C	0.147	0.405	1.000	Do Not Test
0 °C vs. -40 °C	1.457	4.004	<0.001	Yes
0 °C vs. -20 °C	0.0392	0.108	1.000	Do Not Test
-20 °C vs. -40 °C	1.418	3.896	<0.001	Yes

Comparisons for factor: Temperature within acidic treatment

Comparison	Diff of Means	t	P	P<0.050
23 °C vs. -40 °C	1.914	5.258	<0.001	Yes
23 °C vs. -20 °C	0.692	1.902	0.350	No
23 °C vs. 0 °C	0.400	1.098	1.000	Do Not Test
0 °C vs. -40 °C	1.514	4.160	<0.001	Yes
0 °C vs. -20 °C	0.293	0.804	1.000	Do Not Test
-20 °C vs. -40 °C	1.221	3.356	0.005	Yes

Comparisons for factor: Treatment within 23 °C

Comparison	Diff of Means	t	P	P<0.05
HDPE vs. Acidic Treatment	7.768	21.341	<0.001	Yes
HDPE vs. No Treatment	6.553	18.004	<0.001	Yes
HDPE vs. Alkaline Treatment	5.681	15.607	<0.001	Yes
Alkaline vs. Acidic Treatment	2.087	5.734	<0.001	Yes
Alkaline vs. No Treatment	0.872	2.396	0.104	No
No Treatment vs. Acidic	1.215	3.338	0.006	Yes

Comparisons for factor: Treatment within 0 °C

Comparison	Diff of Means	t	P	P<0.05
HDPE vs. Acidic Treatment	3.872	10.637	<0.001	Yes
HDPE vs. No Treatment	2.202	6.050	<0.001	Yes
HDPE vs. Alkaline Treatment	1.532	4.209	<0.001	Yes
Alkaline vs. Acidic Treatment	2.340	6.428	<0.001	Yes
Alkaline vs. No Treatment	0.670	1.841	0.401	No
No Treatment vs. Acidic	1.670	4.587	<0.001	Yes

Comparisons for factor: Treatment within -20 °C

Comparison	Diff of Means	t	P	P<0.05
HDPE vs. Acidic Treatment	5.867	16.120	<0.001	Yes
HDPE vs. No Treatment	4.603	12.647	<0.001	Yes
HDPE vs. Alkaline Treatment	3.274	8.996	<0.001	Yes
Alkaline vs. Acidic Treatment	2.593	7.124	<0.001	Yes
Alkaline vs. No Treatment	1.329	3.651	0.002	Yes
No Treatment vs. Acidic	1.264	3.473	0.004	Yes

Comparisons for factor: Treatment within -40 °C

Comparison	Diff of Means	t	P	P<0.05
HDPE vs. Acidic Treatment	3.447	9.469	<0.001	Yes
HDPE vs. No Treatment	2.196	6.032	<0.001	Yes
HDPE vs. Alkaline Treatment	1.050	2.886	0.025	Yes
Alkaline vs. Acidic Treatment	2.396	6.584	<0.001	Yes
Alkaline vs. No Treatment	1.145	3.147	0.011	Yes
No Treatment vs. Acidic	1.251	3.437	0.004	Yes

A result of "Do Not Test" occurs for a comparison when no statistically significant difference is found between two means that enclose that comparison. For example, if you had four means sorted in order, and found no difference between means 4 vs. 2, then you would not test 4 vs. 3 and 3 vs. 2, but still test 4 vs. 1 and 3 vs. 1 (4 vs. 3 and 3 vs. 2 are enclosed by 4 vs. 2: 4 3 2 1). Note that not testing the enclosed means is a procedural rule, and a result of Do Not Test should be treated as if there is no significant difference between the means, even though one may appear to exist.

APPENDIX G

Result of the Effect of Fiber Content and Fiber Treatment on the Density of RPF reinforced HDPE

Table G.1. Effect of untreated and treated raffia palm fibers on thermo-physical properties of high density polyethylene composites.

Polymer	Fiber Content (wt. %)	Melting Temperature (°C)	Heat of Fusion (J/g)	Crystallization Temperature (°C)	Heat of Crystallization (J/g)	Fractional Crystallinity (%)
HDPE Raw Fiber	-	142.8	180.3	111.7	189.8	62.2
	5	139.3	176.4	114.2	183.9	64.0
	10	137.6	175.0	115.0	179.5	67.0
	20	141.0	177.2	113.8	172.7	76.4
	30	139.4	162.2	114.9	161.0	79.9
NaOH Treated Fiber	5	139.94	189.6	112.8	187.3	68.8
	10	139.64	179.2	115.2	184.6	68.7
	20	140.45	163.2	114.7	164.0	70.3
	30	138.76	159.9	114.5	153.9	78.8
H ₂ SO ₄ Treated Fiber	5	139.2	190.2	115.8	185.7	69.0
	10	138.4	181.3	115.9	187.0	69.4
	20	139.3	173.0	115.6	171.3	74.6
	30	139.0	155.8	115.7	152.4	76.7

APPENDIX H

Result and Statistical Analysis of the Effect of Fiber Content and Fiber Treatment on the Water Absorption Behaviour of RPF reinforced HDPE

Table H.1. Effect of untreated and treated raffia palm fibers on water absorption behaviour of high density polyethylene composites.

Polymer	Fiber Content (wt.%)	Water Saturation Level (wt.%)	
		1st stage	2nd stage
HDPE	-	0.26	-
Raw Fiber	5	0.15	0.21
	10	0.15	0.25
	20	0.15	0.25
	30	0.26	0.41
	NaOH Treated Fiber	5	0.10
NaOH Treated Fiber	10	0.15	0.25
	20	0.20	0.31
	30	0.26	0.36
	H ₂ SO ₄ Treated Fiber	5	0.10
H ₂ SO ₄ Treated Fiber	10	0.15	0.20
	20	0.20	0.25
	30	0.26	0.31

Table H.2. SigmaPlot two-way analysis of variance of the effect fiber content and fiber treatment on the water absorption behaviour of raffia palm fiber reinforced high density polyethylene.

Source of Variation	DF	SS	MS	F	P
Fiber Load	3	0.136	0.0453	15.643	<0.001
Treatment	3	0.0400	0.0133	4.611	0.009
Fiber Load × Treatment	9	0.0581	0.00646	2.231	0.046
Residual	32	0.0926	0.00289		
Total	47	0.327	0.00695		

Dependent Variable: Water Absorbed (wt.%).

Main effects cannot be properly interpreted if significant interaction is determined. This is because the size of a factor's effect depends upon the level of the other factor. The effect of various levels of fiber load depends on what level of treatment is present. There is a statistically significant interaction between fiber load and treatment ($P = 0.046$).

All Pairwise Multiple Comparison Procedures (Bonferroni t-test):

Comparisons for factor: Fiber load

Comparison	Diff of Means	t	P	P<0.050
30 wt.% vs. 5 wt.%	0.149	6.779	<0.001	Yes
30 wt.% vs. 10 wt.%	0.0924	4.205	0.001	Yes
30 wt.% vs. 20 wt.%	0.0752	3.426	0.010	Yes
20 wt.% vs. 5 wt.%	0.0737	3.354	0.012	Yes
20 wt.% vs. 10 wt.%	0.0171	0.779	1.000	No
10 wt.% vs. 5 wt.%	0.0565	2.574	0.089	No

Comparisons for factor: Treatment

Comparison	Diff of Means	t	P	P<0.050
No Treatment vs. Acidic	0.0747	3.402	0.011	Yes
No Treatment vs. HDPE	0.0408	1.858	0.434	No
No Treatment vs. Alkaline	0.0117	0.535	1.000	Do Not Test
Alkaline vs. Acidic Treatment	0.0630	2.867	0.044	Yes
Alkaline Treatment vs. HDPE	0.0291	1.324	1.000	Do Not Test
HDPE vs. Acidic Treatment	0.0339	1.543	0.796	No

Comparisons for factor: Treatment within 5 wt.%

Comparison	Diff of Means	t	P	P<0.05
HDPE vs. Acidic Treatment	0.120	2.731	0.061	No
HDPE vs. No Treatment	0.0717	1.633	0.673	Do Not Test
HDPE vs. Alkaline Treatment	0.0514	1.170	1.000	Do Not Test
Alkaline vs. Acidic Treatment	0.0686	1.561	0.770	Do Not Test
Alkaline vs. No Treatment	0.0204	0.464	1.000	Do Not Test
No Treatment vs. Acidic	0.0482	1.098	1.000	Do Not Test

Comparisons for factor: Treatment within 10 wt.%

Comparison	Diff of Means	t	P	P<0.05
Alkaline vs. Acidic Treatment	0.0540	1.230	1.000	No
Alkaline Treatment vs. HDPE	0.0157	0.358	1.000	Do Not Test
Alkaline vs. No Treatment	0.0101	0.229	1.000	Do Not Test
No Treatment vs. Acidic	0.0440	1.001	1.000	Do Not Test
No Treatment vs. HDPE	0.00567	0.129	1.000	Do Not Test
HDPE vs. Acidic Treatment	0.0383	0.872	1.000	Do Not Test

Comparisons for factor: Treatment within 20 wt.%

Comparison	Diff of Means	t	P	P<0.05
No Treatment vs. Acidic	0.0570	1.298	1.000	No
No Treatment vs. HDPE	0.0403	0.917	1.000	Do Not Test
No Treatment vs. Alkaline	0.0123	0.280	1.000	Do Not Test
Alkaline vs. Acidic Treatment	0.0447	1.018	1.000	Do Not Test
Alkaline Treatment vs. HDPE	0.0280	0.637	1.000	Do Not Test
HDPE vs. Acidic Treatment	0.0167	0.381	1.000	Do Not Test

Comparisons for factor: Treatment within 30 wt.%

Comparison	Diff of Means	t	P	P<0.05
No Treatment vs. HDPE	0.189	4.304	<0.001	Yes
No Treatment vs. Acidic	0.150	3.406	0.011	Yes
No Treatment vs. Alkaline	0.0651	1.481	0.890	No
Alkaline Treatment vs. HDPE	0.124	2.823	0.049	Yes
Alkaline vs. Acidic Treatment	0.0846	1.925	0.379	No
Acidic Treatment vs. HDPE	0.0394	0.898	1.000	No

Comparisons for factor: Fiber load within no treatment

Comparison	Diff of Means	t	P	P<0.05
30 wt.% vs. 5 wt.%	0.261	5.937	<0.001	Yes
30 wt.% vs. 10 wt.%	0.183	4.175	0.001	Yes
30 wt.% vs. 20 wt.%	0.149	3.387	0.011	Yes
20 wt.% vs. 5 wt.%	0.112	2.551	0.094	No
20 wt.% vs. 10 wt.%	0.0346	0.788	1.000	Do Not Test
10 wt.% vs. 5 wt.%	0.0774	1.762	0.525	Do Not Test

Comparisons for factor: Fiber load within alkaline treatment

Comparison	Diff of Means	t	P	P<0.05
30 wt.% vs. 5 wt.%	0.175	3.993	0.002	Yes
30 wt.% vs. 10 wt.%	0.108	2.465	0.116	No
30 wt.% vs. 20 wt.%	0.0960	2.186	0.217	Do Not Test
20 wt.% vs. 5 wt.%	0.0794	1.807	0.481	No
20 wt.% vs. 10 wt.%	0.0123	0.279	1.000	Do Not Test
10 wt.% vs. 5 wt.%	0.0671	1.528	0.818	Do Not Test

Comparisons for factor: Fiber load within acidic treatment

Comparison	Diff of Means	t	P	P<0.05
30 wt.% vs. 5 wt.%	0.159	3.629	0.006	Yes
30 wt.% vs. 10 wt.%	0.0777	1.770	0.518	No
30 wt.% vs. 20 wt.%	0.0562	1.279	1.000	Do Not Test
20 wt.% vs. 5 wt.%	0.103	2.350	0.151	No
20 wt.% vs. 10 wt.%	0.0216	0.491	1.000	Do Not Test
10 wt.% vs. 5 wt.%	0.0817	1.859	0.434	Do Not Test

A result of "Do Not Test" occurs for a comparison when no significant difference is found between two means that enclose that comparison. For example, if you had four means sorted in order, and found no difference between means 4 vs. 2, then you would not test 4 vs. 3 and 3 vs. 2, but still test 4 vs. 1 and 3 vs. 1 (4 vs. 3 and 3 vs. 2 are enclosed by 4 vs. 2: 4 3 2 1). Note that not testing the enclosed means is a procedural rule, and a result of Do Not Test should be treated as if there is no significant difference between the means, even though one may appear to exist.